

SPECTROCHEMICAL TRACE-ELEMENT ANALYSIS IN STEELS AND
FERROUS ALLOYS

by

JOHN ERIC CHESTER B.Sc., A.R.C.S.

A thesis submitted for the Degree of
Doctor of Philosophy
of the
University of London

Department of Chemistry
Imperial College of Science and Technology
London S.W.7

October 1971

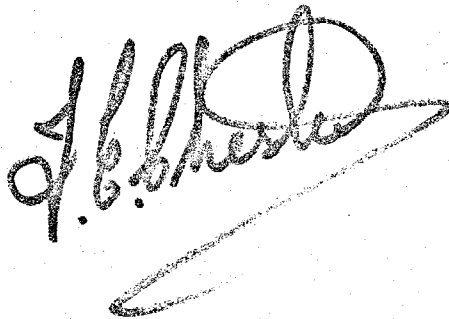
Acknowledgement

All work in this thesis is original except where due acknowledgement is made, and was carried out at Imperial College between October 1967 and September 1970,

I wish to thank Professor T.S. West and Dr. R.M. Dagnall for their help and encouragement, without which this work would not have been undertaken.

I also wish to thank my colleagues at Imperial College and the photocopying departments of Imperial College and Pilkington Brothers for their aid in preparing this thesis.

Finally I should like to thank the Welding Institute for the funds to carry out this study.



J. B. Sherwin

ABSTRACT

The first part of this work was concerned with the use of a ternary complex, formed by the sensitisation of the aluminium catechol violet complex with cetyltrimethylammonium bromide, for the determination of aluminium.

A solvent extraction system was developed using benzoic acid in ethyl acetate to extract the aluminium away from a number of interfering species, principally iron and some divalent cations. The aluminium was then back-extracted into aqueous solution for subsequent determination. EDTA was used as a mass masking agent for small quantities of interfering cations.

A number of other ternary complexes of the first-row transition elements with catechol violet and cetyltrimethylammonium bromide were prepared for the first time. The extinction coefficients were measured and a preliminary investigation of the compositions was undertaken.

It is suggested that the iron catechol violet cetyltrimethylammonium bromide complex is suitable for further development as a spectro-photometric reagent.

The middle section of this work was concerned with the development of a sensitive flame spectrophotometric method for boron, using the emission from the BO_2 radical in an oxygen-hydrogen-nitrogen co-axial flame.

The technique was found to depend for its sensitivity upon the anomalously high volatility of boric acid in absolute methanol to achieve an indirect nebuliser efficiency approaching 60%.

The latter part of the work was concerned with the calculation of free atom concentrations of elements in a

number of flames.

The atomisation of boron in five analytical flames was studied using this method using a digital computer to generate graphs of the dependence of atomisation upon flame stoichiometry.

This computer technique was also used to study the anomalously low sensitivity of determination of zirconium in the nitrous oxide acetylene flame. Data for titanium were also generated as a comparison.

The study showed that condensed zirconium carbide is formed in the fuel-rich flame, seriously reducing atomisation. In fuel-lean flames zirconium oxide species occur to lower the atomisation.

Notation

Because of the limitations of the typeface used, the following notation has been employed in this work.

Temperature

Temperatures are generally written thus:-

2000K for 2000 degrees Absolute (Kelvin)

2000C for 2000 degrees Centigrade (Celsius)

Contracted Notation for Numbers

Large or very small numbers are generally written in the contracted form thus :-

1.0E-04 for 0.00010 (1.0×10^{-4})

2.3E+05 for 230,000 (2.3×10^5)

(This notation is standard usage for computers with a limited typeface.)

Contents

Chapter	Title	Pages
1.	An Absorption Spectrophotometric Technique for the Determination of Aluminium Employing Ternary Complexes.	1.1 - 1.31
2.	Further Investigation of Ternary Complex Systems for Solution Absorption Spectrophotometry.	2.1 - 2.18
3.	A Flame Spectrophotometric Technique for the Determination of Boron.	3.1 - 3.32
4.	Computer Calculations of Boron Free-Atom Concentrations in Analytical Flames.	4.1 - 4.78
5.	Computer Calculations of Titanium and Zirconium Free-Atom Concentrations in the Nitrous Oxide Acetylene Flame.	5.1 - 5.34

Appendix

A Digital Computer Program to Determine Species Concentrations by the Minimisation of Free Energy	A.1 - A.25
---	---------------

Total 218 pages

CHAPTER 1

AN ABSORPTION SPECTROPHOTOMETRIC TECHNIQUE FOR THE DETER-
MINATION OF ALUMINIUM EMPLOYING TERNARY COMPLEXES.

Introduction.

The use of ternary complexes in analytical chemistry is well established for a great number of applications. These applications may be divided into two main types; those where the ternary complex is formed to be extracted with later determination of one of the components, not necessarily the analyte, and those where the ternary complex is determined spectrophotometrically.

Examples of the first type are; the determination of boron by formation of barium borotartrate followed by determination of the barium either by flame photometry ¹ or X-ray fluorescence ², and the determination of niobium by formation of molybdenum blue from the ternary phosphomolybdate ³.

Examples of the second type are much more numerous including the determination of molybdenum and antimony ⁴, tin ^{5,6}, silver ⁷, rare earths ⁸, fluoride ^{9,10}, and the classical determination of phosphorus as phosphomolybdate.

BAILEY ¹¹ has subdivided the types of ternary complexes into five categories depending on the nature of each of the three components. These categories are: 1. complex anions such as FeCl_4^- or SbCl_6^- which form colored complex products with cationic chromophores such as triphenylmethane dyestuffs or with other cations to form complexes suitable for the determination of the cation. 2. complexes of cations and complex mixed ligands such as phosphomolybdate. 3. complexes between a cation and two anionic ligands. 4. complexes made by the combination of a cation, an anion, and an uncharged species such as 1,10 phenanthroline. 5. complexes formed in the presence of and modified by micellar aggregates.

The ternary complexes investigated in this study form part of the fifth category.

A further three-way categorisation is possible. Ternary complexes used for absorption spectrophotometry may be considered as having one of three origins of colour formation. First the colour may be totally characteristic of one of the components, for example the ion association products formed by the reaction of tetrafluoroborate with Crystal Violet ¹², or Brilliant Green ¹³. In these techniques, the complex is normally extracted from unreacted reagent. Nearly all elements forming anionic complexes in highly acid solutions may be determined this way.

Second, the colour may be totally unrelated to the colour of any of the components, usually due to a charge transfer mechanism. e.g. Cu(I) neocuproin nitrate ¹⁴.

Third, the colour may be formed as a modification of the original colour of one of the complex components. This group includes the cerium/lanthanum fluoride Alizarin system ¹⁰, the Xylenol Orange rare earth cetylpyridinium bromide system ⁸, and the Catechol Violet metal surfactant system. In this latter system, the metal may be almost any cation and the surfactant may be any cationic one such as cetyltrimethylammonium salts or gelatine.

The system selected for this study was the one of Catechol Violet (CV) and cetyltrimethylammonium bromide (CTAB) with various cations.

Catechol Violet was initially prepared as a metallochromic indicator principally for complexometric titrations of such metals as Co, Ni, Mn, Zn, Mg, Cd ¹⁵, Cu ¹⁶, Bi ¹⁷.

Because of its structure (Fig. 1.1) with two complexing nuclei, it is extremely useful for this purpose and will give complexes with a large number of metals.

Its use as a colorimetric reagent for a variety of metals has since been described. It is especially useful as a reagent for polyvalent metals and a number of methods for zirconium ^{18,19,20,21}, molybdenum, tungsten and vanadium ²², bismuth ^{23,24}, and titanium ²⁵. This list is not exhaustive merely representative and many more references are available.

Few references to its use for determining divalent metals are available, the reasons being that it is unstable in alkaline solution at the point of maximum formation of those complexes, and it not a very selective reagent. One reference to its use for copper ²⁶ states that Pb, Ag, Hg, Bi, Zn, Sn, Sb, Ni, Cr, Fe, Mg, Ca, Sr, Ba all interfere so that it is only suitable for pure solutions. Further the determination must be carried out in neutral solution and is not very sensitive.

More recently, the effect of dispersing agents such as gelatine and CTAB has been reported as giving improved sensitivity, and several methods for various metals have been published ^{4,5,6}. A characteristic of the complex under the conditions used by these authors is the bathochromic shift in the wavelength of maximum absorbance.

This shift has been attributed to the reaction of the various basic functional groups within the gelatine with the remaining acidic protons on the CV nucleus. ²⁶

The object of this research was to continue the investigation into this effect to elucidate the exact mechanism and develop analytical methods based upon it. The point of

commencement of this study was the observation of the formation of an aluminium-CV-CTAB complex during an earlier study ⁴.

Apparatus

The apparatus used for this study consisted of a Unicam SP600 visible spectrophotometer with matched 1cm quartz cuvettes. For easier plotting of spectra, use was also made of a Unicam SP800 and a Beckmann DB600 scanning spectrophotometers.

Reagents

Al stock	0.001M	0.2267g of A.R. $\text{NH}_4\text{Al}(\text{SO}_4)_2 \cdot 12\text{H}_2\text{O}$ dissolved in 500ml distilled water.
CV	0.001M	0.1932g of CV dissolved in 500ml distilled water
CTAB	0.001M	0.36447g CTAB dissolved in 1 litre distilled water
Mixed Reagent		0.1546g CV & 1.458g CTAB dissolved in 2 litres distilled water
pH10 Buffer		50ml conc NH_3 solution diluted to 350 ml, pH adjusted to 10.2 with conc HCl and diluted to 400ml.
EDTA	0.1M	7.5g of EDTA(GPR free acid) dissolved in 200ml of water using the minimum conc NH_3 , pH adjusted to 9.5 and diluted to 250ml.
Ascorbic acid	5%	5g GPR ascorbic acid in 100ml water prepared fresh every 2 days
Hydroxylamine	10%	10g $\text{NH}_2\text{OH} \cdot \text{HCl}$ in 100ml water
1,10 Phenanthroline	2%	2g 1,10 phenanthroline (GPR) in 100ml water.

Benzoic Acid	5%	25g benzoic acid(GPR) dissolved in 500ml ethyl acetate(GPR)
Ammonium Benz- oate	10%	10g ammonium benzoate(GPR) dissolved in 100ml water
Ammonium Acetate	50%	50g ammonium acetate in 100ml water.

All reagents were A.R grade except for the CV CTAB and where otherwise stated.

Preliminary Investigation.

Initially the ternary complex was prepared in pH4.5 solution and the wavelength of maximum absorption was found to be 680nm. A study to find the optimum pH for formation of the complex disclosed that this was in alkaline conditions. Under these conditions, CV decomposes very rapidly owing to oxidation by dissolved oxygen. It was found that ascorbic acid and hydroxylamine were suitable protective reagents. The investigation of pH dependence was carried out with and without these protective reagents, and the results (without protection) are presented as Fig.1.2.

The optimum pH for the formation of the complex is at pH10. Higher pH values result in a higher blank absorbance, and the very rapid oxidation of the chromophore even in the presence of protective agents. Without these protective agents, decomposition is measurably slow at pH values less than 10 and, absorbances measured at a fixed time after addition of the alkaline buffer are reproducible.

The behaviour of the blank solution under these conditions is also interesting; the behaviour of CV is summarised in Fig.1.1; mixed CV CTAB solutions also display a green phase at about pH 7.

The optimum pH selected for the remainder of this study was pH10. All further investigations were made using solutions containing 5ml of 5% ascorbic acid per 100ml final solution volume except where specifically stated.

The optimum reagent ratios were also determined. These were found to be 2:1 CV:Al and 5:1 CTAB:Al. It was not found possible to use these ratios in practice as the complex precipitated if the CTAB level was held at this low level.

Measurement of the complex stability with time indicated that the complex slowly precipitated forming a turbid solution, and levelling the absorption curve. This effect could be reduced by increasing the CTAB concentration, and the final value selected as most suitable for solutions for measurement was $5.0E-04M$. This value was selected as a compromise between higher values with greater stability, and the tendency of the highly concentrated stock CTAB solution to become turbid.

The physical behaviour of solutions of ternary complexes containing CTAB was found to be rather peculiar. DAGNALL⁶ found that solutions containing Sn(IV)-CV-CTAB became decolorised with time. A brief investigation by the author disclosed that a major cause of this decolorisation is that the complex becomes firmly adherent to any glassware with which it is in contact. This effect has been previously reported by the author⁴, and the order of importance of this effect was found to be Sn-Mo-Al. The Sn complex required concentrated acid to remove it from glassware whereas the others could be removed by acetone as well as acid. The other most important effect peculiar to these complex solutions is the slow precipitation of the ternary complex. As previously

noted, this may be reduced or delayed by the use of greater CTAB concentrations, but it cannot be stopped completely.

CTAB stock solutions were also found to precipitate slowly. This effect was not found to be important in solutions less than 0.001M although it is measurable. In more concentrated solutions the effect is much more noticeable but it was found possible to delay this precipitation indefinitely by constant stirring, or reverse it by gentle heating. This effect is not true precipitation rather it must be considered as aggregation of the micelles to form larger micelles.

CV solutions also deteriorate slowly with time, but this deterioration was found to be due to the growth of molds in the solution. As CTAB is a very valuable germicide it was found to be very effective in preserving CV solutions against this deterioration, and the use of mixed reagent solutions was found to be very convenient.

This behaviour has an effect upon the analytical usefulness of these complexes. In the case of the Sn and Mo complexes, a definite value has been ascribed to the molar extinction coefficient. In this study, the effective molar extinction coefficient was found to vary according to the age of the complex and the state of the CTAB stock solution used for preparation of the complex.

If the CTAB stock solution was allowed to become slightly turbid, the blank absorbance was increased without a corresponding increase in the absorbance of the complex. This behaviour tended to reduce the effective extinction coefficient and sensitivity.

The age of the complex was much more important since

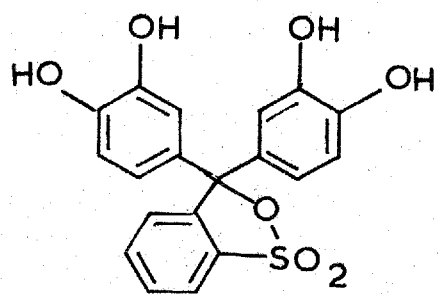
rapid measurement of the absorbance of the complex immediately after formation indicated an extinction coefficient about 40% higher than that derived from measurement some 20 minutes later. No way could be found of stopping this rapid initial decrease in complex absorbance, but after about 20 minutes the rate of decrease had so decreased that the absorbance decreased by only a further 15% over the next 24hrs.

For these reasons, it was not possible to ascribe an exact value to the molar extinction coefficient. However, exhaustive investigation showed that, for any set of solutions prepared from the same stock solutions at the same time the effective extinction coefficient was constant. Thus it was considered that this system was satisfactory for development as an analytical technique.

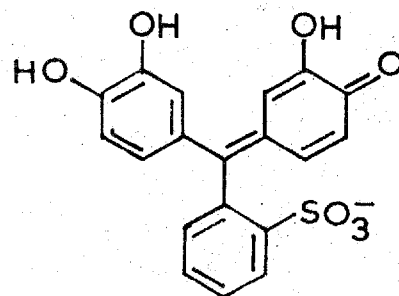
Under the conditions which were adopted as standard (i.e. final solution concentrations of 1. ascorbic acid 0.25% 2. CV $5.0 \times 10^{-5}M$ 3. CTAB $5.0 \times 10^{-4}M$ and pH10) and permitting a colour development time of 20 minutes, the effective molar extinction coefficient was found to be very near to 53,000 at 670nm.

The spectra of the complex and other components are given as Fig.1.3. This shows the spectra of: a. the Al-CV binary complex, b. CV alone, c. CV-CTAB, d. CV and cetylpyridinium bromide (CPB), e. Al-CV-CTAB, and f. Al-CV-CPB. All concentrations are as given in the previous paragraph; CPB was used to replace CTAB in two solutions to show the effect of using a different cationic surfactant.

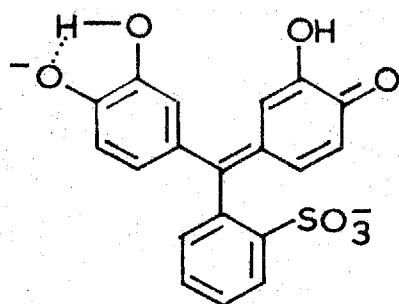
The next stage in this study was the determination of the composition and structure of this complex. The earlier determination of the optimum reagent ratios indicated a



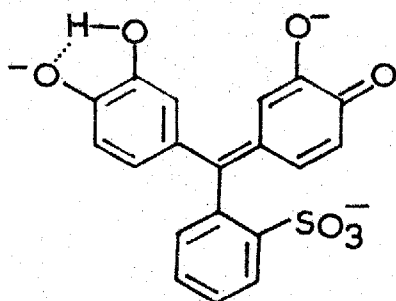
solid



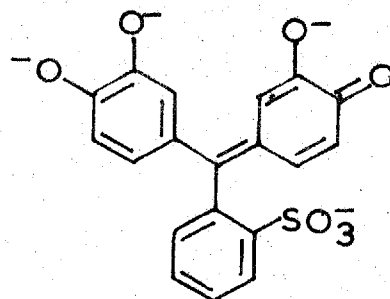
yellow pH 3



orange pH 6



purple pH 7-10



blue pH 11

Fig. 1.1

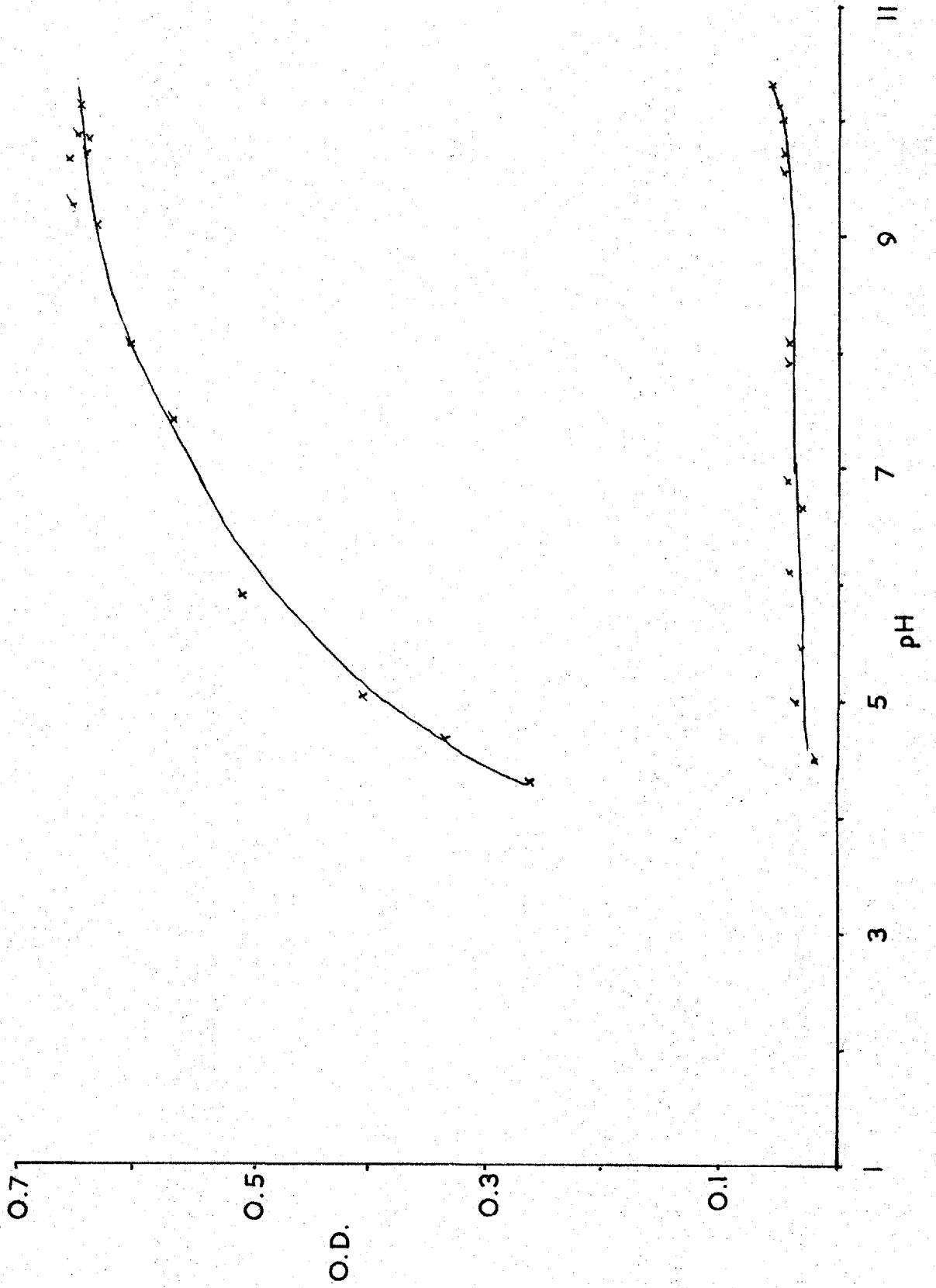


Fig.1.2

complex ratio of Al:CV:CTAB of 1:2;5. To confirm this a set of potentiometric titrations was performed with the results shown in Fig.1.4. These titrations were performed on solutions containing various combinations of; 5ml 0.01M Al, 10ml 0.01M CV, and 25ml 0.01M CTAB. A blank titration was also performed. The titrant used was 0.2M NaOH solution.

The titration graph for pure Al solution shows clearly the loss of 3 equivalents of protons followed at pH9 by the stepwise loss of a further proton.

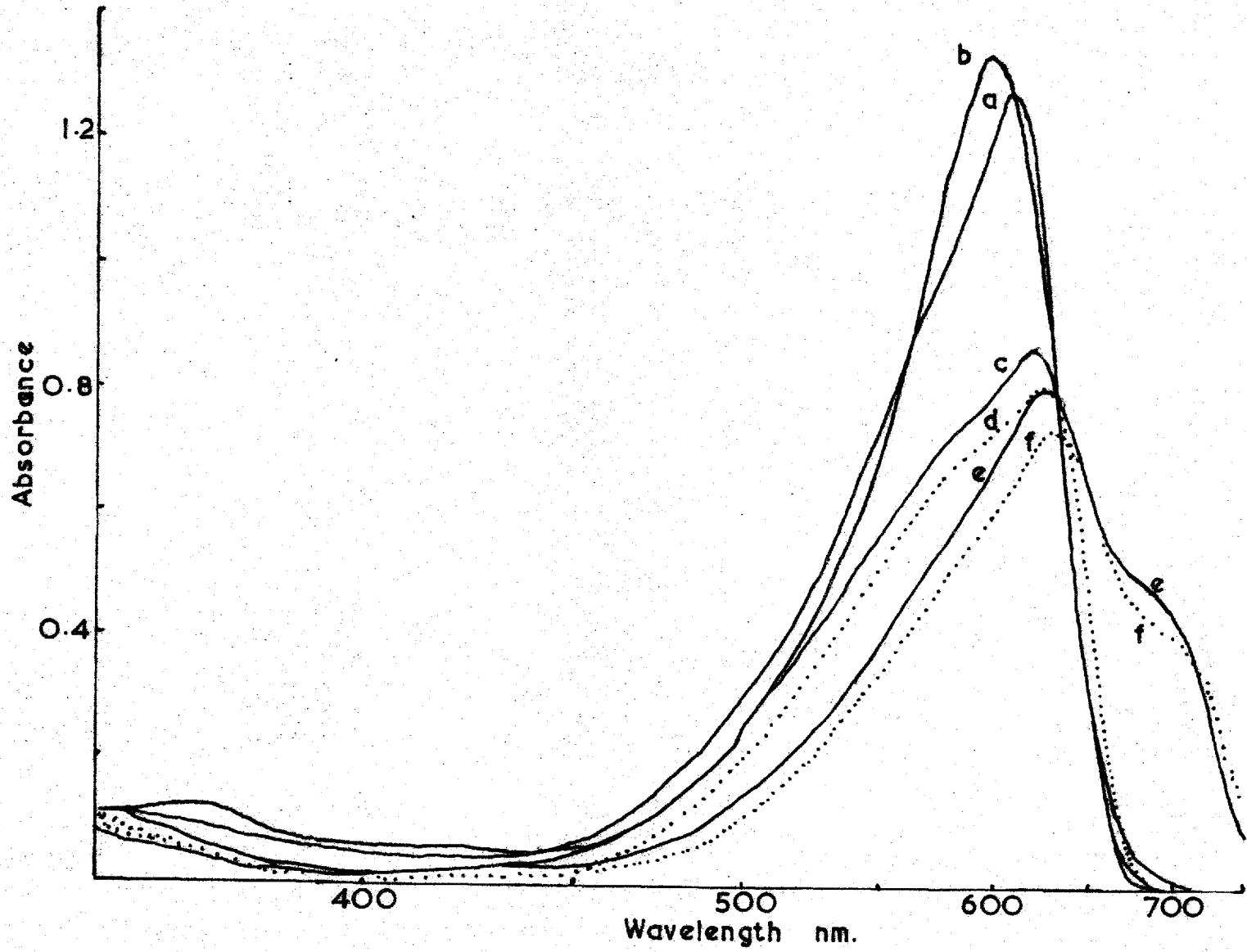
For the CV solution, there is the immediate loss of a strong acid proton presumably from the sulphonic acid group. The curve then indicates the loss of another proton from pH5-7 followed by the gradual loss of a very weak acid proton from pH7-10. After this the curve is too indistinct to permit interpretation. These changes may be attributed to the stages shown in Fig.1.1.

The binary complex displays the characteristics of losing 6 equivalents of protons up to pH6 followed by the loss of a further 2 equivalents of protons in a step at pH6-7.(N.B. these figures refer to equivalents of protons per mole of aluminium)The final stage of this process is thought to be the formation of an anion of the form shown within the brackets in Fig.1.5. The step where 2 equivalents of protons are lost is probably due to the loss of protons from the outer two complexing centres.

The ternary complex shows much the same behaviour as the binary, but all the protons are lost at much lower pH values indicating much more polar bonding. The final structure of the complex is thought to be that shown in Fig.1.5.

The complex was found to be extractable into CHCl_3 ,

Fig. 1.3



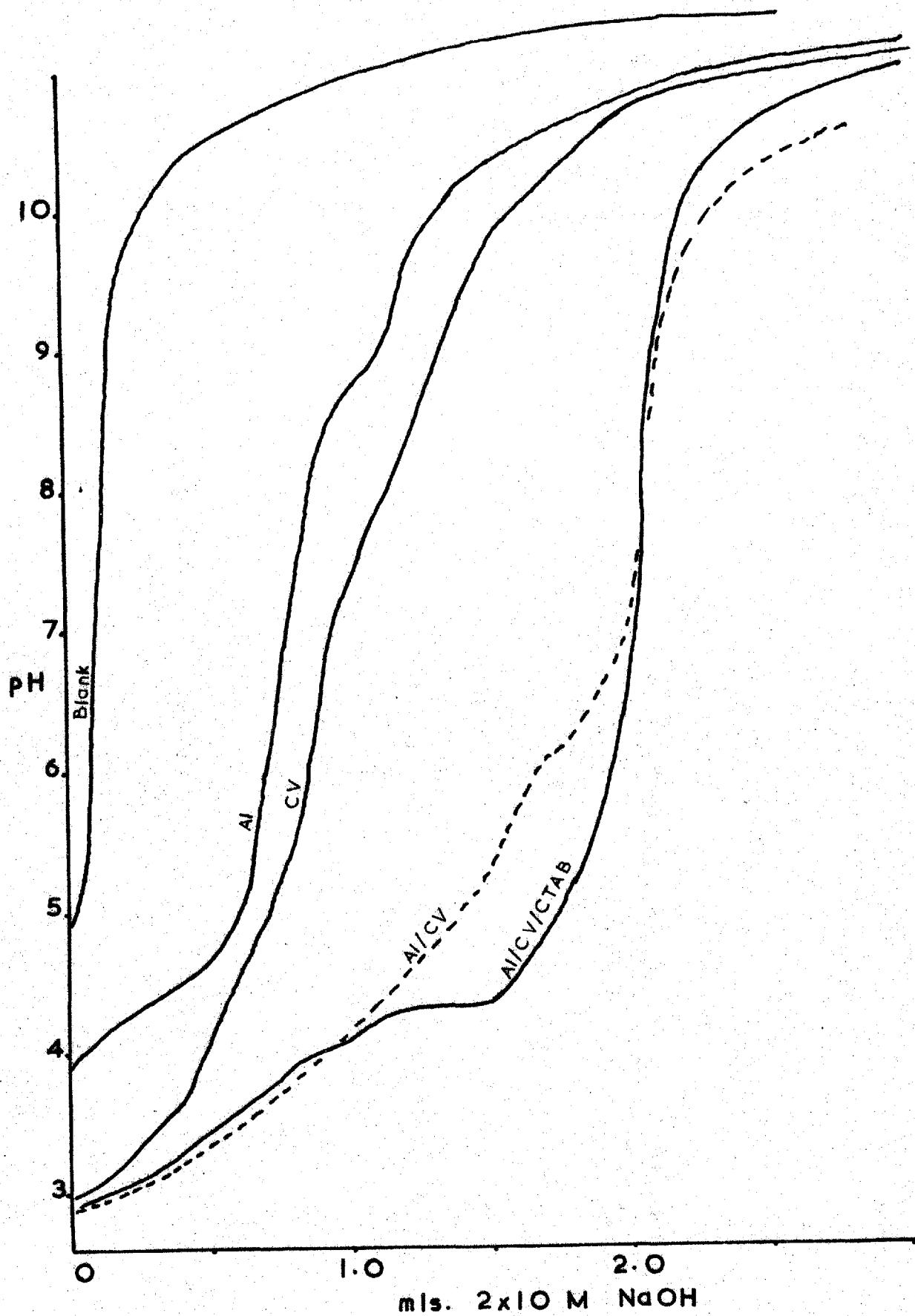


Fig.1.4

but the extraction was not straightforward and it was not thought possible to use it for an analytical method.

Shaking a solution of the complex with chloroform for several minutes did not appear to give any extraction, but if the system was left standing for several minutes after shaking, the aqueous layer became decolorised. During this period, the colour from the complex was observed to become concentrated in the interface between the layers and after a few minutes more, the chloroform layer assumed the colour of the complex. At this point, shaking immediately restored the colour to the aqueous layer, decolorising the chloroform. Standing for several minutes thereafter produced the exact sequence of events originally observed leading to the chloroform layer once more assuming the complex colour. Once an extraction had been carried out, this procedure could be repeated many times. The preferred state for the system appeared to be with the complex wholly in the chloroform layer.

The use of very high excesses of CTAB merely led to almost total formation of very stable emulsions which could not be separated.

Calibration curves were plotted to examine the useful analytical range for the technique developed, and these are given as Fig.1.1 a. & b. They extend over a concentration range from $1.0E-07M$ to $2.0E-05M$, a range of from 0.0027ppm to 0.54ppm of Al in the final solution. The calibration was linear over the whole of the range within experimental error. The magnitude of the probable error in measurement at the low end of the range is some 33% if taken as an absolute value of 0.002 absorbance units. The lower curve in Fig.1.6 a. was obtained using an absorptiometer and a No.608 filter.

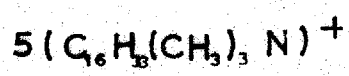
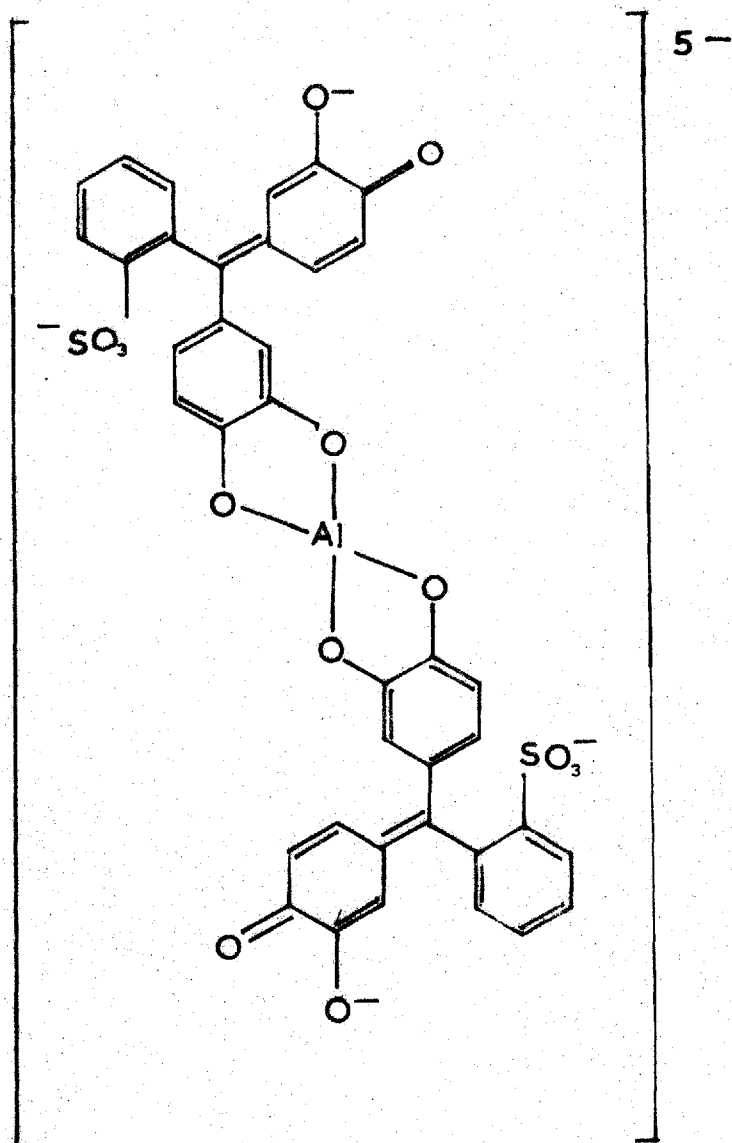


Fig. 1.5

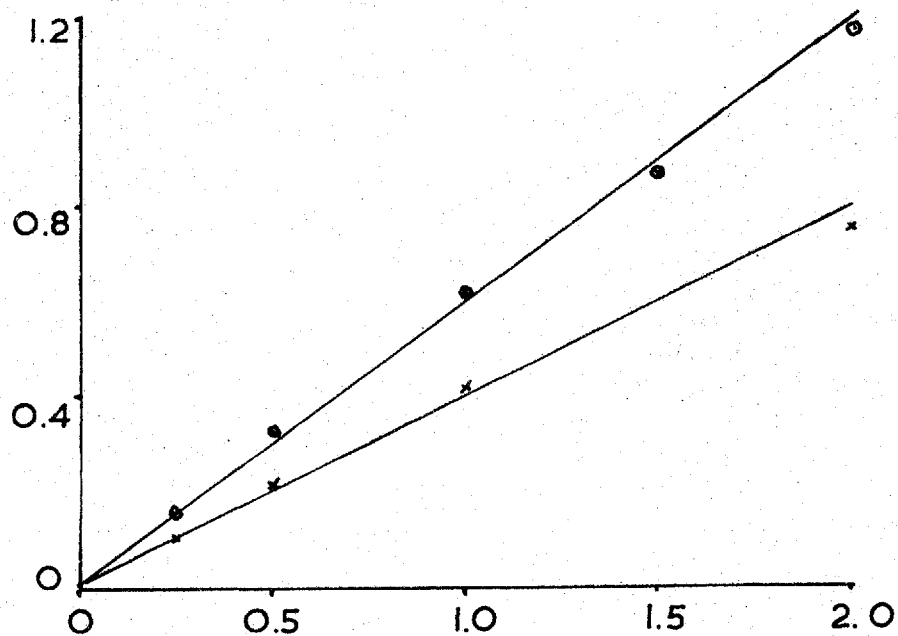


Fig.1.6 a.

Absorbance
(Al concentration x 100,000)

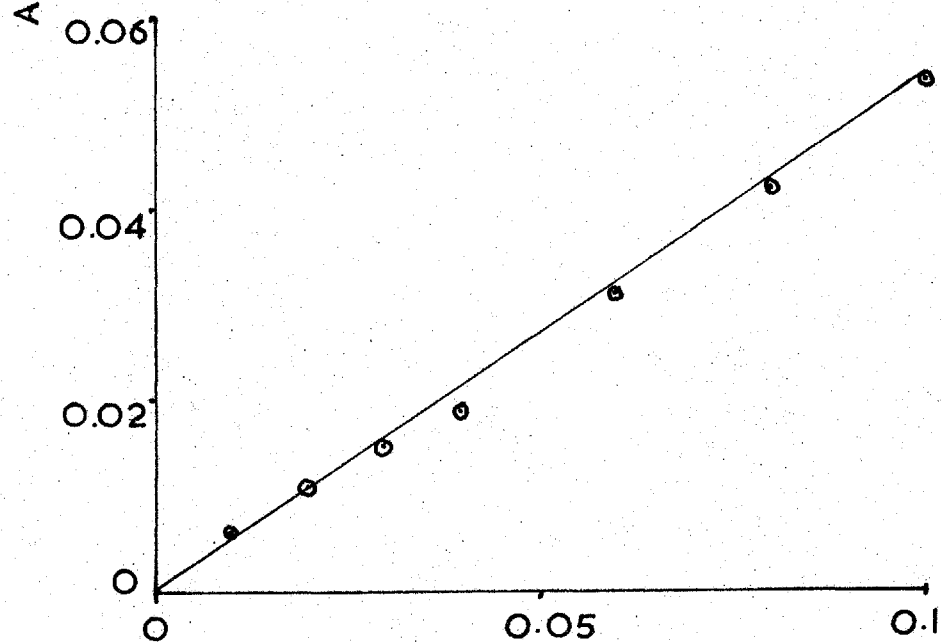


Fig.1.6 b.

The possible effect of interferences was investigated. Briefly stated, all metals in valency states 2,3 and 4 that were investigated interfered seriously with the formation of the ternary complex. Oxidising species also attacked the CV leading to turbid solutions. Certain others such as Cr(III) interfered by forming bulky precipitates in the alkaline conditions. Interfering anions were found to include tartrate, acetate, EDTA if present in the original solution and large concentrations of fluoride (more than 100-fold molar excess over Al). Notwithstanding the observed interference of EDTA, it was decided to attempt the use of EDTA as a mass masking agent. The aluminium EDTA complex is slow to form and it has been reported as being unstable in ammoniacal solution ²⁷.

Addition of 5ml of 0.1M EDTA solution per 100ml of the final solution for measurement was found to remove the interference caused by a number of elements a table of most of the interferences investigated is given below.

<u>Interference</u>	<u>Excess</u>	<u>No EDTA</u>	<u>EDTA</u>
Blank		0.067	0.120
Standard		0.600	0.655
Cu	100	0.486	0.658
Mg	"	0.720	0.638
Co	"	0.99	0.628
Ni	"	1.20	0.620
Hg(II)	"	1.07	0.805
Cr(III)	"	0.505	0.585
Be	25	0.95	0.84
Blank		0.070	0.111
Standard		0.610	0.610
Fe(III)	100	0.880	0.850
Fe(II)	"	1.21	1.12
Mo(VI)	"	0.632	0.645
Gd(III)	20	1.30	1.21
Zr(IV)	10	1.27	0.87
Bi(III)	50	1.39	1.85
Cd	10	0.750	0.605
U(VI)	"	1.6	1.30

<u>Interference</u>	<u>Excess</u>	<u>No F</u>	<u>100 F</u>	<u>500 F</u>
Standard B(H ₃ BO ₃)	10	0.650 0.639	0.630 0.630	0.855
Standard PO ₄ (III)	100	0.582 0.560		

The reason for the number of standard solutions used is the variation between separate sets of determinations. Each standard solution refers to the whole of the next block of results.

In addition to those interferences noted above, large concentrations of sodium were found to increase the absorbance of the blank and reduce the overall sensitivity. For this reason, it was decided to use the corresponding ammonium salts for all large additions of such solution constituents as the EDTA added for masking.

A solvent extraction technique was developed from one reported by MORRISON & FREISER²⁸ using benzoic acid and ethyl acetate. The technique given was found to give incomplete extraction when used for this study. The modifications that were necessary were the use of 5% benzoic acid in ethyl acetate as the extraction medium, the use of ammonium benzoate instead of sodium benzoate, and the formation of the aluminium benzoate at pH4 to improve the recovery. A full description of the technique is given later.

Interferences with this extraction were ascorbate, tartarate, and o-phosphate. Chromium also interfered by precipitation in the aqueous phase before extraction, obscuring the phase boundary and possibly occluding some of the organic phase. Anomalously, chromate was not found to interfere as seriously as chromium(III) probably because the boundary of the phases was not so heavily obscured. Because of the need to reduce any iron(III) present in the original

sample solution, hydroxylamine must be used and this will reduce any chromate present. The iron(II) so formed from any iron(III) is masked with o-phenanthroline, and the red complex formed renders the phase boundary easily visible.

A table of results of interferences removed by this extraction and the use of EDTA in the final solution is given below.

<u>Interference</u>	<u>Excess</u>	<u>Signal</u>
Blank		0.112
Standard		0.667
Hg	100	0.640
Standard		0.618
Fe+CrO ₄	50+10	0.604
Cu	100	0.622
Standard		0.589
Co	100	0.570
Ni	"	0.570

It was not found possible to remove the interference due to Be, Cr(III), rare earths, V(V), and Zr(IV). Antimony, and titanium were not extracted but the results were equivocal and further research is necessary on these points.

Suggested Technique for the Determination of Aluminium

Prepare a calibration curve by pipetting 1-10ml portions of 0.0001M aluminium solution into 100ml volumetric flasks. Add 25ml of the mixed reagent solution followed by 5ml of 5% ascorbic acid solution and 5ml of the pH10.2 buffer solution. After 20 minutes development time, add 5ml of 0.1M EDTA solution and make up to 100ml. Measure the absorbance at 670nm against a reagent blank. The curve is a straight line passing through the origin.

Test samples may be treated similarly. If interfering species are present, the following procedure may be used.

For both calibration and test solutions, transfer

appropriate aliquots to 100ml separating funnels. Add 1ml of 10% hydroxylamine solution, 5ml of 10% ammonium benzoate solution, 2ml of 2% 1,10 phenanthroline solution, and 2ml of 50% ammonium acetate solution. Adjust the pH to 7.5 to 9 if necessary, add 10ml of 5% benzoic acid solution in ethyl acetate. Shake vigorously for about 1 minute, separate the phases discarding the lower(aqueous) layer, and back-extract the organic layer with two 10ml portions of 1M hydrochloric acid. Combine these extracts in 100ml volumetric flasks, add 25ml of the mixed reagent solution and 5ml of 5% ascorbic acid solution. Add conc. ammonia solution dropwise until the solution turns green. Add 5ml of the buffer followed 20 minutes later by 5ml of 0.1M EDTA solution.

Measure as before.

The order of addition of the reagents is important. All glassware that has been in contact with ternary complex solutions should be washed after use to remove the adherent film that builds up on it. This is especially important for the cuvettes used for measurements.

Conclusions

Although the complex composition has been elucidated, a number of questions have not been answered. The potentiometric titrations showed that both binary and ternary complexes exist in the fully deprotonated form. However their spectra are quite different. That of the binary complex resembles that of the purple alkaline form of CV shown in Fig.-1.1. That of the ternary complex resembles that of the fully ionised alkaline form. This latter point is difficult to verify as the fully ionised form of CV is very unstable and oxidises too quickly for a spectrum to be plotted using -

conventional equipment. This could form the basis of further work on these complexes.

One fact is certain; the binary and ternary complexes exist in totally different environments. The binary complex almost certainly forms an anion in true aqueous solution.

In contrast to this, the ternary complex appears to be an electrically neutral species, and, from the observed fact that the cetyltrimethylammonium cation forms insoluble salts with bulky anions such as iodide or perchlorate, it is apparent that the ternary complex is not in aqueous solution.

Exactly what the environment of the ternary complex is is uncertain and indeterminable by the techniques employed in this study. Considering the spectra presented in Fig. 1.3 it may be seen that the substitution of CPB for CTAB has no apparent effect. The unlikelihood of further coordination of a quaternary nitrogen atom is not sufficient to explain this similarity completely. The similarity may well imply that the molecules of the complex are totally within the CTAB micelles. If adsorbed on the surface of the micelles, some contribution to the properties of the complex would be expected from the electrical properties of the surface layer. These properties are likely to be different for CPB and CTAB so that an observable difference might be expected. This is not necessarily so and further work is needed to resolve this matter.

The most likely situation appears to be that the ternary complex exists as a solid salt of CTAB dispersed in the CTAB micelles.

For this reason, it appears to be impossible to determine the true extinction coefficient of this ternary system.

The immediate decrease in absorption of a 'solution' of this complex subsequent to its formation is almost certainly due to the aggregation of the particles of the complex in the CTAB micelles. Formation of the complex in the absence of micelles appears to be impossible in aqueous solution ¹¹. This does not preclude the possibility of using non-aqueous media, but these results would be subject to interpretation, and anomalous extinction coefficients have been observed ²⁹.

However the true extinction coefficient is not thought to be very different from that reported for the 1:2 Sn:CV complex ⁶, i.e. 96000. Realisation of this sensitivity is impossible with the method used for this study, and a different approach must be employed if it is to be realised.

Notwithstanding this loss in absolute sensitivity, this complex and the analytical method developed compare very favorably with published absorption spectrophotometric techniques for aluminium, including those using 8-hydroxyquinoline ^{30 - 33}, Aluminon ^{30,31}, Chromazurol ³⁴⁻³⁶, and Eriochrome Cyanine ^{37,38}. The most sensitive of these techniques ³⁸ gives an effective extinction coefficient of 45000 measured by depletion of the reagent. However, there is a report in the literature of the determination of aluminium using CV which gives an extinction coefficient of 68000 for the binary complex measured at 580nm and at pH6 ³⁹.

This report is in direct contradiction to the results of this study which gives the wavelength of maximum absorbance of the binary complex as 615nm and the extinction coefficient as about 15000. Further, ANTON ⁴⁰ supports the results of this study and states that the binary complex has its peak absorbance at 615nm and an extinction coefficient of about 670 at pH5. In addition, the extinction coefficient

quoted for the binary complex with tin exceeds that obtained by other workers investigating the Sn/CV system, even when sensitised with gelatine^{5,6,41}. The explanation for this disagreement is not known with certainty, but may lie in a difference in nomenclature. The name Catechol Violet may be applied to pyrocatecholpthalein^{42,43}, and this may have led to some confusion between it and CV. The difficulty has been compounded by 'Chemical Abstracts' which definitely refers to one of the above papers⁴² under the index entry γ -sultone of bis-(3,4 dihydroxyphenyl) o-toluenesulphonic acid, the systematic name for CV. With somewhat less certainty, the same confusion may apply to another paper on the determination of boron⁴⁴.

With regard to this latter paper, there is not much evidence for this view, except that boron did not interfere with the determination of aluminium in this study. In opposition to it, the interference of aluminium, even in the presence of EDTA, was reported, which is in agreement with the results of this study.

It must be concluded that strict comparison of results such as these is impossible without the absolute certainty of agreement of nomenclature. In the absence of this assurance, any comparison or discussion is likely to be misleading and highly frustrating.

The major usefulness of this analytical method would appear to be for the determination of aluminium in plain carbon steels. Possible improvements to the method are the stabilisation of the complex in a more highly dispersed state to secure greater sensitivity, and the development of further extraction techniques for the elimination of interferences.

Suggestions for Future Investigation.

This investigation has shown that the formation of this type of ternary complex depends on the presence of a number of acidic functional groups on the chromophore. Ionisation of these groups increases the absorbance of the chromophoric species. Thus it follows that spectrophotometric reagents with a large number of hydroxyl groups will show improvement upon ternarisation. Thus it is suggested that the ternarisation of such systems be studied. One such system that is suggested by the forgoing study is that of pyrocatecholpthalein with a variety of cations. Another spectrophotometric reagent with the necessary acidic hydroxy groups is carminic acid. A short preliminary study of this reagent and its molybdenum complex has been performed, with the result that a ternary complex has been observed which shows increased absorbance and a bathochromic shift in the absorbance peak (Fig. 1.7). Yet another system worthy of study is the CV/CTAB/Zr system. Again the ternary complex has been prepared and the spectrum plotted (Fig. 1.8). Interestingly, the spectrum shows a hypsochromic shift upon ternarisation. This effect has not previously been described. No further investigation of these systems has been performed by the author.

Finally the effect of ternarising agents of different character to CTAB or CPB should be investigated. The use of non-surface-active ternarising agents in non-aqueous media has been reported¹¹. One reagent of completely different structure that appears to be suitable is 4-anilino-1-phenyl-1,2,4-triazolium chloride⁴⁵.

FIG. 1.7

Mo/Carminic Acid / CTAB

- a. CA
- b. Mo/CA
- c. CA/CTAB
- d. Mo/CA/CTAB

pH 5.2

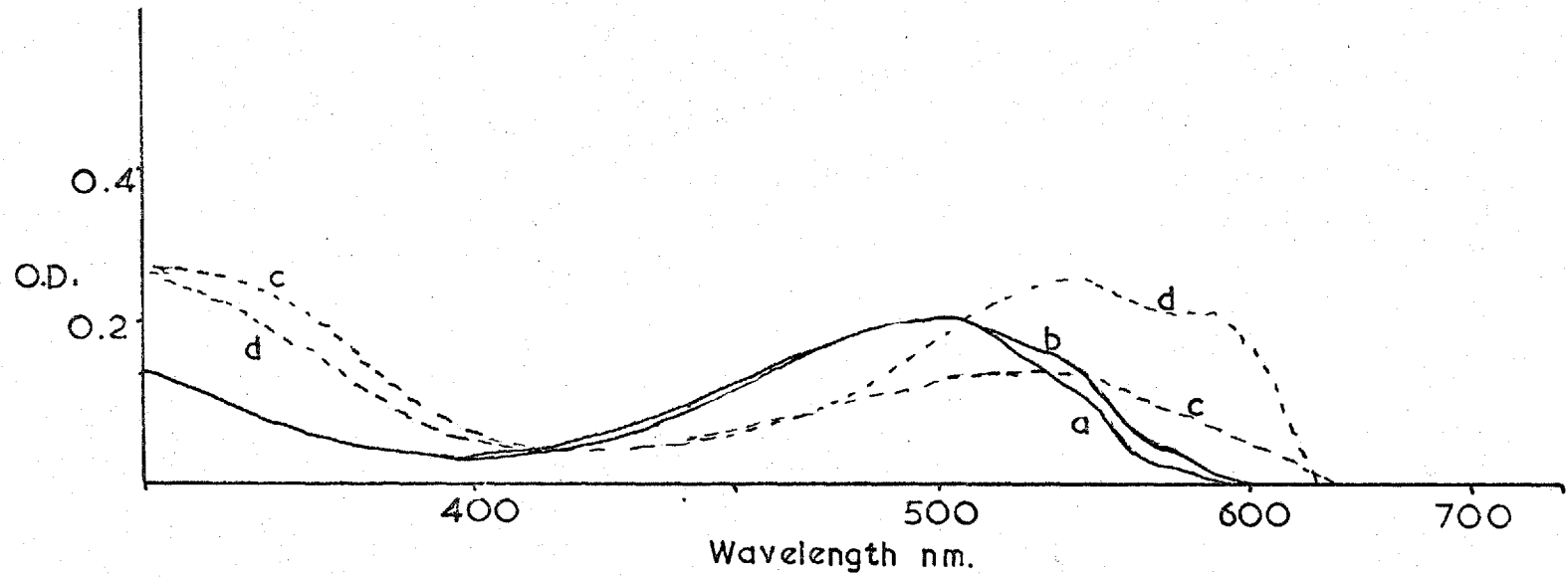
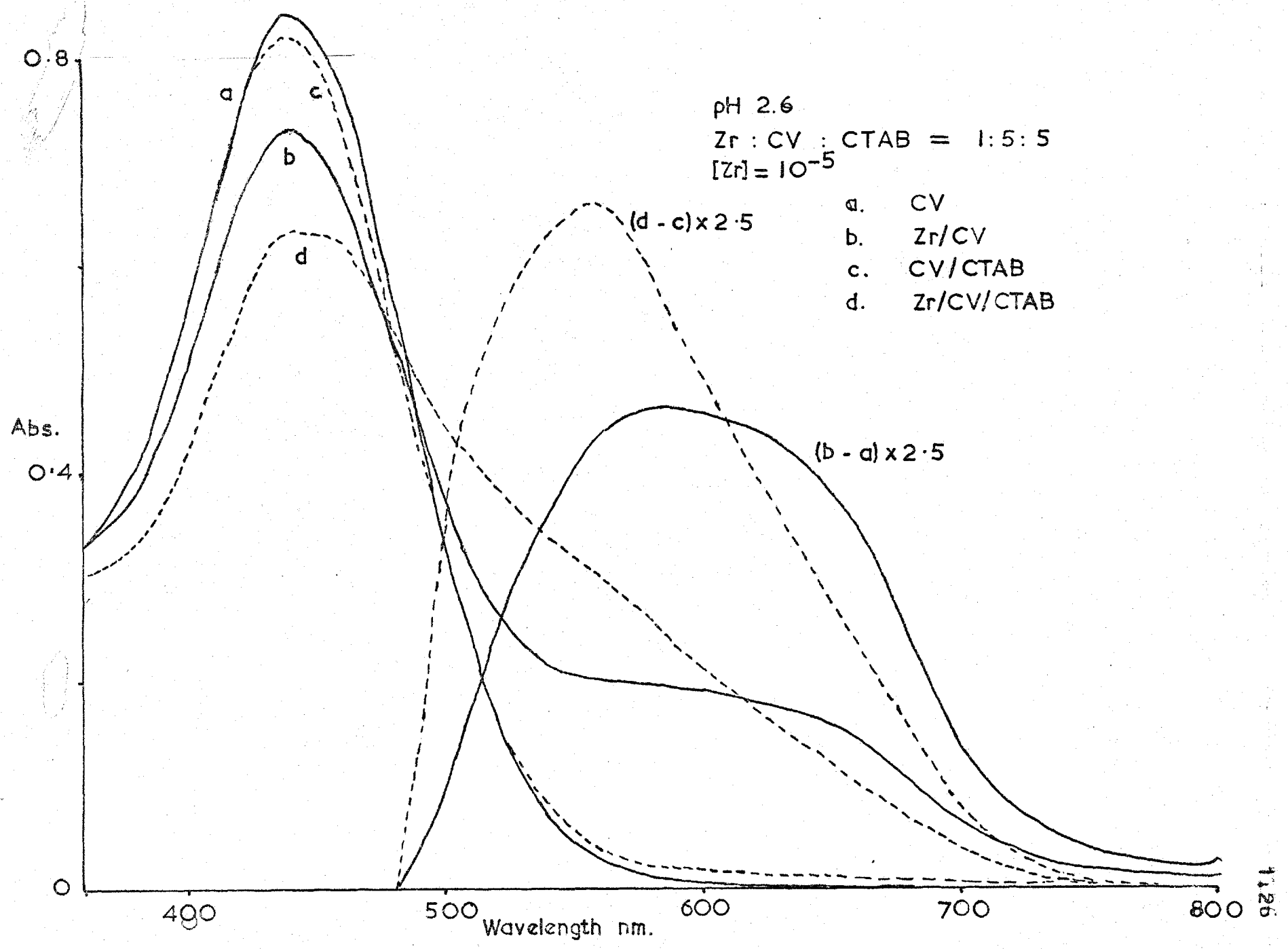


Fig. 1.8



Bibliography

1. E.Bovalini,M.Piazzi
Annali Chimia Roma 48 305 (1958)
2. C.L.Luke
Analytica Chimica Acta 45 377 (1969)
3. G.Norwitz,M.Codell
Analytical Chemistry 26 1230 (1954)
4. B.W.Bailey,J.E.Chester,R.M.Dagnall,T.S.West
Talanta 15 1359 (1968)
5. M.Malat
Z. Anal. Chem. 187 404 (1962)
6. R.M.Dagnall,T.S.West,P.Young
Analyst 92 27 (1967)
7. R.M.Dagnall,T.S.West
Talanta 11 1533 (1964)
8. W.J.de Wet,G.B.Behrens
Anal. Chem. 40 200 (1968)
9. R.Belcher,M.A.Leonard,T.S.West
J. Chem. Soc. 2390 (1958)
10. R.Greenhalgh,J.P.Riley
Analytica Chimica Acta 25 179 (1961)

11. B.W.Bailey
Ph.D.Thesis Imperial College London (1967)
12. I.A.Blyum, T.K.Dushina, T.V.Semenova, I.Y.Scherba
Zavod. Lab 27 644 (1961)
Cf. AA 9 576 (1962)
13. A.K.Babko, P.V.Marchenko
ibid. 26 1202 (1960)
Cf. AA 8 2419 (1961)
14. G.F.Smith, W.H.McCurdy
Anal. Chem. 24 371 (1952)
15. M.Malat, V.Suk, A.Jenickova
Z. Anal. Chem. 145 201 (1955)
16. M.Malat, A.Jenickova
ibid. 147 70 (1955)
17. M.Malat, V.Suk, J.Ryba
ibid. 144 40 (1955)
18. H.Flaschka, M.Y.Farah
ibid. 152 401 (1956)
19. J.P.Young, J.R.French, J.C.White
Anal. Chem. 30 422 (1958)
20. Yu.A.Chernikov, V.F.Luk'yanov, E.M.Kryuzeva
Z. Anal. Chem. 175 155 (1960)

21. G.Staats,H.Brueck
Z. Anal. Chem. 230 271 (1967)
22. A.K.Majumdar,C.P.Savarriar
Naturwissenschaften 45 84 (1958)
- 23 M.Svach
Z. Anal. Chem. 149 416 (1956)
24. M.Malat
ibid. 186 418 (1962)
25. M.Malat
ibid. 201 262 (1964)
26. M.Malat,J.Zelinka
Mikrochimica Acta 228 (1966)
27. J.Kinnunen,B.Merikanto
Chemist Analyst 44 75 (1955)
28. G.H.Morrison,H.Freiser
'Solvent Extraction in Analytical Chemistry' 2nd Edn.
J.Wiley Inc. New York 1962
29. B.W.Bailey
Unpublished Work.
30. E.B.Sandell
'Colorimetric Determination of Traces of Metals' 3rd Edn.
Interscience New York 1959

31. A.G.Owen, W.J.Price
Analyst 85 221 (1960)
32. 'Tables of Spectrophotometric Absorption Data of Compounds Used for the Colorimetric Determination of Elements'. I.U.P.A.C. Commission of Spectrochemical and Other Optical Procedures for Analysis.
Butterworths London 1963
33. R.M.Dagnall, T.S.West, P.Young
Analyst 90 13 (1965)
34. V.N.Tikmonov
Zh. Analit. Khim. 19 1204 (1964)
35. P.Pakalns
Analytica Chimica Acta 32 57 (1965)
36. O.P.Bhargava, W.G.Hines
Anal. Chem. 40 413 (1968)
37. S.Henry, P.Haniset
Ind. Chem. Belge 27 24 (1962)
38. U.T.Hill
Anal. Chem. 28 1419 (1956)
39. K.Tanaka, K.Yamayosi
Japan Analyst 13 540 (1964)

40. A. Anton
Anal. Chem. 32 725 (1960)
41. W.J. Ross, J.C. White
Anal. Chem. 33 421 (1961)
42. V. Patrovsky
Talanta 10 175 (1963)
43. G.K. Singhal, K.N. Tandon
ibid. 14 1127 (1967)
44. Kazuo Hiro
Bull. Chem. Soc. Japan 34 1743 (1961)
45. C. Runti, C. Nisi
Journal Med. Chem. 7 814 (1964)

CHAPTER 2

FURTHER INVESTIGATIONS OF TERNARY COMPLEX SYSTEMS FOR
SOLUTION ABSORPTION SPECTROPHOTOMETRY.

Introduction.

The elucidation of the structure of the aluminium-Catechol Violet(CV)-cetyltrimethylammonium bromide(CTAB) ternary complex has been described in Chapter 1 of this thesis. It was decided to undertake a short complementary study to investigate the effect of varying the cation in the system. The other studies of CV ternary complexes tend to suggest that the complex nature is independent of the cation complexed by the CV ^{1,2}.

The same does not necessarily appear to be true for CV-complexes with anionic species, as indicated by the behaviour of the Sb complex ², and the Zr complex mentioned briefly at the end of the last chapter.

It was decided to limit the number of metal species considered to the members of the first-row transition elements i.e. Sc to Zn. This selection was made to reduce difficulties from the presence of large numbers of metallic species in solution. The chemistry of these elements is well known and is simpler than that of other transition series. The presence of d-electron shells in the metal ions is also a feature that has not been present in any of the elements investigated so far using ternary CV/CTAB complexes.

Previous studies of the binary complexes of these elements has been mainly confined to Ti and V ^{3,4,5} in acidic solution, but one reference exists to the determination of Cu ⁶ in near-neutral solution. Otherwise this reagent has only been used as a complexometric indicator in determinations of these elements. This lack of work must be attributed to the ease of oxidation of CV in alkaline solution where it is most useful for forming complexes with cationic species, and its almost total lack of selectivity. The reported technique for the determination of Cu ⁶ was stated to be effective only for pure solutions.

Experimental.

The procedure selected for this study was standardised as the following:-

A spectrum was plotted followed by the determination of the optimum pH of formation of the complex. Further investigation of the complex was performed at the optimum pH so determined. This further investigation was confined to the construction of constant variation curves for the complex system, neglecting the effect of varying the concentration of CTAB. This latter was regarded as being a standard parameter, as no difference in the nature of the ternary complex has been observed when varying this quantity, until the critical micelle concentration is reached. Thus only the metal:CV ratio was determined.

Buffers used for the constant-variation investigations were acetate based for the Ti and V complexes in acidic solution, and ammonia/ammonium chloride based for alkaline solution.

Alkaline conditions also made the use of protective reagents for the CV necessary. The reagent used was ascorbic acid which had been found to provide protection up to pH10.5.

Initial investigations were performed using a metal concentration in the final solution of 1.0×10^{-5} M. The standard reagent excesses selected for this stage of the study were; CV:metal 5:1, CTAB:metal 50:1. Measurements of absorbance were performed at or near the wavelength of maximum absorbance of the ternary complex.

Results.

The results of this study are incomplete as no way could be devised to form the ternary Cr-CV-CTAB complex in anything approaching 100% yield. This was due to the great kinetic

stability of the hexaquo chromium(III) ion. In acid solution, very little reaction is to be expected as the formation conditions are basically unfavorable. In alkaline solution, the chromium is immediately precipitated as the hydroxide, and the CV will undergo atmospheric oxidation. No attempt was made to provide protection with an inert atmosphere of nitrogen as it was not considered essential to the study.

The other results are presented below.

Spectra.

Only 3 spectra are given, those for the Fe(II), Co(II), and Ti(IV) complexes. The reason for this is simply that these are totally representative of the spectra of all the ternary complexes formed by the elements used for this study.

The Ti(IV) spectrum is virtually identical to that of V and that of Co is nearly identical to those of Ni, Cu, Zn, Sc, & Mn. That of Fe is unique in that it shows an extension of the complex absorbance peak into the near infra-red.

Within the groupings noted above, the only major difference is the value of the extinction coefficient.

The spectra are presented as Figs. 2.1 (Ti) & 2.2 (Fe, Co). The difference in the spectra of the reagent is due to the pH of the solutions used. That in Fig. 2.1 was pH 5; that in Fig. 2.2 was pH 10.

Scandium(III)

The pH dependence is plotted in Fig. 2.3. The optimum pH was found to be pH 8.75 and the extinction coefficient (measured relative to the metal) was 53000.

The constant variation plot is given as Fig. 2.12. This is very confused but indicates that the main complex formed is the 1:1 or 1:1.5 CV:Sc complex. (In all these plots, the metal concentration increases to the right) Some indication is present

of the formation of another complex of the composition CV:Sc 2:1 but this is not clear.

Titanium(IV)

The pH dependence plot(Fig.2.4) shows a clear peak at pH5 and no formation above pH7. The extinction coefficient at 580nm is 45000.

The constant variation plot is given as Fig.2.13. Much clearer than that of Sc, it distinctly indicates the formation of both a 1:1 or 1:1.5 CV:Ti complex and a 2:1 CV:Ti complex. This latter appears to give maximum absorbance at shorter wavelengths.

Vanadium(IV)

The pH dependence plot(Fig.2.5) is similar to that of Ti, but formation is limited at low values of pH. The optimum pH is 5. The measured extinction coefficient is 23000 at 580nm.

The constant variation plot(Fig.2.14) shows the formation of both 1:1 and 2:1 CV:V complexes.

Chromium(III)

Only a constant variation plot is given. This was obtained by leaving solutions to react at pH8.9 overnight and measuring.

The formation of a 2:1 CV:Cr complex is indicated.

Manganese(II)

The pH dependence plot(Fig.2.6) shows that the optimum pH of formation is not achieved within the accessible range but is greater than 10.5. The extinction coefficient is 19000 at 670nm under these conditions.

The constant variation plot(Fig.2.16) was found to give non-reproducible results, and to be of little value. The only tentative result is the indication of the formation of a 2:1 CV:Mn complex.

Iron(II)

The pH dependence plot(Fig.2.7) shows that the optimum pH is about 7, but greater pH values do not decompose the complex.

As previously mentioned, the spectrum is unique, and extends the absorption peak to about 720nm with an extinction coefficient of 63000.

The constant variation plot(Fig.2.17) clearly shows the formation of a 2:1 CV:Fe complex and also a 1:1 complex.

Cobalt(II)

The pH dependence plot(Fig.2.8) indicates an optimum pH value of 9.2. The extinction coefficient is 25000.

The constant variation plot(Fig.2.18) only indicates the formation of a 2:1 CV:Co complex clearly. The non-linearity shown on the right of the plot suggests the formation of other complexes but no inference about the complex ratio may be drawn.

Nickel(II)

The pH dependence plot(Fig.2.9) indicates an optimum pH of 9.0 and an extinction coefficient of 22000.

The constant variation plot(Fig.2.19) is more complex than that of Co, but it also indicates the formation of a 2:1 CV:Ni complex. There are also indications of at least one other complex, but the complex ratio is difficult to assign. It is probably the 1:1.5 CV:Ni complex.

Copper(II)

The pH dependence plot(Fig.2.10) indicates an optimum pH of 8.0. The extinction coefficient is 50000.

The constant variation plot(Fig.2.20) clearly shows the formation of a 2:1 CV:Cu complex, and also a 1:1 complex.

Zinc(II)

The pH dependence plot(Fig.2.11) indicates an optimum pH of 8.5, and an extinction coefficient of 38000.

The constant variation plot indicates the formation of a 2:1 CV:Zn complex and at least one other, but without any clear indication of any other complex ratio.

Experimental Note

The absence of the oxidation states V(V) and Fe(III) is due to the necessity of protecting the CV against oxidation. These species both attack CV leading to turbid solutions.

Conclusions.

The results obtained are highly equivocal about certain points. The use of constant variation plots is in particular suspect and probably susceptible to error. These complexes are known not to be in true solution, so that any investigation which relies upon the measurement of the physical properties of solutions is likely to be somewhat misleading.

As to explaining the variation in properties of the complexes of cationic species within this group, no general conclusion can be drawn. The author cannot explain why for example zinc should give a more highly absorbing complex than nickel.

There does not appear to be any correlation between the measured extinction coefficients and any other published data of the elements. Possibly the difference lies in the relative stability constants of the various complexes, but conditions were chosen such that effectively 100% formation of the complexes should have occurred. The differences between the complexes does not depend upon the formal oxidation state, or Cu and Zn would not be expected to have such high extinction coefficients. The anomalous behaviour of Fe may be attributable, in

part to the possibility of charge transfer occurring. Here again however, this complex is not exceptional in respect of its extinction coefficient when compared with aluminium.

In this regard scandium can be regarded as being outside this group, as it has no d-electrons.

It is possible to regard copper and zinc as also being anomalous as Cu(I) and Zn(II) both have a d^{10} configuration. This sort of reasoning may be applied to Fe(III) which, if present in the high spin configuration, has all five d-electron orbitals occupied by one electron. However Mn(II) can also exist in the high spin state and so this line of reasoning is probably fruitless.

The problem of these complexes still remains unsolved.

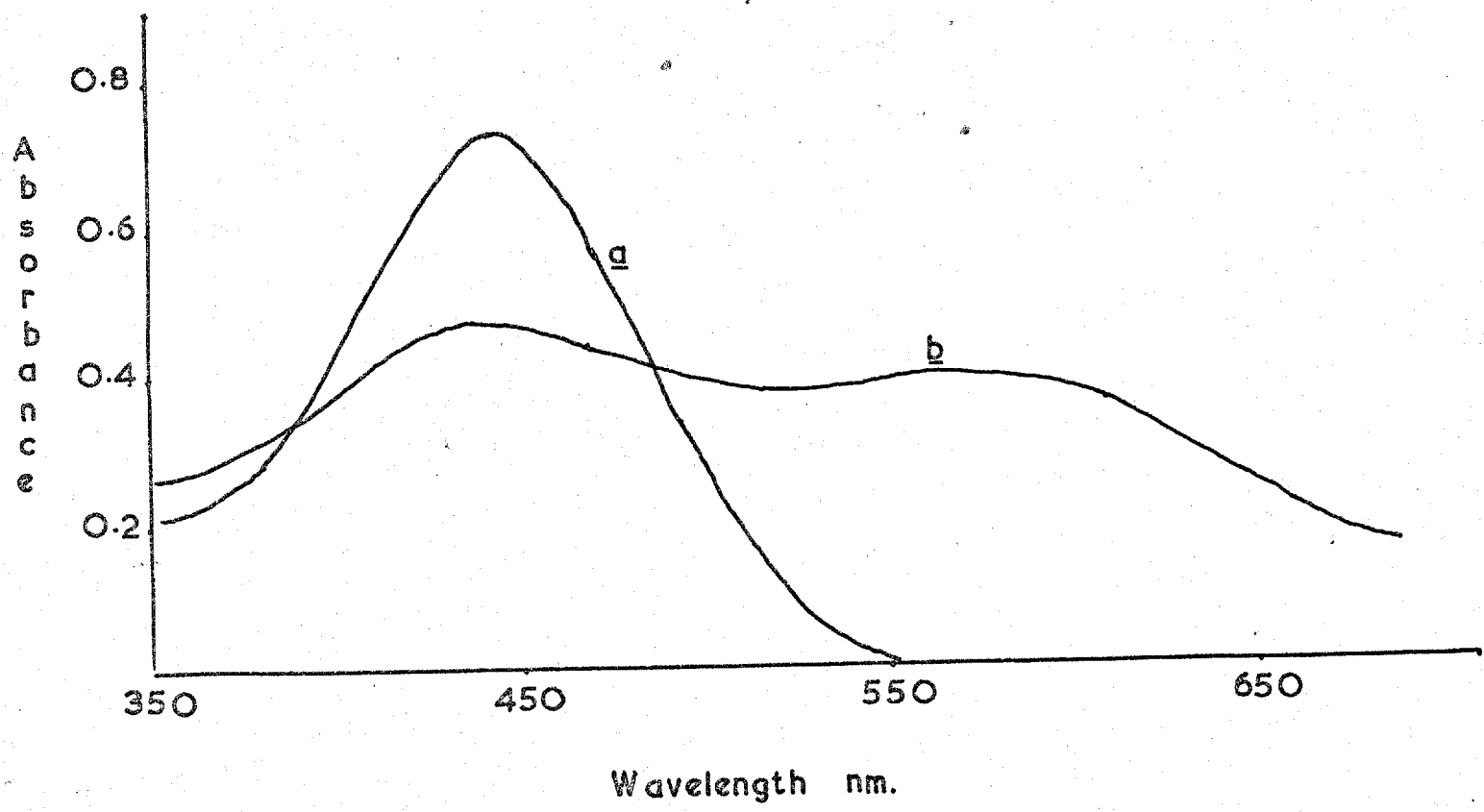
As far as the ternary complexes of Ti and V are concerned their difference from the other complexes is explicable on the basis of their being formed from oxy-anions. (TiO(II) & VO(II)).

Suggestions for Future Work.

In view of the behaviour of these complexes and their practical value in analytical chemistry, it is suggested that a more searching investigation is undertaken into their structure, using physico chemical techniques such as electron-spin-resonance and nuclear-magnetic-resonance spectroscopy.

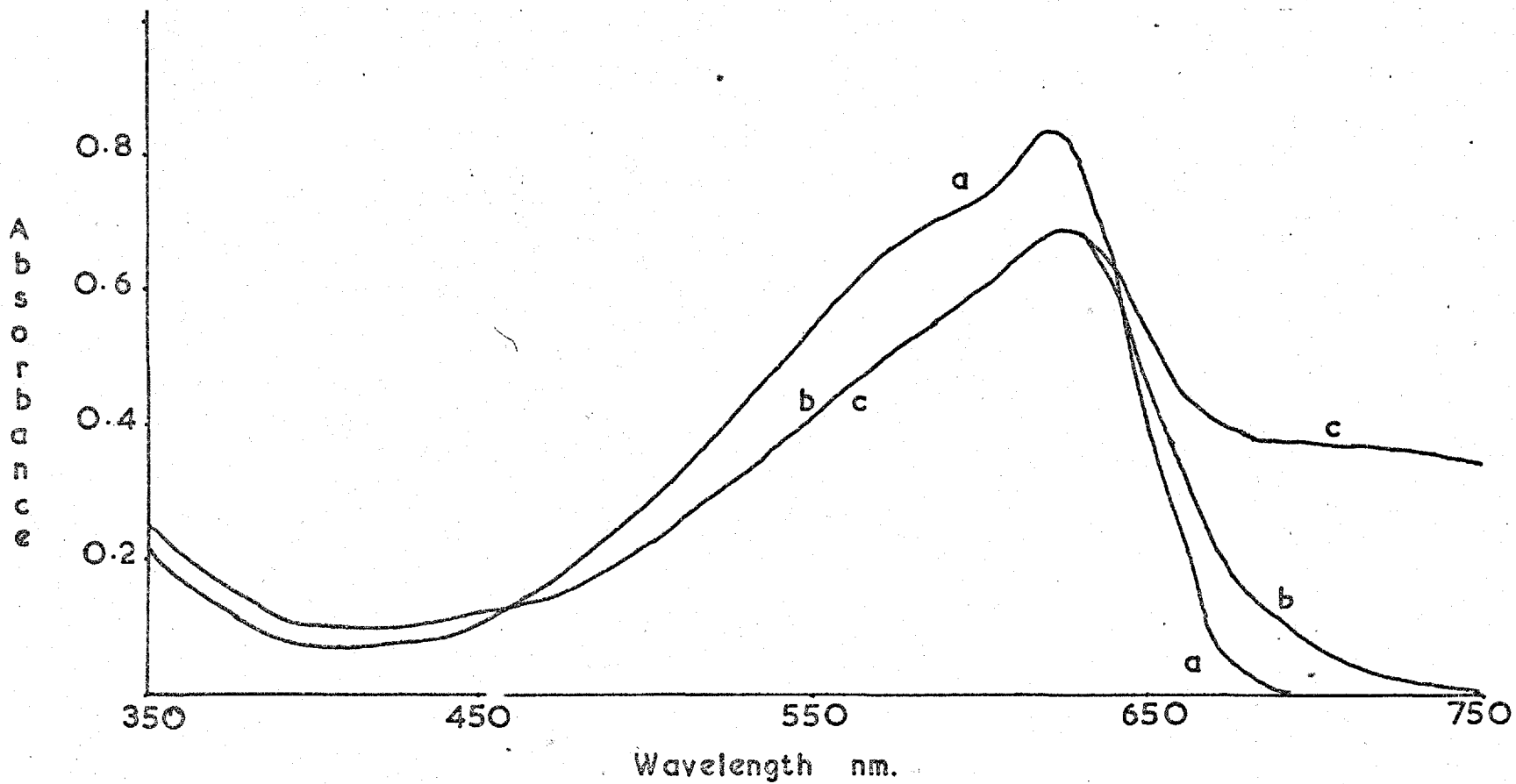
In the field of practical analytical chemistry, it is suggested that a more intensive investigation be undertaken into developing a technique for the determination of iron, using this reagent system.

FIG.2.1



a CV / CTAB
b Ti / CV / CTAB

FIG. 2.2



- a CV / CTAB
- b Co / CV / CTAB
- c Fe / CV / CTAB

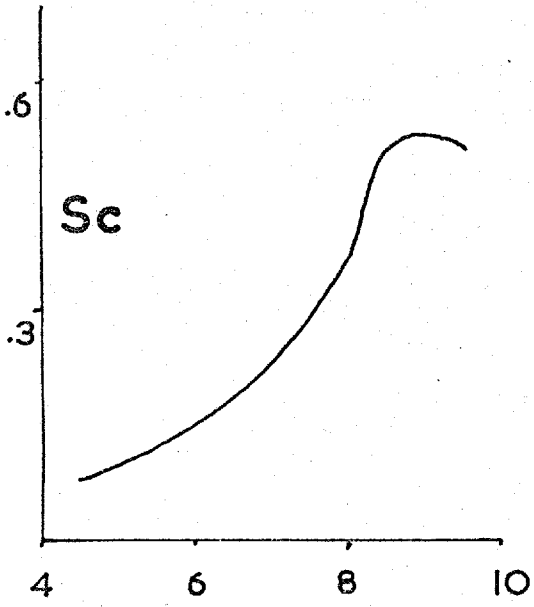


Fig.2.3

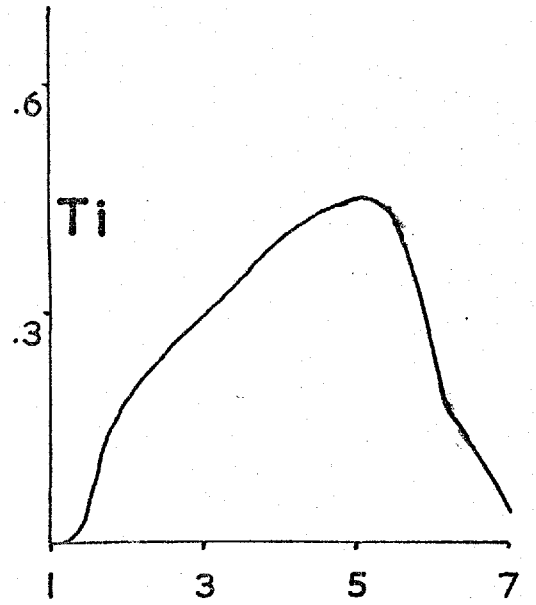


Fig.2.4

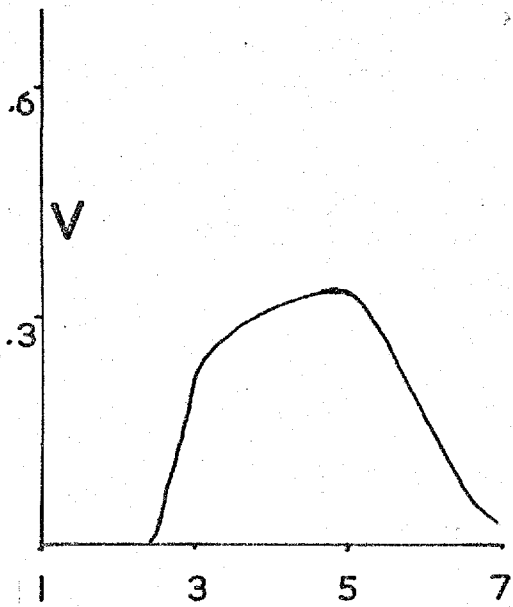


Fig.2.5

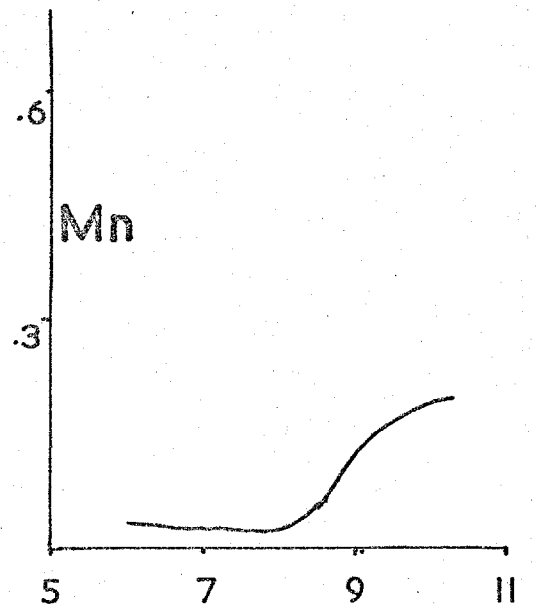


Fig.2.6

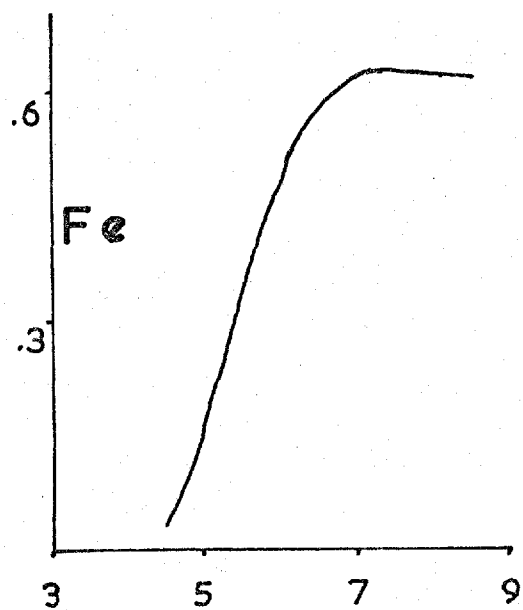


Fig.2.7

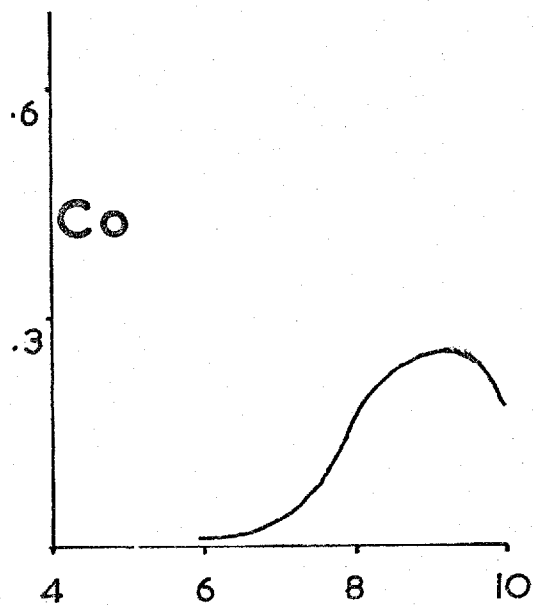


Fig.2.8

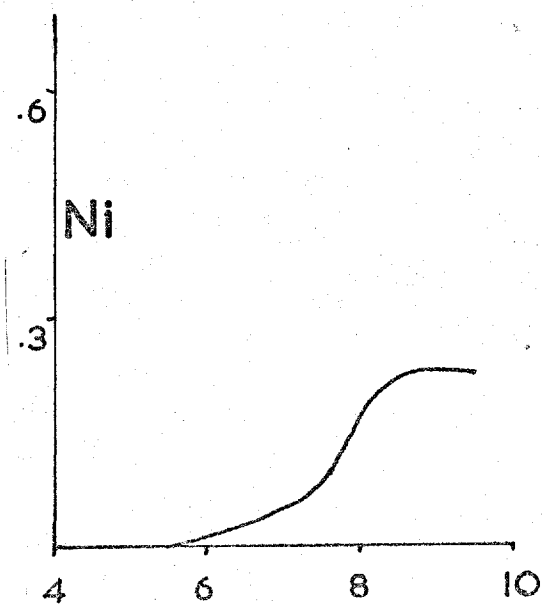


Fig.2.9

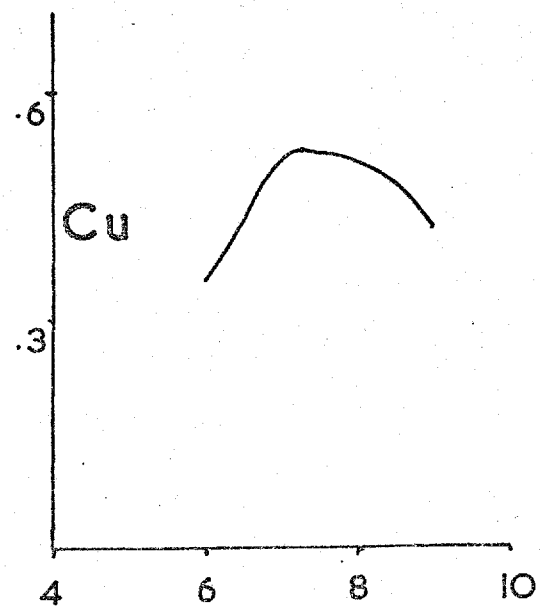


Fig.2.10

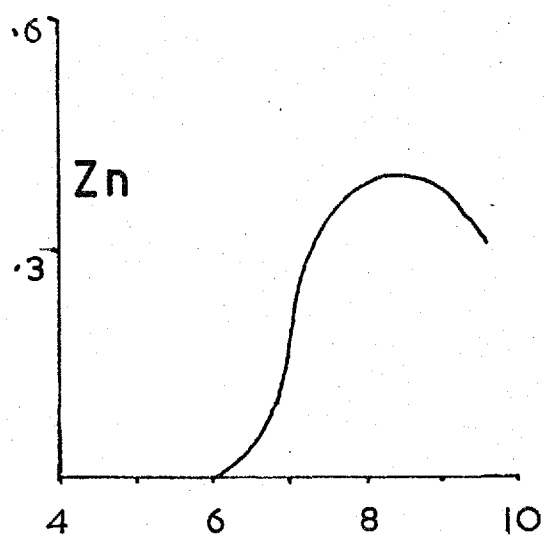


Fig.2.11

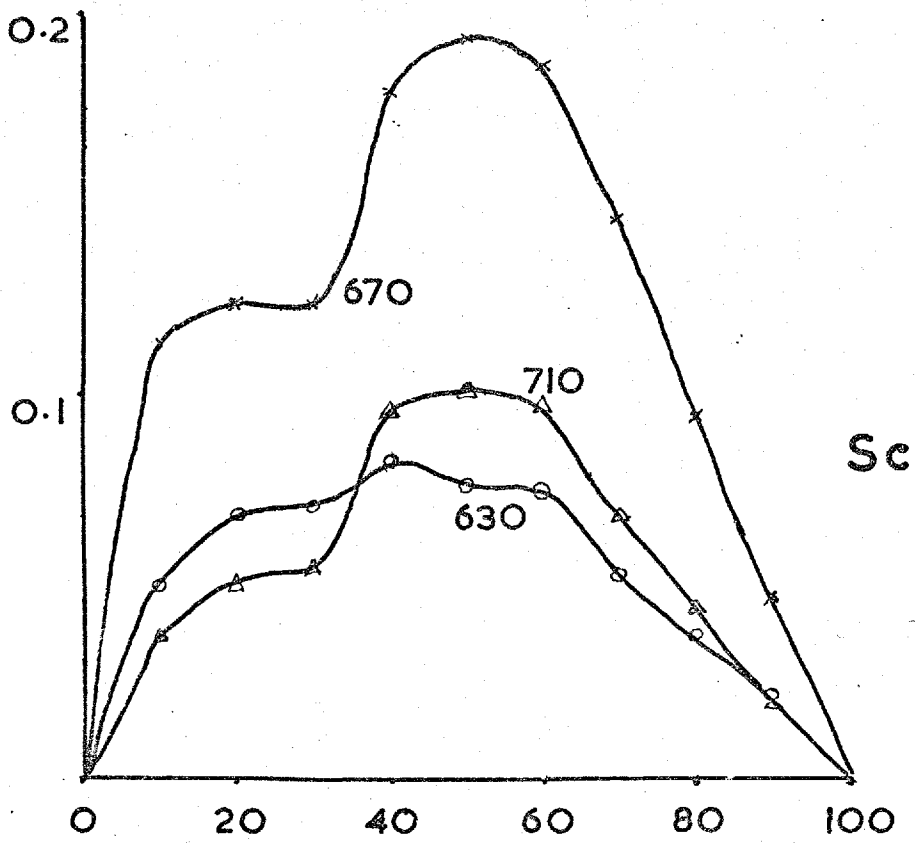


Fig.2.12

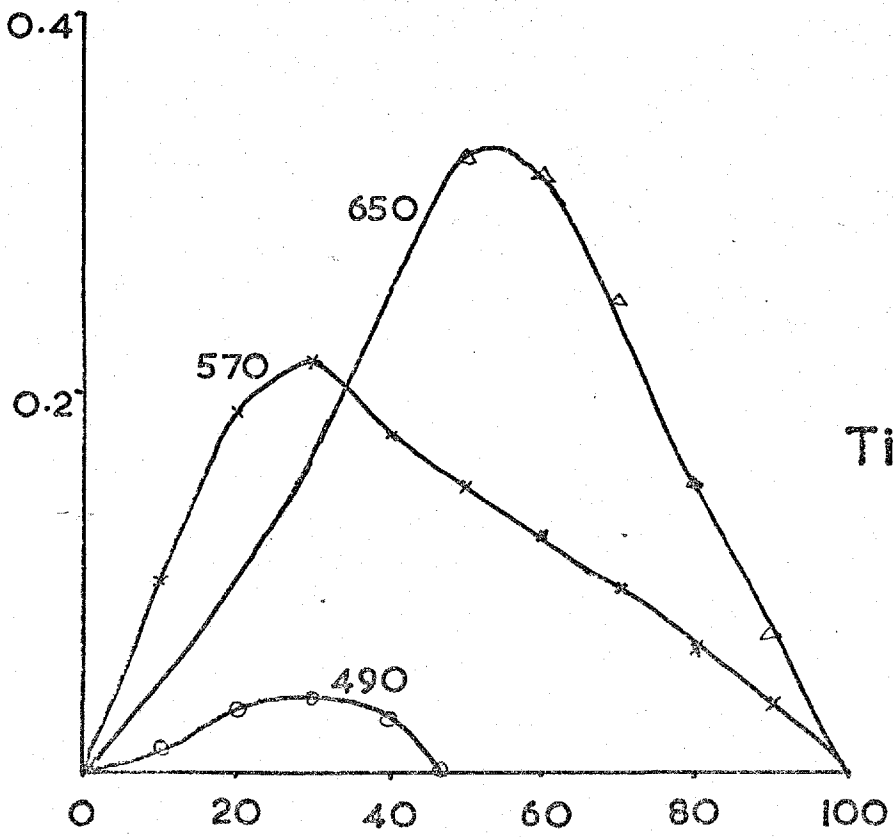


Fig.2.13

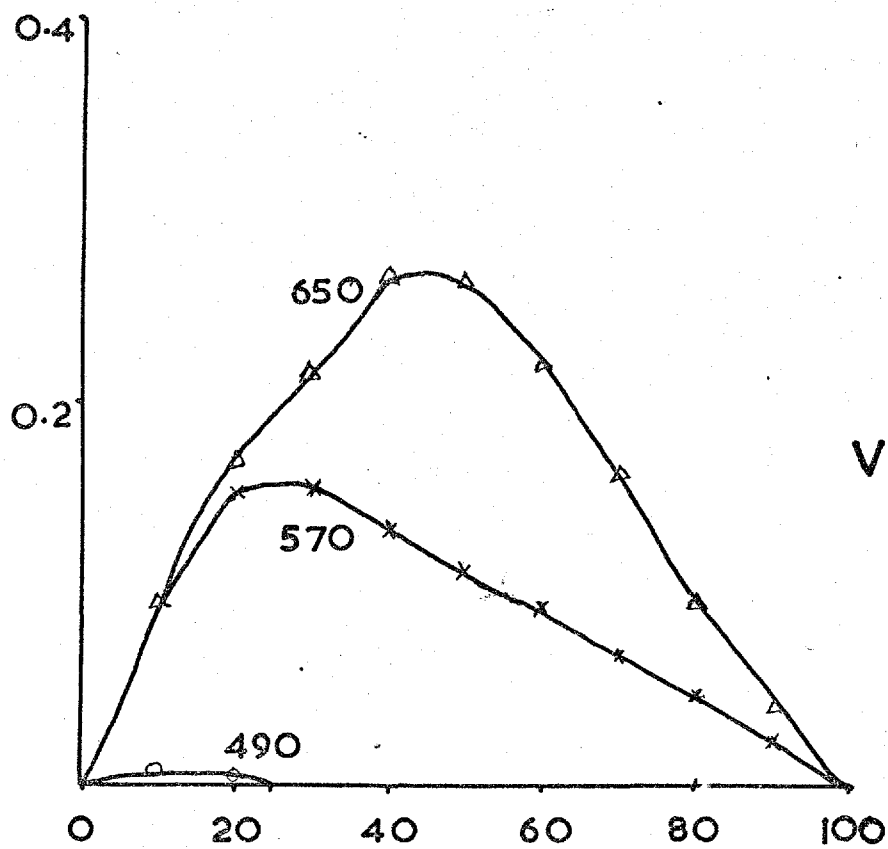


Fig. 2.14

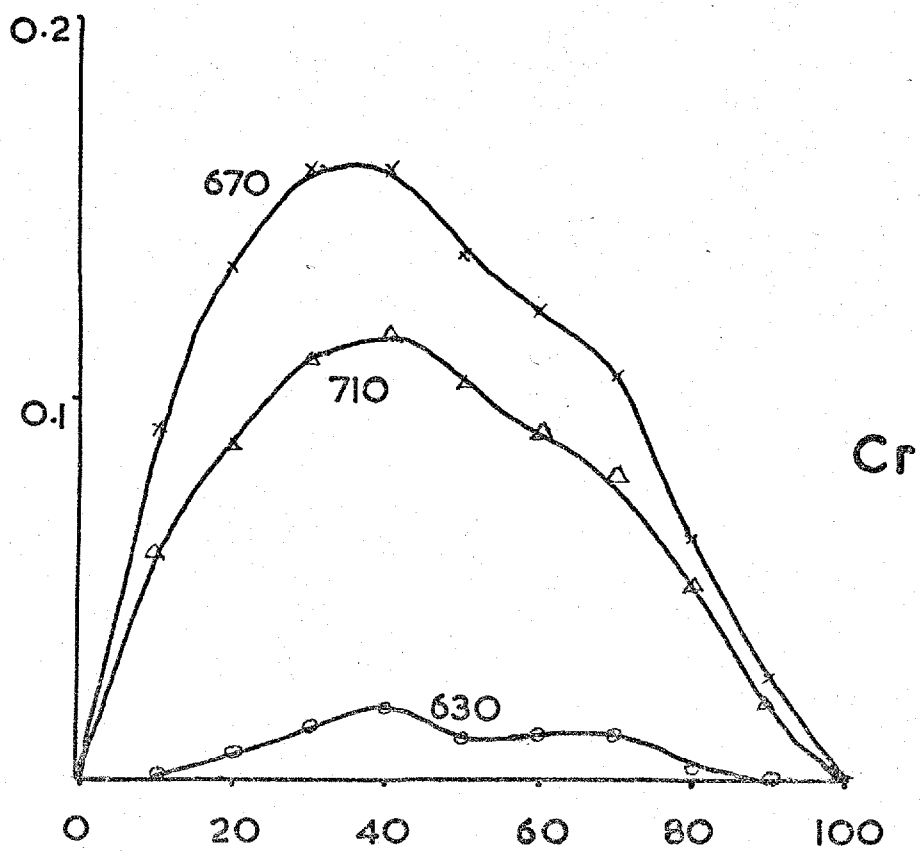


Fig. 2.15

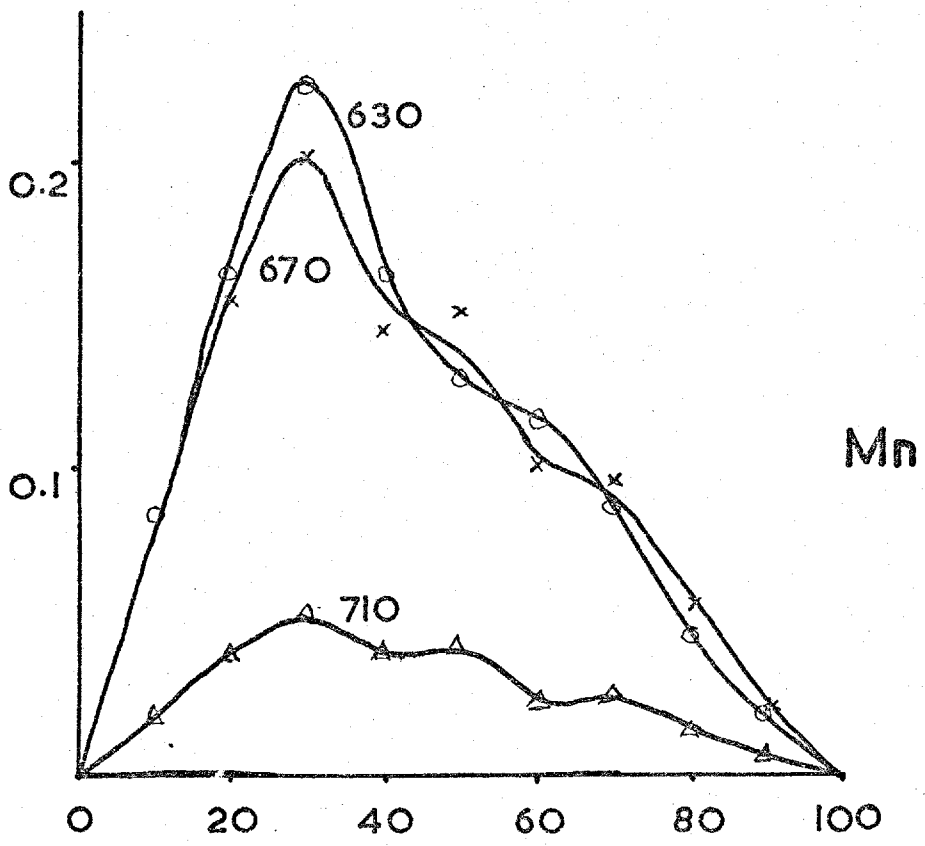


Fig.2.16

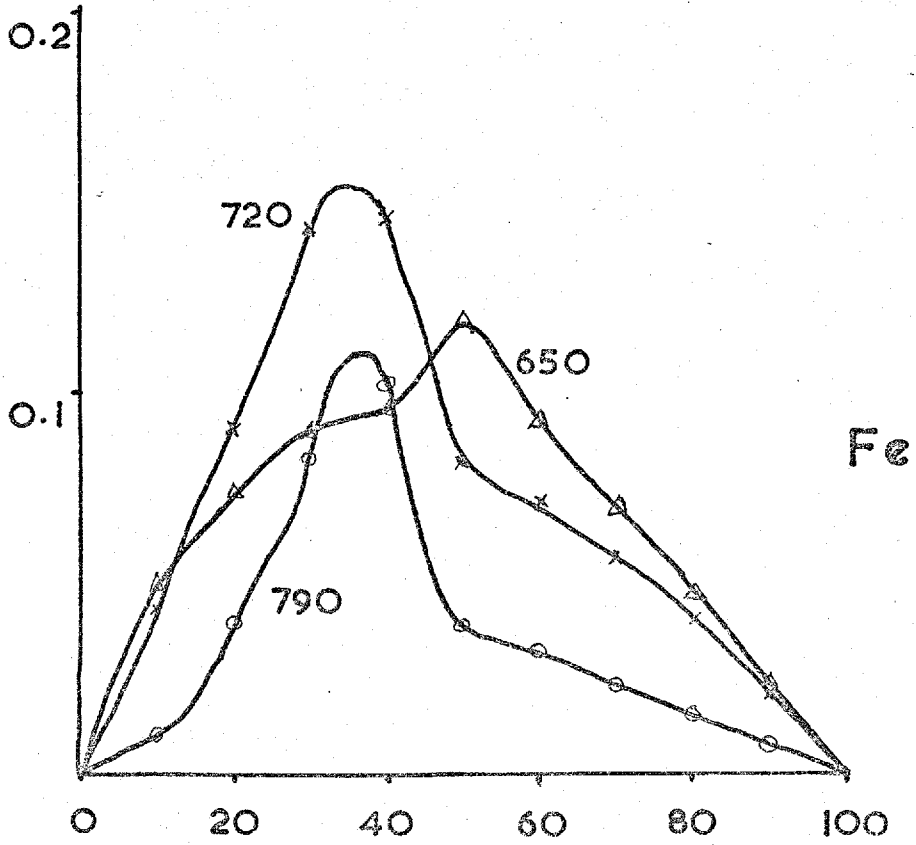


Fig.2.17

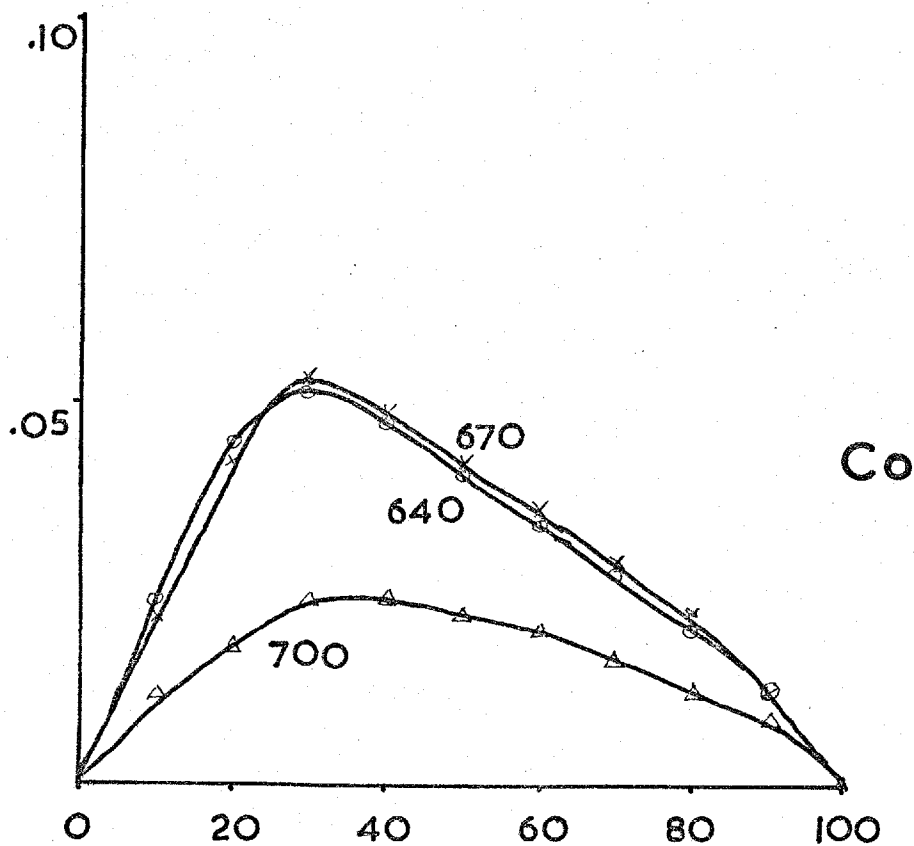


Fig.2.18

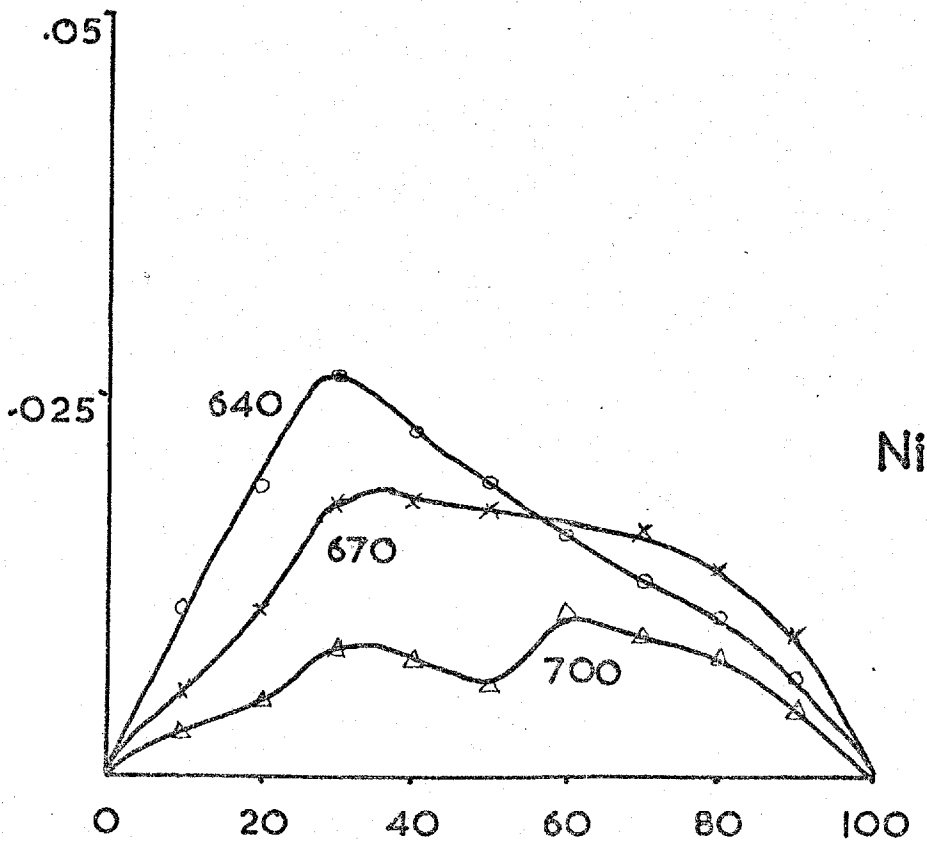


Fig.2.19

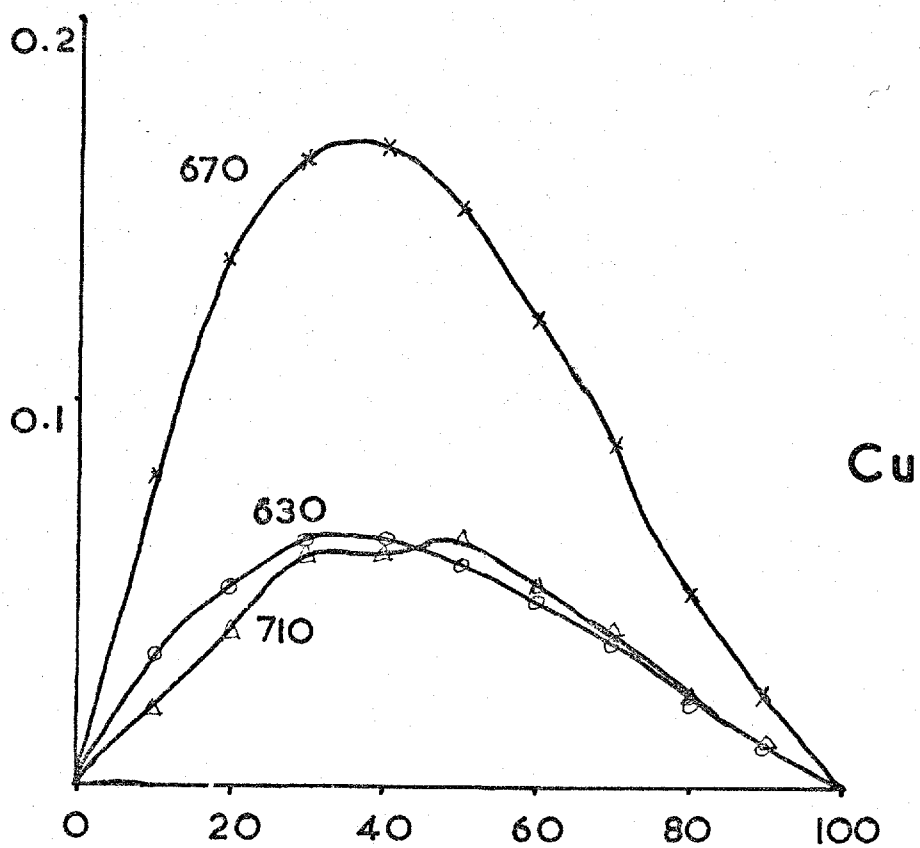


Fig.2.20

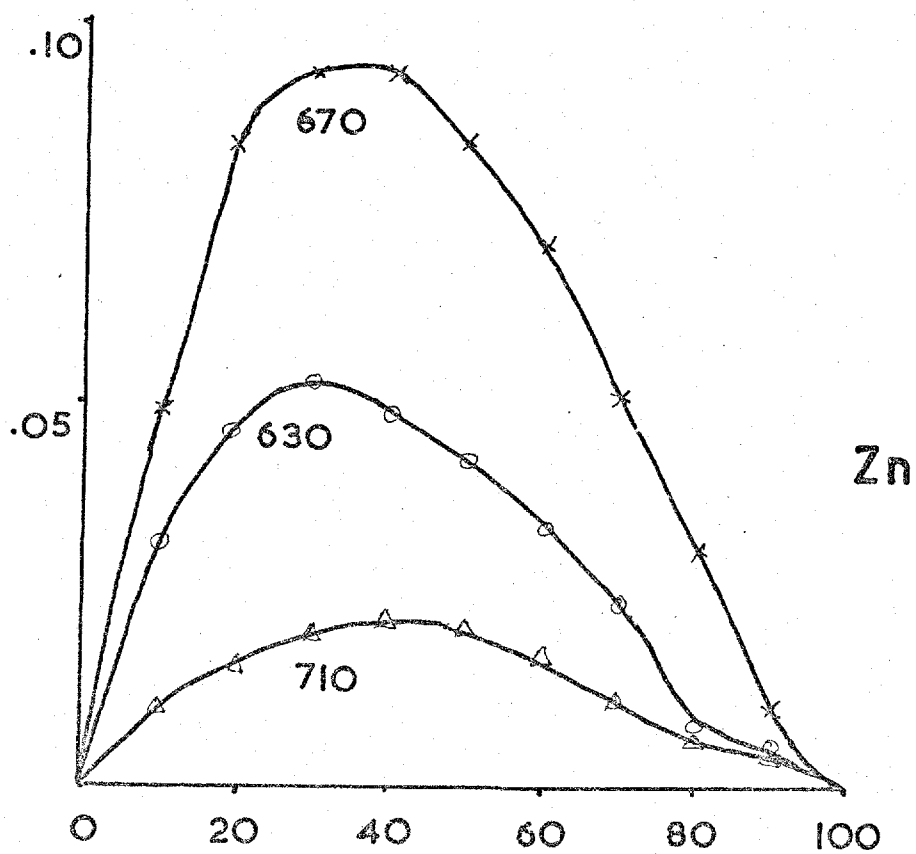


Fig.2.21

Bibliography

1. R.M.Dagnall, T.S.West, P.Young
Analyst 92 27 (1967)
2. B.W.Bailey, J.E.Chester, R.M.Dagnall, T.S.West
Talanta 15 1359 (1968)
3. M.Malat
Z. Anal. Chem. 201 262 (1964)
4. A.K.Majumdar, C.P.Savariar
Naturwissenschaften 45 84 (1958)
5. S.P.Mashran, O.Prakash, J.N.Amasthi
Analytical Chemistry 39 1307 (1967)
6. M.Svach
Z. Anal. Chem. 149 416 (1956)

CHAPTER 3

A FLAME SPECTROPHOTOMETRIC TECHNIQUE FOR THE DETERMINATION
OF BORON.

Introduction Of all the alloying elements employed in steel and ferrous alloys, boron is the one which exerts the most profound effect at low levels.

A boron content of 0.001% in carbon steel exerts an effect upon the working properties and hardenability, of similar magnitude to that imparted by the addition of 0.03% molybdenum.

At this concentration level, the presence of boron exerts a delaying effect upon certain phase transformations in steel, thus improving the hardenability and permitting the use of a thicker ruling section.

More than 0.0025% of boron exerts a deleterious effect, and at concentrations of 0.006 to 0.01%, the steel may become so hot-short as to fragment under its own weight. This is because of the formation of low melting-point components at the grain boundaries. For this reason, it is usual to employ concentrations less than 0.004% to avoid this possibility.

Complications occur because of the extreme ease of oxidation of boron. If hot boron-containing steel is left in contact with an oxygen-containing atmosphere, the boron will oxidise in the surface layers, thus resulting in serious inhomogeneity. This ease of oxidation necessitates the use of fully-killed steels if boron is to be used as an improver. Killing agents such as silicon or aluminium are normally used for these steels.

A further complication is the existence of so-called acid-soluble and acid-insoluble forms of boron present in steel. Acid-soluble boron is soluble in dilute mineral acids, whilst the acid-insoluble form requires the use of vigorous oxidation to render it soluble. The acid-insoluble fraction

is generally thought to be present mainly as the carbide or nitride. The inclusion of zirconium or titanium reinforces the effect of boron as both of these elements form stable immensely hard carbides and nitrides. The effect is used in nitriding and carbo-nitriding steels.

The heat-treatment of a boron containing steel also affects the form in which the boron is present. Prolonged heating at high temperature (austenitisation) may give a supersaturated solution of boron in the steel nullifying the normal effect. Restoration of the original properties may be achieved by normalisation at a later stage.

Other metallurgical applications of boron include the complex alloys used for introducing boron into steel. Typically these contain about $\frac{1}{2}\%$ of boron together with much larger concentrations of other alloying elements such as vanadium and manganese.

Boron is also used as an alloying element in its own right in such alloys as 18:8 austenitic stainless steels. In these boron may be present at the level of some $\frac{1}{2}\%$. Its purpose in these alloys is as a hardening agent. After austenitisation of the alloy at 1100C and quenching which leaves the boron in supersaturated solution, it is heated to 600-700C causing hardening by precipitation at the grain boundaries.

With regard to these important applications and the extremely limited range over which it exerts a beneficial effect in carbon steels, it is immediately apparent that the accurate analysis of trace quantities of boron is of great importance.

It might be expected that a relatively small number of

standard techniques of boron assay would have been developed. Instead, there are a large number of methods in the literature and little general agreement.

For the determination of relatively large quantities of boron in metallic matrices (0.1 to 0.5%), titrimetric methods have generally been employed. These rely upon the formation of boric acid on dissolution of the alloy. The exact finish thereafter is dependent on the matrix and the method of dissolution, although it is general practice to add vicinal diols such as glycerol or mannitol to increase the strength of the boric acid.

In a typical direct technique, YAKOVLEV and KORINA¹ employed dissolution of the sample in dilute hydrochloric acid and oxidation with hydrogen peroxide. Any insoluble residue was fused with sodium carbonate and returned to the main sample. Metals were precipitated as their hydroxides. Aliquots of the resultant solution were treated with citric and hydrochloric acids, and finally titrated potentiometrically with caustic soda in the presence of invert sugar.

Other workers^{2,3,4} have used the same technique of separating iron and other metals with insoluble hydroxides, but there is a considerable risk of losing boron by co-precipitation². This has been reduced by the precipitation of a mixed ferrous-ferrous hydroxide³, or initial sample preparation by fusion with sodium peroxide.⁵

Methods developed by other workers for the titrimetric analysis of relatively large amounts of boron use separations based on ion-exchange^{6,7,8,9,10}. A necessary precaution for these procedures is the elimination of or correction for the presence of boron in the ion-exchange resin¹¹. In

addition, if metals such as chromium or vanadium are also present, they must be in cationic form, and only small concentrations of acid are permissible.

However, the classical separation method for boron is the use of distillation to remove easily-volatile alkyl esters of boron from the reaction mixture. This technique has long been known and is considered standard for the separation of boron ^{12,13}. The only element reported to be distilled along with boron is germanium ¹⁴. However, the presence of fluoride in the reaction mixture may cause interference by reducing the yield ¹⁵.

The distillate from this separation is normally absorbed and hydrolysed in alkali which is then evaporated for concentration of the boron and removal of the alcohol. The finish employed may be titrimetric ^{14,16,17} or any of the colorimetric techniques.

Another separation technique suitable for use with a titrimetric finish is the so-called pyrohydrolysis method ¹⁸ ¹⁹, in which the boron-containing alloy is heated in steam at a temperature of 1100°C. Boron distils as boric acid.

The gravimetric determination of relatively large quantities of boron has been reported ¹³.

The technique used by the majority of workers for the determination of trace quantities of boron is solution absorption spectrophotometry. To this end a large number of methods and reagents have been developed. The best of these methods are those based on curcumin, but the whole range may be studied with advantage.

The slowness of development of these methods is well shown by two sentences from W.T. BRANDE's 'Manual of Chemistry'

published in 1819 ²⁰. "It (boron) is very difficultly soluble in water; the solution reddens vegetable blues. Its solution in spirits of wine burns with a green colour."

These properties still form the basis of the best analytical methods for boron notwithstanding the passage of 150 years.

Most spectrophotometric methods for boron employ either curcumin, carminic acid, quinalizarin and other substituted anthraquinones, or 1:1 dianthrimide or its derivatives.

Another important type of system used is that using the reaction of tetrafluoborate anion with a cationic dyestuff, normally a derivative of thionine, oxazine, or a triphenylmethane derivative.

quinalizarin gives a bluish colour in concentrated sulphuric acid. This colour is very dependent on the acid concentration turning red at lower concentrations. Boron causes this red colour to become blue.

A variety of techniques have been described using visual ²¹ and photoelectric photometry ²², and a number of separation techniques to reduce the effect of interfering elements ^{23,24,25,26}. Other anthraquinones have been investigated, and one, tetrabromochrysozin (tetrabromo-1:8 dihydroxyanthraquinone) has been found to be appreciably more sensitive ²⁷.

These techniques suffer from the inherent disadvantages of the unpleasant nature of the reaction medium, and the sensitivity of the reaction to changes in the acid concentration. Oxidising agents, various metal ions and fluoride also interfere.

The second major spectrophotometric reagent is

1:1 dianthrimide. This was first prepared by ECKERT and STEINER²⁸ who first observed its reaction with boric acid in concentrated sulphuric acid. In recent years it has been applied to the determination of boron by a number of researchers^{29,30,31,32,33}.

Although it is possible to determine boron directly in aluminium alloys, separation of interferences by ion exchange is necessary for steels.

As for quinalizarin, these procedures must be carried out in concentrated sulphuric acid, and the colour developed by prolonged heating. All the same inherent disadvantages are also shared by this reagent.

Carminic acid, a natural dyestuff, has been used by several workers for boron analysis^{34,35,36}. Again concentrated sulphuric acid must be used as the reaction medium and the colour developed by heating. Nitrite, nitrate fluoride, and titanium interfere, and the use of a methyl borate distillation has been advocated³⁴. The reagent has recently been used for an Auto Analyzer method for boron³⁷.

The mainstay of spectrophotometric methods for boron is curcumin which is the coloring matter of turmeric. Its reaction with boron may give two compounds, rubrocurcumin (1:1 complex) or rosocyanin (1:2 complex), and evidence has been adduced for the formation of a 1:3 complex³⁸. Complex formation is thus dependent upon the exact conditions of reaction. The use of oxalic acid to promote the reaction as has been suggested by certain workers^{39,40}, has been implicated as favoring the formation of the rubrocurcumin complex rather than the more sensitive rosocyanin³⁴. Other workers have used other techniques to stabilise the complex formed

such as trichloroacetic acid ⁴¹, reaction in glacial acetic acid and sulphuric acid ³⁸, reaction in phenol and glacial acetic acid ⁴², formation in ethanol under reflux ⁴³, or the use of acetic anhydride ⁴⁴.

In these procedures, formation of the complex is usually preceded by a preliminary methyl borate distillation and absorption in alkali. Direct determination is possible after precipitation of the matrix elements with caustic soda ²⁴.

After the formation of the colour it is necessary in all these methods to remove the purple-colored ionused unreacted curcumin, either by solvent extraction of the complex or curcumin, or by adding ethanol.

Comparison of these methods gives the following results

<u>Reagent</u>	<u>Molar Extinction Coeff't</u>
Quinalizarin	2,700 - 7,000
Carminic Acid	2,100 - 6,500
1:1 Dianthrimide	12,000 - 18,000
Curcumin(oxalate)	37,000
Curcumin(ref.38)	151,000

Other solution spectrophotometric reagents reported in the literature include Catechol Violet ⁴⁵, and Pyrocatechol-phthalein ⁴⁶. (As stated in Section 1 of this thesis, there may be some confusion on nomenclature at this point as this latter paper is indexed in Chemical Abstracts under the entry of; bis(3,4-dihydroxyphenyl) o-toluenesulphonic acid β -sulfone).

The use of cationic dyestuffs has previously been mentioned. PASZTOR and BODE ⁴⁷ have made a study of substituted thionine dyestuffs. HOBSON ³³ states that the method is

subject to disadvantages insofar as non-linear calibration curves were produced, and the separation appeared to be temperature dependent and also sensitive to the polythene bottles used.

Similar comments seem to be applicable to the use of other ion-association systems.

Apart from these methods which form the bulk of analytical methods for boron, a number of other techniques have been reported in the literature.

Spectrography using spark or arc sources has been employed by several workers ^{49,50,51,52}, and the exceedingly low detection limit of 0.00004% has been reported ⁴⁹. These methods suffer from the usual disadvantages of precision and standardisation.

The use of X-Ray fluorescence both direct ⁵³, and indirect ⁵⁴ has been reported. The latter employed the determination of the barium in barium borotartrate.

Spectrofluorimetry using Benzoin ^{55,56} and Quercetin ⁴⁵ has been reported.

Flame spectrophotometric techniques are scarce in the literature. The basic reason for this is the extreme ease of oxidation of boron, and the very high thermal stability of the various oxides of boron. Because of this, conventional flames atomise boron to a negligibly small degree, and the atomic spectroscopy of boron either by emission or absorption techniques is difficult. Even in the best such conventional flame (nitrous oxide acetylene) AMOS and WILLIS ⁵⁷ reported a detection limit of 50ppm.

When the low atomic weight of boron is taken into consideration, this detection limit is some two or three orders

of magnitude worse than that of many other so-called refractory oxide elements, measured in terms of corresponding sample solution molarities.

This problem is not however shared by sources that do not contain any oxygen. Some atomic-spectrophotometric determinations have been made using plasma sources^{58,59,60}. Sensitivities of the order of 1ppm are achievable by these techniques.

Undoubtedly the best technique using conventional flames is that of using the molecular band emissions from the boron species which predominate in these flames. The most useful of these emissions is that of BO_2 which gives a boron-containing flame its characteristic green colour first noticed by BRANDE.²⁰

Few references to this technique exist in the literature exceptions being DEAN⁶¹ who used a flame photometer to determine boron in plating baths, and HERRMANN and ALKEMADE⁶² who achieved a detection limit of 0.11ppm of boron using an oxyhydrogen flame.

The following study was undertaken to devise a rapid method for the determination of boron, particularly in steel, using conventional flame photometry equipment.

Apparatus

The apparatus used in this study consisted of a Hilger Atomspek atomic absorption spectrophotometer. This was modified for operation in the emission mode by the addition of a 400Hz. chopper (H1346) and a backing-off control. This latter addition consisted of a 1000 ohm high precision variable resistor wired as a potential divider across a 9 volt battery. In operation the output from the potential divider

was connected in series with the output signal from the instrument and in opposition to it.

In addition to the spectrophotometer, a Beckmann 5inch strip chart recorder was used to record spectra.

A variety of burners was available, but the one used for the majority of this study was modified from an air-propane burner for the Unicam SP900 flame spectrophotometer. A diagram of this burner and the modifications is given as Fig.3.1.

The nebuliser from the instrument was also modified to suit the requirements of the study. The standard nebuliser body was used but the nebuliser head was removed and that from a Hilger Uvispek flame emission attachment substituted. This was further modified by the substitution of a stainless steel capillary as the sample uptake tube.

The instrumental arrangement adopted for the study was governed by several constraints imposed by the geometry of the instrument. As it is not intended for emission work, the instrument has the monochromator entrance slit set behind a lens housing. The chopper which is necessary for the tuned amplifier installed in the instrument is arranged horizontally between the monochromator slit and a focussing lens. It was thus found impossible to position the flame within 12.5cm. from the monochromator entrance slit, so the arrangement shown in Fig.3.2 was adopted. The flame was imaged on the monochromator slit using the lenses from the instrument and a concave mirror was placed behind the flame to image it in itself improving the brightness. These arrangements necessitated removing all other equipment from the burner section of the instrument.

Modified Unicam SP 900 Burner

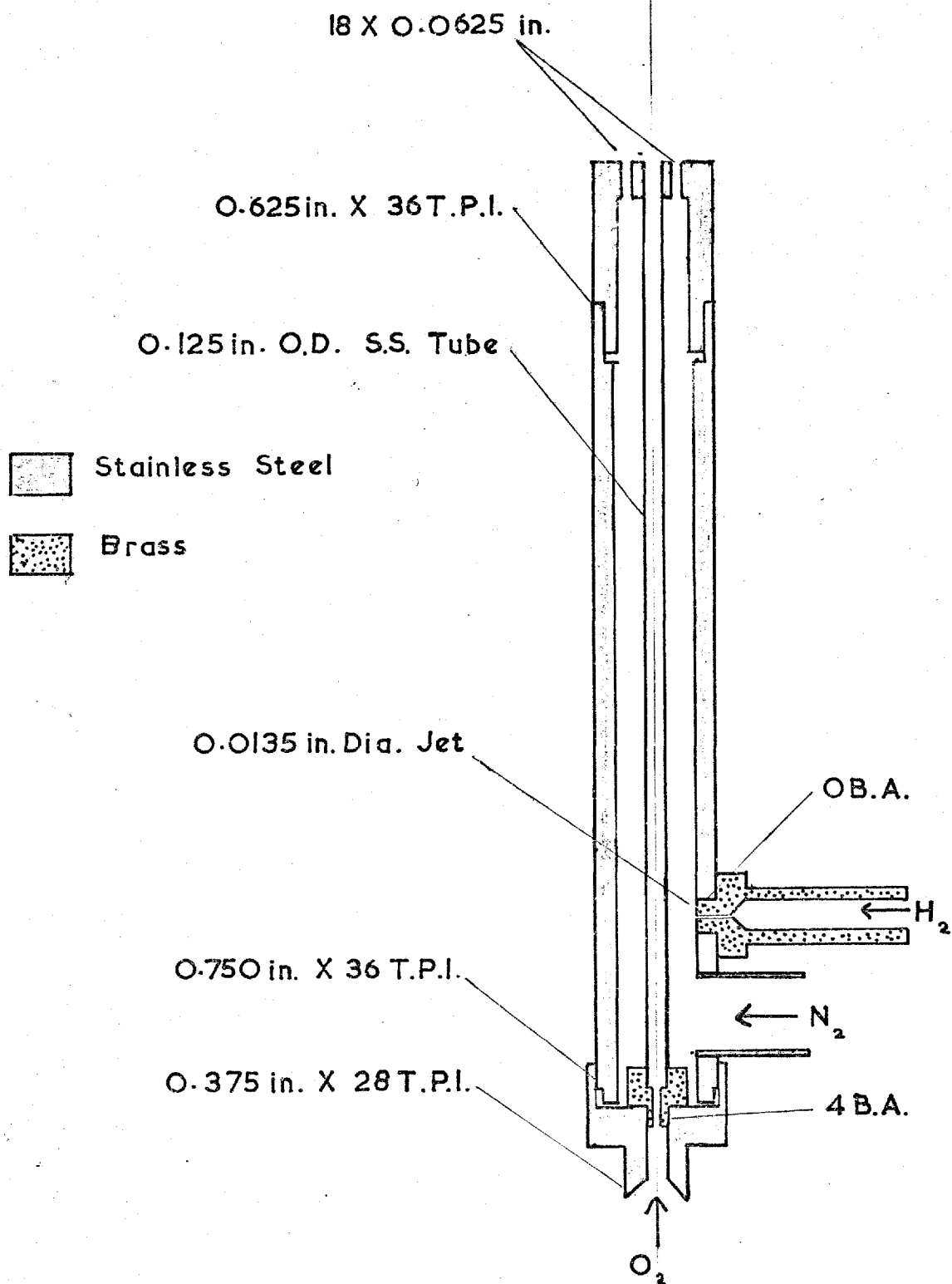
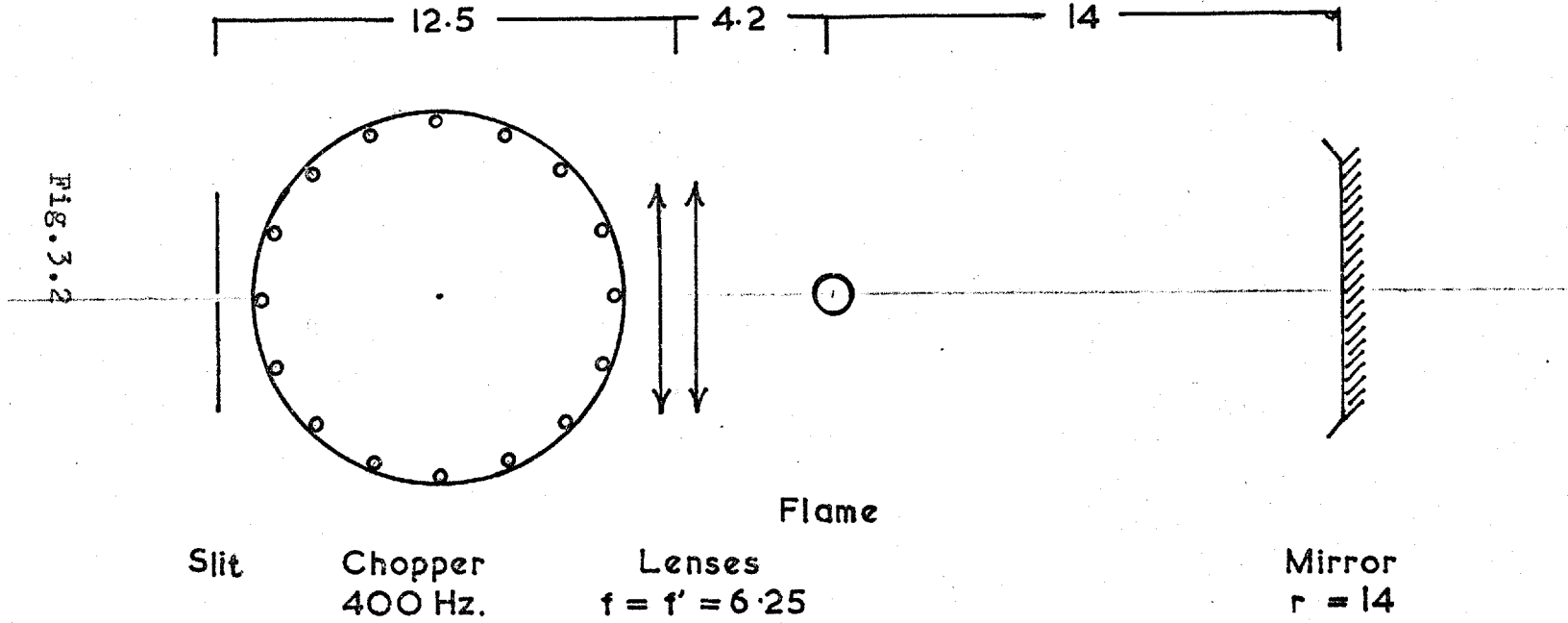


Fig. 3.1

OPTICAL ARRANGEMENT



All dimensions given in cms.

During the latter stages of this study, a distillation apparatus was constructed from silica, to permit comparison of the performance of boron-free and borosilicate glassware. A diagram of this apparatus is given as Fig.3.3. In addition to the apparatus shown a 50ml. round-bottom flask with a B14 cone joint was used; this was also silica. The components for this apparatus including the flask were obtained from Jencons Ltd. of Hemel Hempstead, Herts. at a total price of approximately £11.00, exclusive of the cost of fabrication.

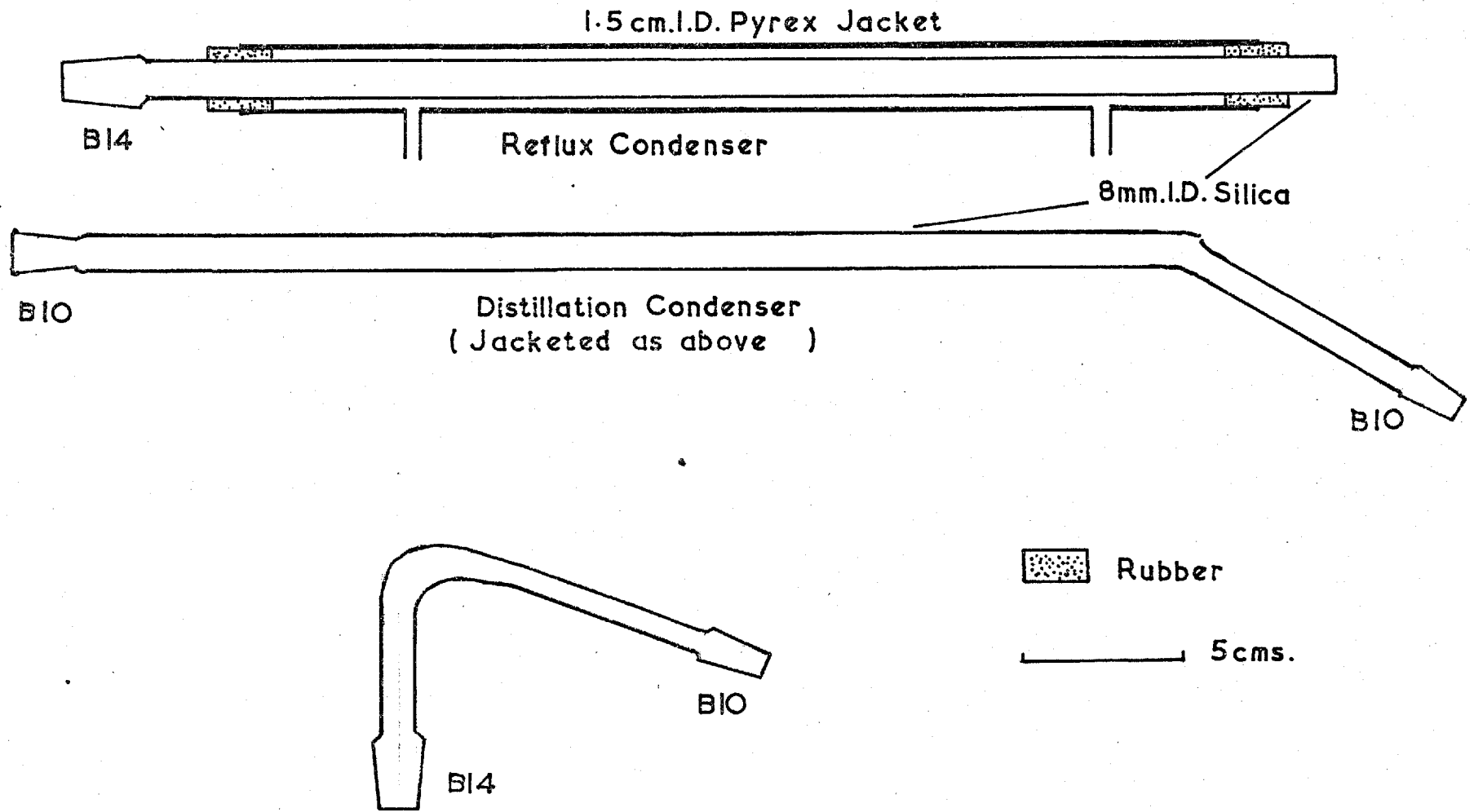
Results.

Preliminary Investigations:

Initially it was desired to investigate the possibility of using the low-background nitrogen-hydrogen flame. It was immediately apparent that this flame was unsuitable, and the injection of oxygen gave greatly increased emission. As it was also desired to use conventional flame photometry equipment as far as possible, using quiet laminar flames and indirect nebulisers, the use of Beckmann-type burners was regarded as undesirable. A series of burners was designed and constructed with the feature of injecting a laminar stream of oxygen above the top-plate, and co-axial with the flame. The remainder of the flame gas circuit consisted of an indirect pneumatic nebuliser driven by nitrogen, and a system for introducing hydrogen into the base of the burner.

The appearance of this type of burner in operation is quite characteristic. The flame consists of three major regions; an outer faintly-luminous hydrogen-air diffusion flame, an inner non-luminous cone of oxygen, and a highly-luminous reaction zone between these two. Virtually the

Fig. 3.3



whole of the green emission from the boron species in the flame is produced by the top of this interconal reaction zone.

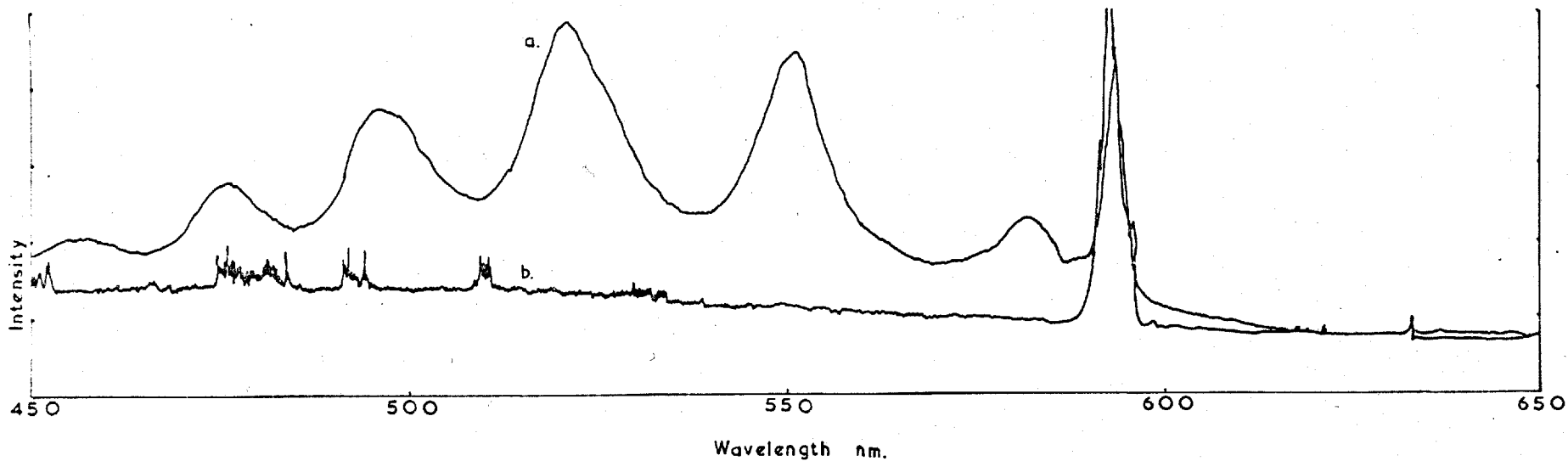
Spectra of this zone with and without boron present were plotted and the spectrum within the range 450 to 650nm is given as Fig.3.4. Spectrum a. is that produced by spraying 100ppm of boron(as boric acid) dissolved in methanol into the flame ; spectrum b. that produced by spraying pure methanol. The baseline of the spectra is not on the zero-line but approximates to the level at the long-wavelength end. This is an instrumental characteristic.

The extremely high emission peak at about 594nm is that of sodium present as an impurity. The other peaks lie at the wavelengths(after correction for instrumental error) 5770,5465,5165,4920,4710, and 4500nm. PEARCE and GAYDON⁶³ give band heads for BO_2 at 6390,6200,6030,5800,5450,5180, 4930,4710, and 4520nm. There is close correspondence between the last six of these band heads in both cases.

It was not found possible to locate other characteristic bands or lines due to boron at these low concentrations. No emission due to atomic boron at 249.7nm could be detected and the major band heads for the BO radical lie within the region of maximum OH band emission between 3050 and 3450nm.

Although the band head at 5165nm gave the highest absolute brightness, it was found preferable to use the 5465nm band, as the background signal was so much lower. The high background level at 5165nm necessitated backing off approximately some 12-times full-scale deflection at maximum sensitivity. Under this treatment, the photomultiplier tube used soon displayed increasing noise and baseline creep.

Fig. 3.4



It was thus decided to use the 5465nm band.

The basic reason for this high background emission was the use of methanol as a solvent. Early in the investigation it was observed that the emission produced by methanolic solutions of boron far exceeded that produced by aqueous solutions. Further investigation showed that methanol was some two orders of magnitude more effective in introducing boron into the flame as was water. This effect was also observable using ethanol, but was much less noticeable when acetone was used as the solvent. As acetone is as volatile as methanol, it was apparent that some other mechanism than that of volatility of the solvent was involved. The nebuliser efficiency was measured using methanol as the solvent.

The procedure followed was to spray a 1ppm solution of boron into the flame until a steady state was achieved. Three 25ml aliquots of the solution were sprayed in turn, collecting the effluent from the nebuliser drain tube during the period for which each aliquot was sprayed. The volume collected was measured and finally all three were combined and sprayed, measuring the resultant emission. The calibration curve for this procedure was linear. The results are as follows:

Signal for 1ppm	40 divisions
Effluent volume 1.	23.0ml
" " 2.	22.8ml
" " 3.	23.0ml
Signal for Effluent	18 divisions
Boron in Effluent $= (22.93 * 18 / 40) / 25$	41.3% of total
Nebuliser Efficiency Solvent	9.28%
" " " " Boron	58.7%

These results clearly show that the boron is present in a form that is more volatile than methanol itself. This is probably trimethyl borate.

This efficiency proved to be very sensitive to small amounts of water in the solvent, more than one percent produced serious reduction in the emission produced by spraying such solutions.

Once this fact became apparent, it was obvious that the sensitivity achievable by this technique would be enhanced by reducing the amount of water in the sample solution, and by designing a nebuliser that would spray the maximum quantity of sample solution in a given time. This latter feature would normally be expected to lead to a high noise level produced by variations in the spraying, and possibly even a reduction in efficiency due to an increase in the size of the droplets in the spray. However in this case the normal mechanism of actual transfer in the form of droplets is relatively unimportant forming at most only 15% of the total, and probably less than that. Because the sample is gaseous, the nebuliser system forms a buffer which effectively screens the analytical signal from short term variations in the nebuliser spraying rate.

This effect is not totally beneficial, as it was found to lead to a serious 'memory effect'. It was found to be necessary to spray any solution for approximately one minute before the signal stabilised. At the solution flow rates used for this study, this lag required some 10ml of sample to be sprayed.

The final arrangement of the nebuliser system which gave the most satisfactory results had a solution flow rate

of 9.2ml per minute using 2 litres of nitrogen per minute at a pressure of 30psi. As previously stated, this nebuliser was adapted from the flame emission attachment for the Hilger Uvispek spectrophotometer. The major modification was the substitution of a wide-bore stainless steel capillary to permit higher solution flow rates. The capillary used had a bore of 0.020in and a length of 2in. The sample uptake tube was made from 1/8in PVC tubing so that the rate of sample uptake was governed solely by the capillary.

This nebuliser was found to be approximately twice as effective as the best commercially available nebuliser which was tested.

The other flame conditions were optimised using this nebuliser and the burner shown in Fig.3.1. These conditions were; hydrogen flow rate 5l.per minute, oxygen flow rate $2\frac{1}{2}$ l.per minute, height of optical axis above burner top 2.5cm.

During the optimisation of these conditions, it was observed that the emission was sensitive to the degree of turbulence of the oxygen flow from the injection tube. Maximum emission was obtained if the flow was quiet and laminar. If the flow was allowed to become turbulent, the emission decreased even if all other conditions including oxygen flow rate were the same.

The reason for this behaviour is not clear but is possibly due either to greater cooling in the turbulent flame, or to the emitting species being deactivated by the presence of oxygen.

The final design of the burner(Fig.3.1) was devised to take this feature into consideration; the oxygen injection

tube was proportioned to prevent the possibility of turbulent flow conditions arising.

Apart from the deleterious effect of water in the sample, the major other interference noticed was sodium, which gave false high readings due to scatter in the monochromator. No solution to this problem, other than the absence of sodium from samples could be found, without reducing the sensitivity of the method. This precluded the use of alkaline absorbent to absorb the methyl borate produced by the standard separation technique. In fact it was found to be almost impossible to prepare aqueous solutions which did not contain unacceptable amounts of sodium, and most of the standard reagents also contained too much sodium.

The answer to this problem was found in the use of pure methanol as the final sample solvent. It was found to be possible to carry out a methyl borate distillation with effectively 100% yield without the use of an alkaline absorbent. This technique is only possible with very dilute solutions of the order of a few ppm, and if sufficient methanol is also distilled to redissolve the methyl borate in the condenser. In use the condenser must be flushed with pure methanol before use and the distillation executed as quickly as possible. In actual practice this is very difficult to achieve, as the sample flask contains concentrated sulphuric acid, and overheating causes the methanol to be lost by oxidation and etherification. The most successful results were obtained using a micro-bunsen burner for heating. In addition, the use of borosilicate glassware was not found to introduce any error, even when used for the reaction flask. Its use is not recommended however.

Experimental Procedure for Boron Determination.

The experimental procedure developed for the determination of boron in steel matrices is as follows:

Weigh out between 0.5 and 1gm of the sample in the form of drillings or turnings, mix with 3gm of sodium carbonate and fuse at red heat in a platinum crucible for about 30 minutes. Grind the fused mass to a fine powder and transfer to a 50ml r.b. silica reaction flask. Up to another 0.5gm of sodium carbonate may be used to aid this transfer. The flask should be set up under reflux and 20ml of conc. sulphuric acid added in small portions. Heat the reaction mixture until all evolution of carbon dioxide ceases, cool in ice and carefully add 20ml of pure methanol (Burroughs A.R. grade) in small portions cooling between each addition. The final addition of methanol should be as small as possible consistent with thorough rinsing of the reflux condenser. Fit a distillation condenser as quickly as possible so as to avoid any possible loss of boron by volatilisation, and distil as quickly as possible but without overheating.

The distillation condenser must be rinsed with methanol immediately before fitting, and the distillation should be observed carefully. Approximately 15ml of methanol must be collected. If any difficulty is noticed distilling the methanol such as vigorous boiling in the reaction flask but little flow of condensate, or if fumes fill the condenser, then the distillation will be incomplete and a low result will be obtained.

The condensate should be collected in a 25ml graduated flask which has previously been washed with concentrated hydrochloric acid and methanol to remove adventitious sodium

or boron contamination. After dilution to the mark with pure methanol the solution is ready for spraying.

It is essential to carry out duplicate determinations, and blanks on the reagents used. Calibration solutions must be prepared, but these may be made up from pure methanol and boric acid (1000ppm=5.7197gm H_3BO_3 per litre)

The calibration curve is measured by spraying pure methanol into the nebuliser until the baseline stabilises, then spraying each solution in turn for at least one minute before taking the reading. The sample solutions should be sprayed next using the same procedure, followed by a check on the stability of the baseline and a check of one or two points on the calibration curve.

A calibration curve should then be plotted and the boron content of the samples calculated. (For a 1gm sample, 1ppm of boron in the final solution=0.0025% boron in the sample.)

Instrumental conditions should be set to give the maximum useful nebulisation rate of the sample using nitrogen gas, and balancing the relative flow rates of the hydrogen fuel and oxygen to give the maximum analytical signal. These conditions should be determined empirically as slight variations may occur. The conditions found to be most satisfactory in this study were a nitrogen flow rate of 2l per min. an oxygen flow rate of 2.5l per min. (at a pressure of 25psi) and a hydrogen flow of 5l per min. (at 5psi) Measurements were taken 2.5cm above the burner top plate.

Care should be taken to avoid draughts, and the monochromator slit should be shielded from daylight as the analytical wavelength is in the visible region of the spectrum.

Results

The calibration curves obtained in this study were all found to be linear up to 2ppm. It was not found possible to measure over a greater range than this at maximum sensitivity because the signal exceeded full scale deflection, and the backing-off control introduced slight non-linearity if the setting was altered during one set of solutions.

Sensitivity was found to be 40% fsd for a 1ppm solution and the noise level did not exceed 1% fsd. The practical determination limit was taken to be 0.05ppm of boron in the sample solution equivalent to a sensitivity of 0.0001%B in the original sample (1gm sample size).

Typical results are given below.

<u>Sample</u>	<u>Wt.</u>	<u>Found</u>	<u>Actual</u> (Certificate)
B.C.S.327	1.0165	0.0035	0.003
"	0.55	0.0024	"
"	0.52	0.0029	"
"	0.58	0.0029	"
B.C.S.329	0.53	0.0077	0.008
"	0.56	0.0081	"
"	0.52	0.0077(5)	"
"	0.55	0.002	"
"	0.528	0.003	"
"	0.53	0.0052	"

The last three results were included to show the effect of poor recovery of methanol. In these determinations it was found impossible to recover a sufficient volume of methanol for the distillation to be successful.

Apart from these results, all are well within the limits of variation shown on the certificates.

The recommended technique of course is for determining total boron in steel. Preliminary investigation indicated that it is also possible to determine soluble boron if this is dissolved in dilute sulphuric acid. This solution should be neutralised with caustic soda and evaporated to dryness in the distillation flask, followed by distillation as detailed above.

Initial dissolution in acids other than sulphuric acid is not recommended as in the case of hydrochloric acid, some acid may distil with the methyl borate, and this will raise the background level. This is probably amenable to blank correction but it is more convenient to use sulphuric acid, as the only decomposition product likely, sulphur dioxide, is innocuous in small concentrations.

Another dissolution method was tried which was successful in attacking a large range of metals. This was the method advocated by EBERLE and LERNER¹⁵ who used bromine in methanol as the solvent for Be, Zr, Th, and U. This method was modified because of the unavailability of boron-free Be, and sulphur dioxide was used to react with excess bromine. Initial results were encouraging but the development of a method using this system was not completed. Difficulties were encountered in the variable amount of bromine necessary to dissolve given sample weights, and in the carry over of bromine-containing species in the distillation, giving rise to a high background. No great difficulties should arise to prevent the development of such a method, but this was not pursued, although initial results were promising. This method has the advantage of being in a non-aqueous medium.

Conclusions

The analytical technique developed appears to be applicable to the determination of boron in any matrix if it can be extracted in a form suitable for a methyl borate separation. The only restriction on this is the presence of halide, fluoride being particularly inimical.

The sensitivity of the method could probably be improved by the use of more suitable equipment, the equipment used was basically unsuitable, and no indication was obtained of the ultimate noise level inherent in the signal. The noise measured appeared to be purely instrumental, as the magnitude of the noise was unaffected by altering the gain of the instrument.

Comparison of the equipment used and commercially-available equipment indicated that the nebuliser was about twice as effective as the best commercial one (Techtron AA4), but this is a specialised application. The whole system gave an approximately four-fold improvement in sensitivity compared with a Beckmann total-consumption nebulising burner.

The whole method is probably capable of substantial improvement, and the further development of the bromine-methanol reagent system would appear to have particular advantages.

Compared with other methods described in the literature this method is relatively quick, simple and of acceptable sensitivity. In addition conventional equipment may be used with the minimum of modification.

Bibliography

1. P.Y.Yaklovlev,G.V.Korina
Zavod. Lab 26 1342 (1960)
2. S.Weinberg,K.L.Proctor,O.Milner
Industrial and Engineering Chemistry Analytical Edn.
17 419 (1945)
3. H.J.Gräbner
Z. Analytische Chemie 186 327 (1961)
4. L.V.Sabinina,T.Y.Styunkel
Zavod. Lab 13 752 (1947)
5. S.Wakamatsu
Japan Analyst 9 22 (1960)
6. Satoru Muto
Bull. Chem.Soc.Japan 30 881 (1957)
7. J.Janousek,K.Studlar
Hutn. Listy. 14 458 (1959)
Cf. AA 7 532 (1960)
8. R.Capelle
Analytica Chimica Acta 25 59 (1961)
9. British Standard Specification 1121 Part 49 (1966)

10. J.R.Martin, J.R.Hayes
Analytical Chemistry 24 182 (1952)
11. D.L.Calliccoat, J.D.Wolszon, J.R.Hayes
ibid. 31 1437 (1959)
12. W.H.Low
J.A.C.S. 28 807 (1904)
13. G.E.F.Lundell, J.I.Hoffman, H.A.Bright
'Chemical Analysis of Iron and Steel'
Chapman and Hall London 1930
14. J.L.Hague, H.A.Bright
US Bureau of Standards R.P.1120 21 125 (1938)
15. A.R.Eberle, M.W.Lerner
Analytical Chemistry 32 146 (1960)
16. R.Bruhlman, L.Piatti
Chimia 11 203 (1957)
17. H.Iinuma, T.Yoshimori
Japan Analyst 9 826 (1960)
Cf. AA 9 3098 (1960)
18. V.R.Wiederkehr, G.W.Goward
Analytical Chemistry 31 2102 (1959)

19. T.Yoshimori,T.Niwa,T.Takenchi
Talanta 11 993 (1964)
20. W.T.Brande
'A Manual of Chemistry' 163
John Murray London 1819
21. G.S.Smith
Analyst 60 735 (1935)
22. A.H.Jones
Analytical Chemistry 29 1101 (1957)
23. G.A.Rudolph,L.C.Flickinger
Steel 112 pp 114,131,149 (1943)
24. H.A.Kar
Metals and Alloys July 1938 p175
25. L.Bahacek,K.Kunzova
Hutn.Listy. 14 710 (1959)
Cf. AA 6 2160 (1959)
26. Z.Vecera,B.Bieber
Hutn.Listy. 13 808 (1958)
Cf. AA 6 2160 (1959)
27. J.H.Yoe,R.L.Grob
Analytical Chemistry 26 1469 (1954)

28. A.Eckert,K.Steiner
Monatscheft für Chemie 35 1131 (1914)
29. G.H.Ellis,E.G.Zook,O.Bandisch
Analytical Chemistry 21 1345 (1949)
30. D.A.Brewster
ibid. 23 1809 (1951)
31. Methods of Analysis Committee
Journal of the Iron and Steel Institute 189 227 (1958)
32. F.J.Langmyhr,O.B.Skaar
Analytica Chimica Acta 25 262 (1961)
33. J.D.Hobson
BISRA Report MG/D/Conference Proc./610/67
34. S.Wakamatsu
Japan Analyst 7 372 (1958)
Cf. AA 6 1321 (1959)
35. I.U.Martychenko,A.M.Bondarenko
Zhur. Anal. Khim. 12 495 (1957)
Cf. AA 5 1225 (1958)
36. E.Piper,H.Hagedorn
Archiven Eisenhüttenwesen 28 373 (1957)
Cf. AA 5 1226 (1958)

37. G.H.King, R.Wood
Paper presented at a Colloquium on the Application of
the Auto Analyzer for Metallurgical and Water Analysis
at the Bloomsbury Centre. 2nd April 1970
38. M.R.Hayes, J.Metcalf
Analyst 87 956 (1962)
39. J.Borrowdale, R.H.Jenkins, C.E.A.Shanahan
Analyst 84 426 (1959)
40. T.S.Harrison
BISRA Report MG/DA/283/63
41. F.W.Lima, C.Pagano, B.Schneidermann
Analyst 85 909 (1960)
42. R.Greenhalgh, J.P.Riley
ibid. 87 956 (1962)
43. M.Miyamoto
Japan Analyst 11 635 (1962)
Cf. AA 11 62 (1964)
44. R.H.A.Crawley
Analyst 89 749 (1964)
45. Kazuo Hiro
Bull. Chem. Soc. Japan 34 1743 (1961)
Cf. AA 9 2672 (1962)

46. V.Patrovsky
Talanta 10 175 (1963)
47. L.C.Pasztor, J.D.Bode
Analytica Chimica Acta 24 467 (1961)
48. L.C.Pasztor
Analytical Chemistry 32 1530 (1960)
49. W.Koch, K.H.Sauer
Archiven Eisenhüttenwesen 35 983 (1964)
Cf. AA 13 1269 (1966)
50. R.F.Anderson
Applied Spectroscopy 14 123 (1960)
51. E.F.Runge, F.R.Bryan
ibid. 15 13 (1961)
52. J.E.Paterson, W.F.Grimes
Analytical Chemistry 30 1900 (1958)
53. B.L.Henke
Chemical Engineering News 41(47) 40 (1963)
54. C.L.Luke
Analytica Chimica Acta 45 377 (1969)
55. C.A.Parker, W.J.Barnes
Analyst 85 828 (1960)

56. G.Elliott,J.A.Radby
Analyst 86 62 (1961)
57. M.D.Amos,J.B.Willis
Spectrochimica Acta 22 1325 (1966)
58. R.Mavrodineanu,R.C.Hughes
Developments in Applied Spectroscopy 3 305 (1963)
59. R.H.Wendt
U.S.E.E.C. Published Report 15-T-51 (1965)
60. H.Goto,I.Atsuya
Z. Analytische Chemie 240 102 (1968)
61. J.A.Dean
Analyst 86 621 (1960)
62. R.Herrmann,C.T.J.Alkenade
'Flame Photometry' Interscience New York (1963)
63. R.W.B.Pearse,A.G.Gaydon
'The Identification of Molecular Spectra'
Chapman Hall London.

CHAPTER 4

COMPUTER CALCULATIONS OF BORON FREE-ATOM CONCENTRATIONS
IN ANALYTICAL FLAMES.

Introduction. The method adopted for this study was a digital computer program for the minimisation of free energy. This program used the method of OLIVER et al.¹ as applied to the technique developed by WHITE JOHNSON and DANTZIG² The program was written by C.F.ANDERSON⁴ and modified in this department to suit the Imperial College IBM 7094 computer installation using a PUFFT (Purdue University Fast Fortran) compiler and the University of London CDC 6600 installation using a RUN compiler . A routine was written to make use of the CALCOMP graph-plotting facility available at the latter installation. A more comprehensive description of the program is given at the end of this thesis.

The basis of the free-energy minimisation method is that, when a system comes into equilibrium at constant pressure, the Gibb's free energy is at a minimum for the whole system. Thus, if the set of differential equations for the free energy be solved, then the equilibrium values of the species concentrations may be directly determined. No knowledge of kinetic data or equilibrium constants is necessary as the condition of minimum free energy is sufficient to uniquely define the system. However, as the necessary differential equations are in general non-linear, it is necessary to resort to an iterative method of solution in default of an exact method.

The method employed by this program was one using the technique of Lagrangian multipliers.

Characteristics of the Program. The program has the capacity to consider systems containing up to 10 elements and 9 condensed species. The number of gaseous species able to be considered is relatively unimportant as these do not enter

into the solution of the matrix set up by the program. For reasons of computer size and time limitation it was found most convenient to limit the total to no more than 60 species. A further restriction imposed by the method is that of not including as many or more condensed species as there are elements in the system. Neglect of this point will cause the program to fail due to the matrix becoming singular.

It is obvious that many systems do not fulfil these criteria so that consideration of all possible species in these flames is impossible. In cases such as these a number of preliminary runs were undertaken to eliminate those species present in negligible concentrations. In the case of solid species the criterion chosen was that the species was never shown as present when included in any run. Fortunately this did not lead to the necessity of excluding any solid species known to be present. For simplicity in operation the program assumes that any solid species present at less than $1.0E-06$ moles/mole is not present.

Gaseous species are permitted to have values ranging to $1.0E-35$ by the program as these values are not used in the matrix. (For condensed species these values would lead to serious rounding errors)

Gaseous species values of less than the reciprocal of the Avogadro number are clearly meaningless and the criterion used generally was a value of less than $1.0E-16$.

Consideration of the basis of the method indicates that omitting any species affects all other species present to the same degree providing that species does not contain a large proportion of any of the elements present in the system.

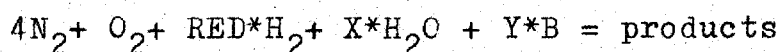
Input. This was by means of punched cards.

The information supplied was thermodynamic data, data for the output headings and amount of output, and data to permit the program to consider a number of differing flame stoichiometries.

The method of varying the flame stoichiometry was as follows:-

Consider an air-hydrogen flame containing boron introduced by means of a nebulised aqueous solution.

The formal equation is:-



where RED, X, Y, are constants .

At the point of formal stoichiometry the value of RED is 2.0. (Normally no account is taken of the contribution of any water introduced into the flame)

Under normal conditions of operating an analytical flame the only parameter varied is the fuel-gas flow rate as pneumatic nebulisers are normally employed, and varying the gas flow rate through one will generally affect its efficiency. Thus it may be seen that the only part of the equation above which varies with stoichiometry is the factor RED.

Although it is possible to enter all the factors directly as a set of mole numbers the method actually used was to normalise the set to give more easily comparable results.

The normalising factor was calculated as follows:-

$$DIV = 4 + 1 + RED + X + Y$$

giving mole numbers (B-values) for the elements of

$$B_H = (2 \cdot X + 2 \cdot RED) / DIV$$

$$B_O = (2 + X) / DIV$$

$$B_N = 8/\text{DIV}$$

$$B_B = Y/\text{DIV}$$

(the symbol B is used in the program)

A further feature was the possibility of permitting Y to remain constant so that the amount of metal added to the flame each time is the same for each mole of input gas. Whilst not strictly in accordance with practice this feature permits easy comparison of the results for a number of flames. This feature was in fact used for the study of boron atomisation in flames.

Output. Two forms of output were produced by the program; printed output from a line-printer and CALCOMP graph plotter output.

The printout was in two forms; mole numbers of species present per mole of gas input, and volume percent of flame gas products. In addition the stoichiometry of each flame and the average molecular weight are output.

The CALCOMP output was in the form of individual 5" square graphs, one for each species, of \log_{10} (percent of the species concentration)(ordinates) vs. fuel/oxidant ratio(abscissae). Three temperatures are considered on each graph and a separate line and set of symbols plotted for each. In the case of metal-containing species the ordinates are \log_{10} (percent of total metal present as that particular species).

All tables of species concentrations in this section were taken from this printout and the graphs of species concentrations are actual CALCOMP output.

Advantages and Limitations of the Method.

The major advantage of this method using free energy

minimisation is that no account need be taken of the path traced by the system to reach the position of equilibrium. Thus merely including the relevant thermodynamic data for all possible species is sufficient to permit the determination of the equilibrium position. This is in strong contrast to the complications necessary when considering the equilibrium constant data ^{1,5}.

Since no path to final equilibrium is specified, this method must be considered equivalent to taking the elements present in the proportions of their respective mole numbers heating the mixture to the final temperature and allowing the system to attain equilibrium.

The disadvantages are twofold; first it may not be possible to consider all the species present, and second the practical system may depart from the ideal behaviour assumed for the purposes of calculation.

The assumptions made are:

- i) All gaseous species are assumed to exhibit ideal-gas behaviour.
- ii) All condensed species are mutually immiscible.
- iii) True thermal equilibrium is achieved.
- iv) The composition of the system is described by the set of mole numbers used.

In the case of species not available for consideration it is obviously impossible to include them but, experience has shown that if these are minor species no great error is caused by their omission. The effect of such an omission is to redistribute their component elements throughout the system without affecting the ratios of the other species seriously. This only applies when the species concerned does

not contain a significant fraction of any of the elements present in the system, or the system is not near a critical ratio e.g. a C/O ratio of unity. Omission of a major species is not tolerable as this will cause a serious error in the calculation.

The JANAF Thermochemical Tables ⁶ list virtually all species present in hydrocarbon flames above the level of $1.0E-6$ volume percent. This consideration is more serious in the case of metal-containing species where such complete data may be lacking. The effect of omitting such a species will only cause a negligible change in calculated flame composition, but a major change in percentage atomisation. Such omissions are imponderable.

Justification of the first two assumptions may be made on the basis that any errors introduced are known to be small, and no better simple description of the system is available.

Justification of the latter two conditions is more difficult as deviations from them are well known in practical flames. Certain flames such as the oxy-hydrogen and cool (below 2000K) acetylene-air flames display anomalous behaviour in the spectra of the hydroxyl radicals ^{7,8}. Further, certain workers have used the primary combustion zones of flames in emission work ^{9,10}. Under these conditions it would be rash to assume thermal equilibrium, especially as they often display marked chemiluminescence in these zones. This reasoning also applies to turbulent non-premixed flames such as are produced by Beckmann-type burners. In such flames a typical cross-section is likely to include both primary combustion zones and others where

combustion is virtually complete. For these reasons the results of this program are not likely to apply to such flames and may prove highly misleading in cases where chemiluminescence contributes to the analytical signal.

These limitations thus confine the usefulness of the following work mainly to absorption or fluorescence spectrometry, since in these techniques quiet pseudo-laminar premixed flames are generally employed. Analytical measurements in these flames are made in the transparent interconal zone where the conditions most nearly approach thermodynamic equilibrium. More important, these techniques rely upon the presence in this zone of a population of ground-state atoms of the analyte. The program is designed to calculate this population.

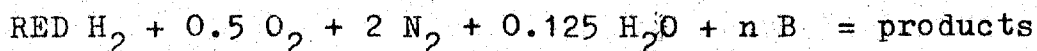
The final assumption of this method, that the system is adequately described by the set of mole-numbers used, is difficult to justify for any practical flame. The major difficulty is over the effect of gaseous diffusion into and out of the flame. This diffusion obviously occurs, but a detailed mathematical description or model of gas behaviour in such a system is beyond the scope of this work. This aspect has thus been largely ignored for the purpose of programming, and consideration is confined to a simple qualitative description of the expected effects which is at the end of the chapter.

Theoretical Calculation of Boron Atomisation in Analytical
Flames.

1. The Air Hydrogen Flame.

This flame has been used for atomic emission spectroscopy of easily-atomised elements but, it has not been extensively employed for atomic absorption spectroscopy (AAS). The maximum temperature attained has been reported variously 2240K ¹¹ , 2270K ⁷ , and 2110K ¹² . For this study however the temperatures used for the composition graphs are 2000K, 2300K, & 2600K. Although this last temperature is impossibly high, it is valuable in certain cases to study higher temperatures in order to seek anomalies or confirm trends. Such an anomaly is the absence of condensed species present in cooler flames.

The formal stoichiometry of the flame was assumed to be according to the equation:-



RED is the parameter previously described.

The water present on the LHS of the equation was calculated on the basis of 0.05 mole of water introduced into the flame by each mole of nebulising gas. This is equivalent to a nebuliser spraying 4ml. of solution per 5l. of nebulising gas and having an efficiency of 5%. Such a value has been found to be typical of equipment used in this laboratory. For nitrous oxide as the nebulising gas the higher value of 0.625 mole per mole was assumed.

For this study the values of RED ranged from 1 to 3 ie up to 200% formally fuel-rich. It must be noted that over this range the added water forms approximately from 2 to 4% of the total feed gas.

The variable 'n' in the equation which simply expresses the notion that when the mole numbers of all other species were normalised before computation, this value was chosen such to give a constant input value for boron. The value chosen for this study was $1.0E-4$.

A preliminary study was undertaken to select the boron containing species to be considered in this and the other analytical flames studied. A list of all species considered is given as Table 4.1a. Species present in concentrations less than $1.0E-12$ moles per mole of flame gas were eliminated from consideration in order to save computer time and avoid difficulties with the matrix manipulation. Reduced lists of the species considered for each flame are given as Tables 4.1b,c,& d.

Results.

The results for this flame are presented as Figs.4.1 to 4.12 and Table 4.2. It must be remembered that although the CALCOMP graphs show results for 2600K the temperature of the air hydrogen flame is no higher than 2300K. An interpretation of the results for each of the major species is given below.

Molecular Hydrogen Fig.4.1

The graph shows a steady gradation from an H/O ratio of 2 to the maximum fuel-richness. The wide spacing at the low end of the scale is merely a characteristic of the logarithmic scale and indicates the dissociation of water at the temperatures considered. At greater fuel-richness this difference is reduced by the general increase in free hydrogen and the scale contraction.

The major reducing species in this flame is probably atomic hydrogen and this exhibits much the same behaviour

as molecular hydrogen. This indicates that these species are in thermal equilibrium. Relative concentration levels are given in Table 4.2.

Atomic Oxygen Fig.4.2

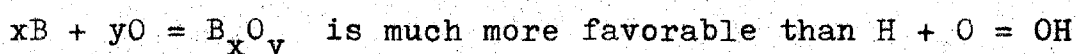
This species is one of the most important oxidising species in this and all other flames considered. It may be seen from the graph that initially, the atomic oxygen level starts at a relatively high value and then falls steadily as the fuel-richness increases. Molecular oxygen (Table 4.2) is present in higher concentrations at near-stoichiometric flames but falls off to approximately one-quarter of the atomic oxygen concentration in very fuel-rich flames. This behaviour shows that molecular oxygen is a more potent oxidising species than atomic oxygen, as would be expected.

Hydroxyl Radical Fig.4.3

Apart from water and molecular oxygen (in fuel-lean flames) this is the most common oxidising species. Its behaviour closely parallels that of atomic oxygen except that the change in concentration from lean to rich flames is some 30-fold, as opposed to the 200-fold change in atomic oxygen.

Atomic Boron Fig.4.4

The feasibility of the AAS determination of boron is dependent upon the concentration of this species. As would be expected the concentration increases with fuel-richness, but at a temperature of 2300K the calculated atomisation is considerably less than 1.0E-07%. This is in an atmosphere containing a 10,000-fold excess of hydrogen over boron. It is immediately apparent that the set of reactions :-



The practical result of this low atomisation would be

that the detection limit of boron would be very high in such a flame.

Boron Monoxide Radical (BO) Fig.4.5

The graph of the concentration of this species displays a rising trend with fuel-richness which was somewhat unexpected. Comparison with the graphs of the other boron-containing species (Figs.4.8-4.12, Table 4.2) confirms this trend for these species with the exception of BO_2 and H_3BO_3 . BO_2 contains some 7.5% of the available boron in the stoichiometric flame at 2300K, and the total change in boron content of all the other species may be accounted for by the change for this species. The concentration of BO_2 is some orders of magnitude greater than that of BO.

The major boron-containing species is the HBO_2 Radical (Fig.4.8) which contains some 92% of the boron in a stoichiometric flame at 2300K. and more than 99% in a fuel-rich flame at the same temperature. Fuel-lean flames might contain less of this species and considerably more BO and BO_2 . Another point of interest is that this species is the first one noted that is favored at lower temperatures.

2. The Nitrous Oxide Hydrogen Flame.

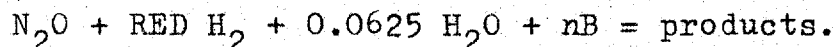
Several workers have investigated this flame for application to analytical spectroscopy ^{13,14,15,16,17}, and some controversy has arisen over its usefulness in this field. Its principal advantage over air-hydrogen is its higher temperature, variously reported as 2820K ¹⁴, 2800K ¹⁶, and 2700K ¹⁷. A further advantage it possesses over oxy-hydrogen is that of a lower burning velocity. This permits the use of conventional nitrous oxide acetylene equipment for

burning premixed stoichiometric flames.

The difference in temperature between this flame and the oxy-hydrogen flame is of the order of 200K ¹¹. The high temperature considered for CALCOMP graph plotting was assumed to show whether the use of the oxy-hydrogen flame would display any significant advantage.

The species considered for this flame are given in Table 4.1b. It was not found necessary to include any condensed species for consideration.

The formal equation for this flame is given by the equation:-



The reasoning leading to these values is as for the air-hydrogen flame. In this case the added water amounted to from $1\frac{1}{2}$ to 3% of the total flame-gas feed.

Results.

The results are presented as Figs.4.13 to 4.24 and Table 4.3. The temperatures considered for the CALCOMP plots were 2400K, 2800K, & 3200K. The practical flame region lies between the two lower temperature graphs.

Molecular Hydrogen Fig.4.13.

This exhibits much the same behaviour as in the air-hydrogen flame. However the graphs cross at greater fuel-richness reversing the order of concentrations. The probable reason for this behaviour is the reduced stability of molecular hydrogen at these high temperatures. In lean flames the presence of higher concentrations of oxidising species present favour the reverse order. The graphs cross at a H/O ratio of approximately 3.

Atomic Oxygen Fig.4.14

As with hydrogen the behaviour of this species closely parallels that of oxygen in the air-hydrogen flame. In this flame the actual concentration is much higher, rising to nearly 0.75% at 2800K in the stoichiometric flame. In addition the curves are much flatter and it may be noted that the scale is only 4/5 of that of the corresponding air-hydrogen graph.

Hydroxyl Fig.4.15

Once again this behaves much the same as in the air-hydrogen flame, merely attaining higher absolute values because of the higher temperatures considered, and lessening of the concentration of diluent nitrogen.

Atomic Boron Fig.4.16

Allowing for the difference of linear scale between this and Fig.4.4, this forms a single series with Fig.4.4. This indicates that, for the purposes of this study, the air-hydrogen and nitrous oxide-hydrogen flames differ only in temperature for their effect on boron atomisation.

This latter observation also applies to the remainder of the species considered for this flame. Thus the trends noted for all species are repeated and extended. The formation of HBO_2 is less favored and the concentration of all other boron-containing species is proportionately increased (with the further exception of H_3BO_3 and B_2O_3). Most notable is the increase in BO and BO_2 .

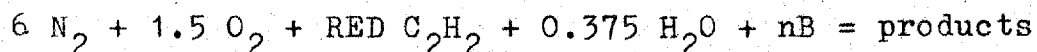
3. The Air Acetylene Flame.

This flame is one of the most widely-used flames for all flame-spectroscopy, particularly for AAS determination of relatively easily atomised elements. Indeed it is specified as standard for most atomic-absorption spectrophotometers using premixed flames.

The temperature of this flame has been measured as:-
2420K ¹³ , 2500K ⁷ , & 2370K ¹⁸ .

The species considered for this investigation are given in Table 4.1c. Solid carbon is the only condensed species in the list.

The formal equation for the flame is given by:-



The values are derived as previously detailed.

Values of RED considered ranged from 1 to 2 giving a C/O ratio range of approximately 0.6 to 1.2 and a feed-gas water content of some 4%.

Results.

These are presented as Figs.4.25 - 4.36 and Table 4.4. The practical flame temperature region lies between 2000K and 2500K. Thus all three temperatures used for the CALCOMP plots (2000K, 2300K, & 2600K) are useful for comparison.

Atomic Carbon Fig.4.25

This species has long been considered the most important reducing species in hydrocarbon flames. As this technique is not capable of considering reaction kinetics this point may not be decided from this study.

From the graph it is immediately apparent that there is a fundamental difference between this flame and the hydrogen flames previously described. The most obvious effect of

this difference is in the shape of the curves which in this case are of a sigmoid shape. There is a sharp increase in the slope of the curves at the point where the C/O ratio most nearly approaches unity. For this particular species the change in concentration on going from a value of RED of 1.6 to 1.7 is some four orders of magnitude.

Apart from this high-gradient section the curves display a steady increase with increasing fuel-richness.

Cyano Radical Fig.4.26

Although suggested as the major reducing species in the nitrous oxide-acetylene flame, this species has not been suggested as a major reducing species in this flame. The CALCOMP plot shows it to be present in concentrations more than 1000-fold greater than atomic carbon.

As with atomic carbon it exhibits a sigmoid dependence upon flame stoichiometry.

Hydrogen Cyanide Fig.4.27

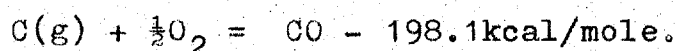
From the calculations of this program this species is indicated as the major carbon-containing species which may be suggested as a reducing agent. The maximum concentration indicated is at a temperature of 2600K and a RED value of 2.0, when the calculated concentration is some 3%.

It has apparently not been suggested as a major reducing agent in analytical flames. Its presence in such flames has been observed by SARGENT¹⁹ who observed a reduction in band emission from CN in a nitrous oxide acetylene flame shielded with hydrogen.

Atomic Oxygen Fig.4.28

The curves for this species are the inverse of those of the previous three species displaying a sharp decrease

in concentration across the line $C/O = 1$. Hydroxyl (Fig.4.29) also displays this dependence. In contrast to this, the concentration of hydrogen (Table 4.4) does not display any such behaviour, instead it exhibits the same type of dependence as in the hydrogen flames. This behaviour of the reducing species in this hydrocarbon flame indicates that there is a very fundamental difference in the reducing properties of this as opposed to hydrogen flames. The basis of this difference lies in the reaction :-



Atomic Boron Fig.4.30

As has been suggested above, this shows much the same behaviour as the other reducing species in the flame. The change in atomisation across the point of maximum gradient is some five orders of magnitude. The maximum degree of atomisation is calculated as $18\frac{1}{2}\%$ at 2600K and a RED value of 2.0. Of course this value is not approached in practice since the air acetylene flame cannot achieve anything near this temperature at this stoichiometry.

Boron Monoxide Radical (BO) Fig.4.31

The behaviour of this species is much more complex than in the hydrogen flames. Again the concentration shows a rising trend with increasing fuel-richness but, two of the curves cross changing the order at maximum fuel-richness.

Boron Dioxide Radical (BO₂) Fig.4.32

This species also shows more complex behaviour analogous to that of BO. In this case all three curves cross at $C/O=1$ indicating that the thermal stability of this species is different in reducing and oxidising conditions.

Boron Monoxide Dimer (B_2O_2) Fig.4.33

This species behaves much as BO does and in fuel-rich flames these two species contain most of the boron present in the flame.

HBO₂ Radical Fig.4.34

In oxidising flames this species contains most of the boron present (up to 99½%). In the fuel-rich flame however, this proportion decreases to approximately 10%. Again this is in sharp contrast to hydrogen flames.

HBO Radical Fig.4.35

Although relatively unimportant in hydrogen flames, this species is much more prevalent in this flame reaching the percent level.

BH₂ Radical Fig.4.36

As with HBO this species is much more important in this flame, particularly in fuel-rich flames. There is a rise in concentration of five orders of magnitude across the line $C/O=1$.

These results emphasise the division of the boron-containing species into those favored by reducing conditions : ie. B,BO, B_2O_2 ,HBO,BH₂ etc. ; and those favored by oxidising conditions BO_2 and HBO₂.

Boron Carbide BC

Although not plotted this species shows an upward trend in very fuel-rich and hot flames. For this reason it is unlikely to be important as these conditions are unlikely to occur in practice.

Solid Carbon

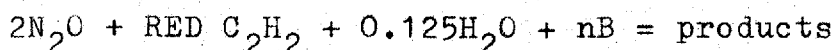
This species first occurs in flames with a RED value of 1.8 and temperatures below 2400K.

4. The Nitrous Oxide Acetylene Flame.

The introduction of this flame into atomic-absorption-spectrophotometry in recent years, has permitted the extension of this technique to many elements which would otherwise prove difficult to determine. Many workers have published papers on the determination of the 'refractory-oxide elements' 13,14,20 21,22,23,24,25,26.

The temperature achieved in this flame has been reported variously as 2800K ¹³, 2900K ²⁶, 2950K ²³, and as 3000K ¹⁴.

The formal stoichiometry of the flame is given by the equation :-



All values used were derived as previously described ; the values of RED considered ranged from 1.0 to 1.5 giving a C/O ratio range of 0.94 to 1.41 and a feed-gas water content of $3\frac{1}{2}\%$ to 4%.

The species considered for this flame are given in Table 4.1c.

Results.

These are presented as Figs.4.37 to 4.48 , and Table 4.5

The temperatures considered for the CALCOMP plots are 2400K, 2800K, and 3200K. The practical range of temperatures is from 2500K to 2950K.

Atomic Carbon Fig 4.37

The level of concentration of this species is considerably higher than in the air acetylene flame at the same temperature. Much of this difference is attributable to the increased percentage of the total flame input formed by carbon.

The concentration curves exhibit the same sigmoid dependence on C/O ratio but, the change in concentration across the line C/O = 1 is somewhat smaller at about three orders of magnitude.

Cyano Radical Fig.4.38

As for atomic carbon the concentration of this species is higher in this flame. The difference in this instance is rather smaller but the behaviour is almost exactly analogous.

Hydrogen Cyanide Fig.4.39

Once again the behaviour of this species is similar to that in the air acetylene flame, the concentrations being of the same order in both flames.

Atomic Oxygen Fig.4.40

The higher temperatures considered for this flame, and the higher input of oxygen to the flame result in a slightly increased concentration of this species.

Hydroxyl Radical Fig.4.41

The same remarks apply to this species as to atomic oxygen.

Atomic Boron Fig.4.42

There is a marked improvement in atomisation in this flame. At a C/O ratio of 1.03 (RED = 1.1) and 2800K, the atomisation is 27½%. Most or all of this improvement must be attributed to the higher temperature considered. Again there is a change of some five orders of magnitude across the line C/O=1.

BO Radical Fig.4.43

This species displays similar behaviour to the air-acetylene flame but shows a very prominent maximum at a C/O ratio of unity. At the temperature of 2800K in fuel-rich flames,

the concentration drops to a constant value of approximately 10% of the boron present.

BO₂ Radical Fig.4.44

As expected, this species shows a monotonic decrease in concentration with increasing fuel-richness, and the sigmoid form of curve. At high values of fuel richness this species contains an insignificant fraction of the boron present.

BO Dimer B₂O₂ Fig.4.45

This again parallels the behaviour of BO but shows characteristics of thermal instability.

HBO₂ Fig.4.46

As in all the flames considered, this contains the bulk of the boron present in fuel-lean flames. In fuel-rich flames the concentration is negligible. This also shows signs of thermal instability.

HBO Fig.4.47

This species displays the same characteristics as BO & B₂O₂ having a maximum at C/O=1.

BH₂ Fig.4.48

This species forms one of the principal boron-containing species in fuel-rich flames. At 2800K and a C/O ratio of 1.03 the boron in the flame is distributed thus:-

BO 34%, BH₂ 32%, B 27%. comprising some 93% of the boron.

Solid Carbon

This first appears at a C/O ratio of 1.08 (RED=1.15) and persists to 2400K.

5. The Oxygen Cyanogen Flame.

The main factors determining the maximum temperature of a flame are; the heat of combustion, the specific heat of the flame products, and the thermal stability of the products. If the flame products are not thermally stable, then the energy of combustion will be dissipated in producing species with high levels of electronic potential energy but relatively less thermal energy. Thus the flame temperature will be lowered.

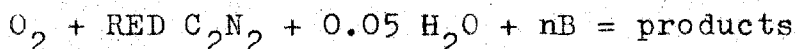
The combustion products of the stoichiometric oxygen-cyanogen flame are nitrogen and carbon monoxide, both of which are extremely thermally stable. The heat of combustion is also high at 126.7kcal/mole at STP. For these reasons, the oxygen cyanogen flame is one of the hottest known. The temperature has been reported as; greater than 4500K²⁷, 4640K²⁸, 4850K²⁹. CONWAY et al.²⁸ found that the temperature of the fuel rich flame decreased more rapidly than that of the lean flame corresponding to it. This latter observation is in accordance with the theory as cyanogen is more easily dissociated than oxygen.

This effect is even more pronounced when water is introduced, as the pure flame contains no hydrogen species. BARTHOLMAY & VALLEE²⁹ found that the temperature was decreased by 500K by the addition of water, and attributed the decrease to the presence of easily dissociated species such as OH.

Hotter flames are known such as ozone-cyanogen, oxygen carbon subnitride, and ozone carbon subnitride. (carbon subnitride C_4N_2 is the nitrile of acetylene dicarboxylic acid) Temperatures as high as 5500K have been reported³⁰.

These flames are much more dangerous than the oxygen cyanogen flame which is considered dangerous because of the poisonous and explosive nature of cyanogen. No analytical applications have been reported.

The formal stoichiometry is given by the equation:-



The values of RED considered were from 0.5 to 1.5 giving a C/O ratio of from 0.5 to 1.5. The feed-gas water content varied between 2 and $3\frac{1}{2}\%$. Species considered are given in Table 4.1 d.

Results

The results are presented as Figs.4.49 to 4.60 and as Table 4.6. The temperatures considered for the CALCOMP plots were 4100K, 4500K, and 4900K.

The practical flame temperature range is difficult to estimate owing to the presence of water, but it would probably be at the low end of the range studied. This problem is further complicated as the environment in the pure and water-containing flames is so different. Only the water containing flame was studied in any detail but, the results are thought to be valid in all particulars but that of temperature. This follows as a result of the characteristics of the program. These points must be borne in mind when interpreting the results of this study.

Atomic Carbon Fig.4.49

This displays the characteristic sigmoid curves typical of carbon-containing flames. The curves are somewhat less steep than those of the hydrocarbon flames, indicating a more gradual transition. The values of actual concentration are much higher approaching the percent range in rich flames.

Cyano Radical Fig.4.50

This behaves similarly to atomic carbon and achieves a comparable concentration in fuel-rich flames.

Atomic Oxygen Fig.4.51

As is to be expected, this shows the inverse behaviour to the reducing species. The curves are again less steep than in the hydrocarbon flames, and the absolute concentrations are higher, reaching the percent level in lean flames.

Atomic Boron Fig.4.52

The results for this species show the characteristics expected, giving degrees of atomisation ranging from the low percent range in lean flames to 95% in rich flames. This range shows clearly how stable the oxides of boron are compared to carbon monoxide, even at these elevated temperatures.

Boron Monoxide Radical Fig.4.53

In fuel-lean flames this is one of the most important boron-containing species and, together with BO_2 comprises some 90% of the boron species. The curves display a similar maximum to that in the nitrous oxide acetylene flame at a C/O ratio of slightly less than unity.

Boron Dioxide Radical BO_2 Fig.4.54

Although of the same order of concentration as BO in lean flames, the concentration of this species decreases much more rapidly with increasing fuel-richness until, in the richest flames, it is four orders of magnitude less than that of BO.

Boron Monoxide Dimer B_2O_2 Fig.4.55

This behaves much the same as BO but has a lower absolute concentration.

Boron Oxide B_2O_3 Fig.4.56

This species is much less significant than the other boron oxide species but otherwise behaves much the same.

HBO Radical Fig.4.57

The importance of this species is limited by the low hydrogen content of the flame but, its behaviour is similar to that of the other boron oxide species.

Boron Carbide BC Fig.4.58

This behaves as a reduced species, increasing to a concentration of the order of 0.1 to 1% in fuel rich flames.

Boron Nitride BN Fig.4.59

Another reduced species, this reaches the level of 0.1% in fuel-rich flames.

 BH_2 Radical Fig.4.60

This species is not very important in this flame, probably because of the low hydrogen content.

Conclusions and Discussion

For the above study to be of any value and to secure valid conclusions, it is necessary to interpret the results and to correlate them with practical experience.

It is obvious that many of these results indicate boron atomisation efficiencies that are not achieved in practice. The two major sources of this hiatus are: inaccuracies in the data or omission of species, and difficulties in predicting the actual temperatures and stoichiometries of practical flames. Another minor source of error is the departure of practical flames from ideal behaviour and equilibrium. This last consideration may be very serious under certain conditions completely vitiating the results but, the flame conditions studied were chosen to minimise this error.

The first category of possible error is largely imponderable. In the absence of evidence to suggest this type of error, no action may be taken. The possibility of this type of error should not be forgotten however.

The second source of error is somewhat more amenable to qualitative or semi-quantitative treatment.

The most easily eliminated source of error is that of flame temperature. All the flames have been considered over a range of temperatures to permit selection of the appropriate temperature for the conditions under study. Actual allocation of the temperature to be used is dependent upon the correct estimation or measurement of the temperature achieved in a practical flame. This is itself not a simple matter in many cases.

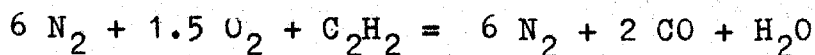
with the exception of the oxygen-cyanogen flame, the range considered may be assumed to be adequate to cover the range of practical flames used for AAS or atomic fluorescence spectroscopy(AFS). In the case of the oxygen cyanogen flame, the temperature of the water-containing flame is severely reduced and, the fuel-rich flame is also much lower in temperature than the stoichiometric flame. Nonetheless this flame would still be analytically useful even 1500K cooler than the theoretical maximum. The study considered such high temperatures merely to include data on the expected performance of very high-temperature flames. All flames studied show somewhat similar behaviour in that, as the stoichiometry varies from the ideal, the temperature falls. It must be noted that the equations used for the computer study give the flame composition accepted as 'stoichiometric' for each flame if the value of RED is taken as 1.0.

This choice and the choice of the range of RED values in each case (except for the nitrous oxide acetylene flame) places the analytically-useful region of flame stoichiometry in the centre of the CALCOMP plots. In the case of nitrous-oxide acetylene flames, the fuel-lean flame is not used in either AAS or AFS, and the useful range of stoichiometry is smaller. Hydrogen flames are generally burned considerably fuel-rich so that the analytically useful region is again in the centre of the plot. This practice leads to some reduction flame temperature from the theoretical maximum but gives better shielding from the surrounding atmosphere and a more stable flame. The optimum condition for these flames is one of slight fuel-richness to achieve the highest temperature possible consistent with a reducing atmosphere. The results of this study clearly show that the atomisation of an element with stable oxides is very sharply temperature-dependent and this is a severe limitation on the use of these flames.

The major conclusion to be drawn from this study about the usefulness of hydrogen flames is, that they are poor for AAS and AFS of refractory-oxide elements because of the sharp temperature-dependence of atomisation. Thermal effects are more important than chemical effects. Thus the most useful hydrogen flame is the hottest almost regardless of composition. The flame that fulfills this condition is the oxy-hydrogen flame and no advantage should result from using nitrous oxide as the oxidant.

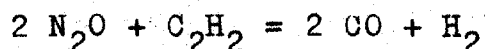
The evaluation of carbon-containing flames is more complex. In practice a balance must be maintained between the necessity of employing a strongly-reducing environment and that of maintaining a high-temperature one.

In the case of the air-acetylene flame the study results suggest that a fuel-rich flame (C/O ratio greater than 1) can be employed for the determination of boron by atomic spectroscopy. When such a flame is burnt however, it is found that the temperature is much less than the theoretical maximum. The accepted equation for the stoichiometric flame is:



and the C/O ratio is 0.66 at this stoichiometry. It is at once apparent that a flame having a C/O ratio of 1.0 is 50% fuel-rich. The probable temperature of such a flame is less than 2000K. JENKINS ³¹ states that such flames do not achieve complete thermal equilibrium for some distance above the primary reaction zone. Another characteristic of such a flame is the presence of solid carbon in relatively high concentrations. This solid carbon is much less effective a reducing agent than the gaseous carbon species. In addition, there is the possibility of occlusion of an analyte by the solid phase.

For the nitrous oxide acetylene flame the equation defining the stoichiometric flame is given by :



The C/O ratio at this stoichiometry is 1.0 and in contradistinction to the air acetylene flame, the major products are reducing agents. Basically it is this characteristic that makes the nitrous oxide flame so valuable for AAS and AFS of refractory-oxide elements. A very reducing, very high temperature environment may be maintained. Little of the carbon present in the flame appears as solid until the C/O ratio exceeds 1.1.

The significance of these criteria is emphasised by the

results of work by BUTLER & FULTON ¹³ , and DE GALAN & SAMAEY ⁸ who found that nitrous oxide alkane (propane or butane) flames were ineffective for atomic spectroscopy of refractory-oxide elements, although the temperatures achieved in these flames are of the same order as the nitrous oxide acetylene flame (2800K).

The reason given for this by DE GALAN & SAMAEY is that these flames achieve their maximum temperature at a C/O ratio of 0.29 to 0.35, and sooting commences at a C/O ratio of 0.55. The results of this study confirm that there would be no significant atomisation of a refractory-oxide element at this stoichiometry.

The major distinction of the acetylene flame is that the maximum temperature is achieved at a C/O ratio of about 1.0 and C/O ratios of up to 1.1 are achievable without excessive sooting.

The second main source of error inherent in interpreting the results of this study lies in the difficulty of assigning a set of mole numbers to describe a practical flame. The main source of this type of error is mixing with the ambient atmosphere by diffusion processes and turbulence.

As has been previously stated, no mathematical treatment has been attempted, but a qualitative account of some of these processes and techniques to reduce their importance is given below. Although of a general nature these comments apply to the particular case of boron in such flames.

The main diffusion effect observed in analytical flames is the inward diffusion of atmospheric oxygen leading to a reduction in free-atom concentration of any elements present that form refractory oxides.

This is a serious limitation and a number of techniques have been developed for preventing this diffusion. These take the form of separators to shield the flame gases from the surrounding atmosphere. Separation is achieved by using a solid, usually silica, separator or a stream of inert gas arranged to flow parallel to the flame gases.

Mechanical separators may be independently heated to extend the high-temperature interconal zone of flames over a greater volume than otherwise possible, giving increased path-length for AAS or AFS 32,33.

The major problems associated with the use of mechanical separators are; the cooling effect, contamination of the separator by analyte, or sooting of viewing windows if these are used. The first two effects may be reduced by external heating of the separator, but the usefulness of this is limited by the melting point of the separator material. This is about 2000K for silica, but in practice the maximum usable temperature is somewhat lower due to softening. Other refractories of higher melting point may be used such as alumina or silicon carbide. The latter has the advantage that it is electrically-conducting. Little work appears to have been carried out using these refractories.

Contamination of the separator is very difficult to eliminate completely and must normally be tolerated as a steady variation in background signal.

Gaseous separation has several obvious advantages; the smaller cooling effect, less contamination of the flame by retention of the analyte, and the transparency of the shield gas.

A variety of techniques have been used for gaseous

shielding, but all have the feature of producing a laminar flow of gas parallel to the axis of the flame.

The simplest and most effective separators employed consist of alternate strips of corrugated and flat sheet metal ^{34,35}, or short lengths of capillary tubing ³¹ .

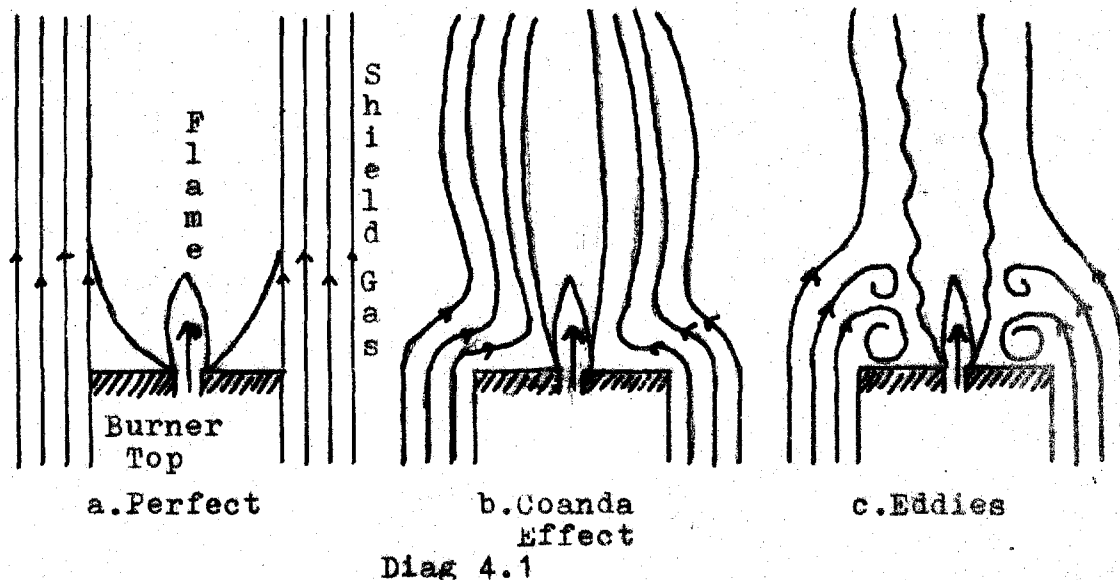
One difficulty encountered with these systems is the impossibility of ensuring matching of the velocities of the flame and shield gases. This leads to turbulence and mixing and a decrease in flame temperature. This decrease is about 300K for a nitrous oxide acetylene flame shielded with nitrogen and somewhat less for argon shielding ³⁶ . A further contributory factor is the removal of the secondary combustion zone from around the interconal zone. The possibility of shielding flames with other flames such as hydrogen diffusion flames or flames of the same composition as the inner one has been explored by SARGENT ¹⁹ . The use of hydrogen shielding was found to give reduced formation of such beneficial species as CN. The use of flames shielded by others of similar composition has been found to be advantageous and preliminary investigations by the author tended to confirm this.

The use of such flame shielding is not a complete solution as the analytical section of the flame is surrounded by a luminous outer cone strongly emitting in the range 305 to 345nm. For elements with resonance lines within this range this may be an insuperable difficulty.

The mixing of the shielding gas with the flame gas may well be exacerbated by the Coanda effect which may occur in some types of burner available. Diag.4.1a.& b. show this effect diagrammatically ³⁷.

This effect is less likely in burners using capillary separators as the gas streams from the capillaries break away immediately upon leaving the from the capillary tips. Subsequently the gas streams may remain laminar for a large distance above the separator. This behaviour is a consequence of the small diameter/length ratio of the capillaries. According to GAYDON & WOLFARD ³⁸ the minimum length of tube necessary to ensure laminar flow is given by the expression $L=0.06r.R$ where r is the radius of the tube and R is the Reynolds Number. For small capillaries the length of the tube is correspondingly small and high eflux velocities may be used before turbulence occurs.

The use of widely separated shield gas and burner gas orifices should be avoided, or the condition shown in Diag.- 4.1c. may well prevail.



The effect of poor aerodynamic design on analytical burners is best observed in the case of long-path separated burners.

Fuel rich flames burning on such burners almost invariably tend to break away from the top plate of the burner

at either end of the slot.

A simple consideration of the mixture flow properties of these burners indicates that the mixture flows more slowly from the ends of the slot, and the highest eflux velocity is at the centre.

This flame lifting at the ends must be due to the sideways flow of the shield gas across the top of the burner. The ends of the burner slot are more vulnerable to this effect because of their asymmetry with respect to this flow.

Shielding the slot with flow-fences on the top-plate reverses this trend and the flames tend to break away in the centre.

Another feature, possibly retrograde, in the aerodynamic design of burners is the introduction of burners with the top shaped to inhibit the build-up of solid carbon on the edges of the burner slot. These generally rely upon slot edges of thin section or raised above the level of the rest of the burner top. Presumably these edges heat up to a temperature at which the carbon is combusted. It follows however that, if a flame is so fuel-rich that elemental carbon is present in the combusted gas mixture in sufficient concentration to exceed the saturation vapour pressure, then there is no way of burning off deposited carbon using surplus oxidant in the fuel gas mixture. The necessary oxygen for this process must be derived from the atmosphere, and the efficacy of the design must rely upon a process deleterious to analytical flame spectroscopy.

It must be remembered that these effects will also be present in unshielded burners but, the net effect may well be much more serious because of the presence of free oxygen.

The plan of analytical burners is also important in determining the amount of inward diffusion of the surrounding atmosphere. Round plan burners have a smaller area of contact with the ambient atmosphere than long path slot burners of the conventional AAS pattern. This may well be implicated in the contradictory results claimed for the nitrous oxide hydrogen flame ^{12,15}. Round flame burners are however not as suitable for AAS as long path ones, and it may be necessary to employ multi-pass arrangements to secure the full advantage of the larger interconal volume produced by these burners.

There is one more diffusion effect which is present in flames. This is the selective outward diffusion of low molecular weight species. This diffusion process leads to a reduction in the actual concentration of such species as atomic and molecular hydrogen in the centre of the flame. Again no treatment of this process has been attempted in this study.

Notwithstanding these criticisms, it is concluded, that the ideal systems described and studied in this investigation approximate reasonably closely to the conditions prevailing in the interconal zones of hot flames burning premixed fuel mixtures. It is to be expected that closer agreement will be obtained for flames where this zone is extended such as those produced by the technique of flame shielding.

Insofar as the results of this study apply to the flame atomic spectroscopy of boron, it is concluded that the most suitable flame type for this work is a high temperature (greater than 2800K) carbon fuelled flame burning at a C/O ratio greater than unity. The most suitable flames for this are the oxygen cyanogen, nitrous oxide acetylene, and very

fuel-rich oxygen acetylene flames.

Comparison of practical results with this study is difficult as so few results have been reported by other workers. Table 4.7 gives the relevant results from the study by DE GALAN et al.⁸ with the comparable results from this study. As so few results are comparable, it is difficult to draw any firm conclusions and the matter must be held in abeyance pending any further work measuring practical atomisation levels in analytical flames. Generally the results do not appear to be contradictory and the conclusions drawn by DE GALAN are supported by this study.

Bibliography

1. R.C.Oliver, S.E.Stephanou, R.W.Baier
Chemical Engineering Feb.19 121 (1962)
2. W.B.White, S.M.Johnson, G.B.Dantzig
Journal of Chemical Physics 28 751 (1958)
3. B.R.Kubert, S.E.Stephanou
'Kinetics, Equilibria and Performance of High Temperature Systems' Edited G.S.Bahn, E.E.Zukoski
Butterworths London (1960)
4. C.H.Anderson
Paper presented at the Pittsburgh Conference on Analytical Chemistry and Applied Spectroscopy. March 1968
5. B.F.Dodge
'Chemical Engineering Thermodynamics' p526
McGraw Hill New York (1944)
6. JANAF Interim Thermochemical Tables
Dow Chemical Corp. Midland Mich.
7. R.Mavrodineanu, H.Boiteux
'Flame Spectroscopy' Wiley New York (1965)
8. L.de Galan, G.F.Samaey
Spectrochimica Acta 25B 245 (1970)

9. R.Herrmann,C.T.J.Alkemade
'Flame Photometry' Interscience New York (1963)
10. V.A.Fassel,R.B.Myers,R.N.Knisely
Spectrochimica Acta 19 1187 (1963)
11. R.Friedman
3rd. Symposium on Combustion p110
Williams & Wilkins Baltimore (1949)
12. R.Smith,C.M.Stafford,J.D.Winefordner
Analytical Chemistry 41 946 (1969)
13. L.R.P.Butler,H.A.Fulton
Applied Optics 7 2131 (1968)
14. J.B.Willis
Applied Optics 7 1295 (1968)
15. R.M.Dagnall,K.C.Thompson,T.S.West
Analyst 93 153 (1968)
16. J.B.willis,V.A.Fassel,J.A.Fiorino
Spectrochimica Acta 24B 157 (1969)
17. M.P.Bratzel Jr.,R.M.Dagnall,J.D.winefordner
Analytical Chemistry 41 1527 (1969)

18. E.Pungor
'Flame Photometry Theory' p162
D.Van Nostrand Co. London (1967)
19. M.Sargent
Ph.D.Thesis London (1970)
20. D.W.Golightly
U.S.A.E.C. Published Report 15-T-26 (1965)
21. M.D.Amos, J.B.Willis
Spectrochimica Acta 22 1325 (1966)
22. G.F.Kirkbright, M.K.Peters, T.S.West
Talanta 14 789 (1967)
23. G.F.Kirkbright, M.K.Peters, M.Sargent, T.S.West
Talanta 15 663 (1968)
24. A.Hell, W.F.Ulrich, N.Shifrin, J.Ramirez-Munoz
Applied Optics 7(7) 1317 (1968)
25. G.F.Kirkbright, M.Sargent, T.S.West
Talanta 16 1467 (1969)
26. J.B.Willis, J.O.Rasmuson, R.N.Kniseley, V.A.Fassel
Spectrochimica Acta 23B 725 (1968)

27. N.Thomas, A.G.Gaydon, L.Brewer
Journal of Chemical Physics 20 369 (1952)
28. J.B.Conway, A.V.Grosse, R.H.wilson Jr.
J.A.C.S. 76 499 (1953)
29. A.F.Bartholmay, B.F.Vallee
Analytical Chemistry 28 1753 (1956)
30. A.D.Kirshenbaum, A.V.Grosse
J.A.C.S. 78 2020 (1956)
31. D.R.Jenkins
Spectrochimica Acta 25B(2) 47 (1970)
32. D.N.Hingle, G.F.Kirkbright, T.S.West
Analyst 93 522 (1968)
33. D.N.Hingle, G.F.Kirkbright, T.S.west
ibid. 94 864 (1969)
34. R.S.Hobbs, G.F.Kirkbright, M.Sargent, T.S.west
Talanta 15 997 (1968)
35. R.S.Hobbs, G.F.Kirkbright, T.S.west
Analyst 94 554 (1969)
36. S.Vetter
Personal communication.

37. I.Reba

Scientific American 214(6) 84 (1966)

38. A.G.Gaydon,H.G.Wolfhard

'Flames' Chapman Hall London (1953)

Table 4.1 a.

Species Considered for Boron-containing Flames.

B	BO	BO ₂
BC	BH ₂ O ₂	BH ₃
H ₃ BO ₃	BN	B ₂ H ₆
B ₂ O ₂	B ₃ O ₃ N ₃	B ₃ N ₃ H ₆
BH	HBO	HBO ₂
BH ₂	B ₂	B ₂ O ₃
B ₃ H ₃ O ₆	B ₁₀ H ₁₄	B ₅ H ₉
C	C ₂	C ₃
CH	CH ₂	CH ₃
CH ₄	C ₂ H ₄	C ₂ H ₂
CN	HCN	HCNO
C ₂ N ₂	CHO	CH ₂ O
CO	CO ₂	H
H ₂	OH	H ₂ O
O	O ₂	HO ₂
N	N ₂	NH
NH ₂	NOH	NO
NO ₂	N ₂ O	
B(c)	BN(c)	B ₂ O ₃ (c)
C(c)		

c = condensed

Table 4.1 b.Species Considered for Nitrous-oxide & Air Hydrogen Flames.

B	BO	BO ₂
HBO	HBO ₂	B ₂ O ₂
B ₂ O ₃	H ₃ BO ₃	BH
BH ₂	BH ₃	H
H ₂	O	O ₂
OH	H ₂ O	N
N ₂	NH	NH ₂
NO	NO ₂	N ₂ O

Table 4.1 c.Species Considered for Nitrous-oxide & Air AcetyleneFlames.

B	BO	BO ₂
B ₂ O ₂	B ₂ O ₃	HBO
HBO ₂	H ₃ BO ₃	BH
BH ₂	BH ₃	BC
C	C ₂	C ₃
CN	HCN	C ₂ N ₂
HCNO	CH	CH ₂
CH ₃	CH ₄	C ₂ H ₂
CHO	CH ₂ O	CO
CO ₂	H	H ₂
OH	H ₂ O	O
O ₂	N	N ₂
NH	NH ₂	NO
C(c)		

c = condensed

Table 4.1 d.Species Considered for Oxygen Cyanogen Flame.

B	BO	BO ₂
B ₂ O ₂	B ₂ O ₃	HBO
HBO ₂	H ₃ BO ₃	BH
BH ₂	BH ₃	BN
BC	C	C ₂
C ₃	CN	HCN
C ₂ N ₂	HCNO	CH
CH ₂	CH ₃	CHO
CH ₂ O	CO	CO ₂
H	H ₂	OH
H ₂ O	HO ₂	O
O ₂	N	N ₂
NH	NH ₂	NO
NO ₂	N ₂ O	NOH

Table 4.2

Results for the Air Hydrogen Flame.

H/O Ratio Species & Temp.	2.000	3.778	5.555
H ₂ 2000k	3.21E-01	2.42E+01	3.90E+01
2300k	1.18E+00	2.40E+01	3.86E+01
2600k	3.07E+00	2.34E+01	3.75E+01
H 2000k	9.17E-03	7.97E-02	1.01E-01
2300k	1.04E-01	4.72E-01	5.99E-01
2600k	6.70E-01	1.85E+00	2.34E+00
O 2000k	2.11E-05	2.15E-05	1.07E-05
2300k	2.98E-02	1.16E-03	5.78E-04
2600k	2.21E-01	2.48E-02	1.25E-02
O ₂ 2000k	1.01E-01	1.05E-05	2.62E-06
2300k	3.66E-01	5.50E-04	1.37E-04
2600k	9.16E-01	1.15E-02	2.92E-03
OH 2000k	1.05E-01	9.27E-03	5.88E-03
2300k	5.08E-01	8.90E-02	5.65E-02
2600k	1.62E+00	5.00E-01	3.19E-01
B 2000k	2.13E-13	1.69E-10	7.63E-10
2300k	1.98E-10	2.16E-08	9.79E-08
2600k	3.77E-08	8.67E-07	3.92E-06
BO 2000k	1.35E-04	1.36E-03	2.46E-03
2300k	4.08E-03	2.16E-02	3.91E-02
2600k	5.36E-02	1.72E-01	3.14E-01
BO ₂ 2000k	2.03E+00	2.59E-01	1.86E-01
2300k	7.52E+00	1.93E+00	1.40E+00
2600k	1.92E+01	8.57E+00	6.35E+00
HBO 2000k	6.08E-06	4.87E-04	1.22E-03
2300k	1.34E-04	2.93E-03	7.35E-03
2600k	1.36E-03	1.11E-02	2.79E-02
HBO ₂ 2000k	9.78E+01	9.96E+01	9.97E+01
2300k	9.24E+01	9.80E+01	9.85E+01
2600k	8.07E+01	9.12E+01	9.33E+01
B ₂ O ₃ 2000k	2.72E-03	3.41E-03	4.35E-03
2300k	3.87E-03	5.11E-03	6.56E-03
2600k	4.50E-03	6.33E-03	8.35E-03
H ₃ BO ₃ 2000k	1.83E-01	1.50E-01	1.15E-01
2300k	4.47E-02	3.94E-02	3.04E-02
2600k	1.32E-02	1.34E-02	1.05E-02

Table 4.3

Results for the Nitrous Oxide Hydrogen Flame.

H/O Ratio		2.000	3.882	5.764
Species & Temp.				
H	2400K	2.30E-01	8.98E-01	1.10E+00
	2800K	2.04E+00	4.49E+00	5.49E+00
	3200K	9.35E+00	1.45E+01	1.73E+01
H ₂	2400K	2.10E+00	3.21E+01	4.85E+01
	2800K	6.27E+00	3.04E+01	4.55E+01
	3200K	1.12E+01	2.70E+01	3.81E+01
O	2400K	7.08E-02	3.31E-03	1.65E-03
	2800K	7.42E-01	1.24E-01	6.33E-02
	3200K	3.82E+00	1.53E+00	8.79E-01
O ₂	2400K	6.76E-01	1.47E-03	3.69E-04
	2800K	1.90E+00	5.29E-02	1.38E-02
	3200K	3.19E+00	5.09E-01	1.69E-01
OH	2400K	9.99E-01	1.83E-01	1.12E-01
	2800K	3.74E+00	1.38E+00	8.58E-01
	3200K	7.81E+00	4.86E+00	3.32E+00
B	2400K	9.07E-10	1.15E-07	3.74E-07
	2800K	4.66E-07	8.91E-06	2.87E-05
	3200K	5.48E-05	2.69E-04	7.18E-04
BO	2400K	8.20E-03	4.84E-02	7.92E-02
	2800K	1.71E-01	5.46E-01	8.96E-01
	3200K	1.59E+00	3.11E+00	4.79E+00
BO ₂	2400K	9.63E+00	2.64E+00	2.11E+00
	2800K	2.80E+01	1.50E+01	1.25E+01
	3200K	5.30E+01	4.15E+01	3.68E+01
HBO	2400K	2.76E-04	6.35E-03	1.28E-02
	2800K	4.17E-03	2.93E-02	5.89E-02
	3200K	2.73E-02	8.33E-02	1.52E-01
HBO ₂	2400K	9.03E+01	9.73E+01	9.78E+01
	2800K	7.18E+01	8.45E+01	8.65E+01
	3200K	4.54E+01	5.53E+01	5.83E+01
B ₂ O ₃	2400K	2.54E-03	4.17E-03	5.58E-03
	2800K	2.80E-03	4.92E-03	6.77E-03
	3200K	2.27E-03	3.68E-03	5.05E-03
H ₃ BO ₃	2400K	4.29E-02	3.30E-02	2.50E-02
	2800K	8.88E-03	8.47E-03	6.61E-03
	3200K	1.46E-03	1.72E-03	1.47E-03

Table 4.4

Results for the Air Acetylene Flame.

C/O Ratio		0.593	0.889	1.185
Species & Temp.				
C	2000K	3.83E-14	6.29E-13	3.34E-09
	2300K	3.39E-12	5.72E-11	9.07E-07
	2600K	1.11E-10	1.84E-08	6.72E-05
CN	2000K	1.77E-08	2.69E-07	1.37E-03
	2300K	1.09E-07	1.70E-06	2.58E-02
	2600K	4.57E-07	7.04E-06	2.42E-01
HCN	2000K	4.47E-06	1.11E-04	6.52E-01
	2300K	3.82E-06	9.99E-05	1.73E+00
	2600K	3.52E-06	9.16E-05	3.52E+00
H ₂	2000K	5.60E+00	1.47E+01	1.98E+01
	2300K	5.19E+00	1.45E+01	1.90E+01
	2600K	4.84E+00	1.38E+01	1.72E+01
O	2000K	3.08E-05	3.18E-06	6.47E-10
	2300K	1.84E-03	1.81E-04	1.23E-08
	2600K	4.15E-02	4.07E-03	1.19E-07
B	2000K	2.44E-10	1.42E-08	2.75E-02
	2300K	2.58E-08	1.61E-06	2.00E+00
	2600K	8.88E-07	5.75E-05	1.85E+01
BO	2000K	2.25E-03	1.35E-02	5.33E+00
	2300K	3.28E-02	2.02E-01	1.70E+01
	2600K	2.37E-01	1.50E+00	1.42E+01
BO ₂	2000K	4.94E-01	2.72E-01	2.45E-02
	2300K	3.73E+00	2.26E+00	1.29E-02
	2600K	1.59E+01	9.92E+00	2.75E-03
HBO	2000K	4.24E-04	4.12E-03	1.88E+00
	2300K	2.25E-03	2.32E-02	2.24E+00
	2600K	7.56E-03	8.11E-02	8.54E-01
HBO ₂	2000K	9.95E+01	9.96E+01	9.28E+00
	2300K	9.62E+01	9.74E+01	6.37E-01
	2600K	8.38E+01	8.84E+01	2.73E-02
B ₂ O ₃	2000K	9.05E-03	3.02E-02	9.42E-01
	2300K	1.26E-02	4.30E-02	2.01E-02
	2600K	1.37E-02	4.93E-02	1.26E-04
BH ₂	2000K	3.76E-08	5.75E-06	1.50E+01
	2300K	2.22E-07	3.87E-05	6.33E+01
	2600K	8.31E-07	1.54E-04	6.15E+01
BC	2000K	4.72E-20	4.50E-17	4.63E-07
	2300K	1.26E-17	1.33E-14	2.62E-04
	2600K	9.12E-16	9.79E-13	1.15E-02
C(S)	2000K	0	0	1.36E+01
	% of 2300K	0	0	9.89E+00
	Total 2600K	0	0	2.55E+00

Table 4.5

Results for the Nitrous Oxide Acetylene flame.

C/O Ratio		0.941	1.035	1.129
Species & Temp.				
C	2400K	5.65E-10	2.55E-06	4.29E-06
	2800K	3.46E-08	1.61E-04	5.25E-04
	3200K	8.30E-07	3.00E-03	1.04E-02
CN	2400K	6.75E-06	2.96E-02	4.90E-02
	2800K	6.61E-05	1.62E-01	5.15E-01
	3200K	1.37E-04	5.77E-01	1.60E+00
HCN	2400K	2.70E-04	1.24E+00	2.10E+00
	2800K	2.39E-04	1.13E+00	3.57E+00
	3200K	2.17E-04	8.02E-01	2.68E+00
H ₂	2400K	1.97E+01	2.18E+01	2.26E+01
	2800K	1.80E+01	2.00E+01	1.98E+01
	3200K	1.40E+01	1.56E+01	1.57E+01
O	2400K	2.84E-04	6.48E-08	3.78E-08
	2800K	1.14E-02	2.52E-06	7.57E-07
	3200K	1.63E-01	4.62E-05	1.31E-05
B	2400K	1.96E-05	3.34E+00	3.89E+00
	2800K	1.23E-03	2.75E+01	3.70E+01
	3200K	2.13E-02	6.47E+01	7.74E+01
BO	2400K	7.10E-01	2.76E+01	1.88E+01
	2800K	6.90E+00	3.43E+01	1.38E+01
	3200K	2.63E+01	1.98E+01	7.67E+00
BO ₂	2400K	3.34E+00	2.97E-02	1.18E-02
	2800K	1.73E+01	1.91E-02	2.32E-03
	3200K	3.73E+01	9.16E-03	8.76E-04
HBO ₂	2400K	9.58E+01	8.95E-01	3.62E-01
	2800K	7.54E+01	8.76E-02	1.05E-02
	3200K	3.59E+01	9.29E-03	8.90E-04
HBO	2400K	7.30E-02	2.98E+00	2.07E+00
	2800K	2.86E-01	1.50E+00	6.00E-01
	3200K	5.07E-01	4.62E-01	1.56E-01
B ₂ O ₃	2400K	4.70E-02	1.61E-02	4.40E-03
	2800K	4.46E-02	2.42E-04	1.19E-05
	3200K	1.83E-02	3.82E-06	1.24E-07
BH ₂	2400K	2.95E-04	5.54E+01	6.72E+01
	2800K	1.32E-03	3.28E+01	4.37E+01
	3200K	2.64E-03	8.93E+01	1.07E+01
BC	2400K	5.92E-13	4.56E-04	8.93E-04
	2800K	8.74E-11	9.08E-03	1.42E-01
	3200K	3.12E-09	3.42E-02	1.42E-01
C(s)	2400K	0	0	5.73E+00
	% of 2800K	0	0	0
	Total 3200K	0	0	0

Table 4.6

Results for the Oxygen Cyanogen Flame.

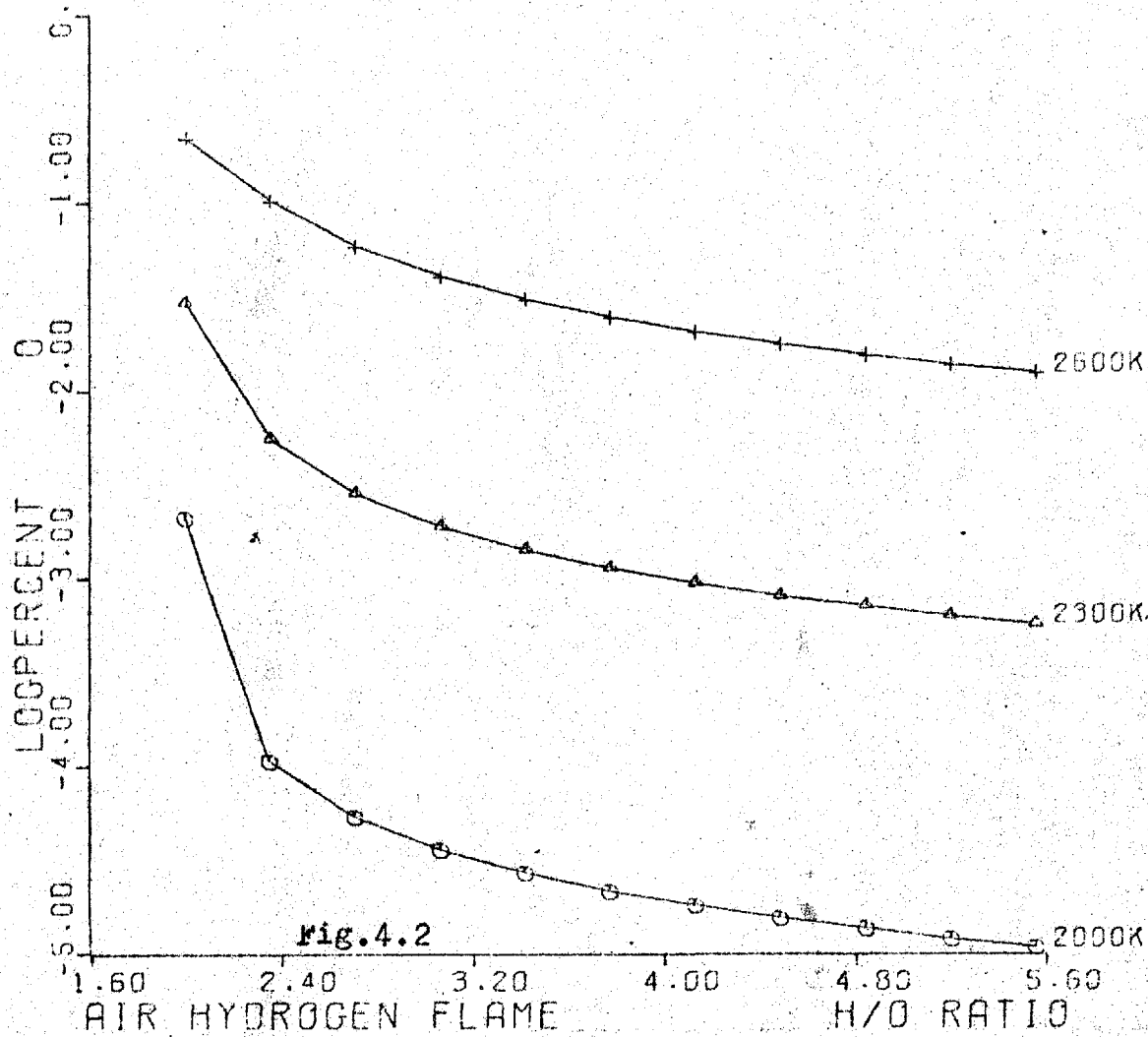
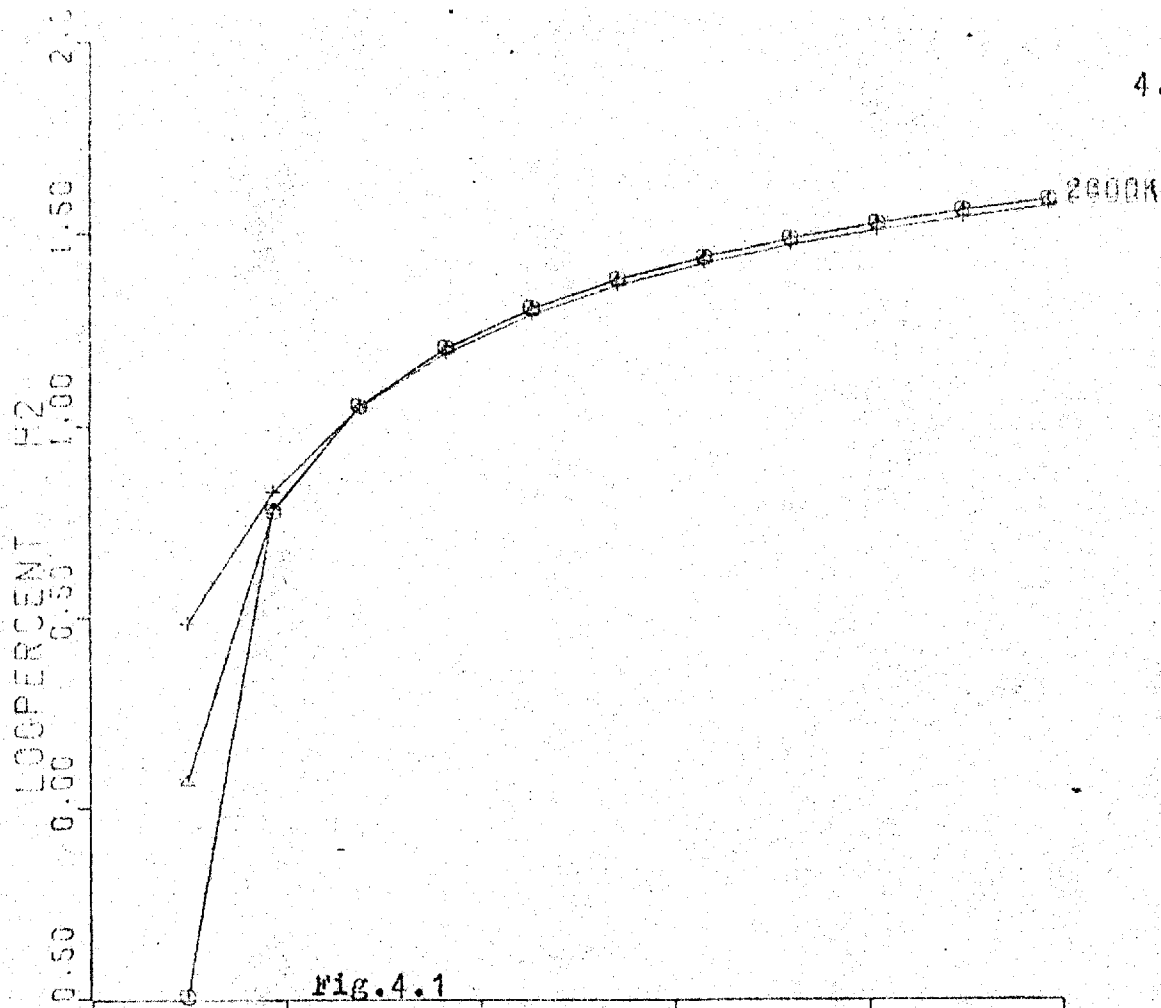
C/O Ratio		0.683	0.976	1.268
Species & Temp.				
C	4100K	8.55E-05	1.50E-03	1.38E+00
	4500K	1.34E-03	2.29E-02	2.92E+00
	4900K	1.42E-02	1.93E-01	4.95E+00
CN	4100K	7.11E-04	1.42E-02	1.23E+01
	4500K	4.60E-03	9.00E-02	1.10E+01
	4900K	2.34E-02	3.63E-01	8.99E+00
O	4100K	1.85E+01	1.35E+00	1.27E-03
	4500K	2.08E+01	1.56E+00	1.04E-02
	4900K	2.16E+01	2.02E+00	6.74E-02
B	4100K	2.06E-01	5.34E+00	9.79E+01
	4500K	2.35E+00	2.86E+01	9.80E+01
	4900K	1.32E+01	6.34E+01	9.79E+01
BO	4100K	4.63E+01	8.73E+01	1.50E+00
	4500K	7.67E+01	7.00E+01	1.60E+00
	4900K	8.06E+01	3.63E+01	1.87E+00
BO ₂	4100K	5.32E+01	7.31E+00	1.18E-04
	4500K	2.09E+01	1.42E+00	2.18E-04
	4900K	6.20E+00	2.61E-01	4.47E-04
B ₂ O ₃	4100K	5.59E-04	1.49E-04	3.98E-11
	4500K	8.70E-05	5.66E-06	1.90E-11
	4900K	8.29E-06	1.65E-07	1.38E-11
BC	4100K	7.00E-08	3.17E-05	5.34E-01
	4500K	3.72E-06	7.76E-04	3.40E-01
	4900K	8.04E-05	5.27E-03	2.08E-01
BN	4100K	6.09E-05	1.79E-03	3.11E-02
	4500K	8.44E-04	1.17E-02	3.84E-02
	4900K	5.55E-03	3.04E-02	4.55E-02

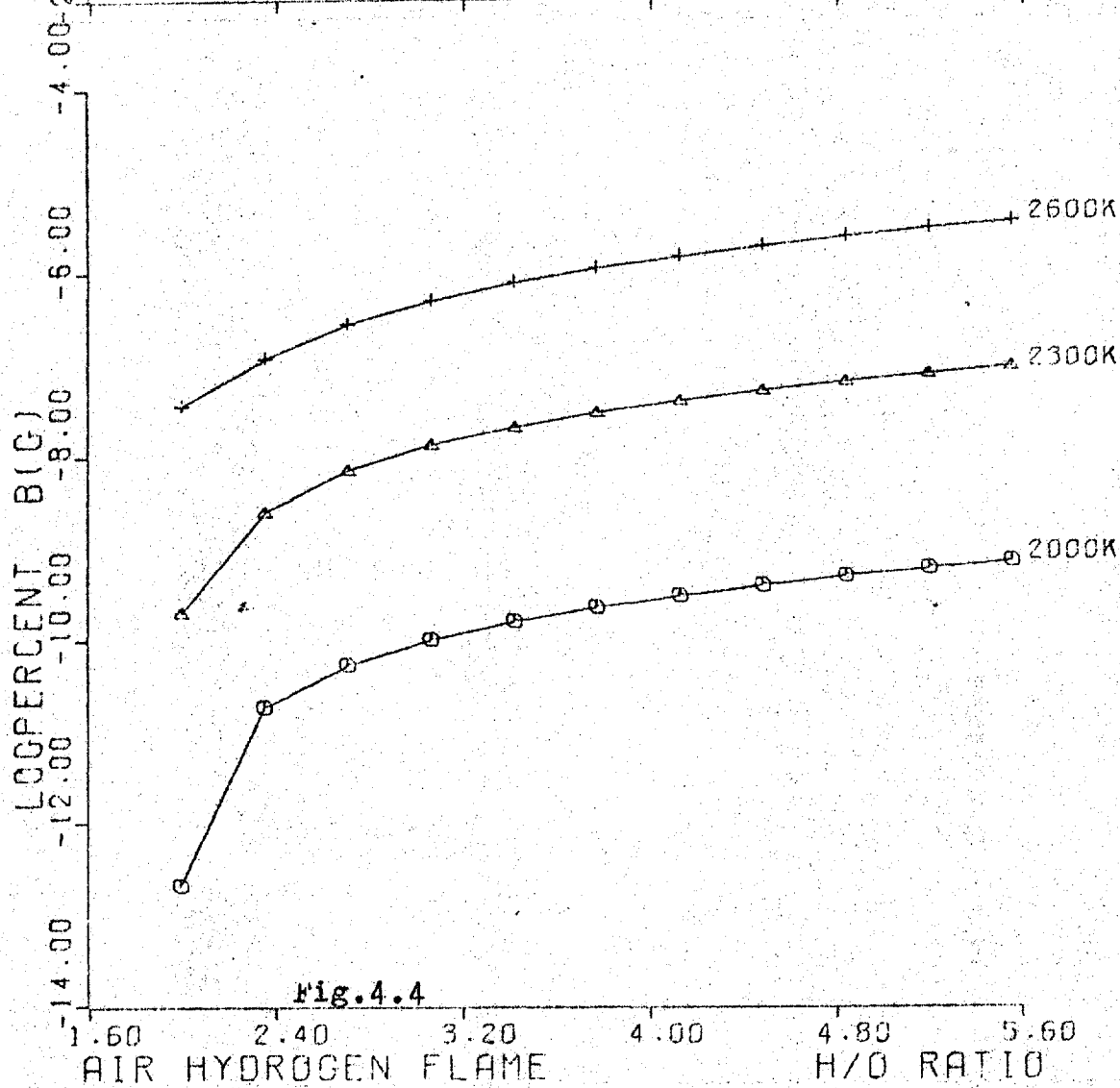
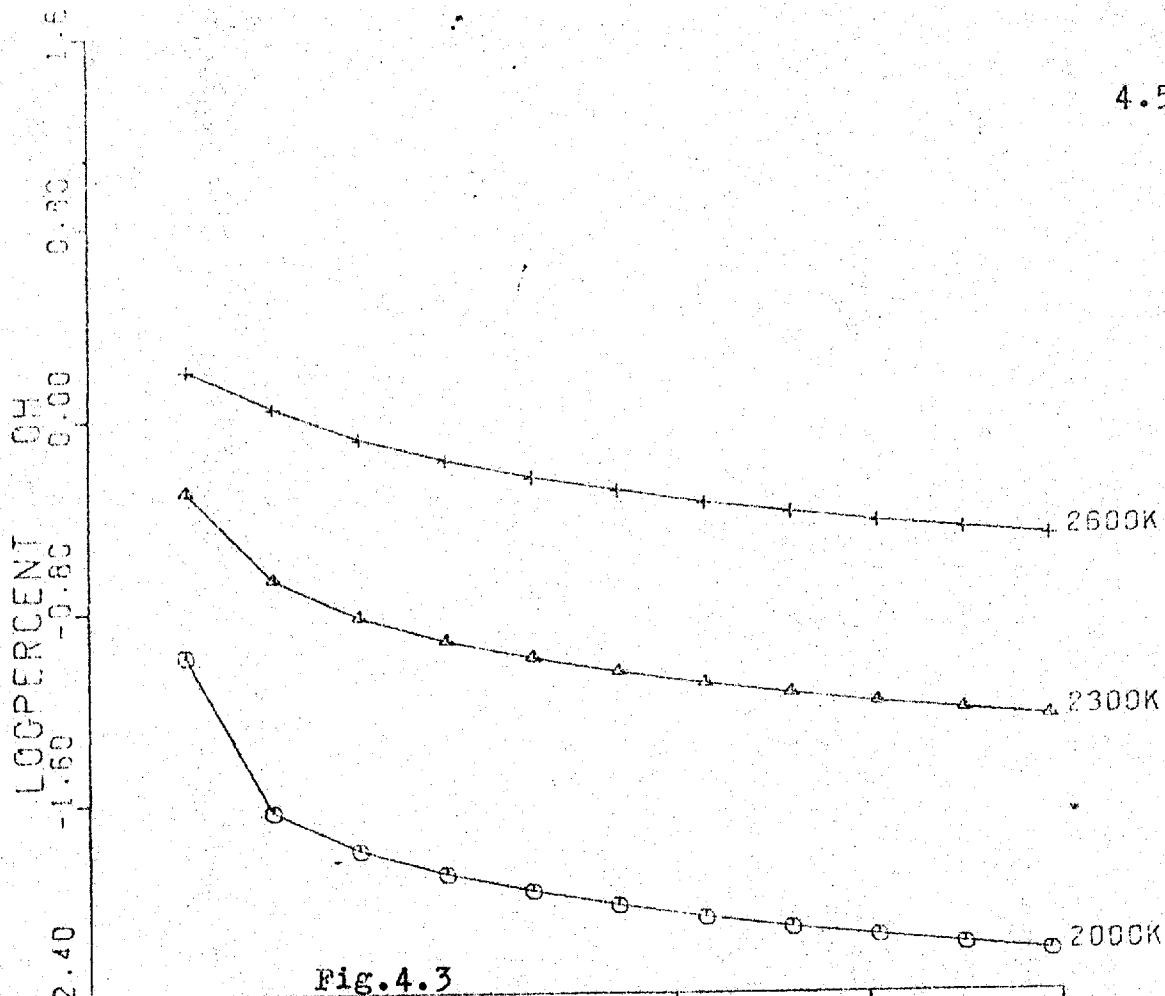
Table 4.7

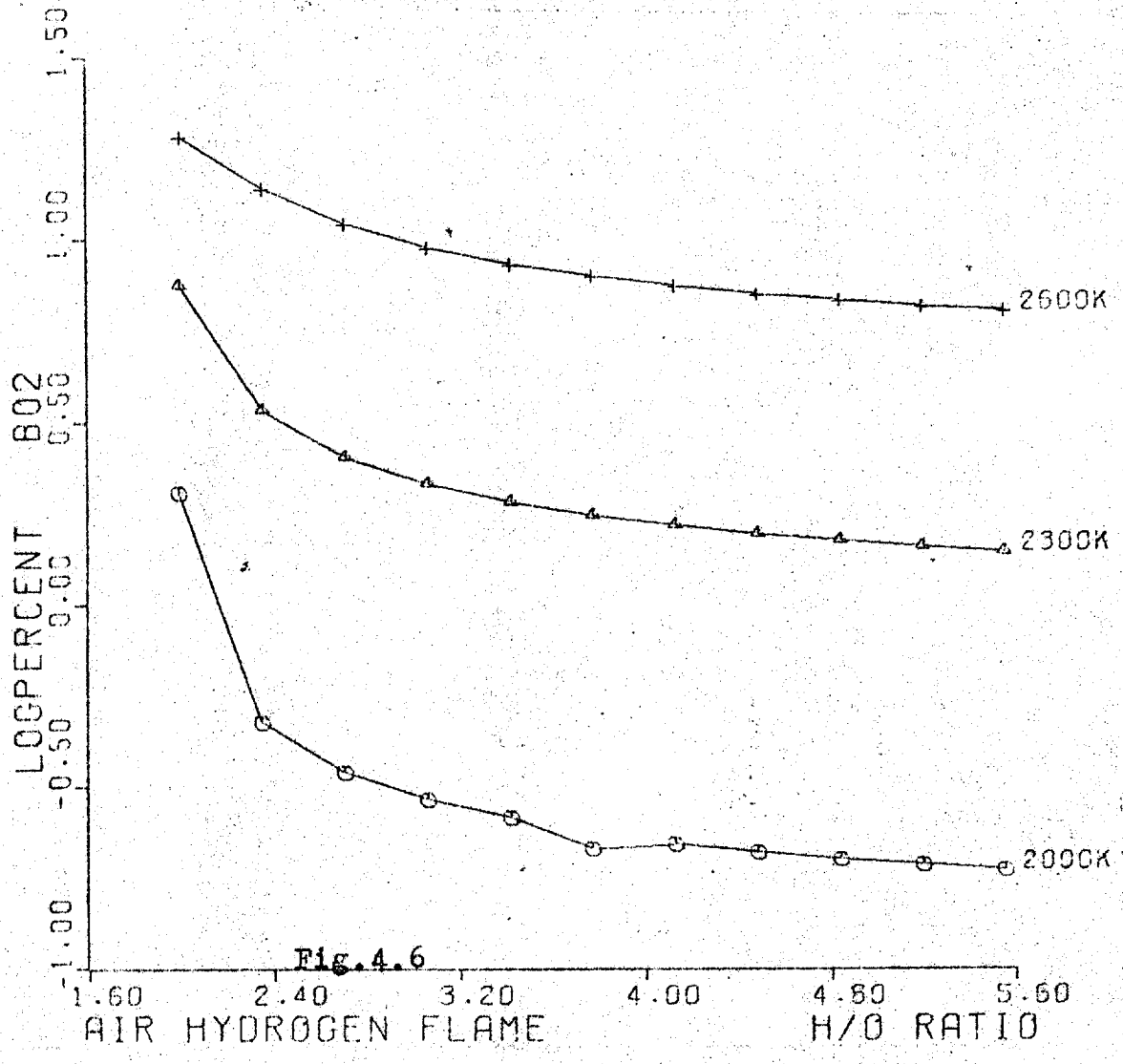
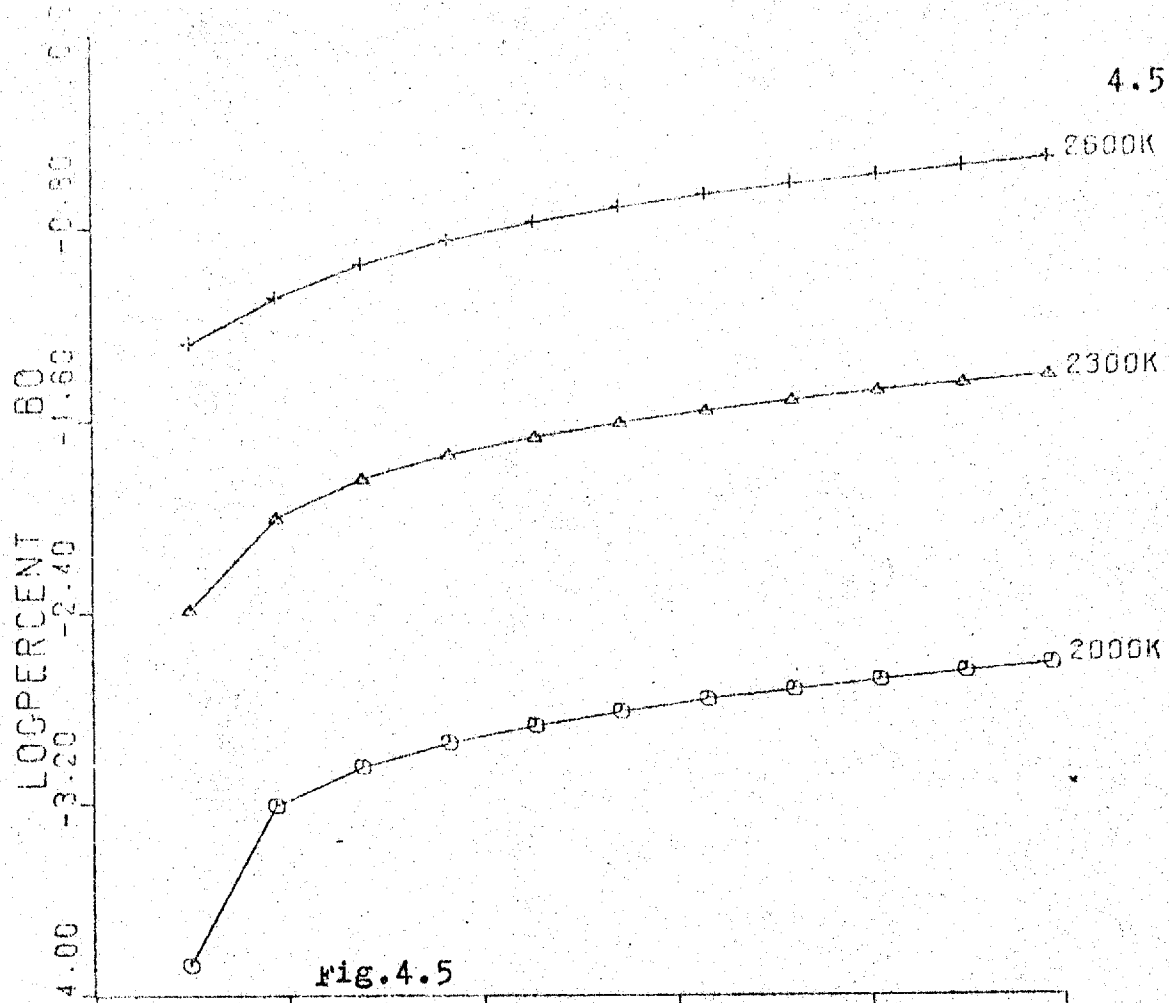
Comparison of Results from this Study and DE GALAN and

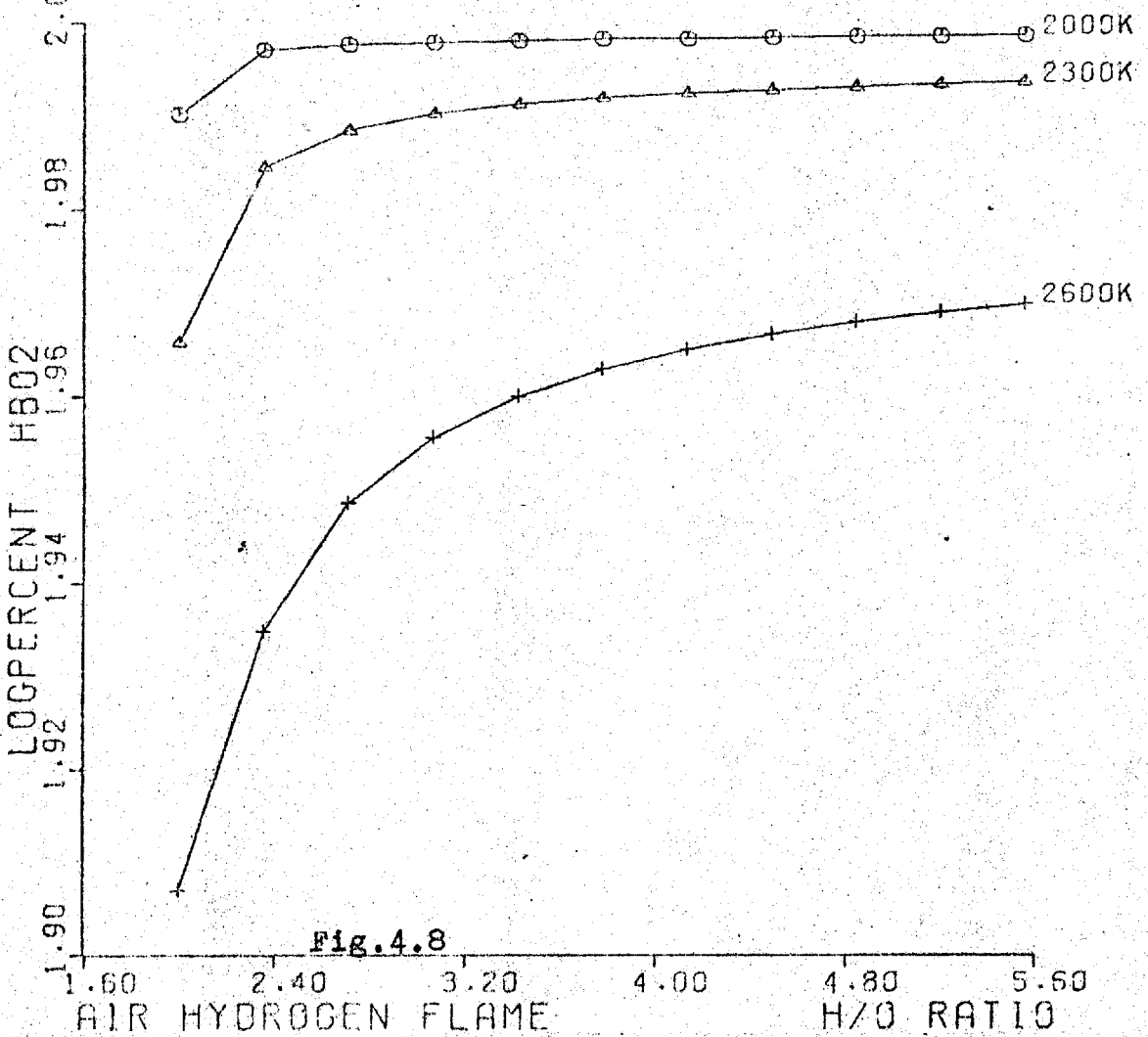
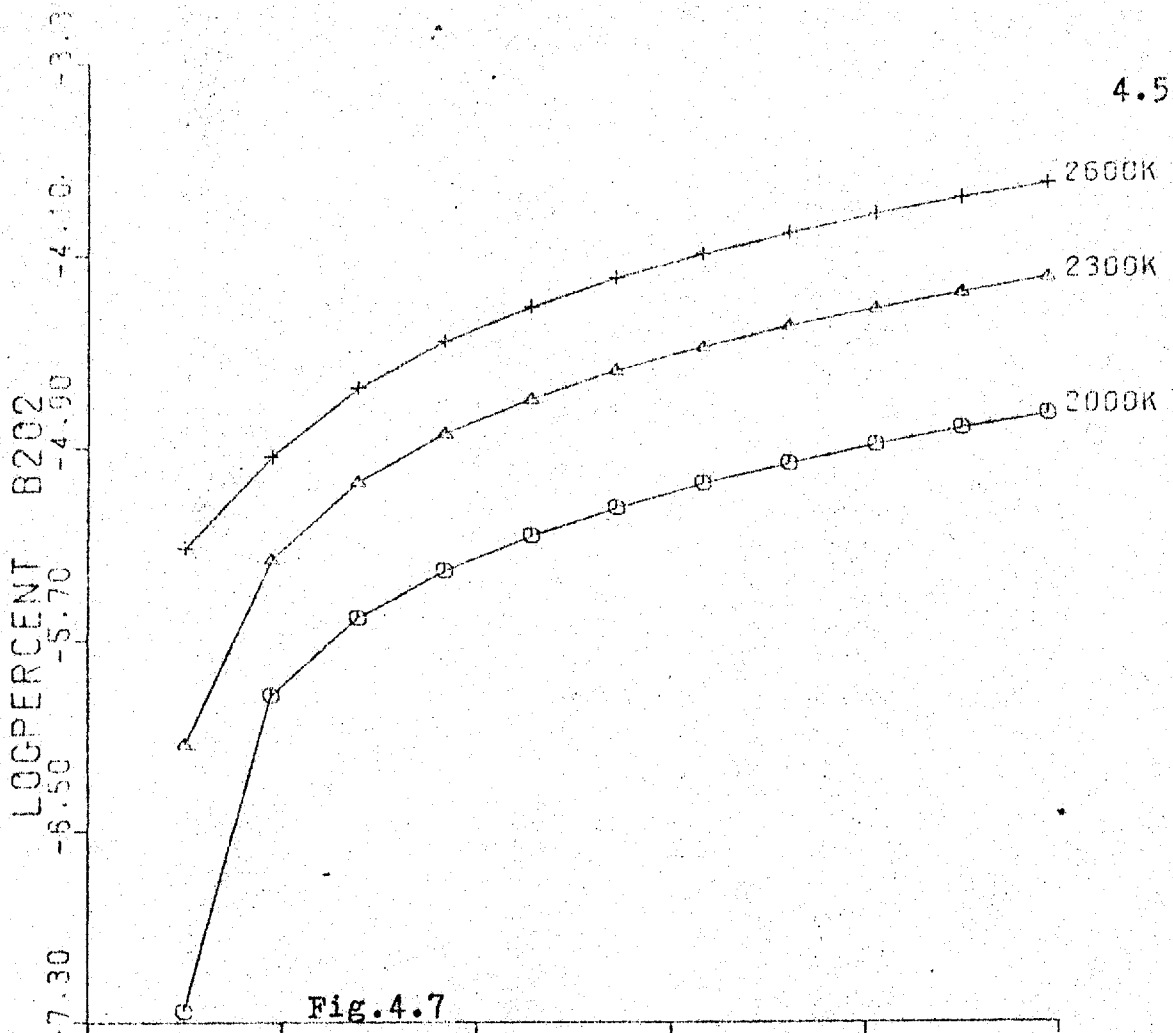
SAMAËY 8.

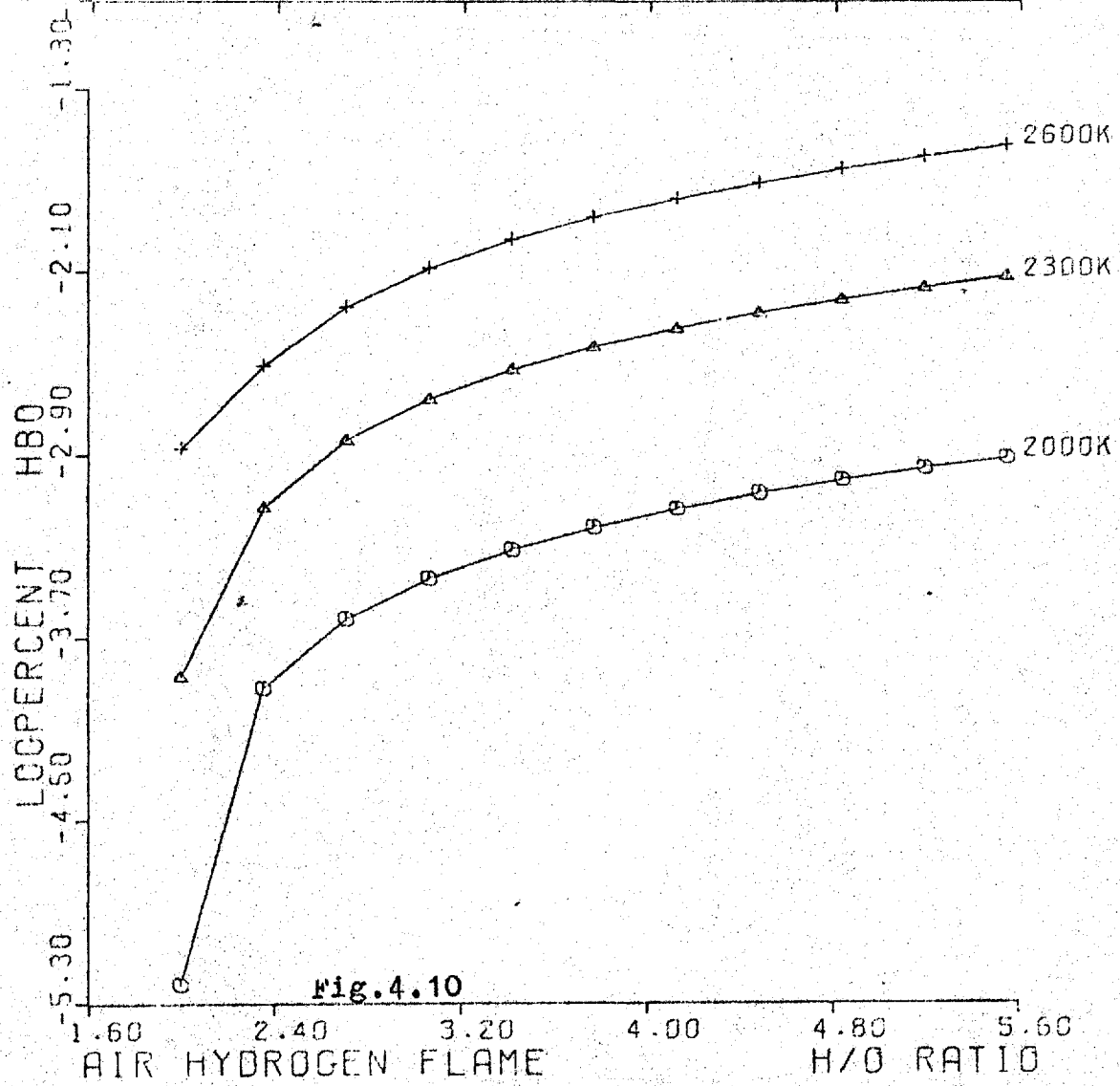
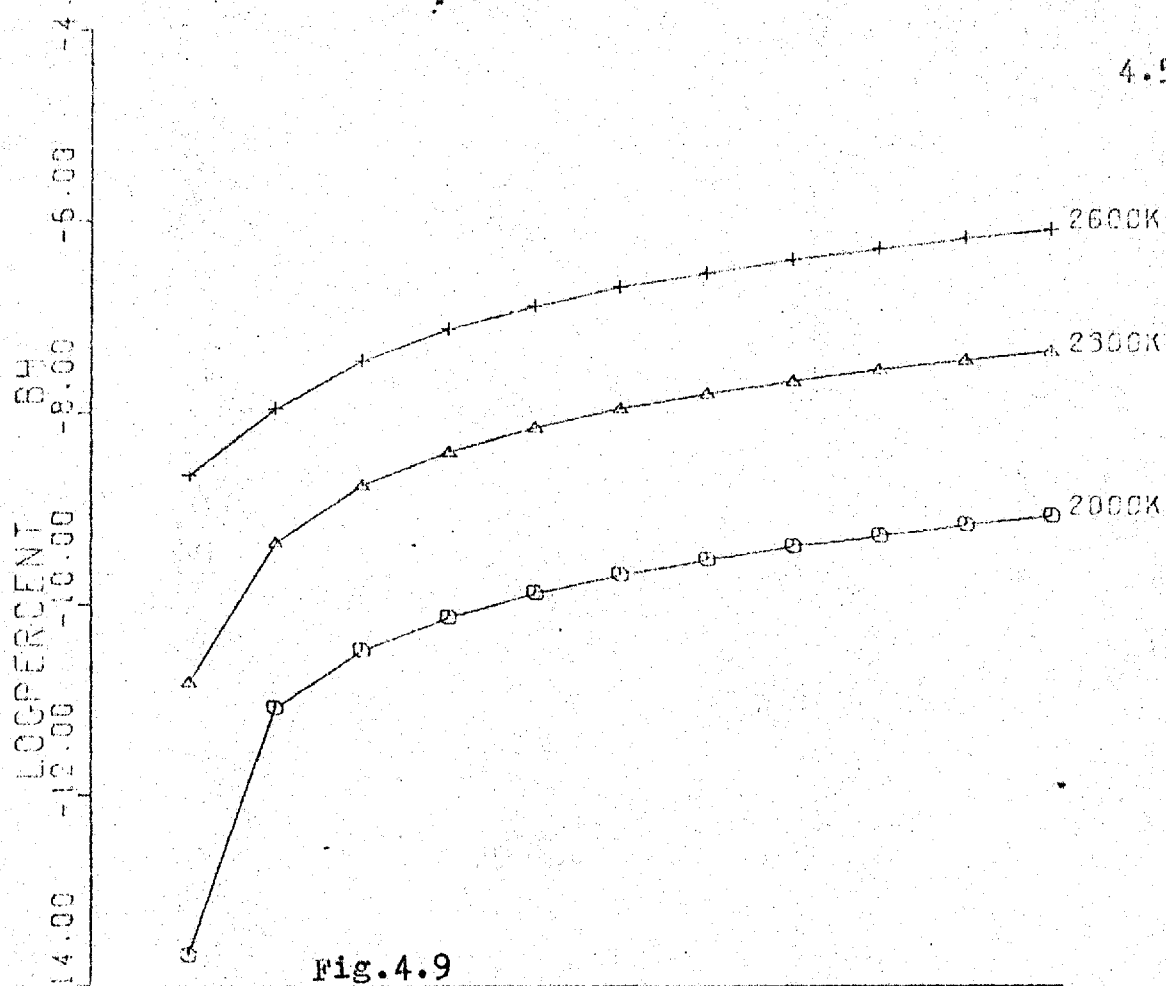
Flame	Temp. Deg.K.	H/O or C/O Ratio	de Galan	This Study
Air/H ₂	2000	5.12	1.0E-03	6.3E-12
N ₂ O/H ₂	2900	3.35	1.0E-03	1.0E-07
Air/C ₂ H ₂	2450	0.45(0.59)	6.0E-04	3.0E-09
N ₂ O/C ₂ H ₂	2950	0.89(0.94)	3.5E-03	2.8E-05











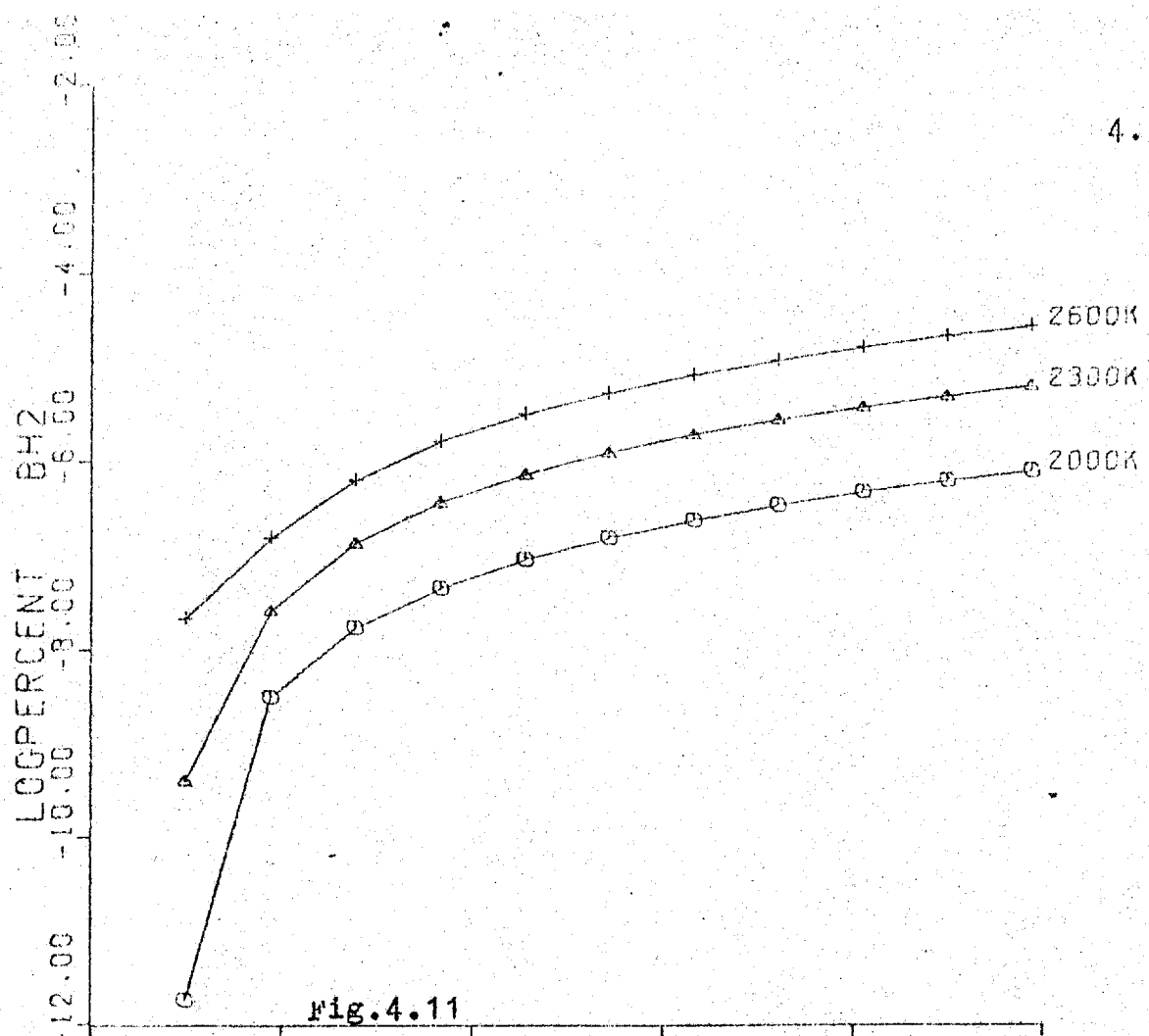


Fig. 4.11

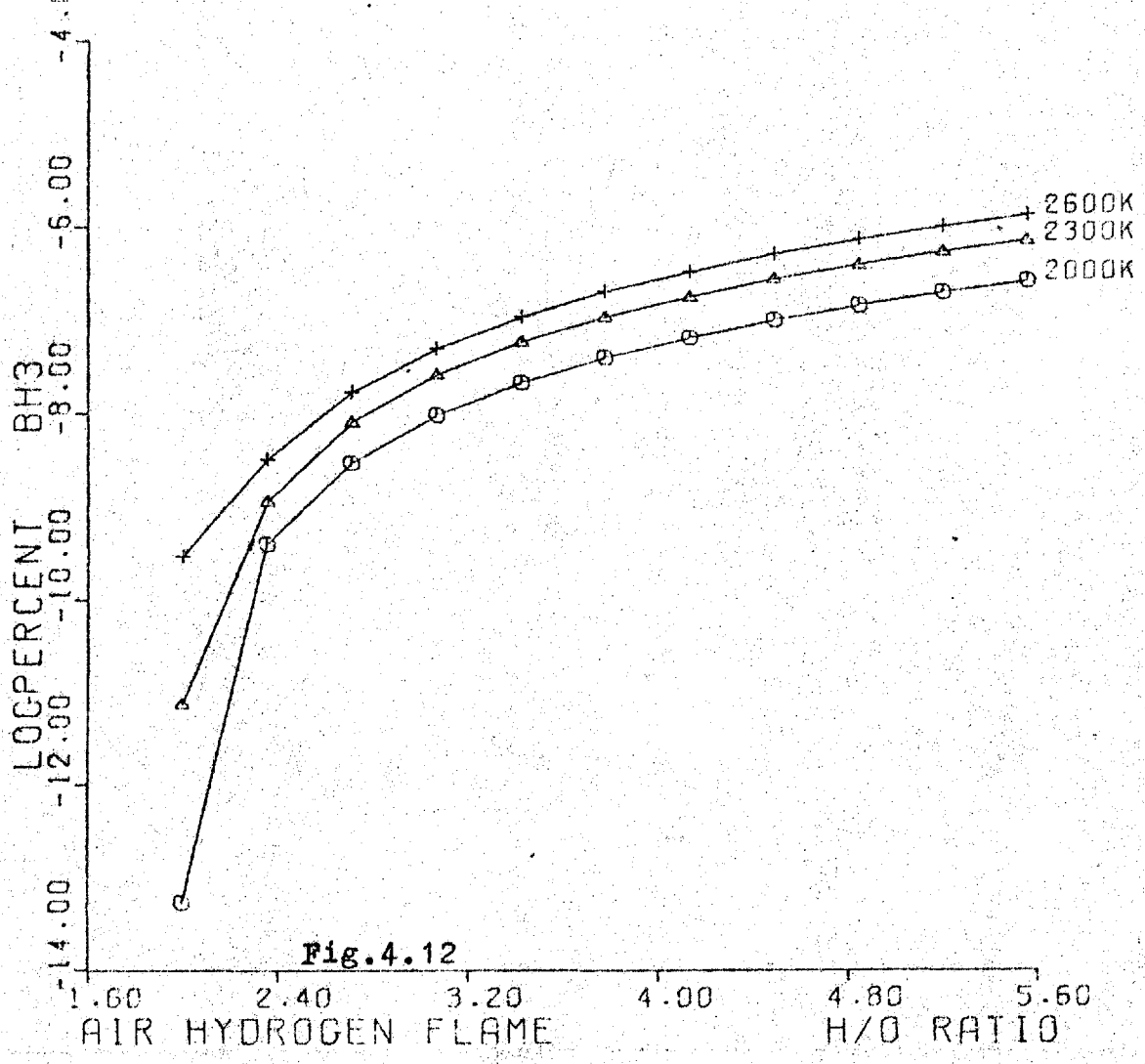
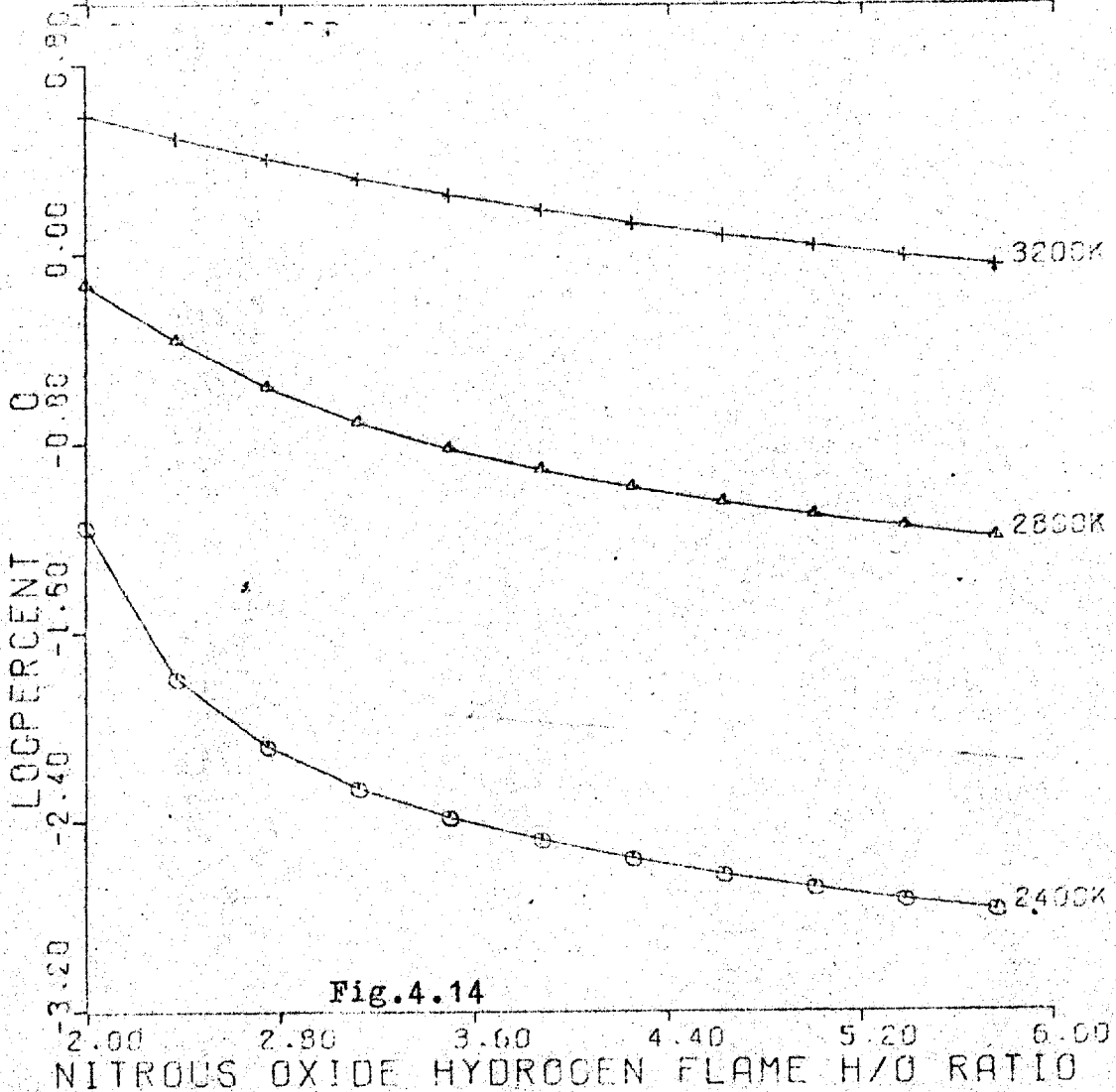
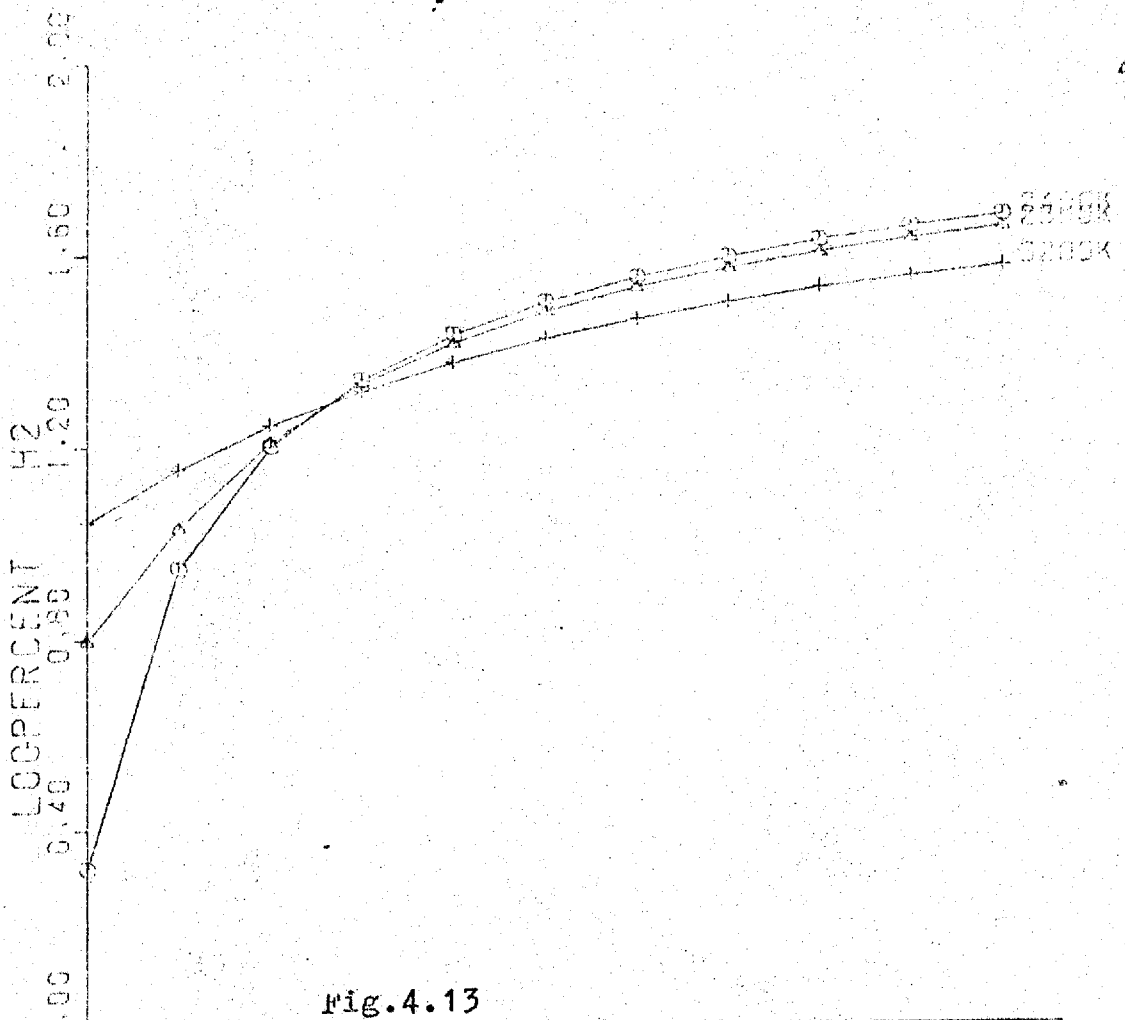
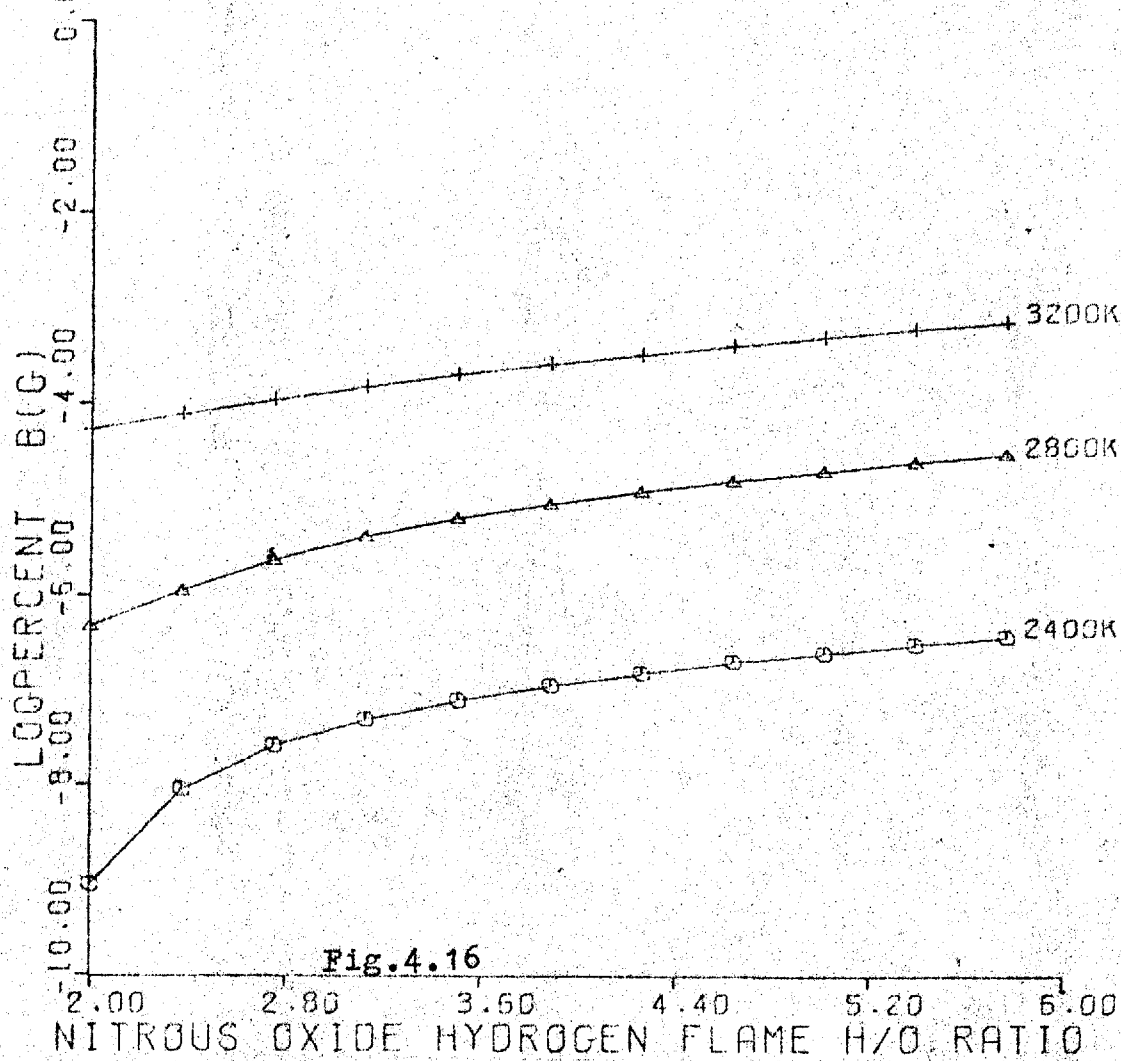
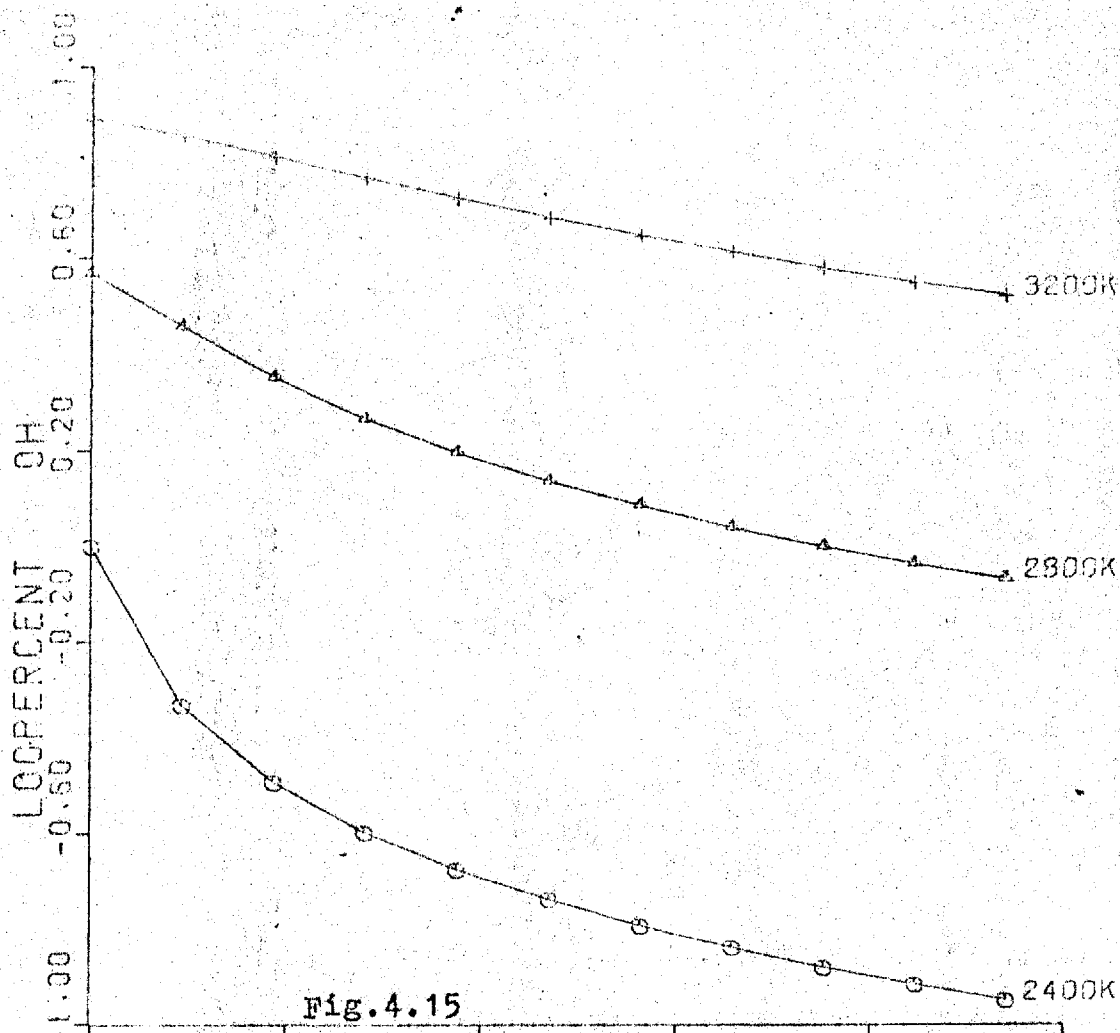
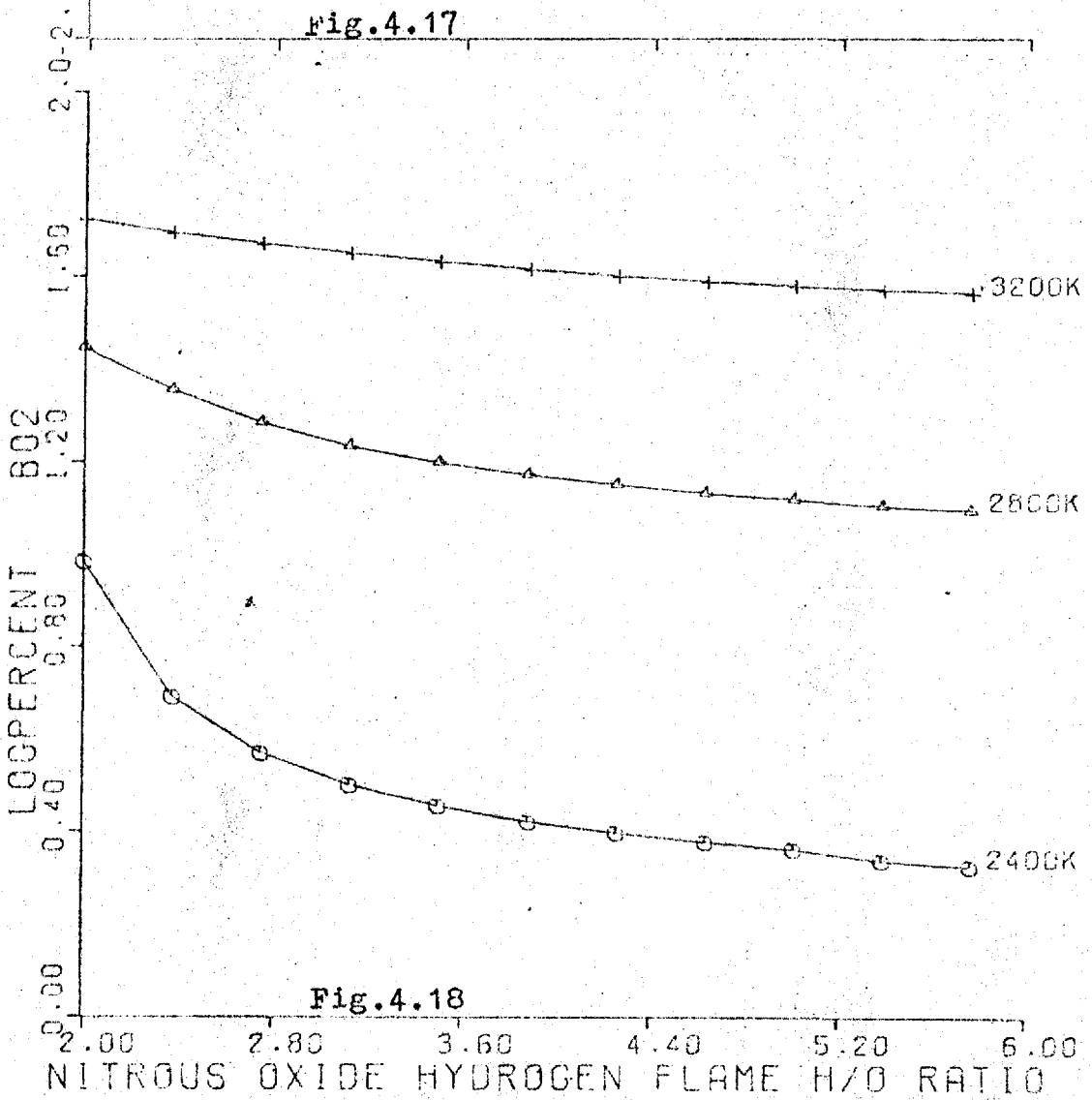
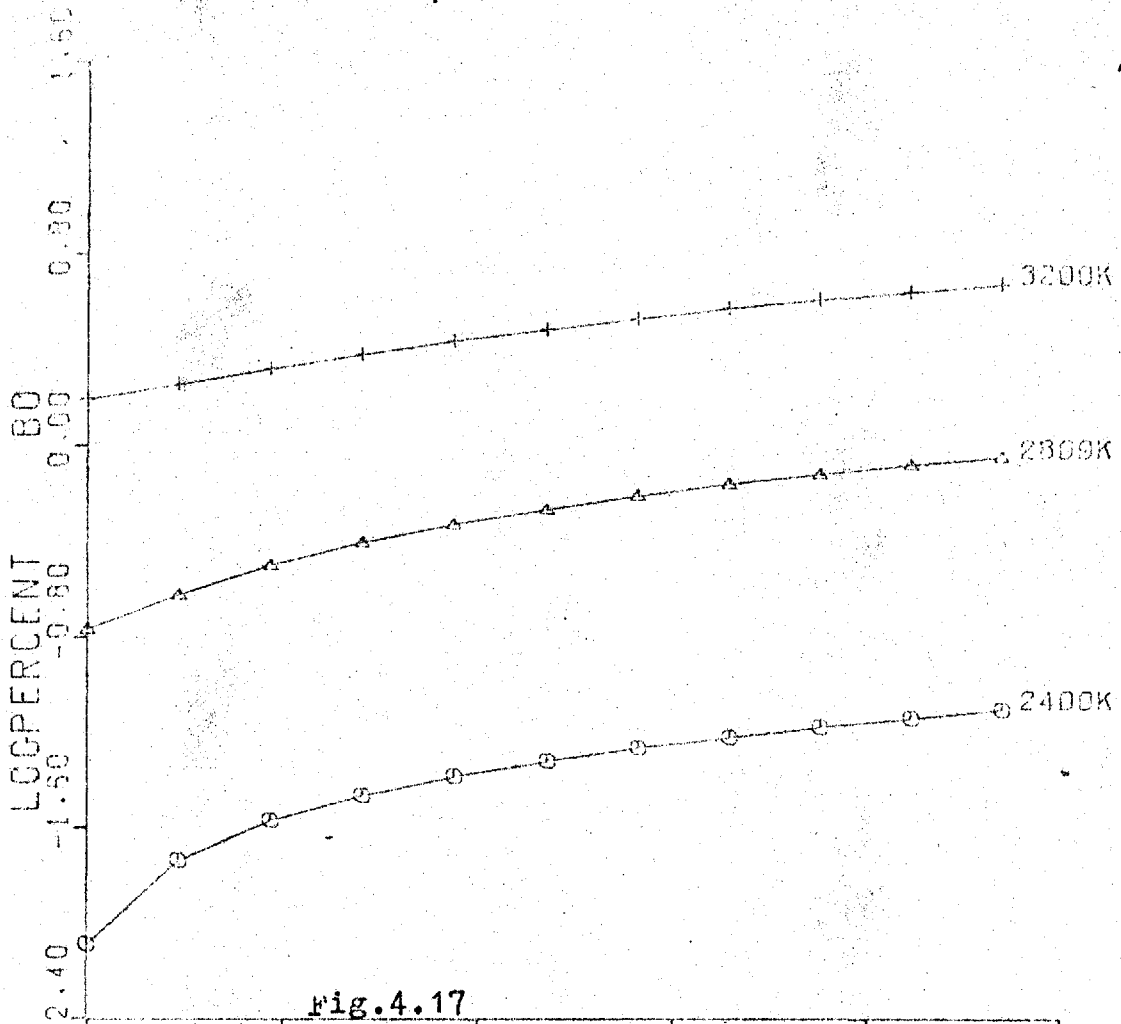


Fig. 4.12







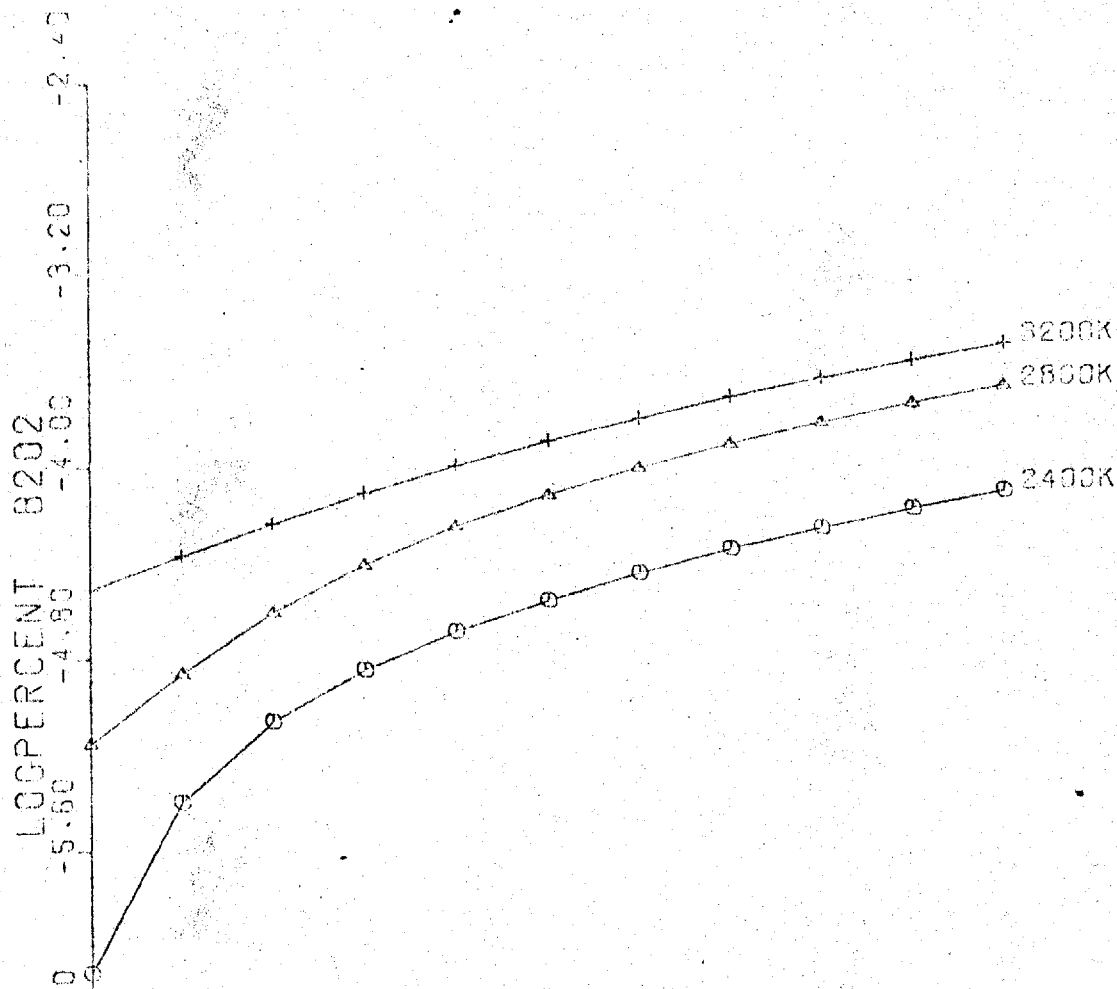


Fig.4.19

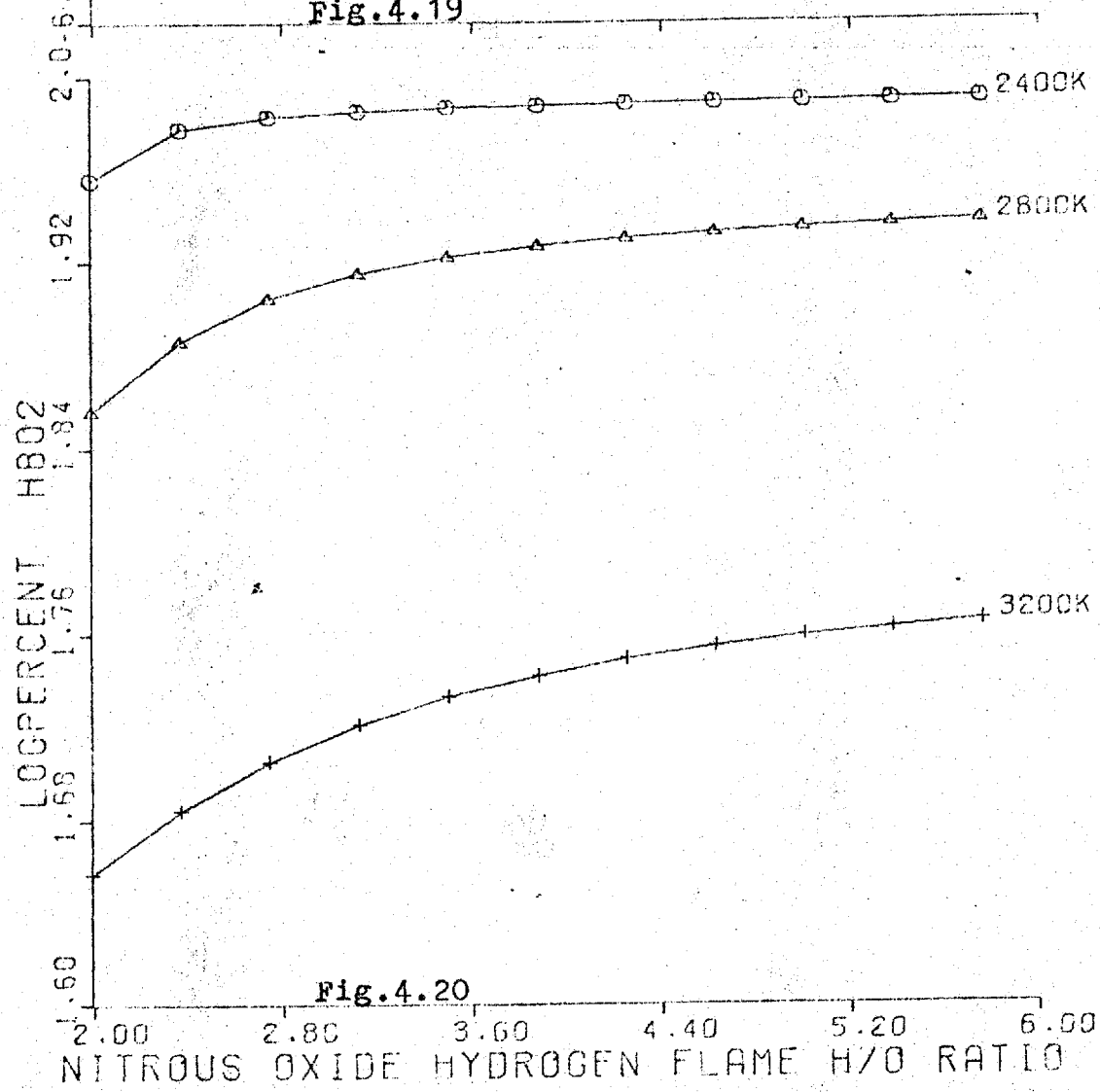
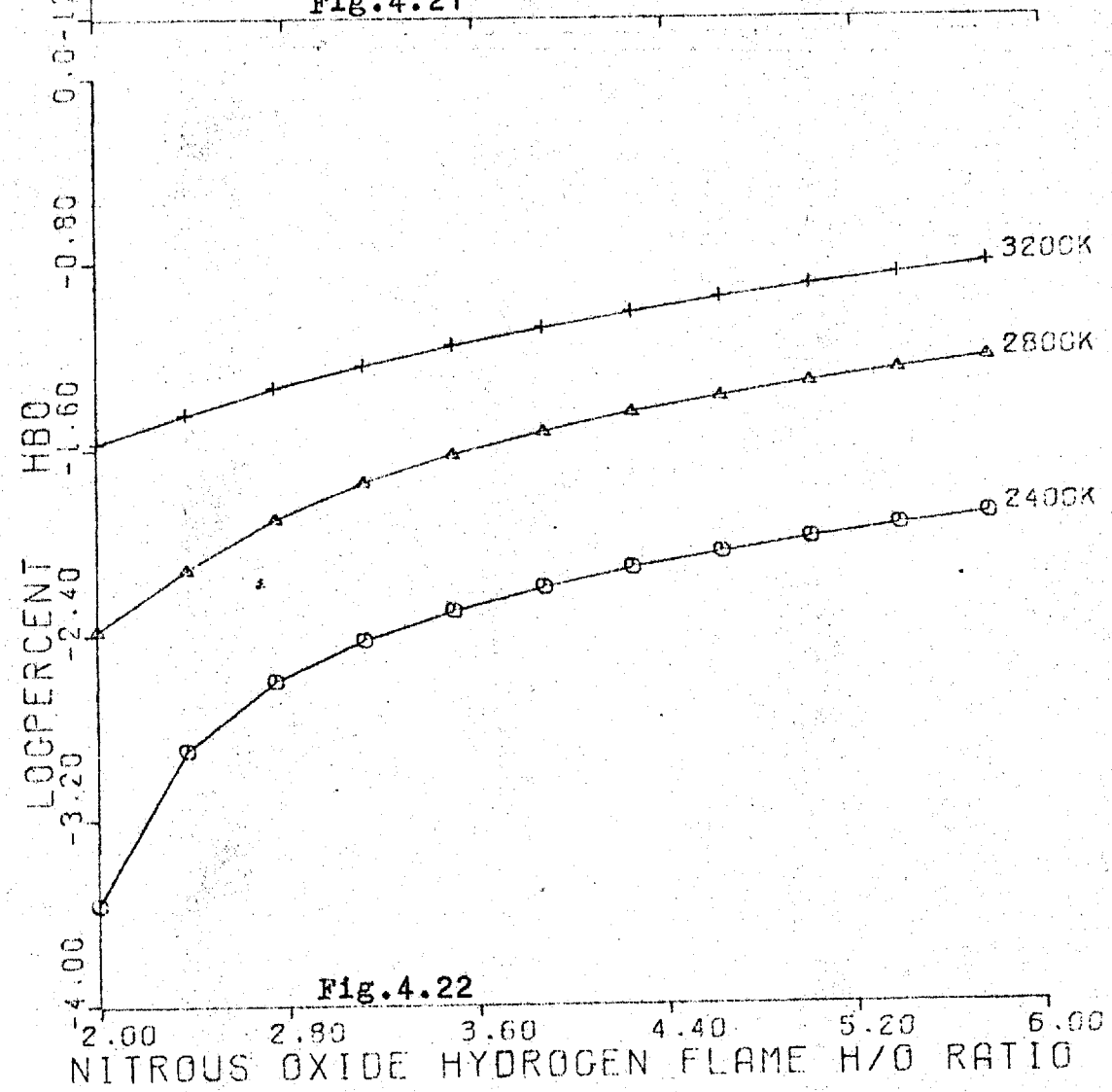
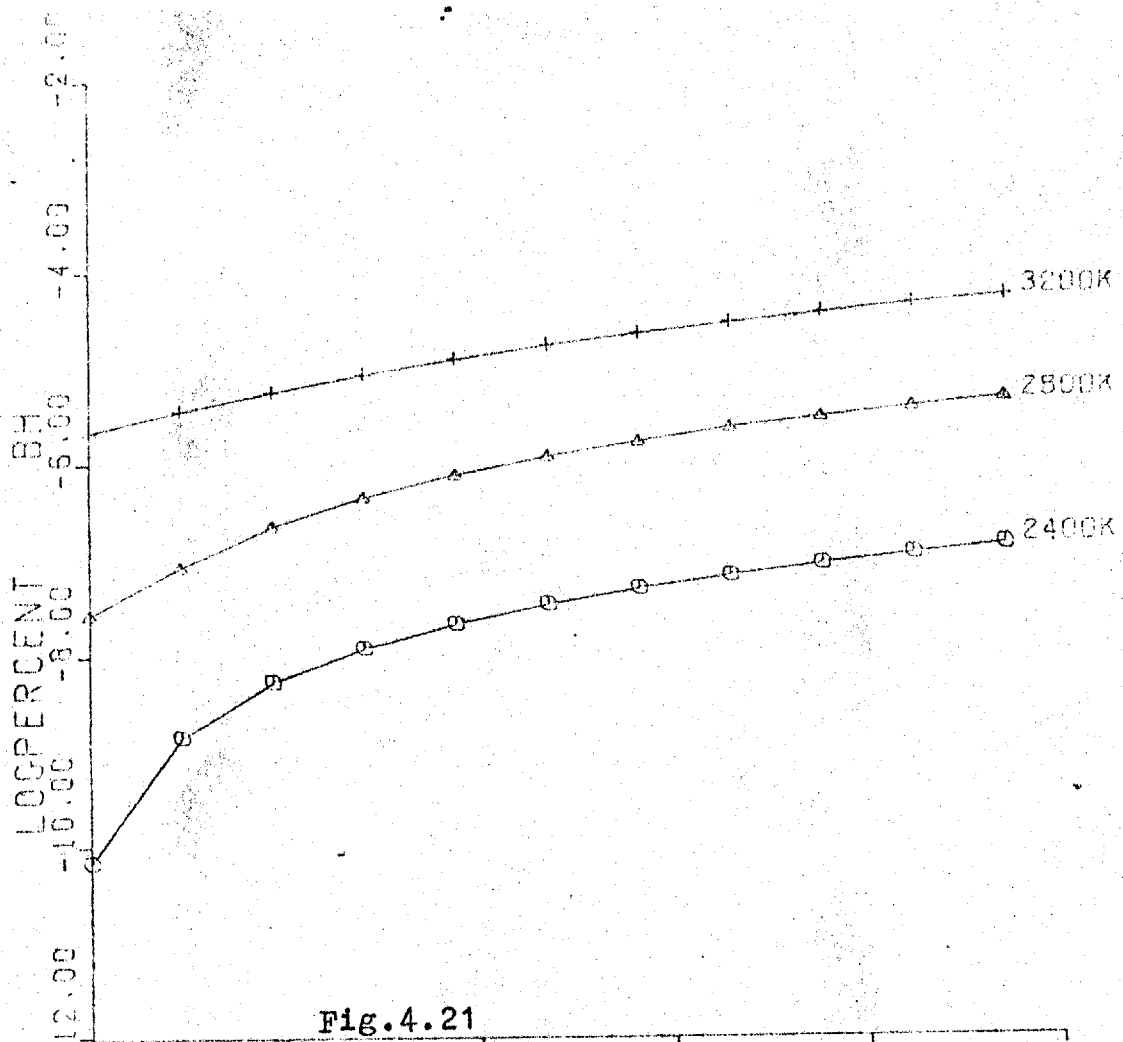
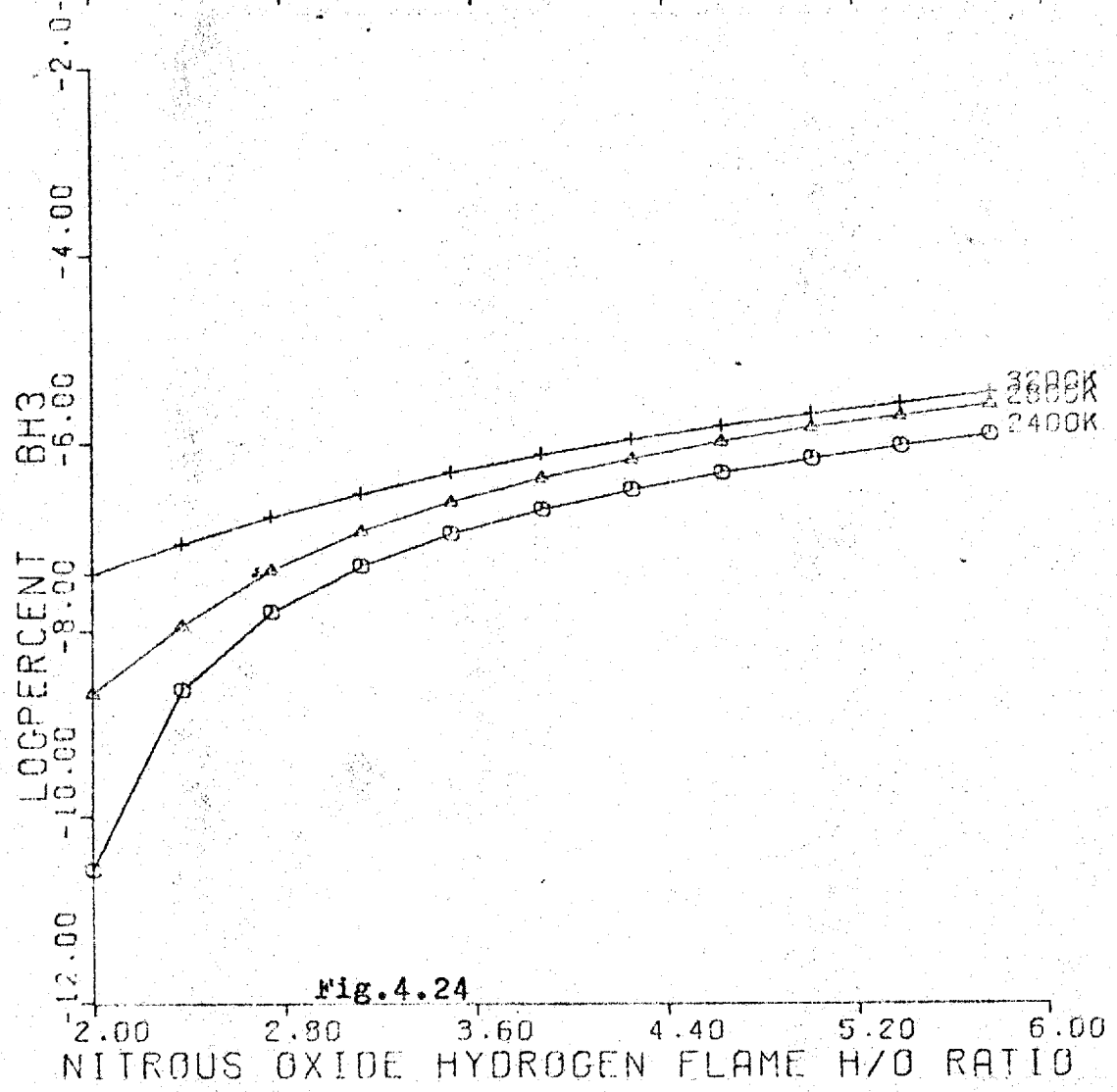
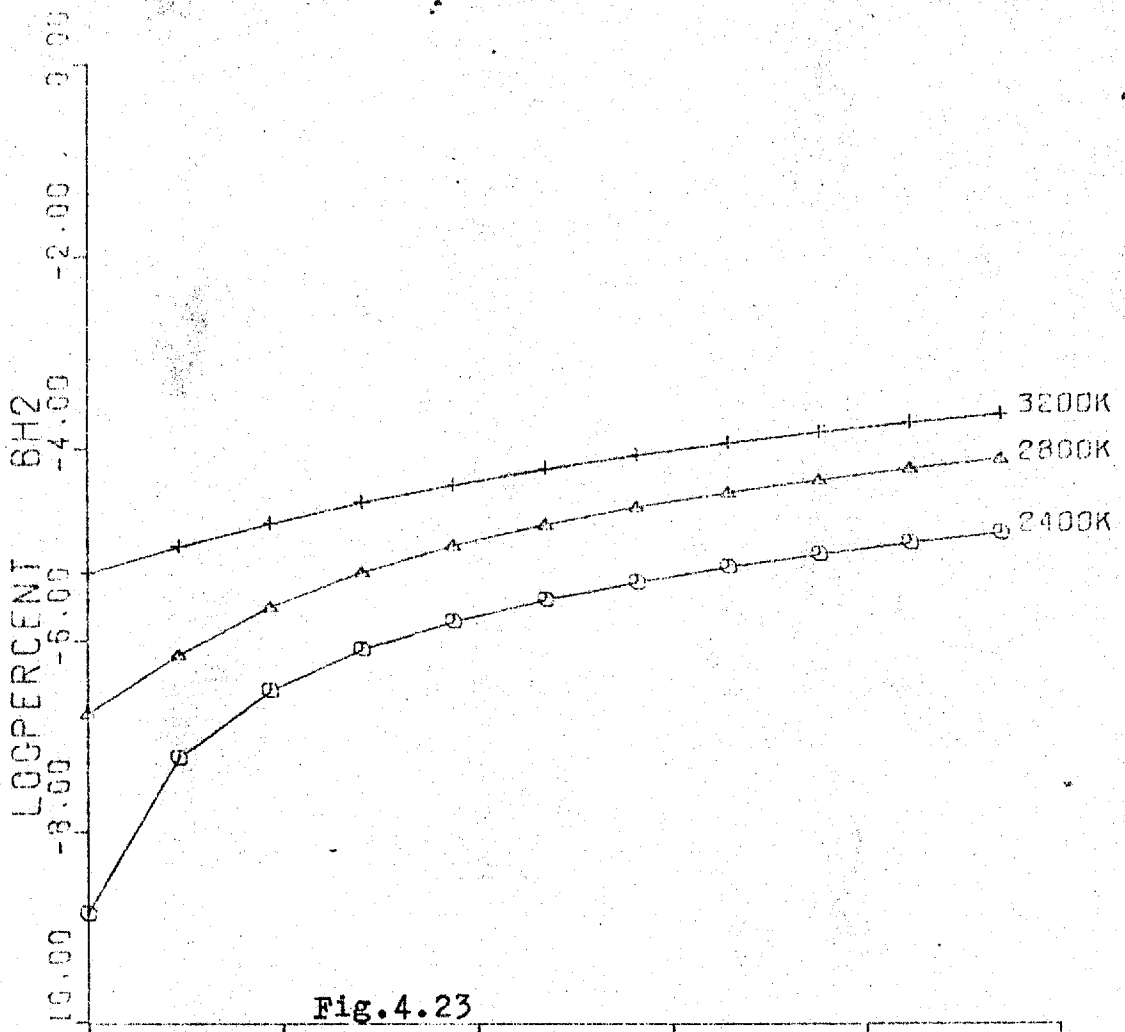


Fig.4.20





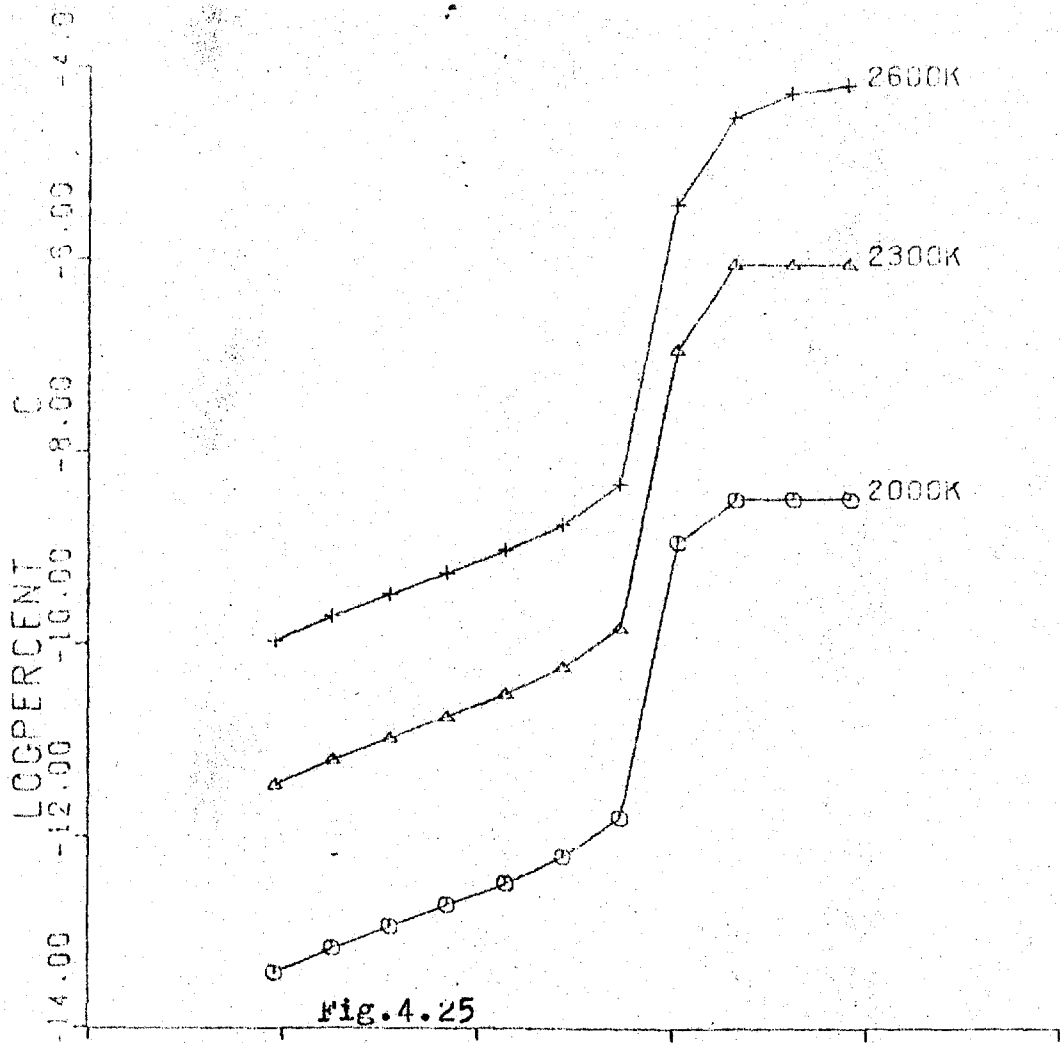


Fig. 4.25

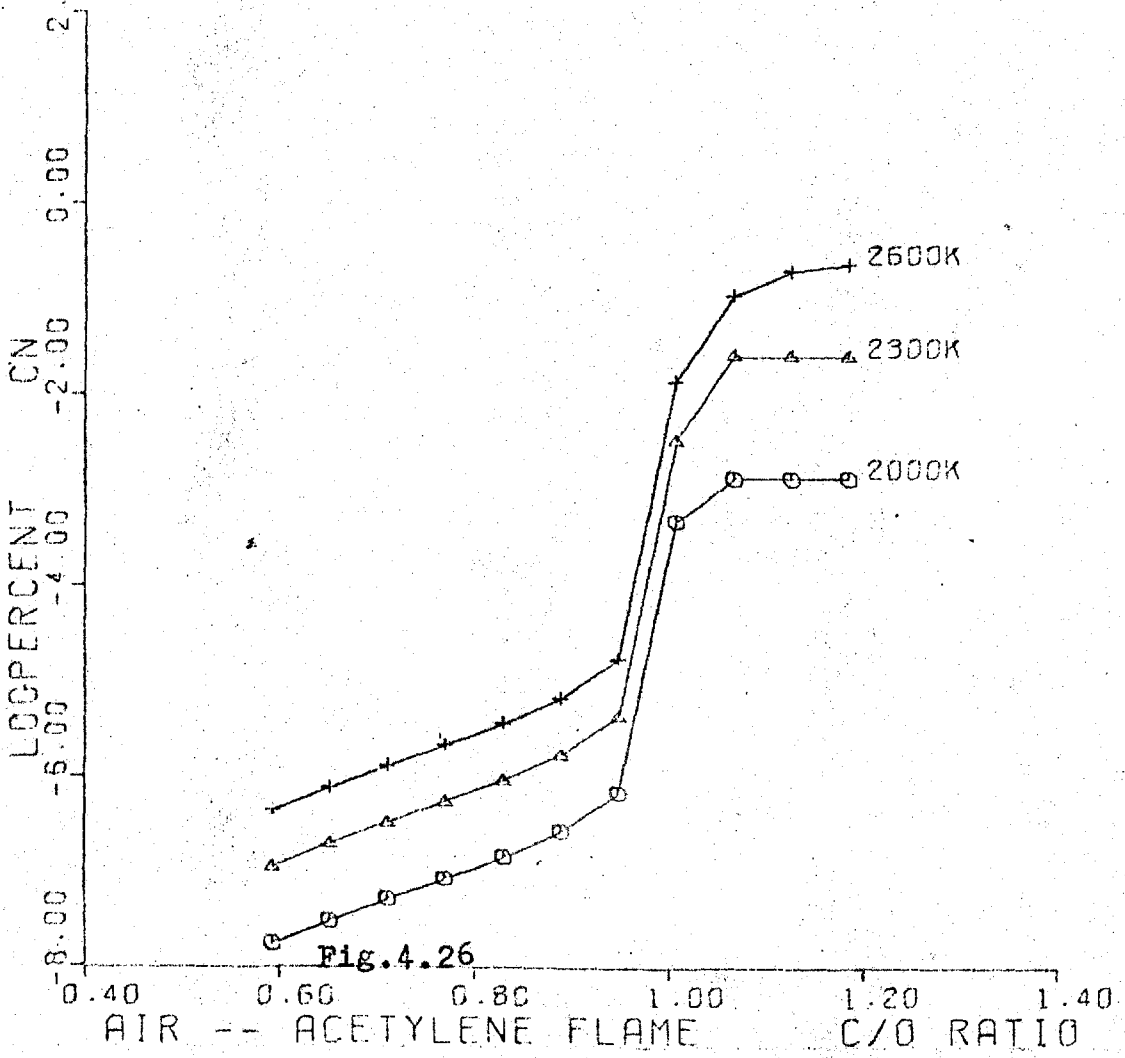
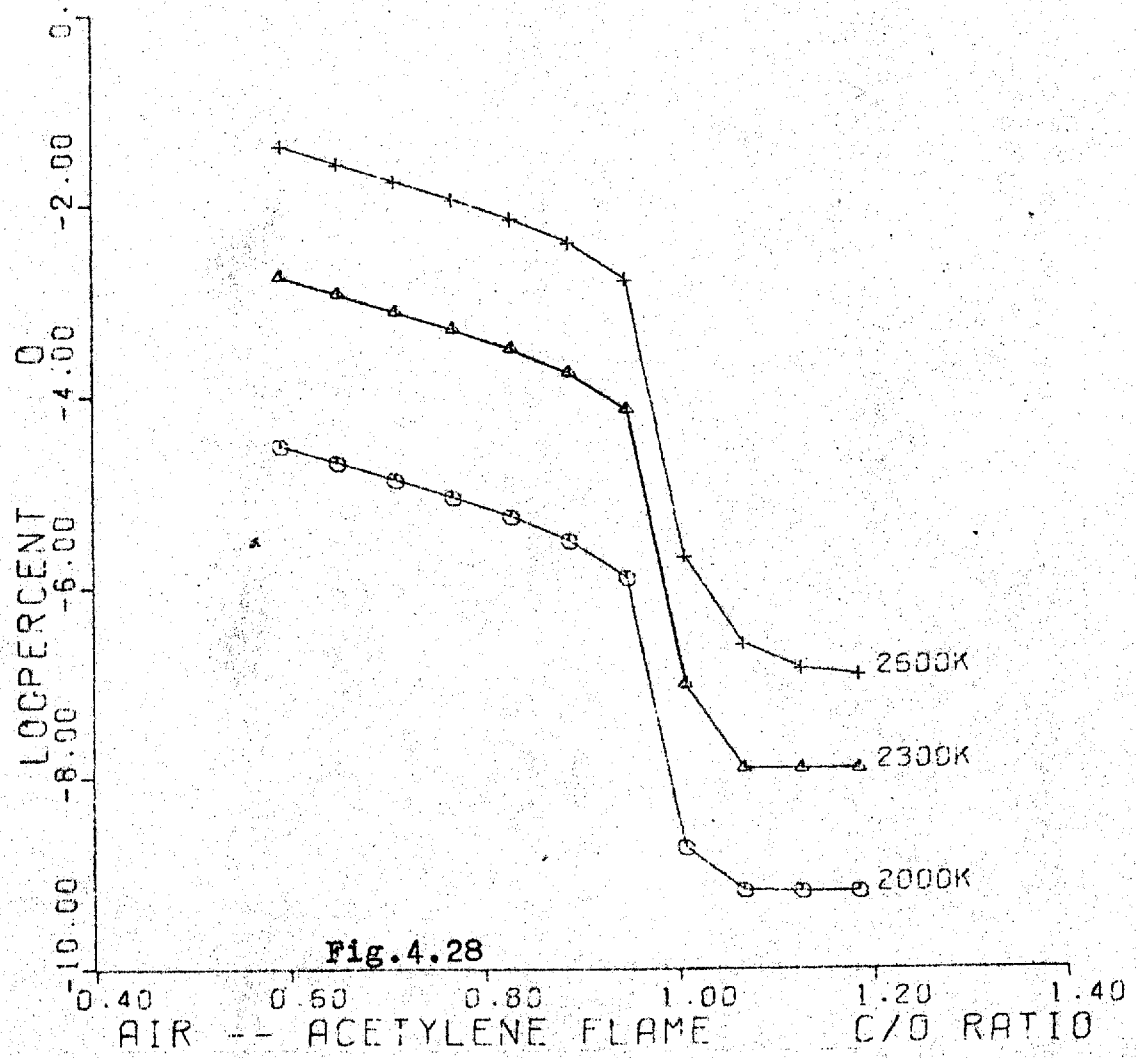
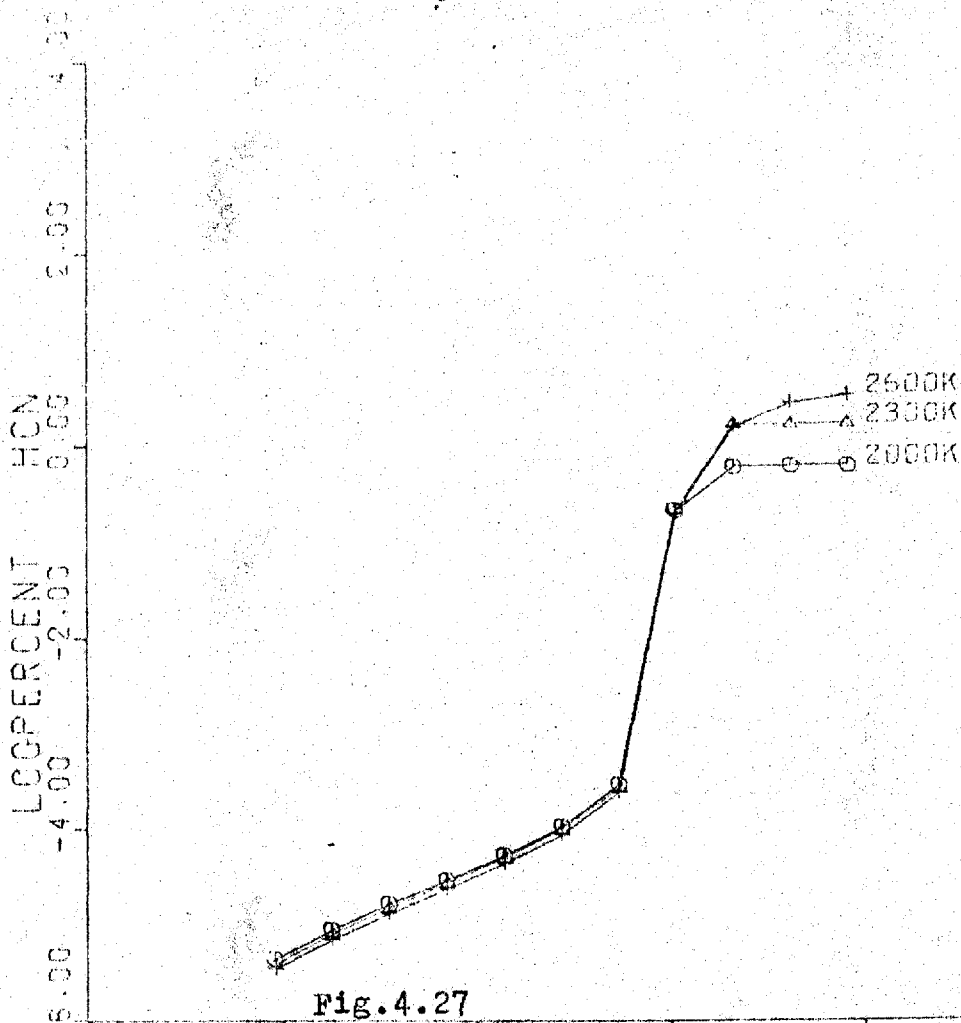
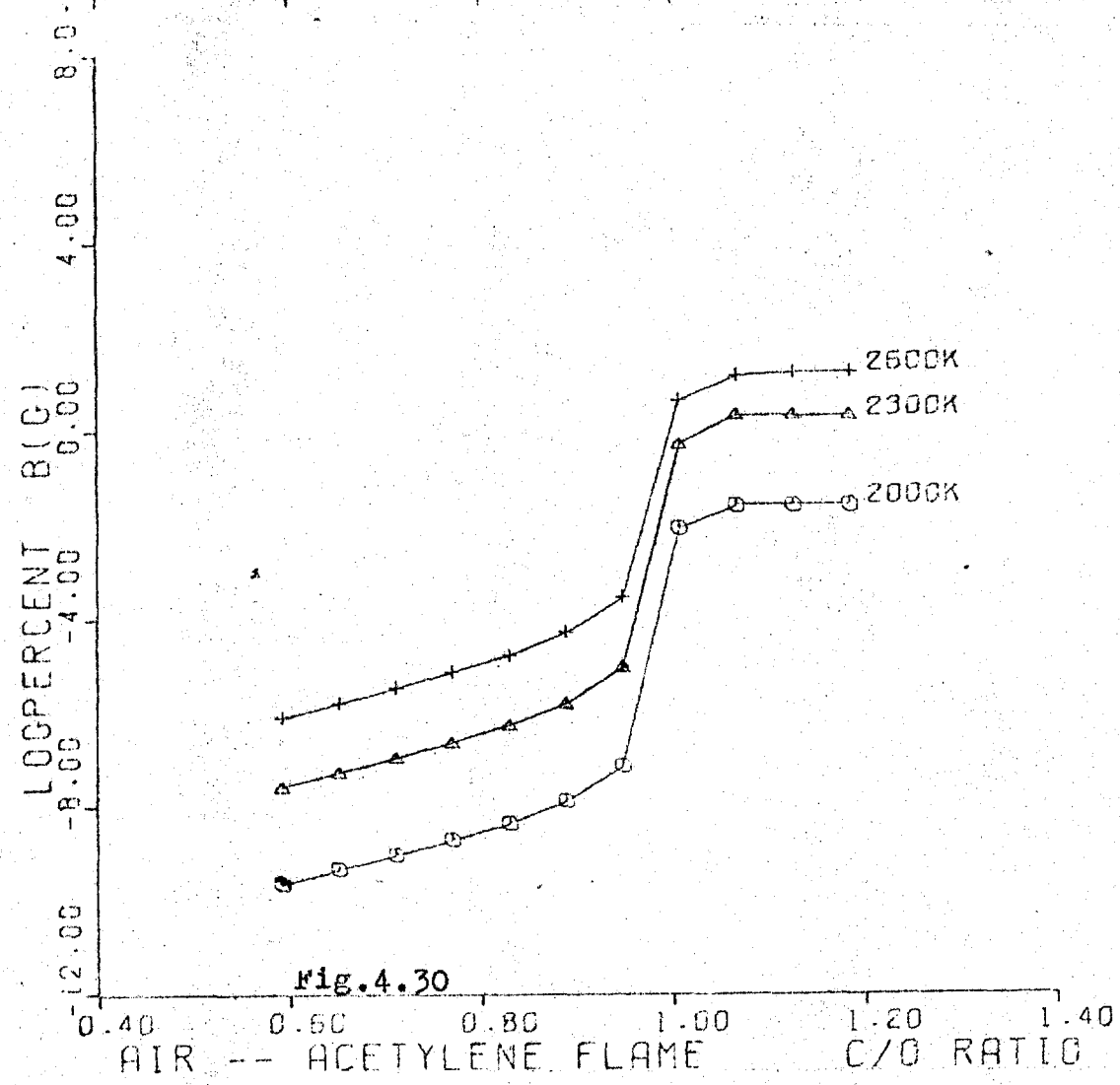
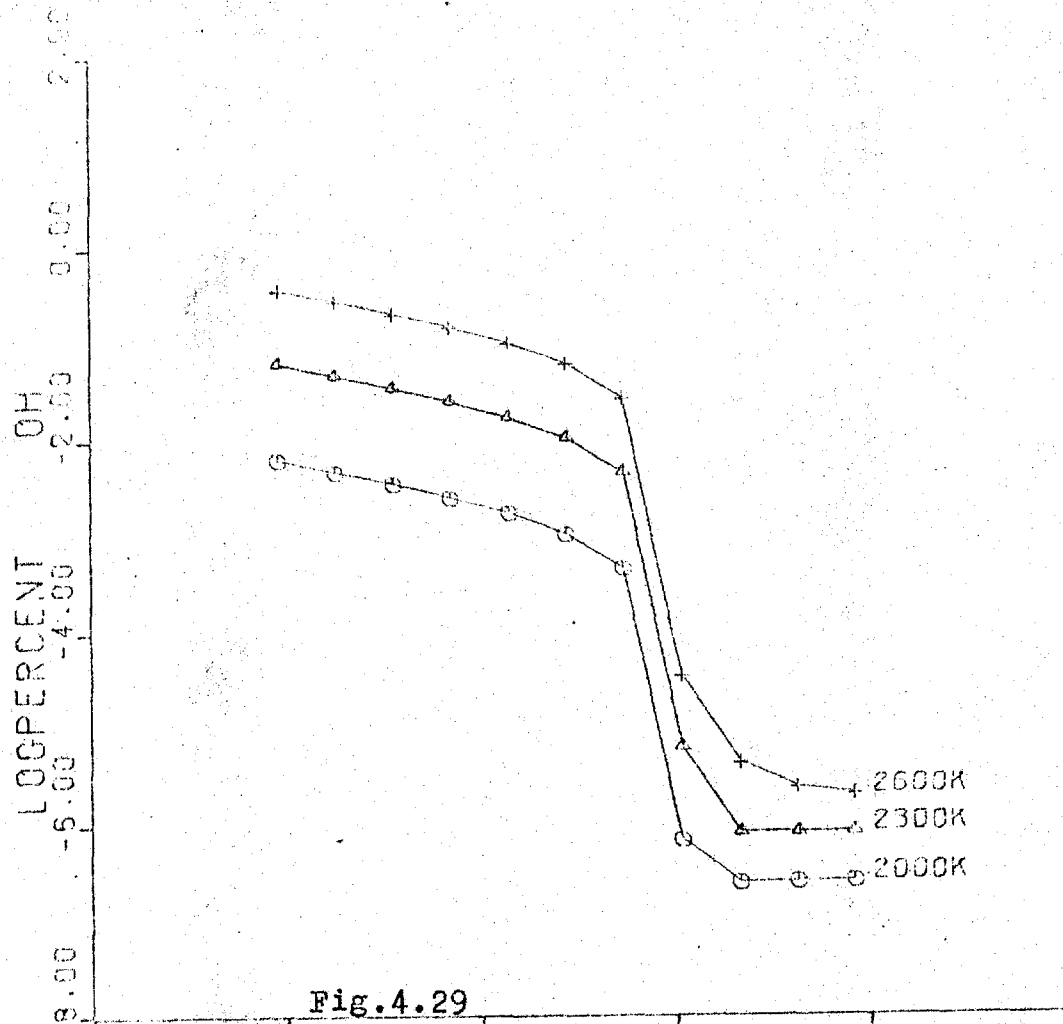
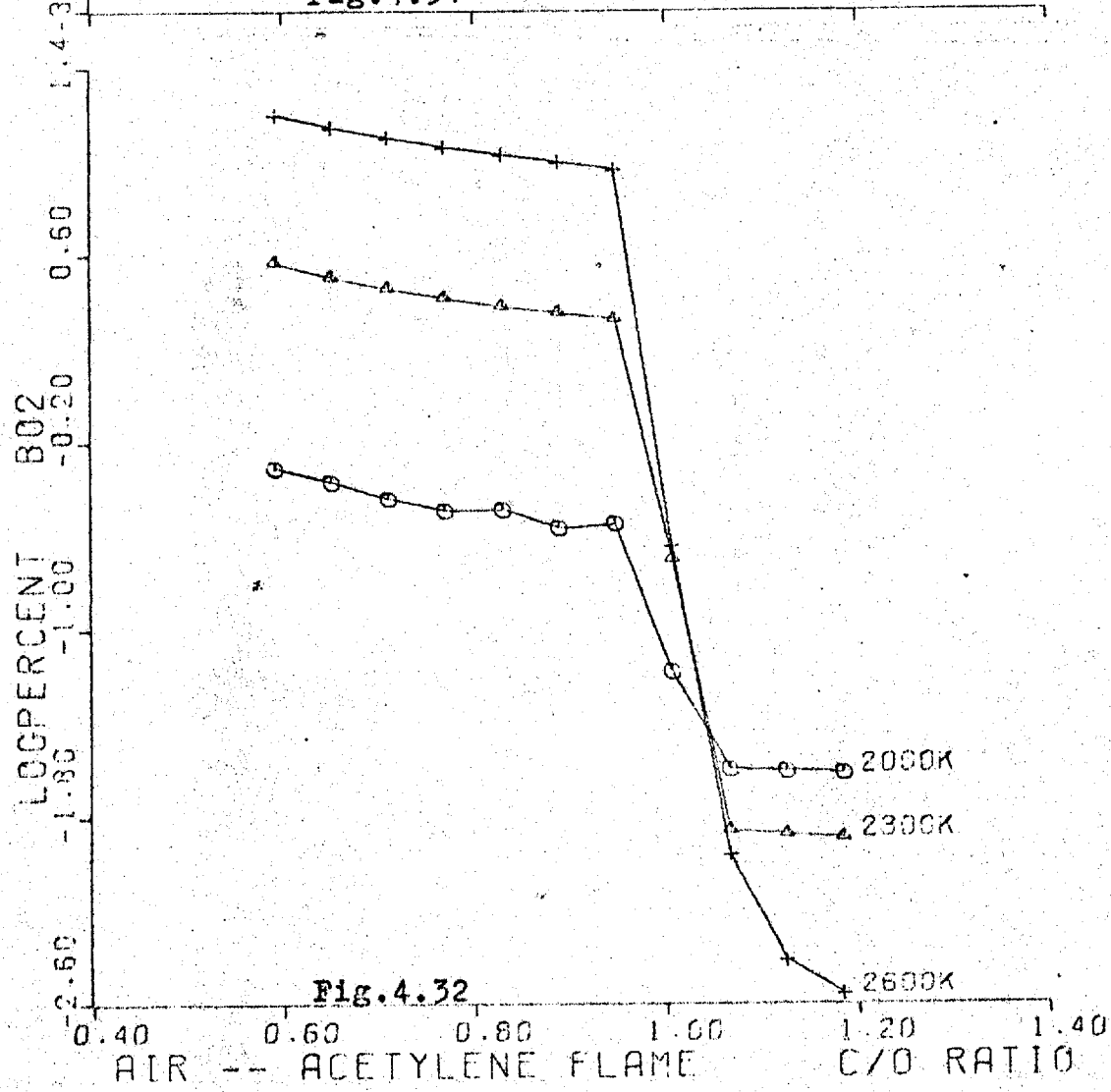
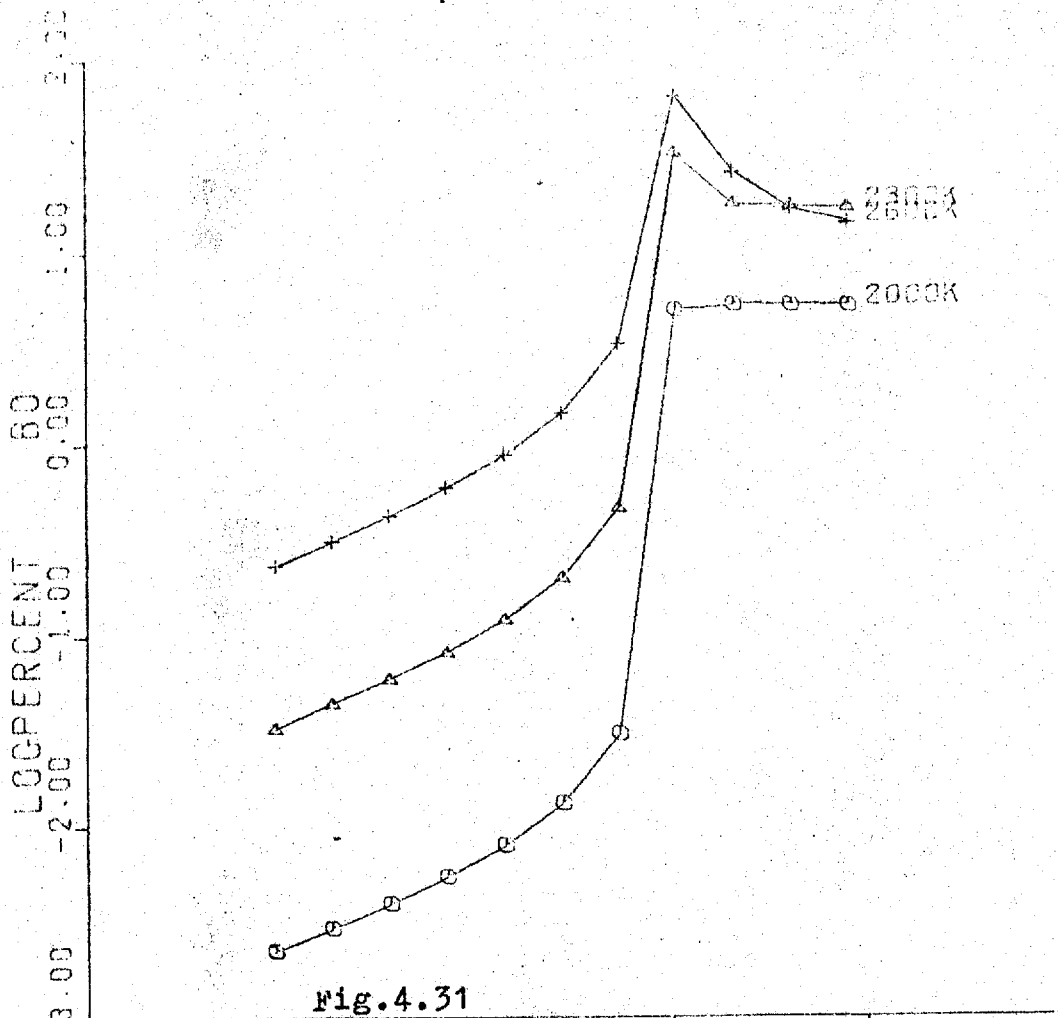


Fig. 4.26







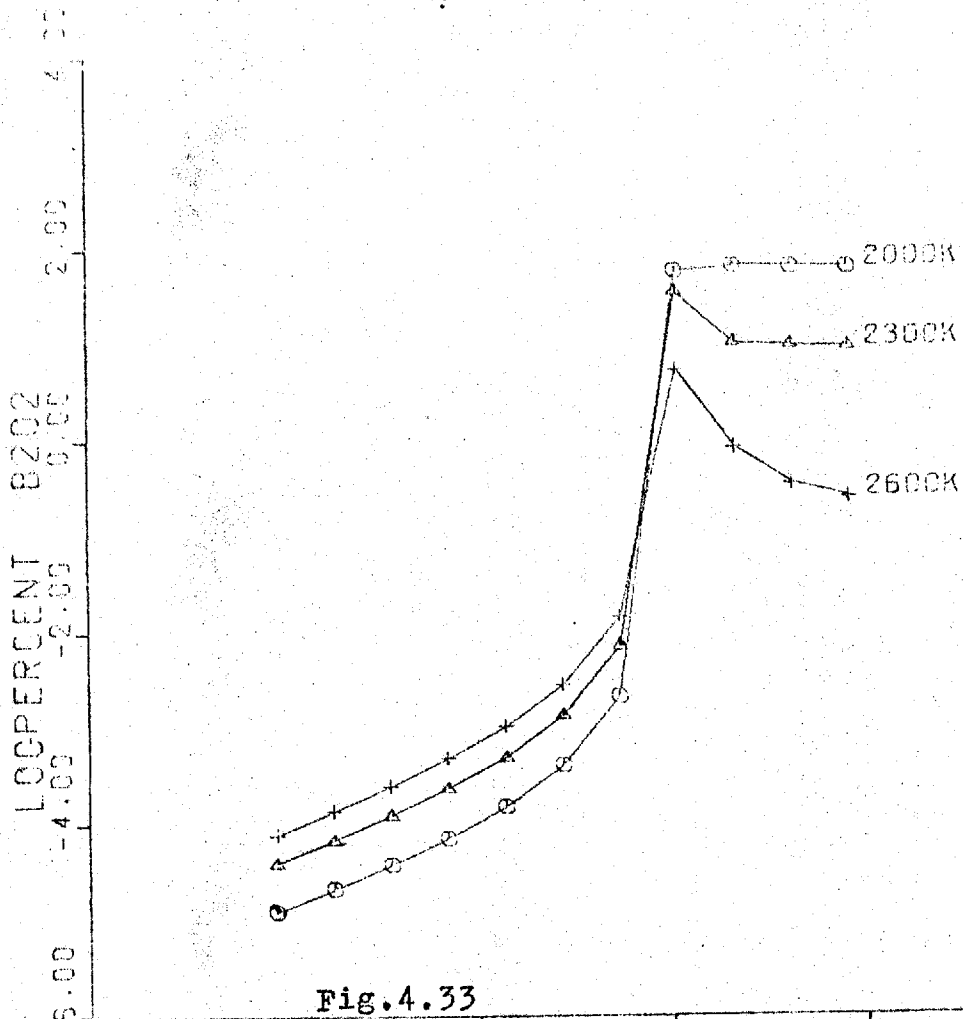


Fig.4.33

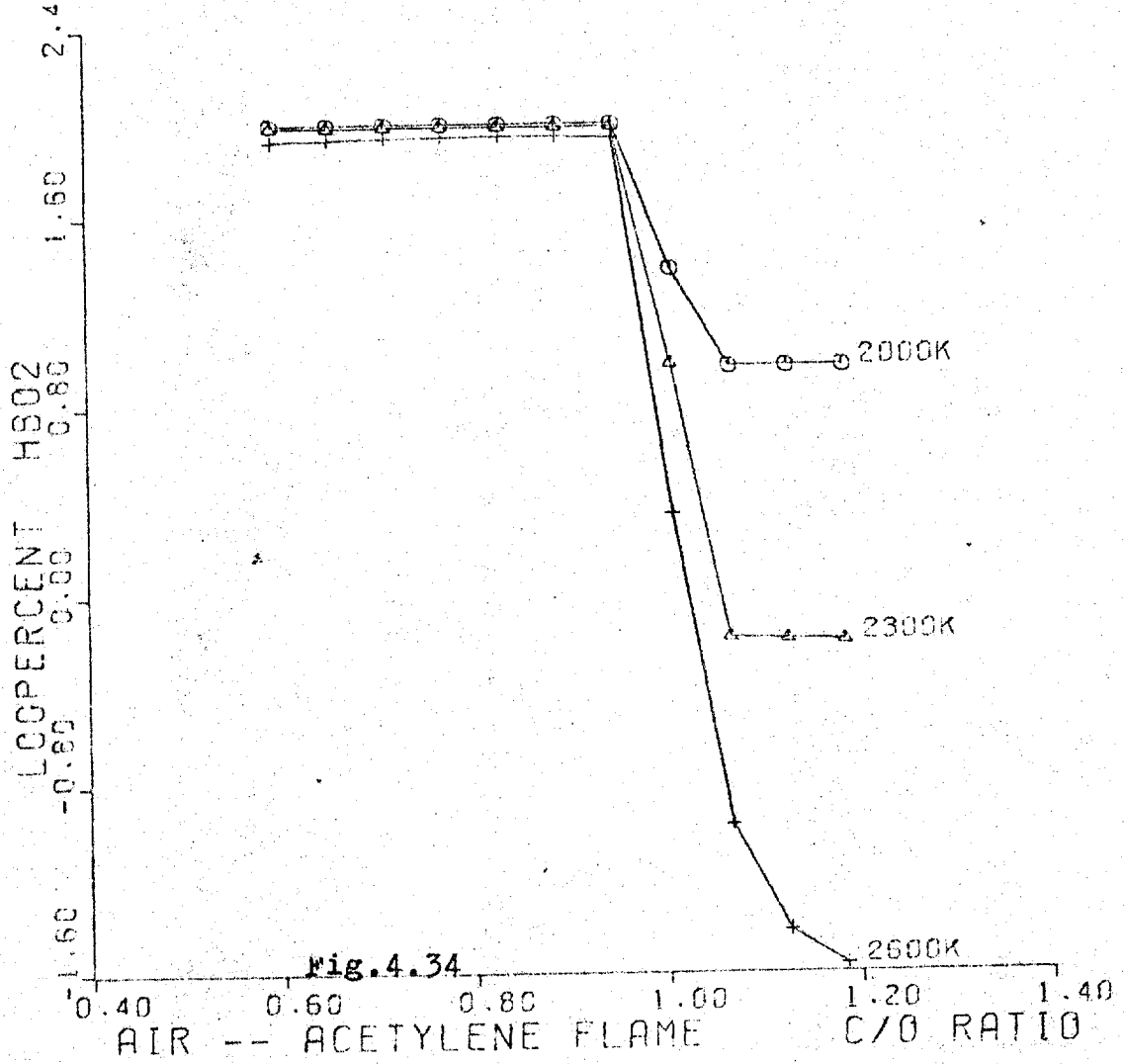


Fig.4.34

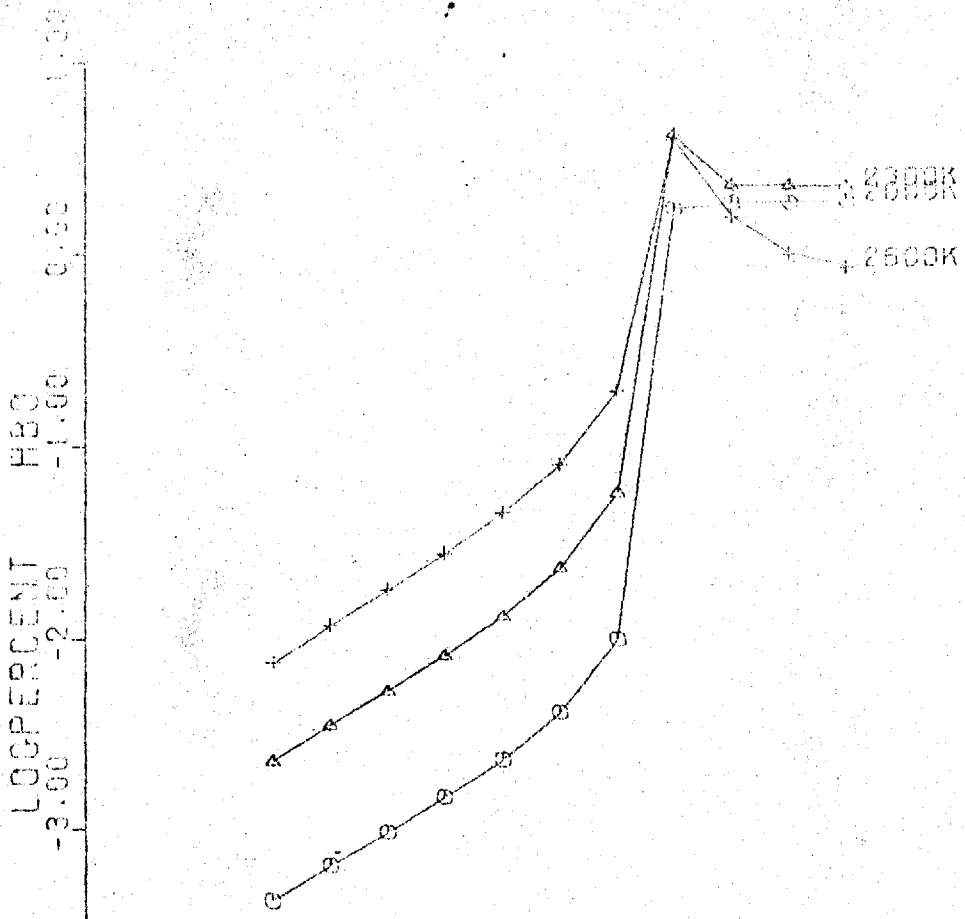


Fig.4.35

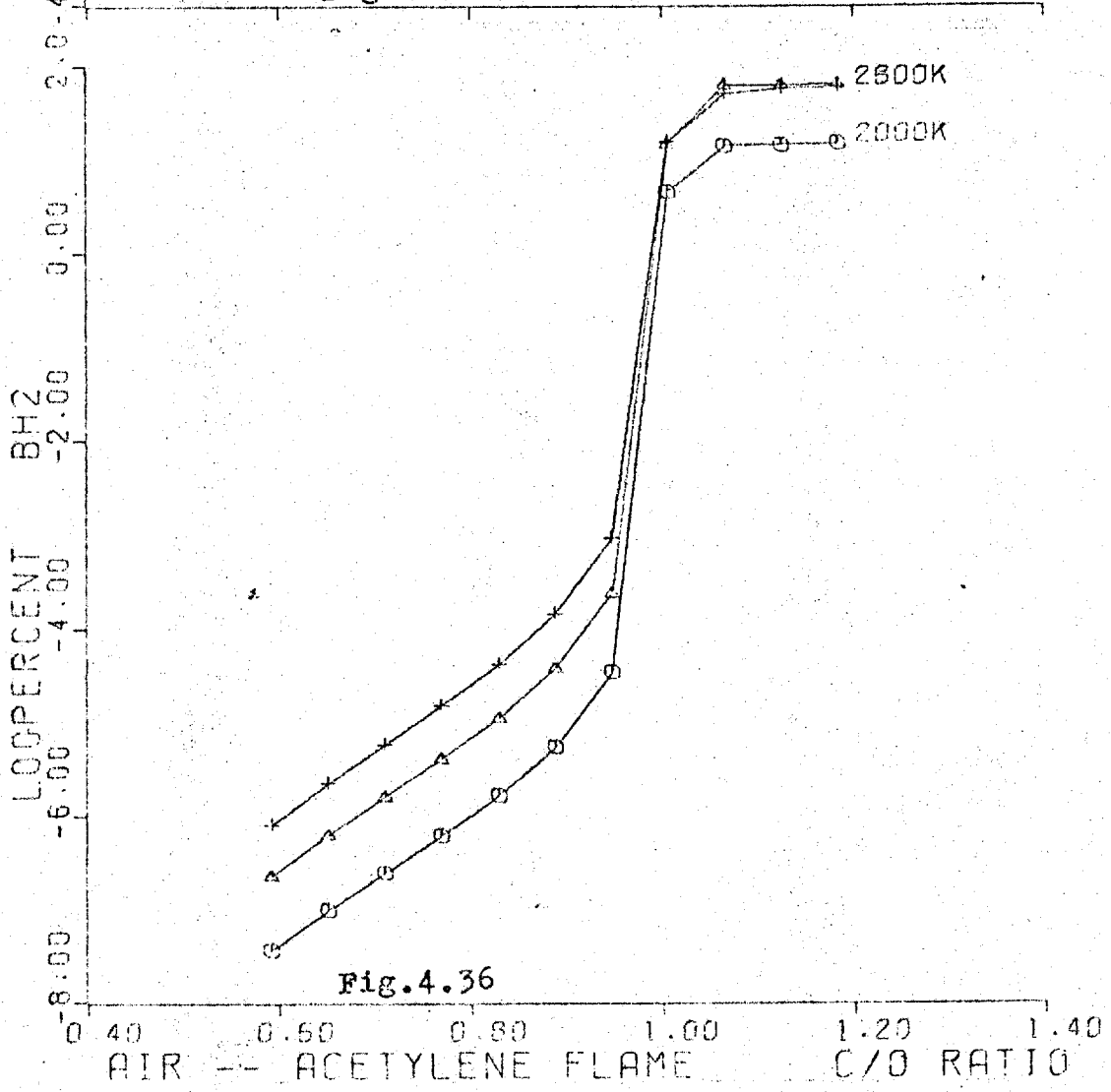


Fig.4.36

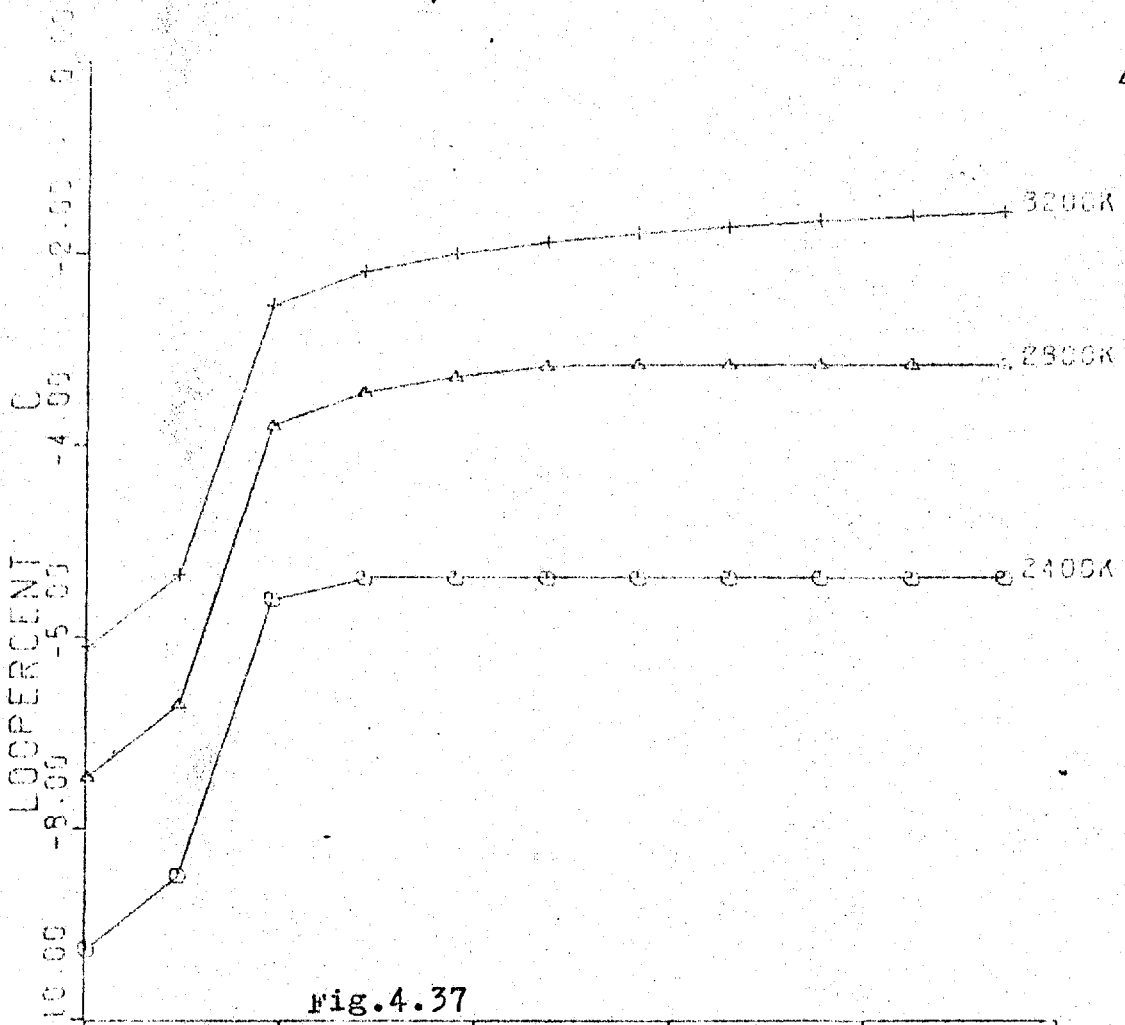


Fig.4.37

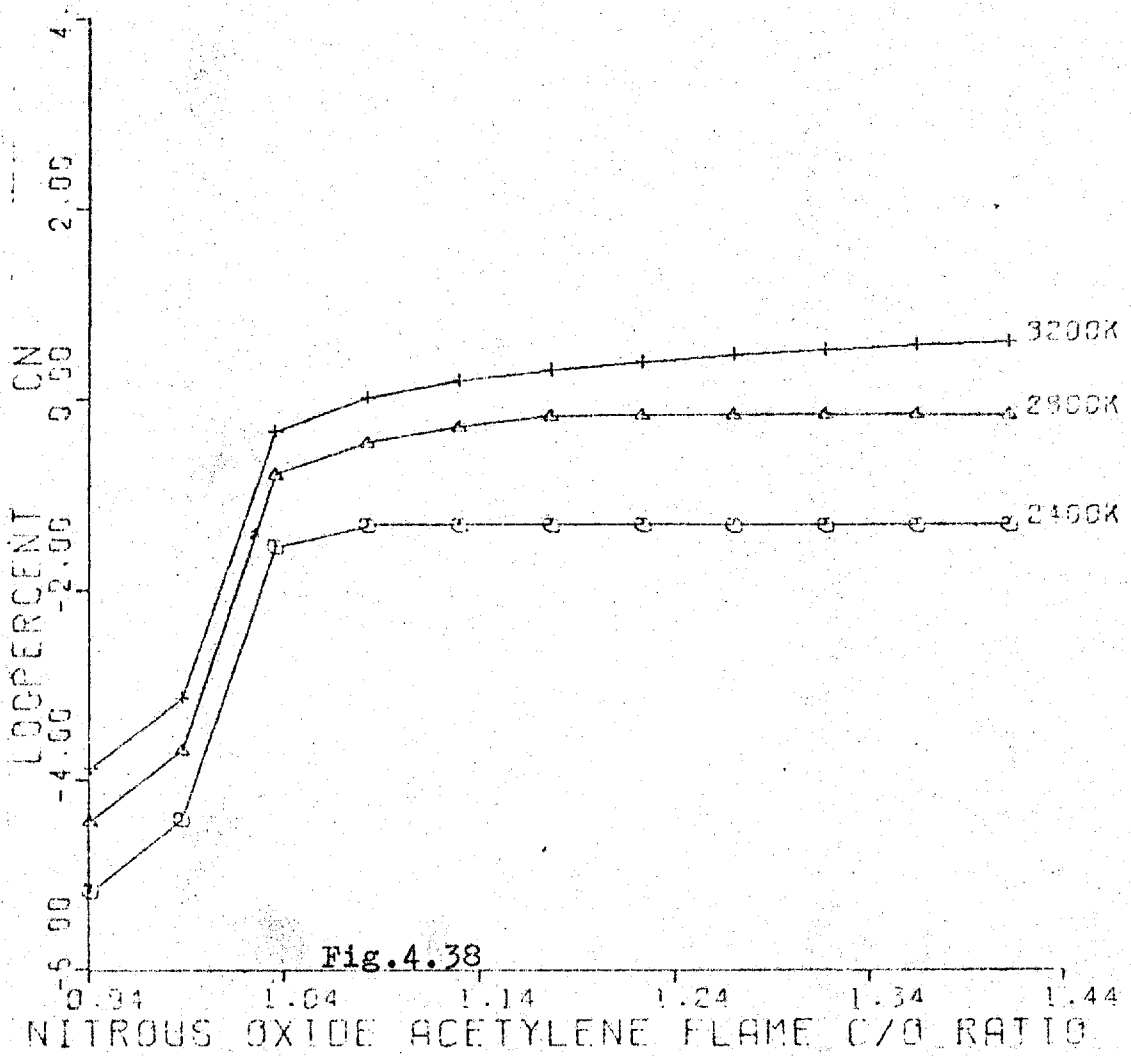
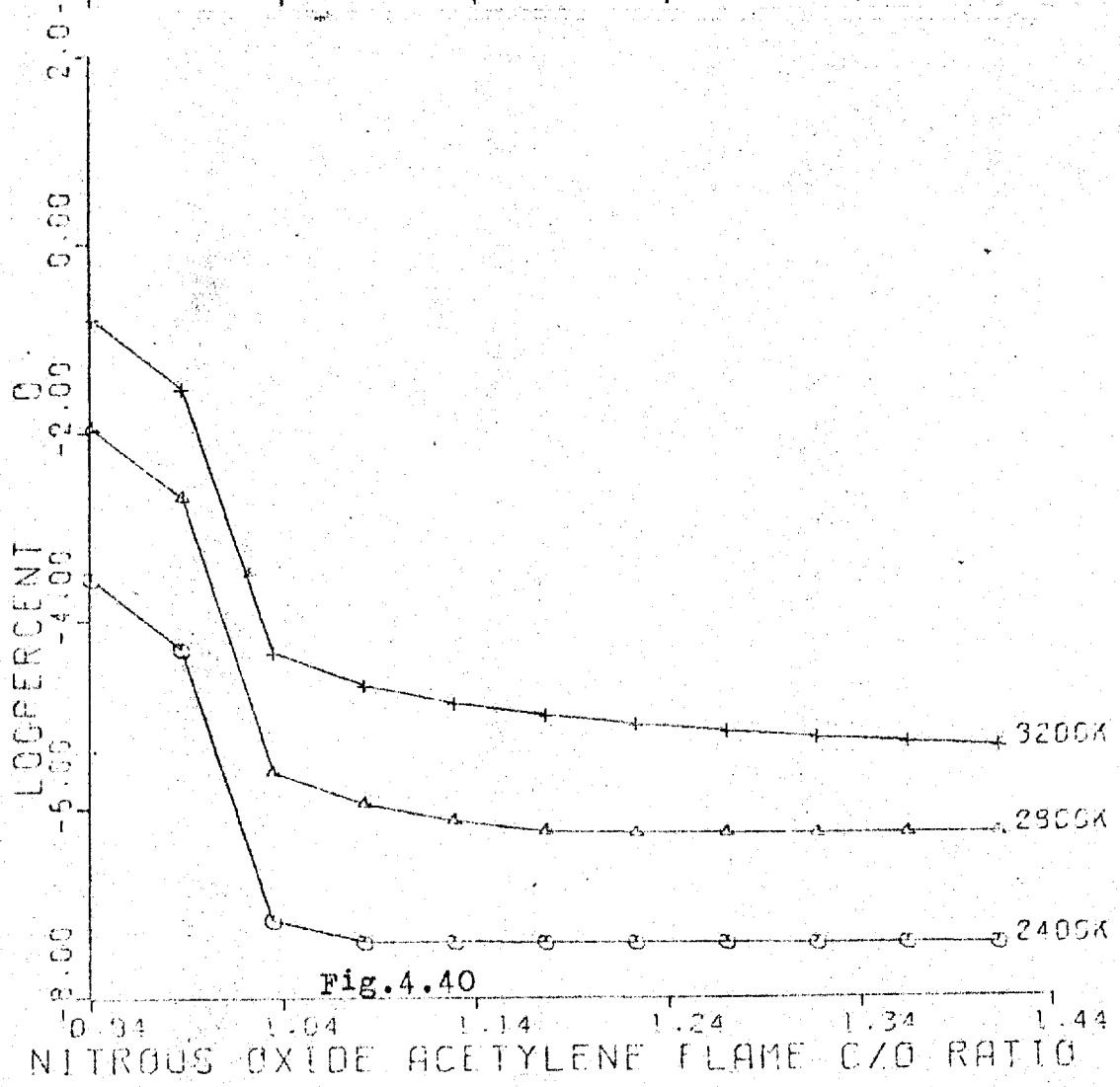
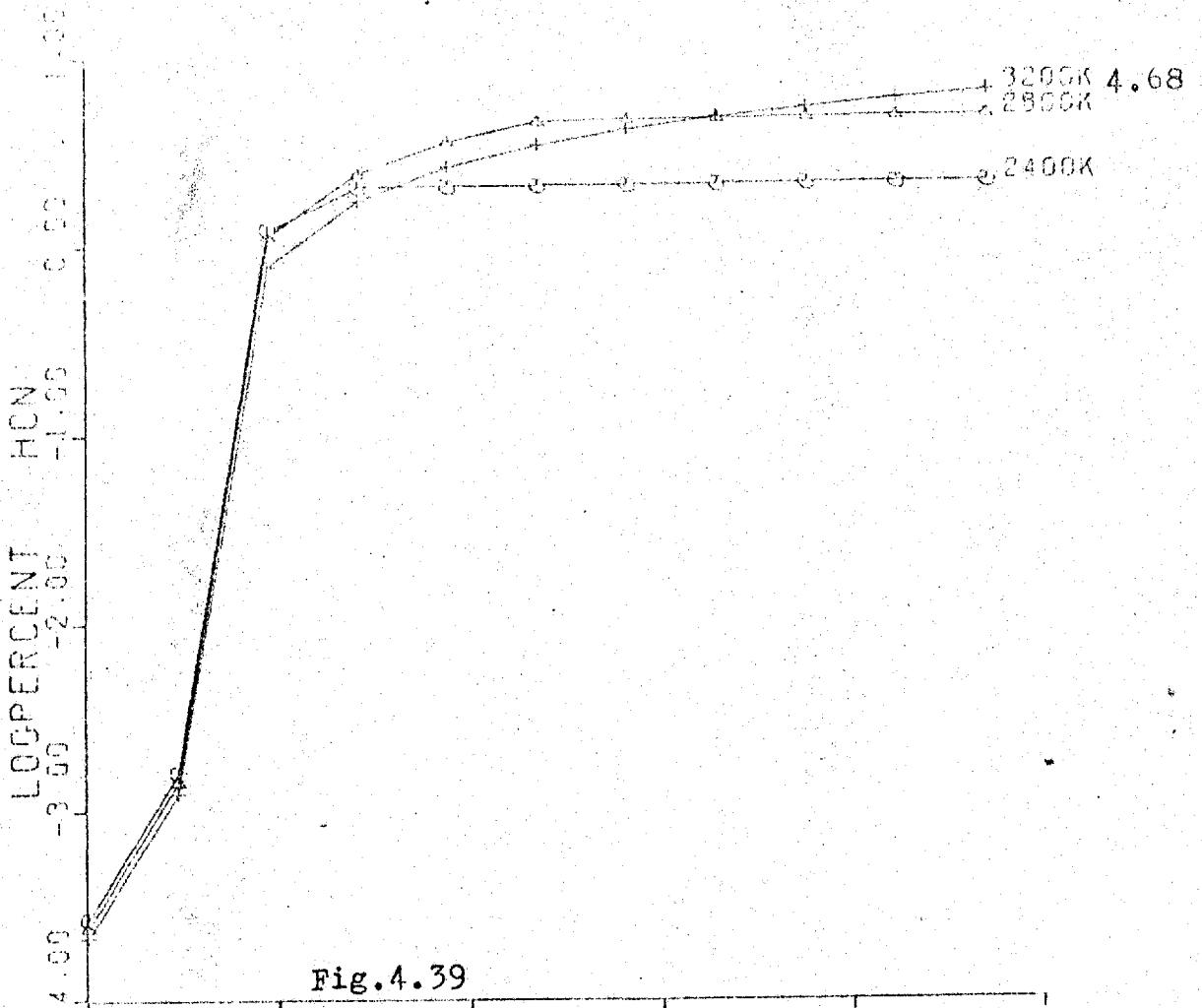


Fig.4.38



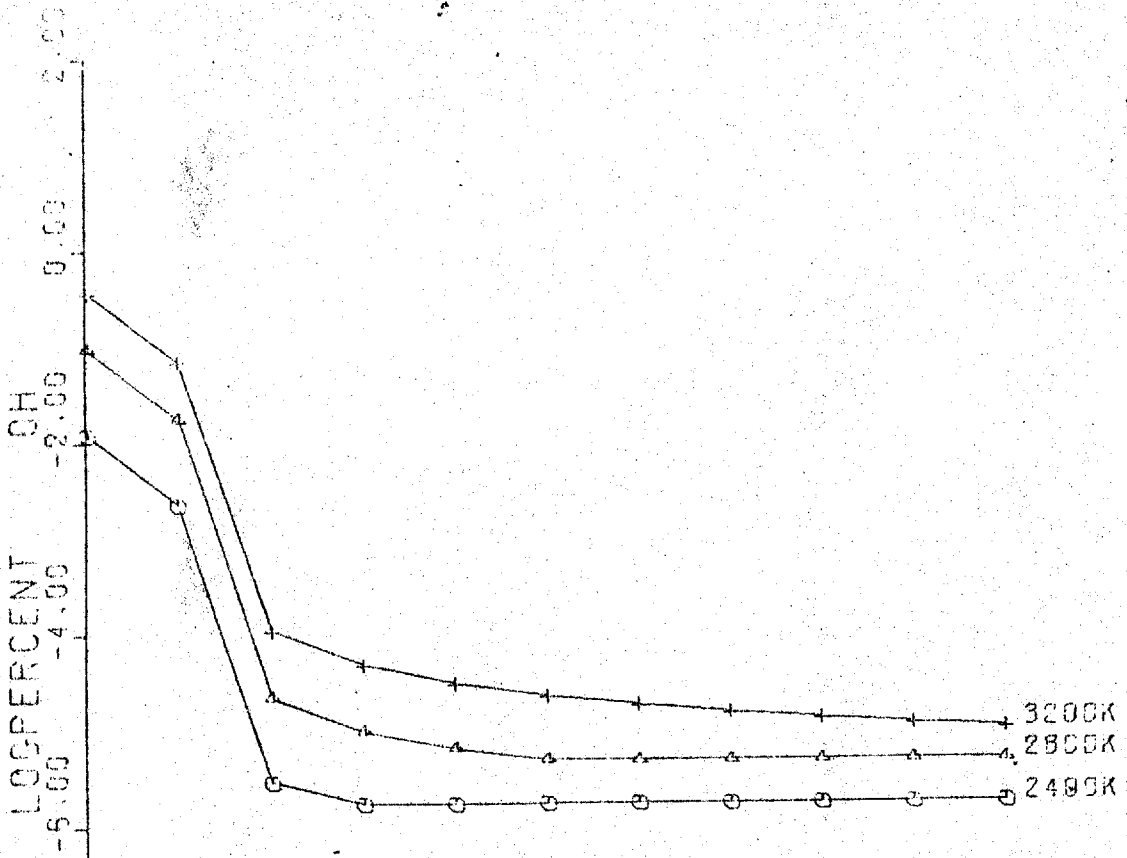


Fig.4.41

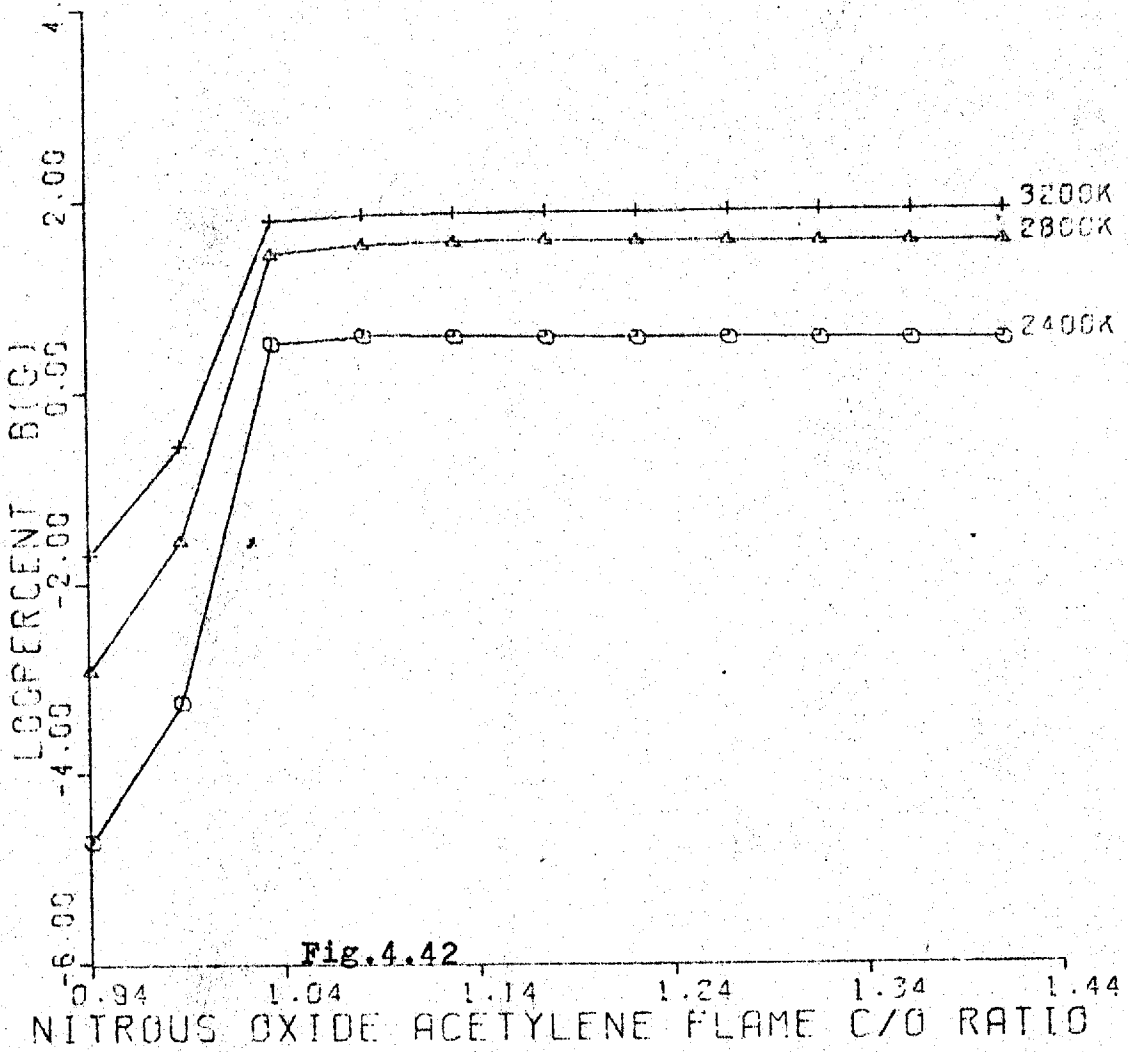


Fig.4.42

NITROUS OXIDE ACETYLENE FLAME C/O RATIO

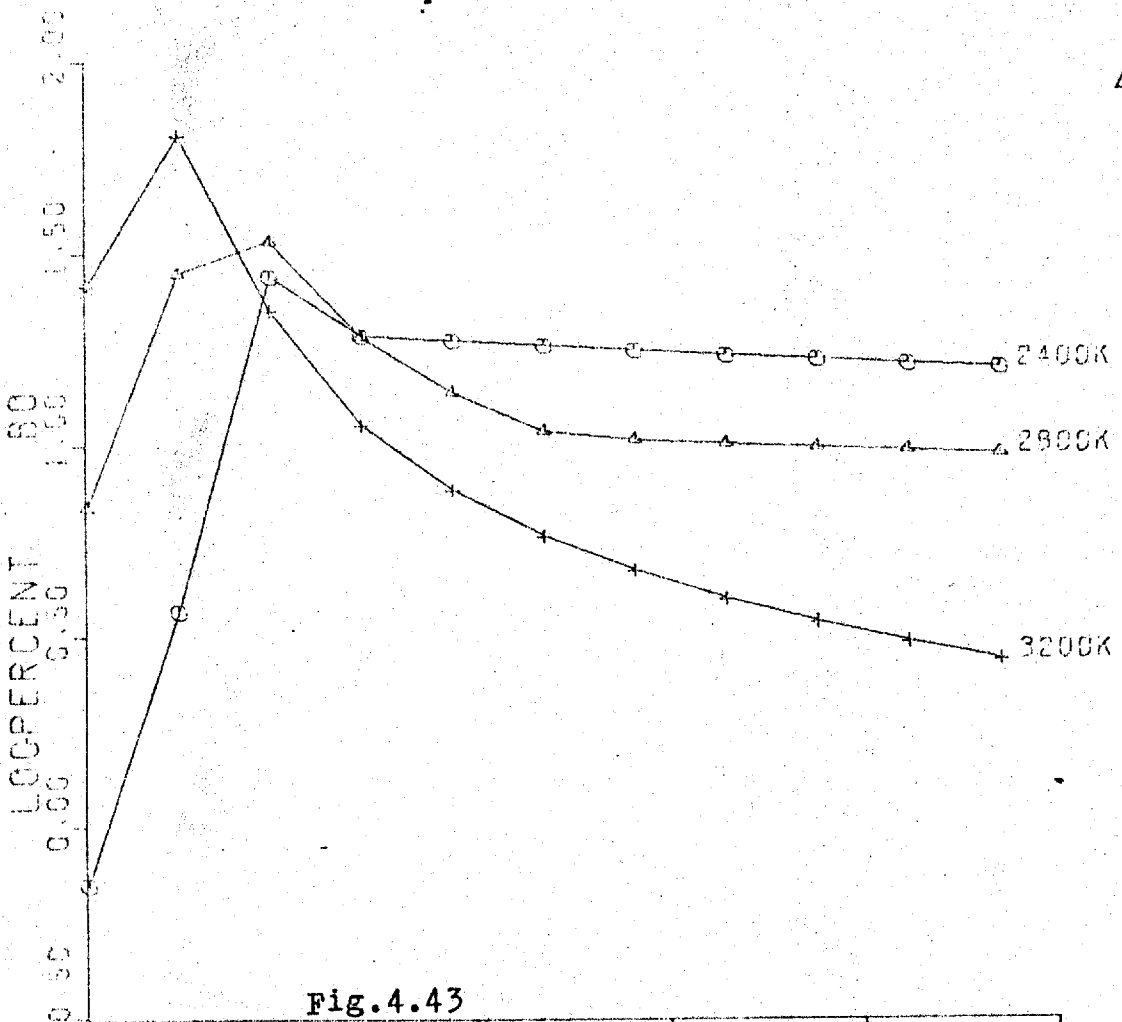


Fig.4.43

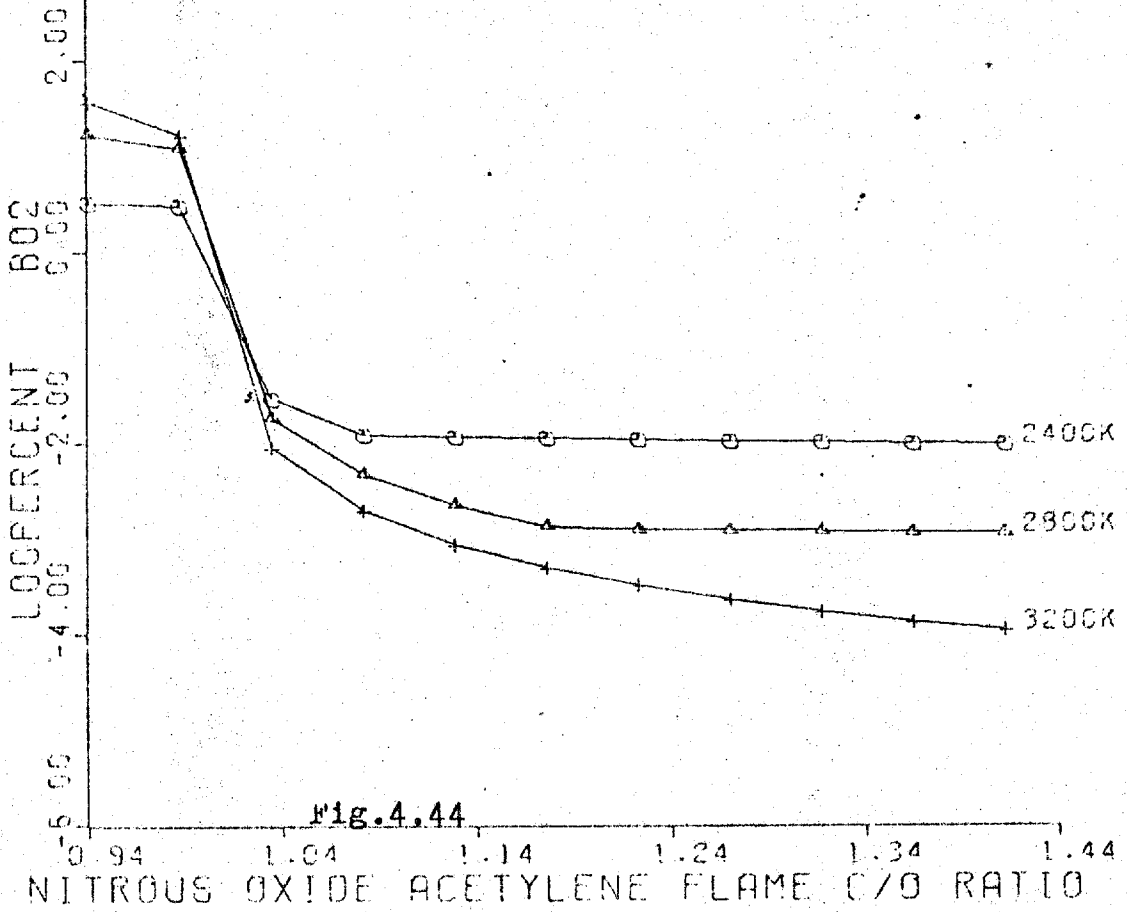


Fig.4.44

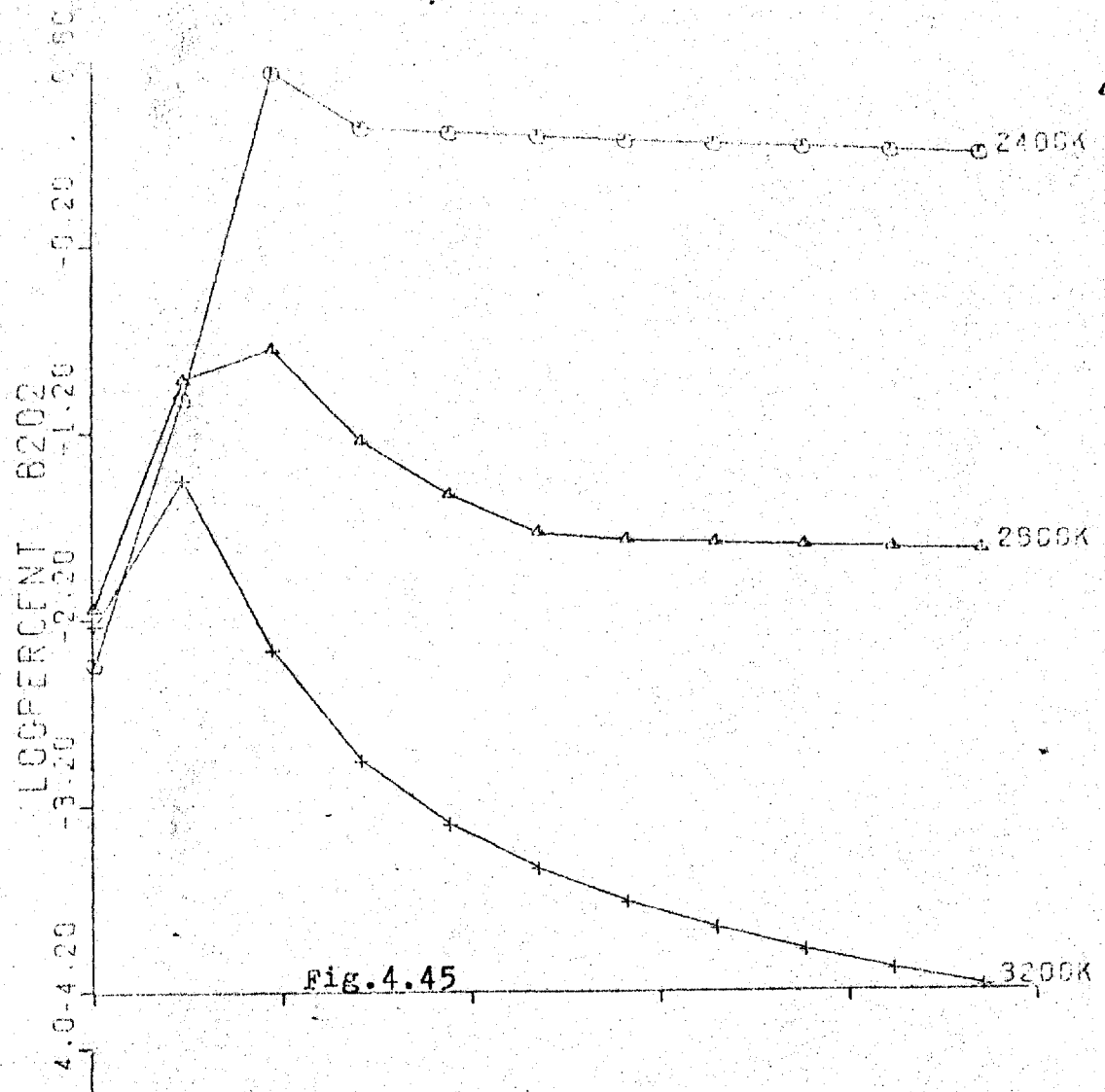


Fig.4.45

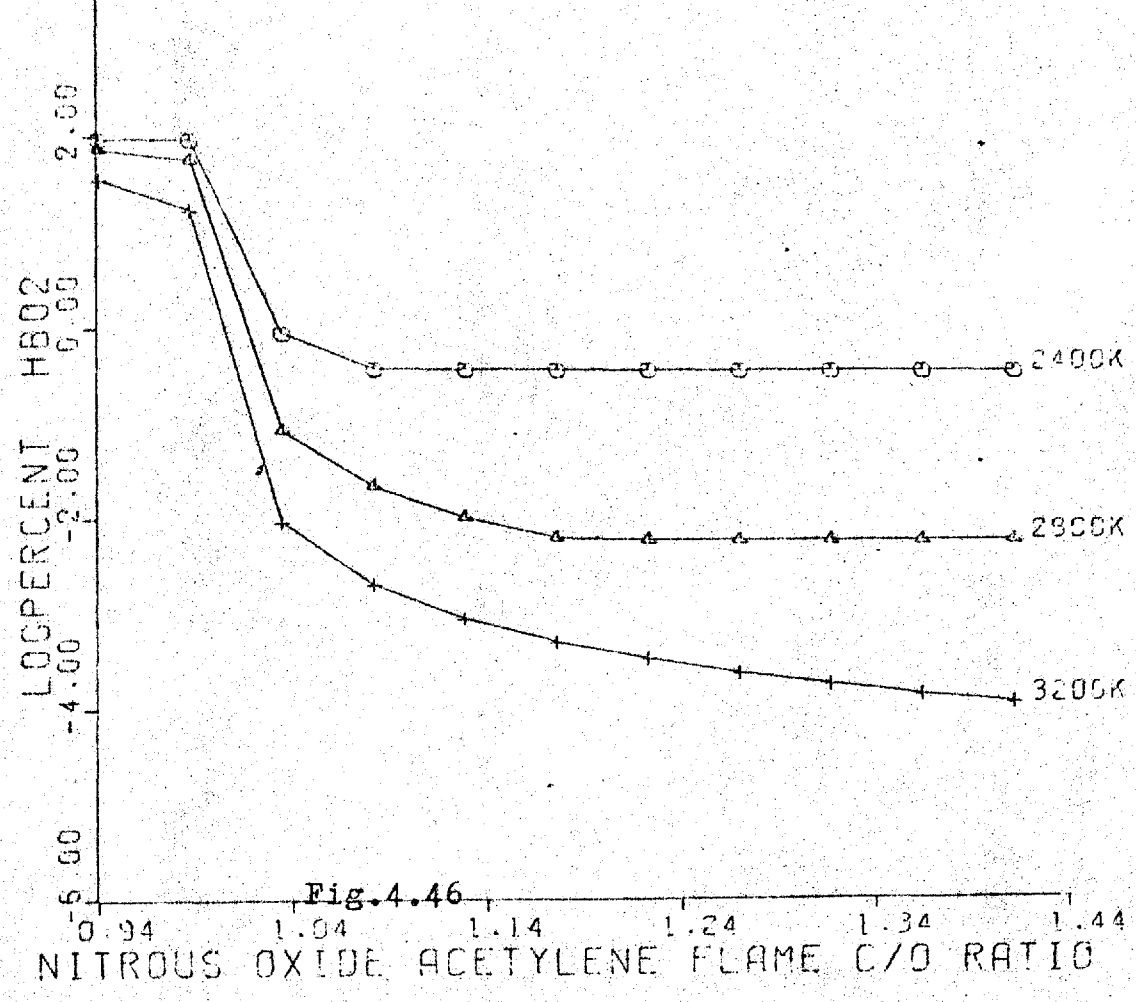
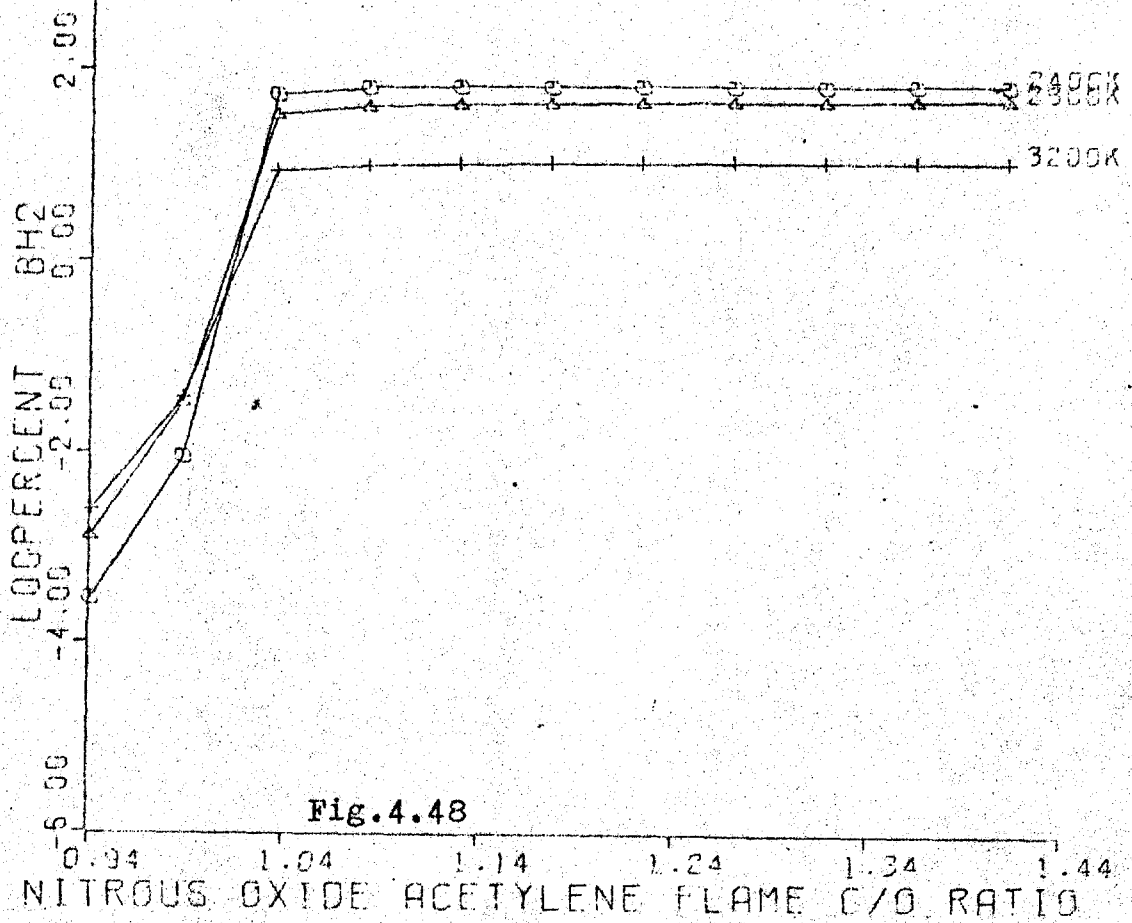
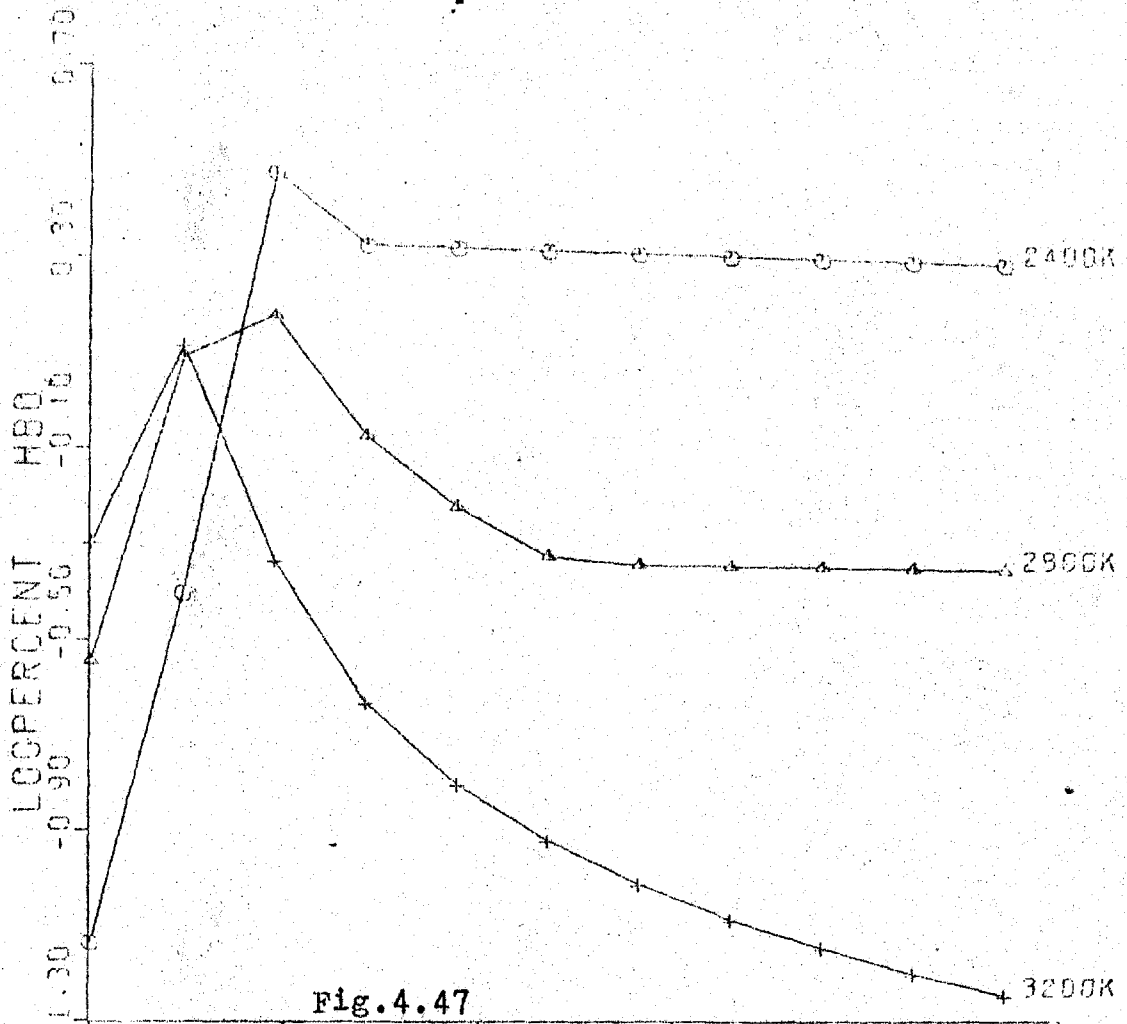


Fig.4.46

NITROUS OXIDE ACETYLENE FLAME C/O RATIO



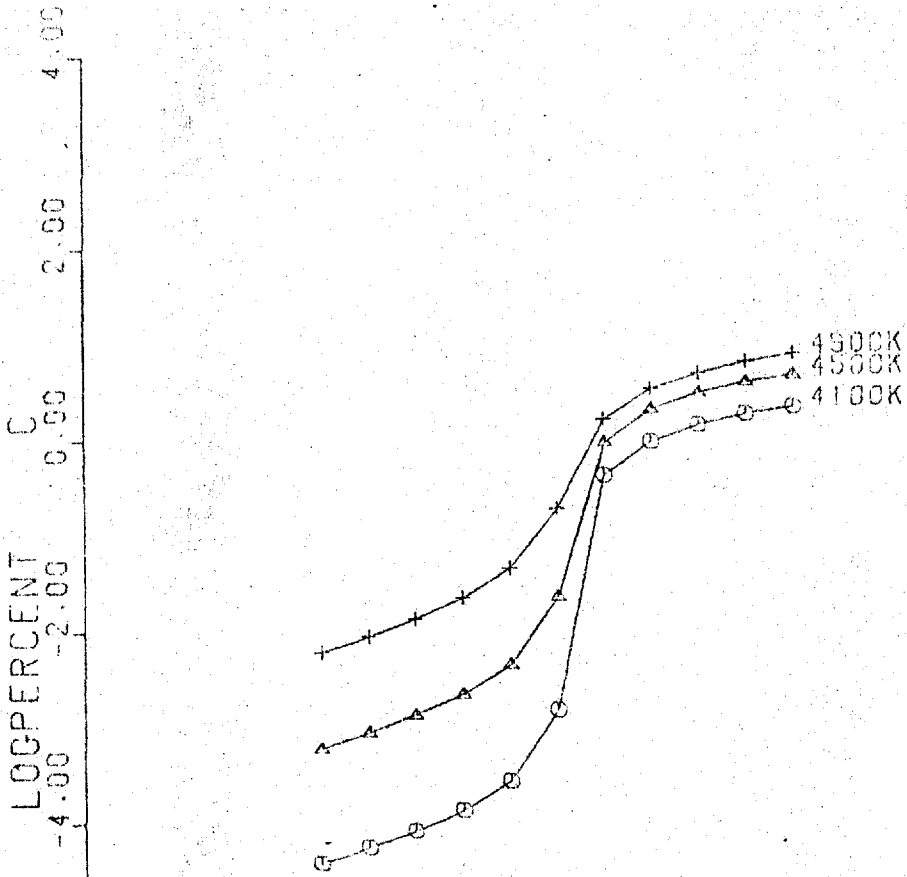


Fig. 4.49

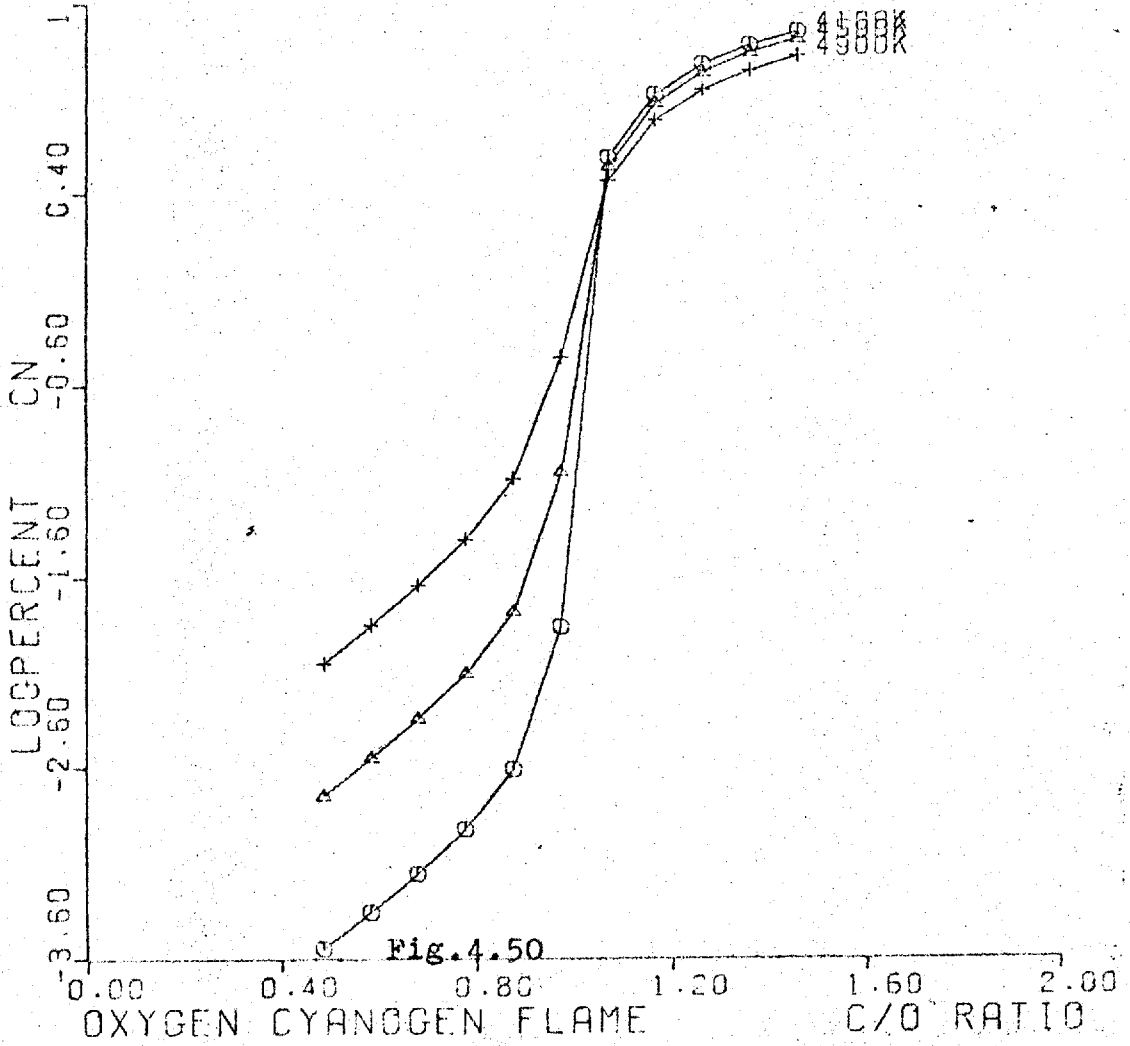
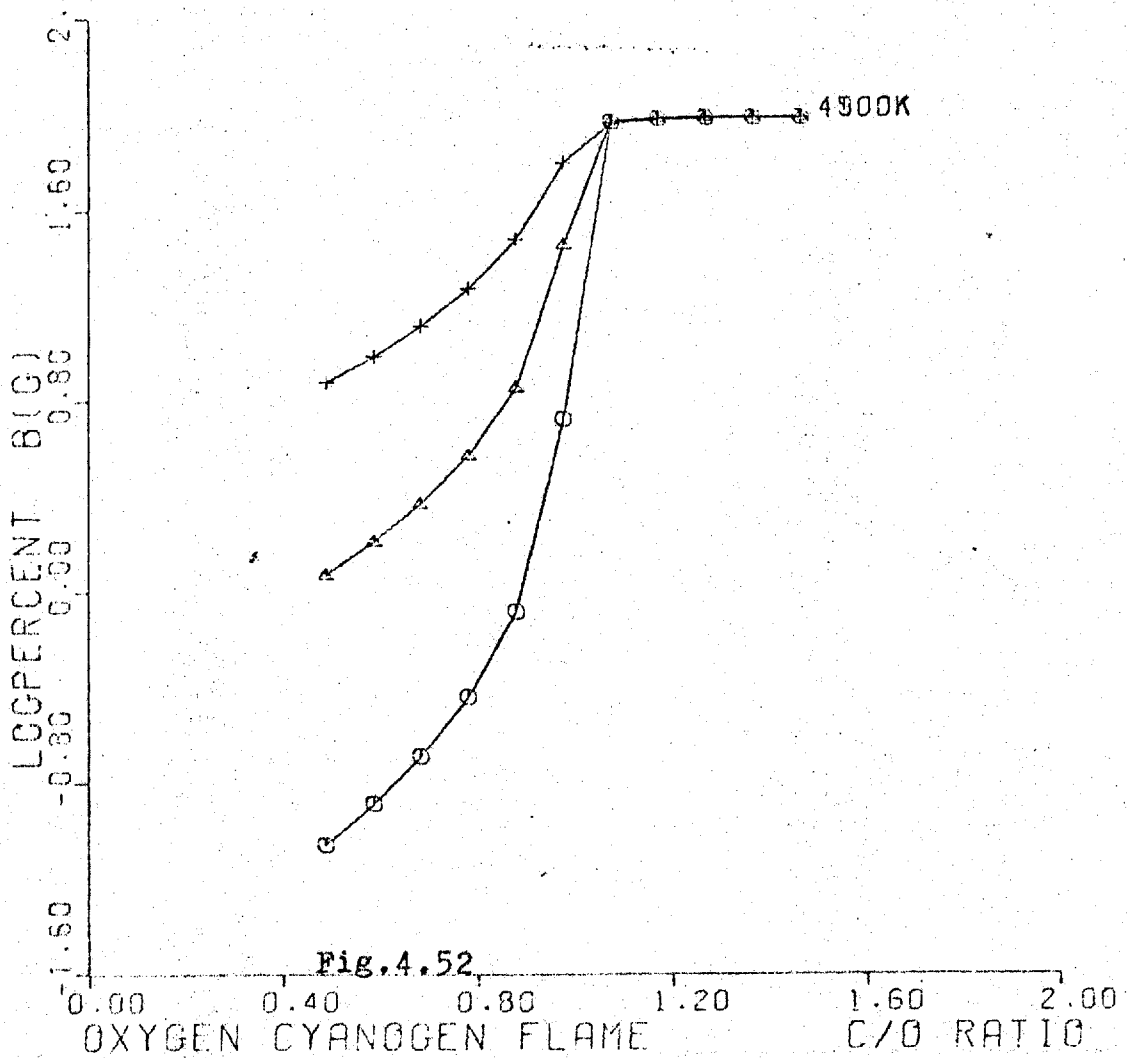
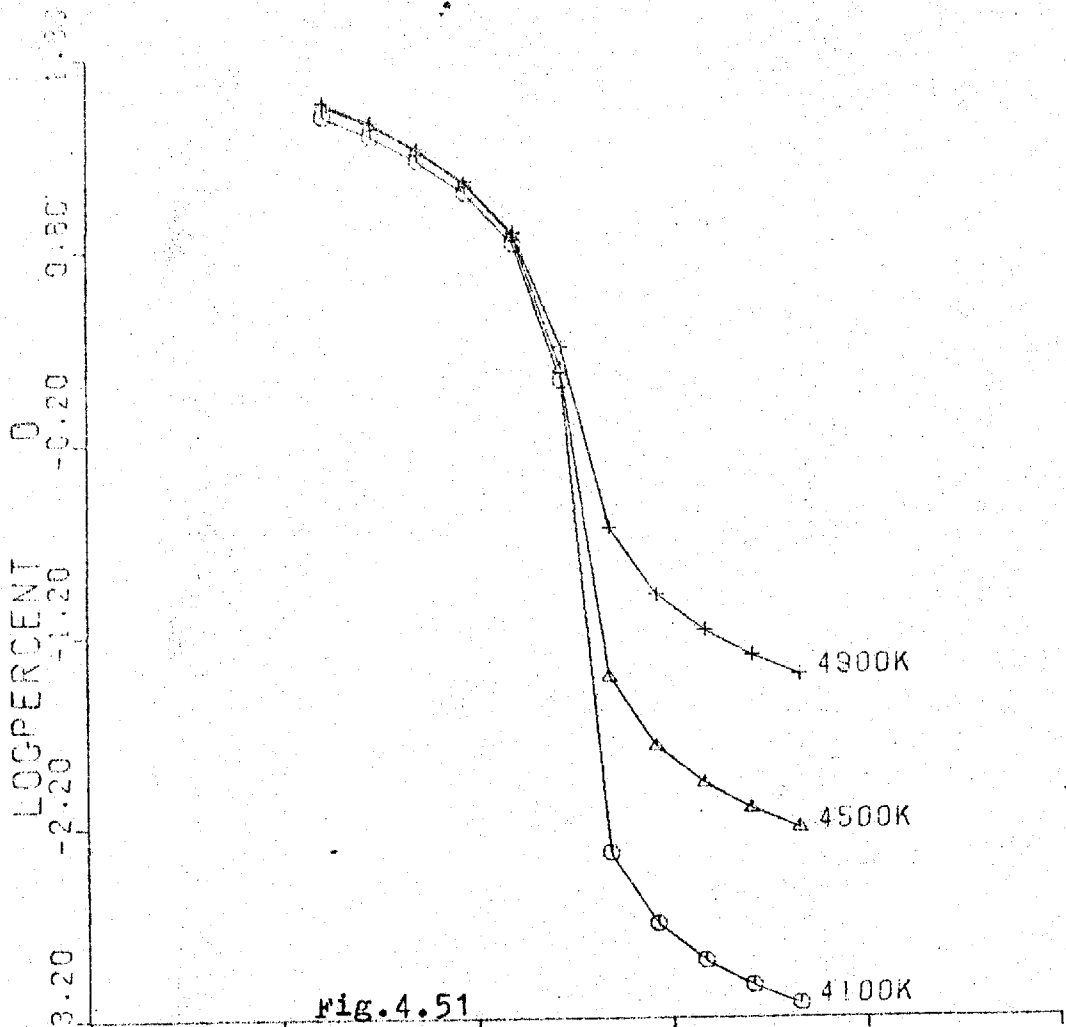


Fig. 4.50



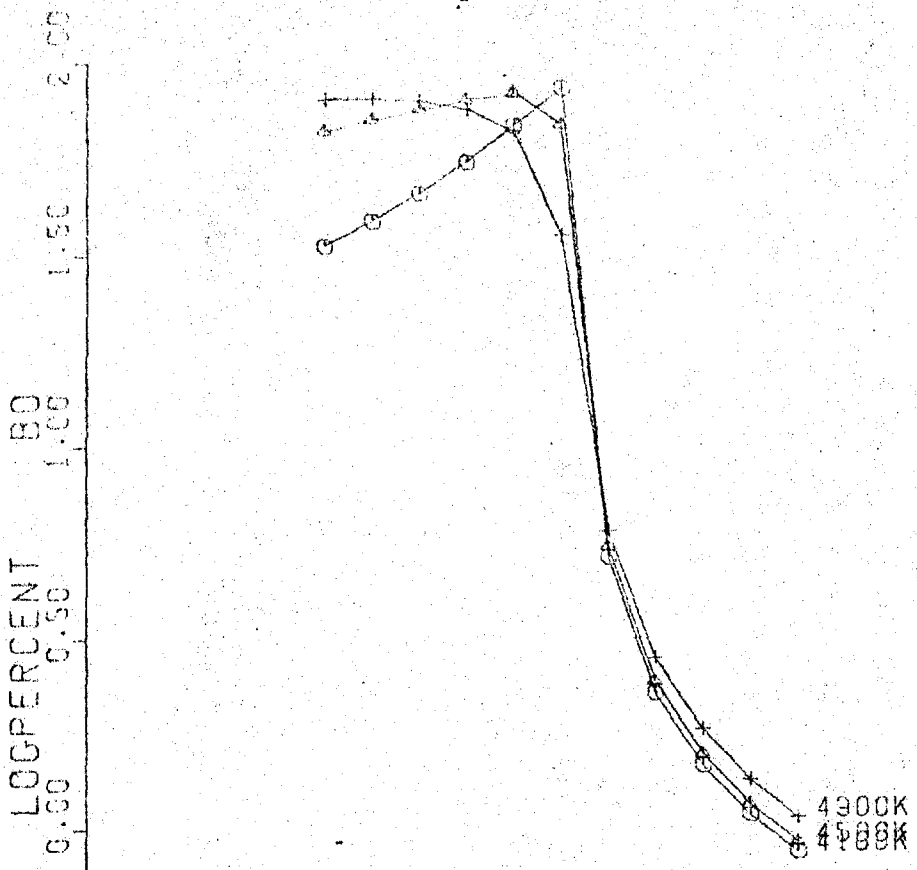


Fig.4.53

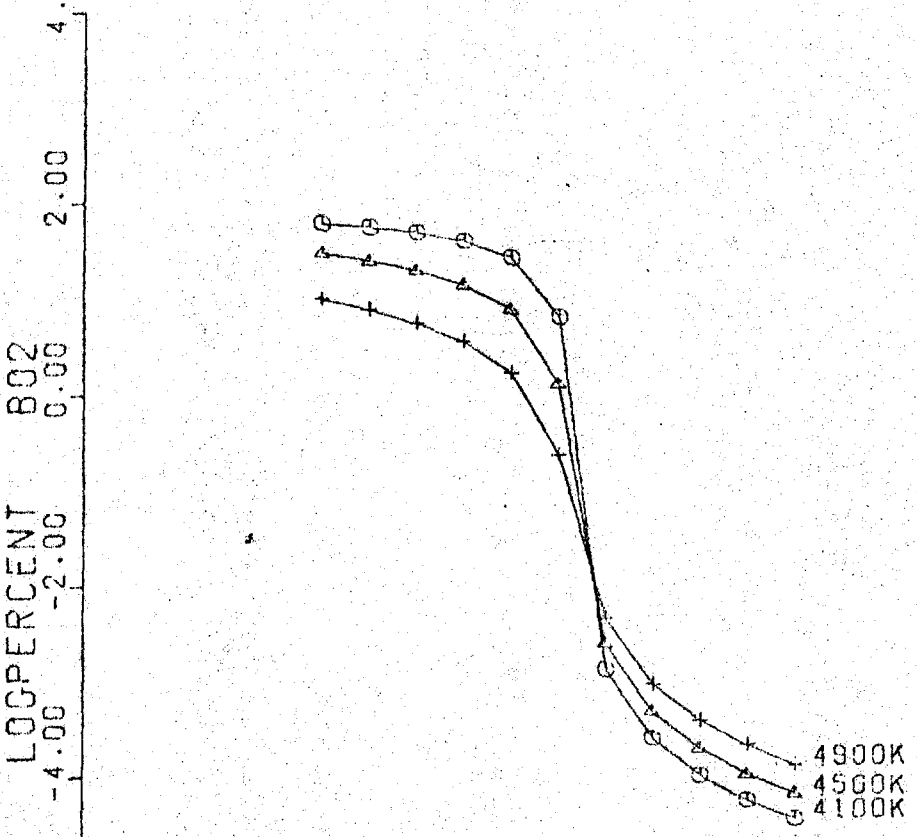
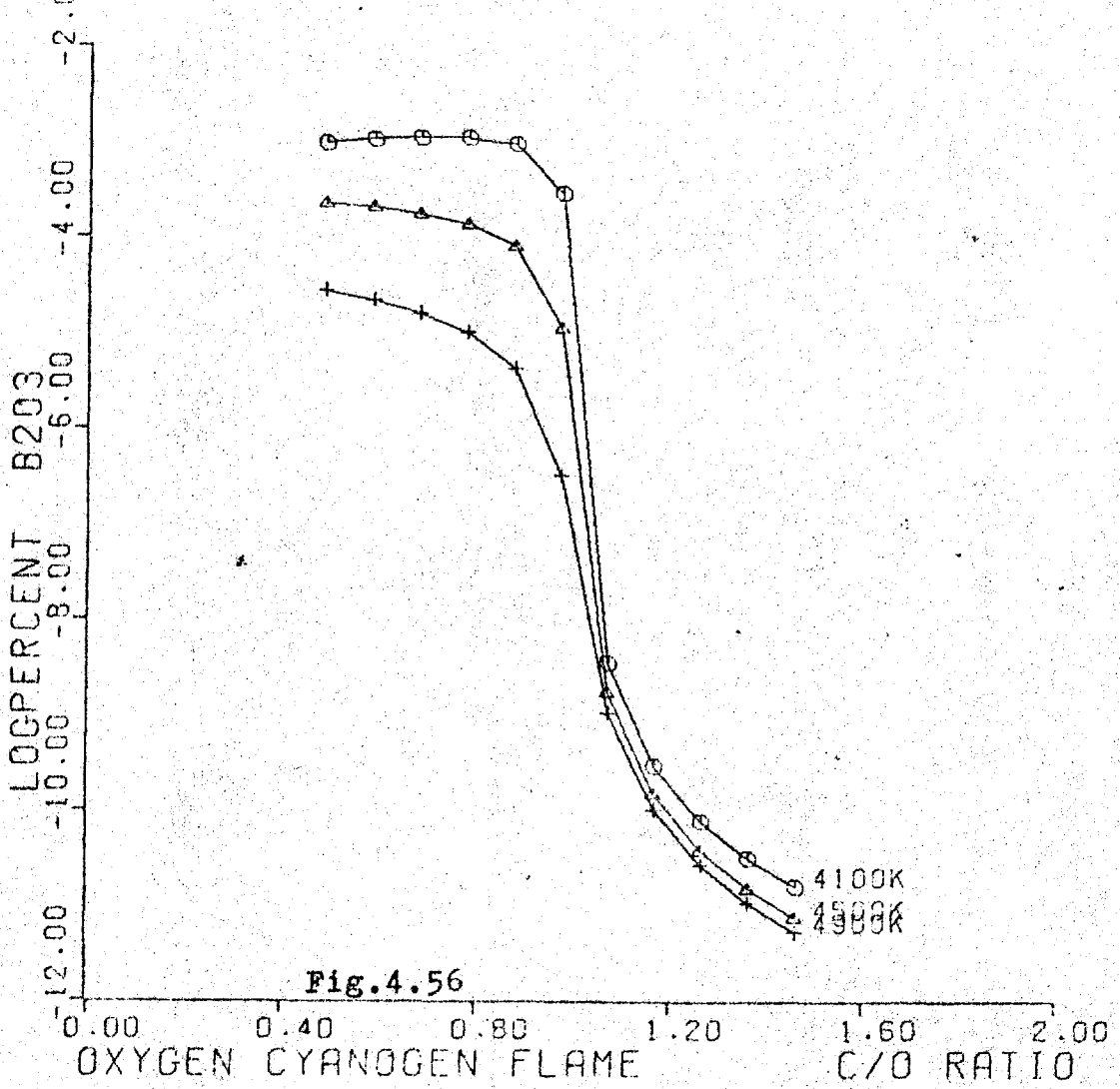
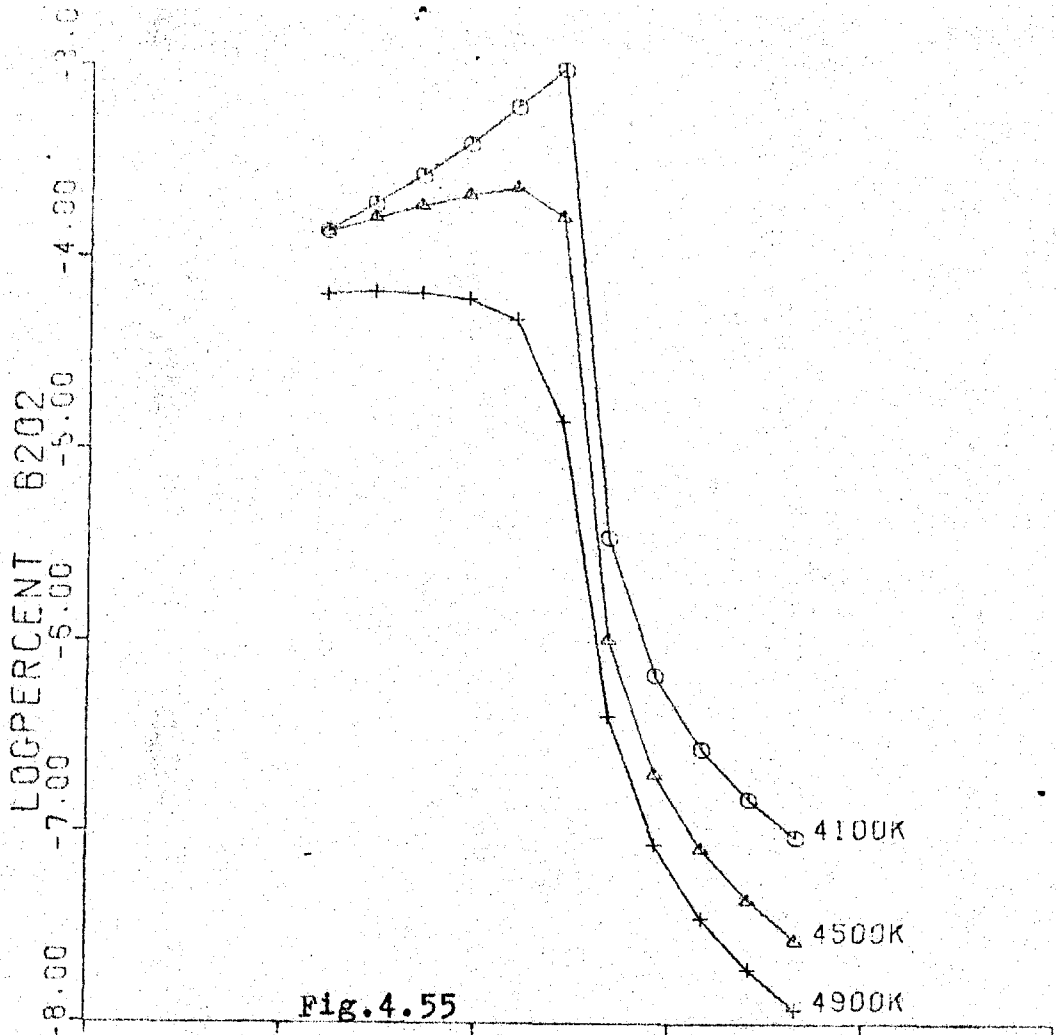


Fig.4.54

OXYGEN CYANOGEN FLAME C/O RATIO



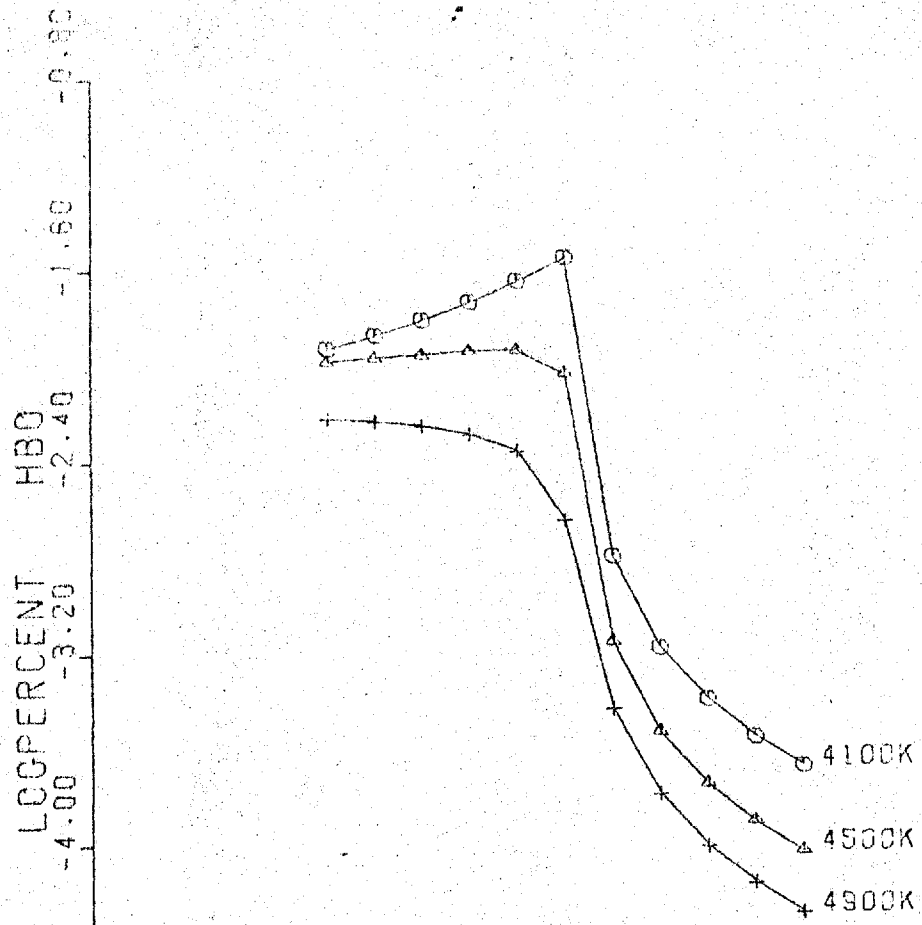


Fig. 4.57

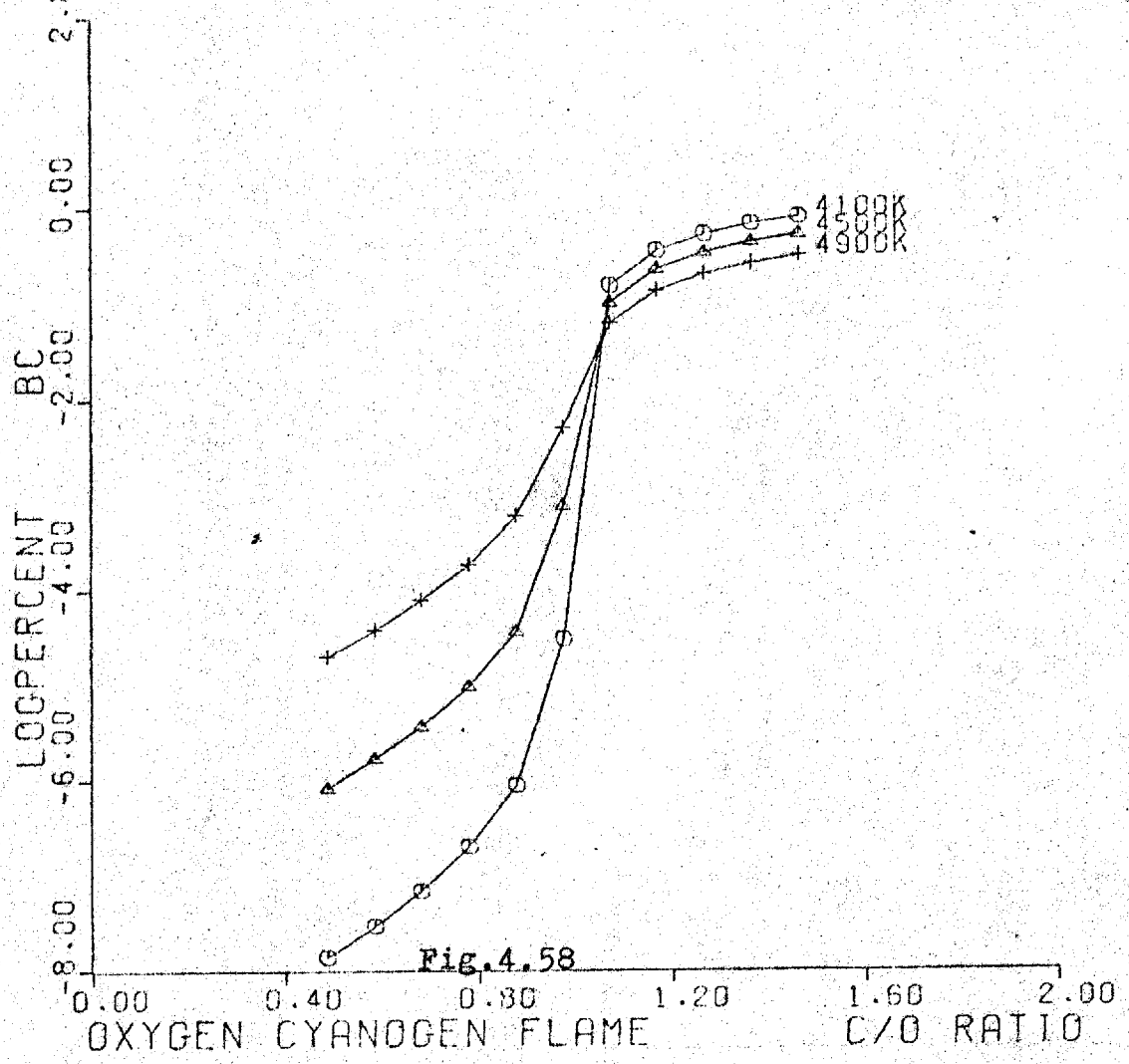
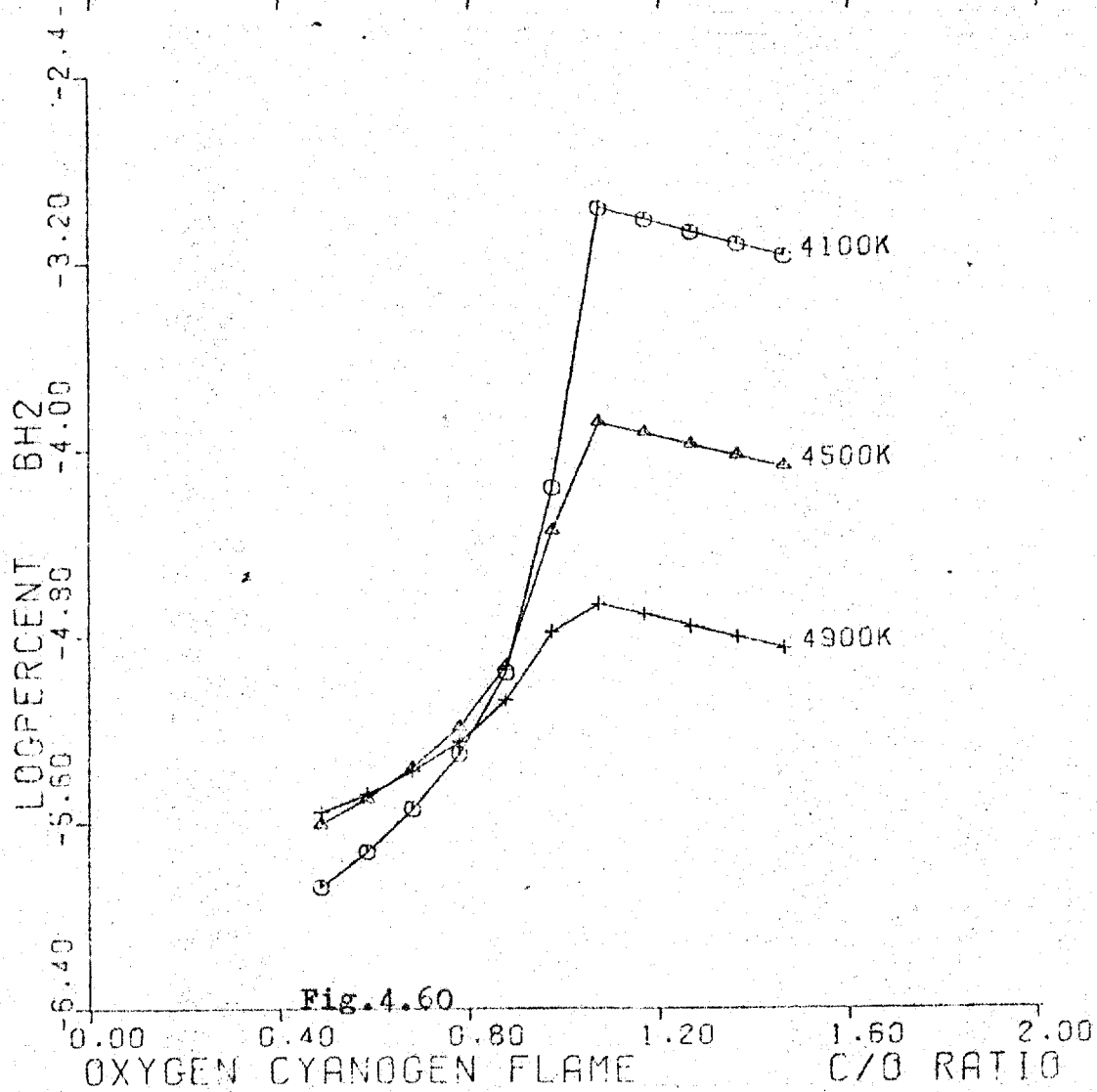
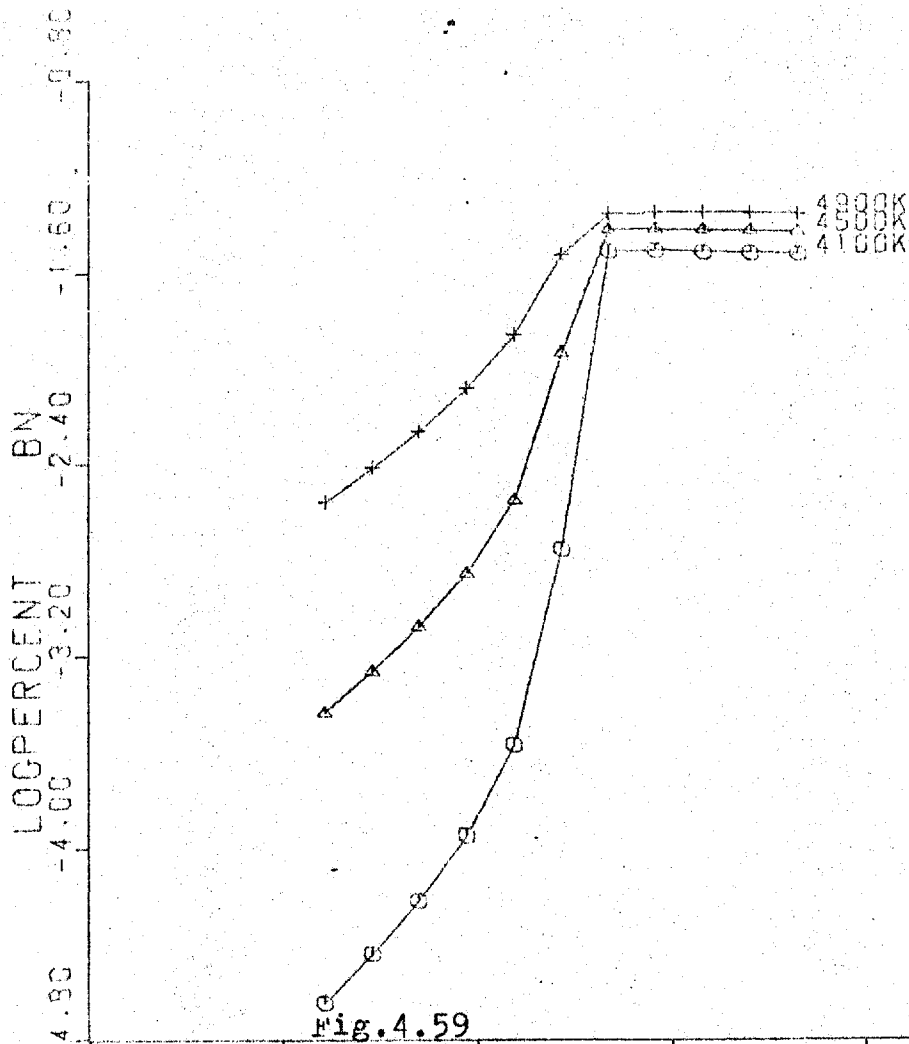


Fig. 4.58



CHAPTER 5

COMPUTER CALCULATIONS OF TITANIUM AND ZIRCONIUM FREE-ATOM
CONCENTRATIONS IN THE NITROUS OXIDE ACETYLENE FLAME.

Introduction.

Since the introduction of the nitrous oxide acetylene flame as an atom reservoir, it has been used for the analytical spectroscopy of a large number of elements which form refractory oxides¹⁻⁸. From the beginning, it has been noticed that the behaviour of zirconium in this flame is somewhat anomalous. AMOS and WILLIS³ reported that the absorption signal was increased by the addition of HF to the sample solution. Later workers^{5,7} have confirmed this, and the indirect determination of fluoride by this method has been suggested⁹. This effect has also been observed for titanium which is zirconium's congener. Even in the presence of HF however, the sensitivity of the determination of Zr is some 5-6 times less than that of titanium. A factor of two of this discrepancy is immediately explicable on the basis of the relative atomic weights (91.22 & 47.90).

The origin of the other 3-fold decrease in sensitivity is not quite so obvious. Two possible sources exist for this discrepancy; the chemical environment, and the oscillator strength of the Zr. Both of these affect the absorption in the expression $\int K_{\nu} d\nu = (\pi e^2 / m_e c) N_0 f$, which gives the integrated absorption in terms of the absorbing species density (N_0) and the oscillator strength (f).

The results of KIRKBRIGHT et al.⁷ strongly suggest that the source of this difference is in the chemical environment of the flame. They found that the small increase in temperature, resulting from shielding a flame with argon rather than nitrogen, produced a significant increase in the sensitivity of determination by Atomic Absorption Spectroscopy (AAS). This is strongly indicative of partial -

atomisation. As with most systems, equilibria tend to follow exponential laws, so that large changes in the position of equilibrium tend to result from small changes in temperature.

The actual change in this system was found to be more than 25% for a probable temperature change of no more than 200K.

As data were available for a large number of zirconium and titanium species in the JANAF Thermochemical Tables, it was decided to undertake a comparative study of the atomisation of these two elements, using the digital computer program described in Chapter 4 to calculate the theoretical values. The availability of suitable data also permitted the study to consider the effect of the presence of fluorine or chlorine in the flames considered.

It was recognised from the start that this approach is not strictly valid, as the effect of using HF in the sample must be to introduce the metal as fluoro-species rather than oxy-species. This suggested that kinetic considerations are very important for this system. As stated in Chapter 4, the program is not equipped to take these factors into consideration. However it was thought that useful results and conclusions might be drawn from the study.

Input to the Program.

The equation chosen to represent the flame is as follows:



The values of RED used varied from 1.0 to 1.5 and the mole number of water introduced was derived as described on p.4.8.

The mole numbers for the metal and the halogen were selected as follows. The value of n was set arbitrarily to 0.0001, and that of m was set such that it would approximate

to a 2% HF solution being used as the sample medium. The same value was also used for the Cl containing flames.

One important difference in technique between this study and the previous one for boron was that the metal mole number was also normalised by division of each mole number by the total. In the first study of boron the boron mole number remained constant at 0.0001; in this study, the metal mole number was varied from 0.000032 to 0.000028 as RED was increased. The exact procedure is described on page 4.3.

The species considered for the study are listed in Table 5.1. Obviously species containing elements not present in a particular flame were not included in the input data for that flame. Not all possible species were considered for each flame. To reduce the computation time and lessen the chance of the program failing to converge, solid species not present in a flame were omitted after a check run. In addition, a number of pure flame species were omitted as these were known from the previous study to be unimportant.

Results.

The results are presented as Tables 5.2 to 5.13, and Figs.5.1 to 5.31

All pure flame species have been omitted from these results. This is because there was found to be no significant difference between their values in the pure flames and those containing metal species. The graphs produced were identical to those produced for the study of boron atomisation (Figs.4.37-4.41, pp4.67-4.69) Reference to these is recommended and the descriptive paragraphs(pp.4.18-4.19)

No reference will be made hereafter to the presence of halogen-containing species which do not contain any metal.

The contribution of these species to the total flame gas composition was found to be negligible with the exception of the atomic species and their hydrogen compounds. The most important other halogen-containing species were not found to exceed $1.0E-04\%$ by volume. The most common were $CClN$, $HOCl$, $NOCl$, CFO , $CHFO$, and $CHFN$.

Where possible differing results for chlorine and fluorine media are presented on the same page.

Species Behaving Similarly in Zr and Ti-containing Flames Atomic Fluorine(Fig.5.1)

This species behaves identically in all flames showing a large decrease in concentration with decreasing temperature, and a small decrease with increasing fuel-richness.

Hydrogen Fluoride(Fig.5.2)

This species is the main reservoir of fluorine in the flame constituting some 95+% of the total. Although it apparently decreases dramatically with high fuel-richness, this effect is mainly one of scale expansion. The decrease is relatively small, but causes relatively large changes in the concentration of other F-containing species.

Atomic Chlorine(Fig.5.3)

This behaves in a very similar fashion to atomic fluorine, but the absolute level of concentration is some two-orders of magnitude higher.

Hydrogen Chloride(Fig.5.4)

Again this species displays similar behaviour to its fluorine congener, with the same overall result.

Titanium Containing Flames.

Atomic Titanium(Fig.5.5)

This species behaves identically in both flames, and displays near 100% atomisation at the higher flame temperatures considered.

(N.B. The graphs for all metal containing species are plotted on the same principle as for the boron study i.e. as \log_{10} % of total metal present. The tables however are given as total of each species present and the total metal concentration is given above as a comparison.)

Titanium Dioxide(Fig.5.6)

Again behaving identically in both environments, this species contains from 25-60% of the total Ti in lean flames, and less than $1.0E-04\%$ in rich flames. It displays the same sigmoid curve displayed by oxidising species in this flame, giving a maximum gradient at a C/O ratio of unity.

Titanium Monoxide(Fig.5.7,5.8)

This species exhibits the characteristics of a typical oxidising species except that it shows an initial rise just below a C/O ratio of 1. The only difference between the Cl-flame(Fig.5.7) and the F-flame(Fig.5.8) is the behaviour of the species at 2800K in very fuel-rich flames. In the presence of F, the species appears to be more favored.

Titanium Monochloride(Fig.5.9)

This species is relatively unimportant but shows characteristics of a reduced species, achieving higher levels in fuel-rich flames. The curve at 2400K shows a peak at C/O=1

Titanium Dichloride(Fig.5.10)

This species is the most important of the Ti/Cl species, reaching the percent level in fuel-rich flames. It shows similar characteristics to $TiCl$ but the order of the curves is inverted, the species is more stable at lower temperature. Again it exhibits a peak at $C/O=1$.

Titanium Trichloride & Tetrachloride(Figs.5.11,5.12)

Both these species behave similarly to each other and to $TiCl_2$. The concentration levels are much lower however.

 $TiOF$ and $TiOF_2$ (Figs5.13,5.14)

These species behave as oxidising species, decreasing across the line $C/O=1$.

 TiF

No graph was included for this species as the absolute concentration is so small as to be negligible.

 TiF_2 (Fig.5.15)

The graph of this species is almost superposable over that of $TiCl_2$, and the same remarks apply.

 TiF_3 (Fig.5.16)

This species behaves similarly to $TiCl_3$, but it has an absolute concentration some two orders of magnitude greater.

Titanium Nitride(solid)

This species does not occur under these conditions.

Titanium Carbide(solid)

This species is only indicated as occurring at low temperatures(2400K) in fuel-rich flames. When it does occur, it is the most important Ti containing species, comprising some 95% of the total titanium present.

Zirconium Containing Flames.Atomic Zirconium(Figs.5.17,5.18)

This species displays slightly different behaviour in F-containing and Cl-containing flames. The difference is in the first three points on the plot, which are lower for the Cl-containing flame. Otherwise the graphs are identical, although the Tables 5.8-5.13 indicate slight differences in favour of the F-containing flame.

The atomisation of Zr never exceeds 55% even in the most favorable conditions, and under the most realistic conditions (2800K C/O=1.03) is nearer 1%.

Zirconium Hydride(Fig.5.19)

This species behaves much like atomic Zr but at only 10% of the concentration. Again there is a decrease in absolute concentration with increasing fuel-richness.

Zirconium Nitride(Fig.5.20)

Again this species shows almost identical behaviour to the previous two species, reaching its maximum concentration at C/O=1 and 3200K.

Zirconium Monoxide(Figs.5.21,5.22)

This species exhibits differential behaviour in F-containing and Cl-containing flames, after the same fashion as atomic Zr. This behaviour appears to be due to the formation of solid ZrO_2 in the Cl-flame at the lower temperature studied 2400K. This does not occur in the F-flame. Thus the plot for the Cl-flame(Fig.5.22) has the first three points of the low temperature curve lower than those on Fig.5.21.

Zirconium Dioxide(Figs.5.23,5.24)

Precisely the same remarks are applicable to this species as are to the previous one. Again the effect of the presence of solid ZrO_2 in the Cl-containing flame is to lower the concentration of this species. Together with the other Zr/O species this forms the great majority of the Zr-containing species in fuel-lean flames.

ZrCl(Fig.5.25)

This behaves like the other Zr reducing species, displaying a peak at C/O=1, and decreasing at greater fuel-richness. The absolute concentration is very small however.

ZrCl₂(Fig.5.26)

Another reducing species, this exhibits much the same characteristics as the others, but shows less temperature-dependence. In fuel-rich flames, it comprises up to some 15% of the total Zr present.

ZrCl₃(Fig.5.27)

This species behaves in a similar fashion to the other zirconium chlorides, but it is intermediate in absolute concentration between ZrCl and ZrCl₂.

Zirconium Fluorides(Figs.5.28-5.31)

These four fluorides behave in a similar fashion to the chlorides described above. In this instance, the difluoride and trifluoride species are almost equally important, but together they comprise at most some 1% of the total Zr present in the flame.

Zirconium Dioxide(solid)

This was found to occur only in the Cl-containing flame, and was eliminated from consideration in the F-containing flame. This procedure is not certain as there is a possibility of synergistic effects. It occurred only at low

temperature in fuel-lean flames, and did not continue into the analytically useful region.

Zirconium Carbide(solid)

This species is not present in fuel-lean flames. In flames where the C/O ratio exceeds unity, it is the most important, comprising up to more than 97% of all Zr present.

The calculations indicate that the behaviour is different in Cl- and F-containing flames. The difference is a factor of 2 at 2800K in the near stoichiometric flames - Tables 5.9 and 5.12. It is also indicated as being formed at 3200K in the F-containing flame but not in the Cl-containing flame. This difference is explicable on the basis of the technique used for calculating solid species concentrations. This is a stepwise process, and species with calculated concentrations less than $1.0E-06$ are excluded from the matrix used for the calculation. As the absolute concentrations of these species are close to this cut-off, it would be easy for a species to be eliminated unexpectedly. The possibility of synergistic action with other condensed flame components also exists. In this instance, solid zirconium dioxide was included in the Cl-flame and not in the F-flame.

Conclusions.

The results of this study are in general agreement with the results obtained in practice. A definite indication is given of the difficulty of atomising zirconium completely in this flame. Within the analytical range of temperature and stoichiometry (approximately 2900K and a C/O ratio from 0.95 to 1.10) there are two opposing mechanisms, both of which tend to reduce the atomisation. If the flame is fuel-

lean, then the majority of the zirconium will be present as oxide species. If it is fuel-rich then the formation of the refractory carbide will remove most of the zirconium present.

Burning the flame at the exact point of $C/O=1$ should give the best compromise, but this is obviously impractical as the slightest variation from this will cause the flame properties to alter considerably.

The same conclusions also apply to the determination of titanium in this flame, but to a lesser degree. Unless the flame is cooled considerably from its maximum temperature of about 2900K, then no great difficulty should be encountered. This is indeed found to be the case, and the recommended conditions for the determination of Ti are to burn the flame slightly fuel-rich ^{3,7}.

In order to obtain the maximum sensitivity of determination of zirconium, it is necessary to use a slightly hotter flame than this one. As shown in Chapter 4, it is still necessary to use a carbon-containing fuel to obtain the best results from conventional flames. Thus three courses of action are possible: use a hotter flame e.g. oxycyanogen, use a hotter non-carbon-containing flame e.g. hydrogen-fluorine, or a plasma source. The latter of these is the most easily feasible, and a compromise, in the form of an augmented nitrous oxide acetylene flame, would probably serve to raise the temperature above the point where zirconium carbide is decomposed. The results indicate that an increase in temperature of only some 400K would serve to reduce the interference by a factor of five.

Table 5.1.Species Considered in the Study.

C	C ₂	C ₃	CN	HCN
C ₂ N ₂	CH	CH ₂	CH ₃	CH ₄
C ₂ H ₂	HCNO	CHO	CH ₂ O	H
H ₂	OH	H ₂ O	O	O ₂
N	N ₂	NH	NH ₂	NO
CO	CO ₂			

Cl-containing Flames Only

Cl	HCl	CCl	CCl ₂	CCl ₃
CCl ₄	CHCl ₃	CH ₂ Cl ₂	CH ₃ Cl	CNCl
HOCl	NOCl	NO ₂ Cl	ClO	ClO ₂
Cl ₂	Cl ₂ O			

F-containing Flames Only

F	HF	F ₂	CF	CF ₂
CFO	CFN	CHFO	CHF ₃	CH ₂ F ₂
CF ₂ O	HO ₂ F	FO	FN	

Ti-containing Flames

Ti	TiO	TiO ₂ (g)	TiC(c)	TiN(c)
TiCl	TiCl ₂	TiCl ₃	TiCl ₄	
TiF	TiF ₂	TiF ₃	TiF ₄	TiOF
TiOF ₂				

Zr-containing Flames

Zr	ZrO	ZrO ₂ (g)	ZrH	ZrN
ZrO ₂ (c)	ZrC(c)			
ZrCl	ZrCl ₂	ZrCl ₃		
ZrF	ZrF ₂	ZrF ₃	ZrF ₄	

(g) = gaseous

(c) = condensed

Table 5.2.Ti/Cl-containing Lean Flame.

C/O = 0.9412		Ti = 0.000032 Cl = 0.000736		
Species	2400K	2800K	3200K	
Ti	3.37E-08	1.66E-07	5.62E-07	
TiO	1.21E-05	1.91E-05	2.41E-05	
TiO ₂	1.98E-05	1.27E-05	7.34E-06	
TiCl	6.45E-16	5.34E-15	2.26E-14	
TiCl ₂	3.13E-08	2.12E-09	2.13E-10	
TiCl ₃	2.01E-12	4.65E-14	1.81E-15	
TiCl ₄	1.25E-16	1.21E-18	2.14E-20	
TiC(c)	0	0	0	
TiN(c)	0	0	0	

Table 5.3.Ti/Cl-containing Near-Stoichiometric Flame.

C/O = 1.0353		Ti = 0.000031 Cl = 0.000713		
Species	2400K	2800K	3200K	
Ti	1.43E-06	2.99E-05	3.06E-05	
TiO	1.18E-07	7.63E-07	3.72E-07	
TiO ₂	4.39E-11	1.12E-10	3.21E-11	
TiCl	2.50E-14	8.79E-13	1.14E-12	
TiCl ₂	1.10E-06	3.15E-07	9.88E-09	
TiCl ₃	6.45E-11	6.37E-12	7.73E-14	
TiCl ₄	6.66E-15	1.51E-16	8.44E-19	
TiC(c)	2.84E-05	0	0	
TiN(c)	0	0	0	

Table 5.4.Ti/Cl-containing Rich Flame.

C/O = 1.1294		Ti = 0.000030		Cl = 0.000692	
Species	2400K	2800K	3200K		
Ti	8.40E-07	2.95E-05	3.00E-05		
TiO	4.01E-08	2.26E-07	1.03E-07		
TiO ₂	8.73E-12	9.92E-12	2.51E-12		
TiCl	1.41E-14	8.54E-13	1.08E-12		
TiCl ₂	6.02E-07	3.03E-07	9.17E-09		
TiCl ₃	3.39E-11	6.01E-12	6.99E-14		
TiCl ₄	1.86E-15	1.40E-16	7.43E-19		
TiC(c)	2.86E-05	0	0		
TiN(c)	0	0	0		

Table 5.5.Ti/F-containing Lean Flame.

C/O = 0.9412		Ti = 0.000032		F = 0.000736	
Species	2400K	2800K	3200K		
Ti	3.36E-08	1.66E-07	5.62E-07		
TiO	1.21E-05	1.91E-05	2.41E-05		
TiO ₂	1.98E-05	1.27E-05	7.34E-06		
TiF	4.01E-18	7.84E-17	7.76E-16		
TiF ₂	3.26E-08	2.91E-09	5.44E-10		
TiF ₃	3.32E-10	3.99E-12	2.30E-13		
TiF ₄	1.95E-14	1.74E-16	6.61E-18		
TiOF	4.72E-08	1.74E-08	7.90E-09		
TiOF ₂	6.55E-10	5.46E-11	8.70E-12		
TiC(c)	0	0	0		
TiN(c)	0	0	0		

Table 5.6.Ti/F-containing Near-Stoichiometric Flame.

C/O = 1.0353		Ti = 0.000031		F = 0.000713	
Species	2400K	2800K	3200K		
Ti	1.43E-06	2.98E-05	3.06E-05		
TiO	1.18E-07	7.60E-07	3.72E-07		
TiO ₂	4.40E-11	1.12E-10	3.21E-11		
TiF	1.55E-16	1.28E-14	2.83E-14		
TiF ₂	1.15E-06	4.30E-07	2.43E-08		
TiF ₃	7.42E-09	5.34E-10	9.35E-12		
TiF ₄	5.68E-13	2.11E-14	2.43E-16		
TiOF	4.18E-10	6.27E-10	1.11E-10		
TiOF ₂	2.26E-12	1.79E-12	1.10E-13		
TiC(c)	2.83E-05	0	0		
TiN(c)	0	0	0		

Table 5.7.Ti/F-containing Rich Flame.

C/O = 1.1294		Ti = 0.000030		F = 0.000692	
Species	2400K	2800K	3200K		
Ti	8.40E-07	2.94E-05	2.99E-05		
TiO	4.01E-08	2.25E-07	1.03E-07		
TiO ₂	8.72E-12	9.89E-12	2.50E-12		
TiF	8.78E-17	1.24E-14	3.65E-14		
TiF ₂	6.25E-07	4.12E-07	2.26E-08		
TiF ₃	3.90E-09	5.05E-10	8.44E-12		
TiF ₄	2.88E-13	1.97E-14	2.14E-16		
TiOF	1.37E-10	1.83E-10	2.97E-11		
TiOF ₂	1.67E-12	5.13E-13	2.89E-14		
TiC(c)	2.86E-05	0	0		
TiN(c)	0	0	0		

Table 5.8.Zr/Cl-containing Lean Flame.

C/O = 0.9412 Zr = 0.000032 Cl = 0.000736

Species	2400K	2800K	3200K
Zr	7.62E-14	2.76E-10	2.51E-09
ZrO	1.18E-08	5.32E-06	9.06E-06
ZrO ₂	1.23E-07	2.67E-05	2.29E-05
ZrCl	6.34E-21	2.98E-17	2.79E-16
ZrCl ₂	1.11E-09	1.50E-08	1.52E-09
ZrCl ₃	5.25E-13	2.01E-12	6.85E-14
ZrH	2.54E-14	4.01E-11	1.74E-10
ZrN	4.48E-19	2.99E-15	4.14E-14
ZrC(c)	0	0	0
ZrO ₂ (c)	3.19E-05	0	0

Table 5.9.Zr/Cl-containing Near Stoichiometric Flame.

C/O = 1.0353 Zr = 0.000031 Cl = 0.000713

Species	2400K	2800K	3200K
Zr	4.34E-10	3.41E-07	1.20E-05
ZrO	1.53E-08	1.46E-06	1.22E-05
ZrO ₂	3.65E-11	1.62E-09	8.76E-09
ZrCl	3.25E-17	3.23E-14	1.21E-12
ZrCl ₂	5.10E-06	1.43E-05	5.94E-06
ZrCl ₃	2.17E-09	1.67E-09	2.43E-10
ZrH	1.52E-10	5.22E-08	8.76E-07
ZrN	2.47E-15	3.58E-12	1.91E-10
ZrC(c)	2.59E-05	1.49E-05	0
ZrO ₂ (c)	0	0	0

Table 5.10.Zr/Cl-containing Rich Flame.

C/O = 1.1294		Zr = 0.000030		Cl = 0.000692	
Species	2400K	2800K	3200K		
Zr	2.54E-10	1.03E-07	1.65E-05		
ZrO	5.23E-09	1.32E-07	4.74E-06		
ZrO ₂	7.26E-12	4.39E-11	9.62E-10		
ZrCl	1.85E-17	9.89E-15	1.61E-12		
ZrCl ₂	2.81E-06	4.43E-06	7.66E-06		
ZrCl ₃	1.16E-09	2.26E-10	3.04E-10		
ZrH	9.10E-11	1.57E-08	1.21E-06		
ZrN	1.43E-15	1.05E-12	2.54E-10		
ZrC(c)	2.73E-05	2.54E-05	0		
ZrO ₂ (c)	0	0	0		

Table 5.11.Zr/F-containing Lear Flame.

C/O = 0.9412		Zr = 0.000032		F = 0.000736	
Species	2400K	2800K	3200K		
Zr	1.81E-11	2.76E-10	2.52E-09		
ZrO	2.80E-06	5.32E-06	9.06E-06		
ZrO ₂	2.92E-05	2.67E-05	2.29E-05		
ZrF	2.00E-20	8.40E-19	1.69E-17		
ZrF ₂	3.20E-10	3.78E-11	9.88E-12		
ZrF ₃	2.63E-09	4.18E-11	2.63E-12		
ZrF ₄	1.13E-11	4.95E-14	1.27E-15		
ZrH	6.04E-12	4.03E-11	1.74E-10		
ZrN	1.06E-16	2.99E-15	4.14E-14		
ZrC(c)	0	0	0		

Table 5.12.Zr/F-containing Near Stoichiometric Flame.

C/O = 1.0353		Zr = 0.000031		F = 0.000713	
Species	2400K	2800K	3200K		
Zr	4.34E-10	3.41E-07	1.48E-05		
ZrO	1.53E-08	1.46E-06	1.51E-05		
ZrO ₂	3.66E-11	1.62E-09	1.08E-08		
ZrF	4.38E-19	9.42E-16	9.01E-14		
ZrF ₂	6.38E-09	3.85E-08	4.77E-08		
ZrF ₃	4.77E-08	3.87E-08	1.15E-08		
ZrF ₄	1.86E-10	4.15E-11	5.05E-12		
ZrH	1.52E-10	5.23E-08	1.08E-06		
ZrN	2.48E-15	3.59E-12	2.36E-10		
ZrC(c)	3.09E-05	2.91E-05	0		

Table 5.13.Zr/F-containing Rich Flame.

C/O = 1.1294		Zr = 0.000030		F = 0.000692	
Species	2400K	2800K	3200K		
Zr	2.54E-10	1.03E-07	1.76E-05		
ZrO	5.23E-09	1.32E-07	5.08E-06		
ZrO ₂	7.25E-12	4.39E-11	1.03E-09		
ZrF	2.47E-19	2.81E-16	1.05E-13		
ZrF ₂	2.47E-09	1.13E-08	5.39E-08		
ZrF ₃	2.50E-08	1.12E-08	1.26E-08		
ZrF ₄	9.39E-11	1.19E-11	5.41E-12		
ZrH	9.10E-11	1.57E-08	1.29E-06		
ZrN	1.43E-15	1.05E-12	2.72E-10		
ZrC(c)	3.01E-05	2.98E-05	6.00E-06		

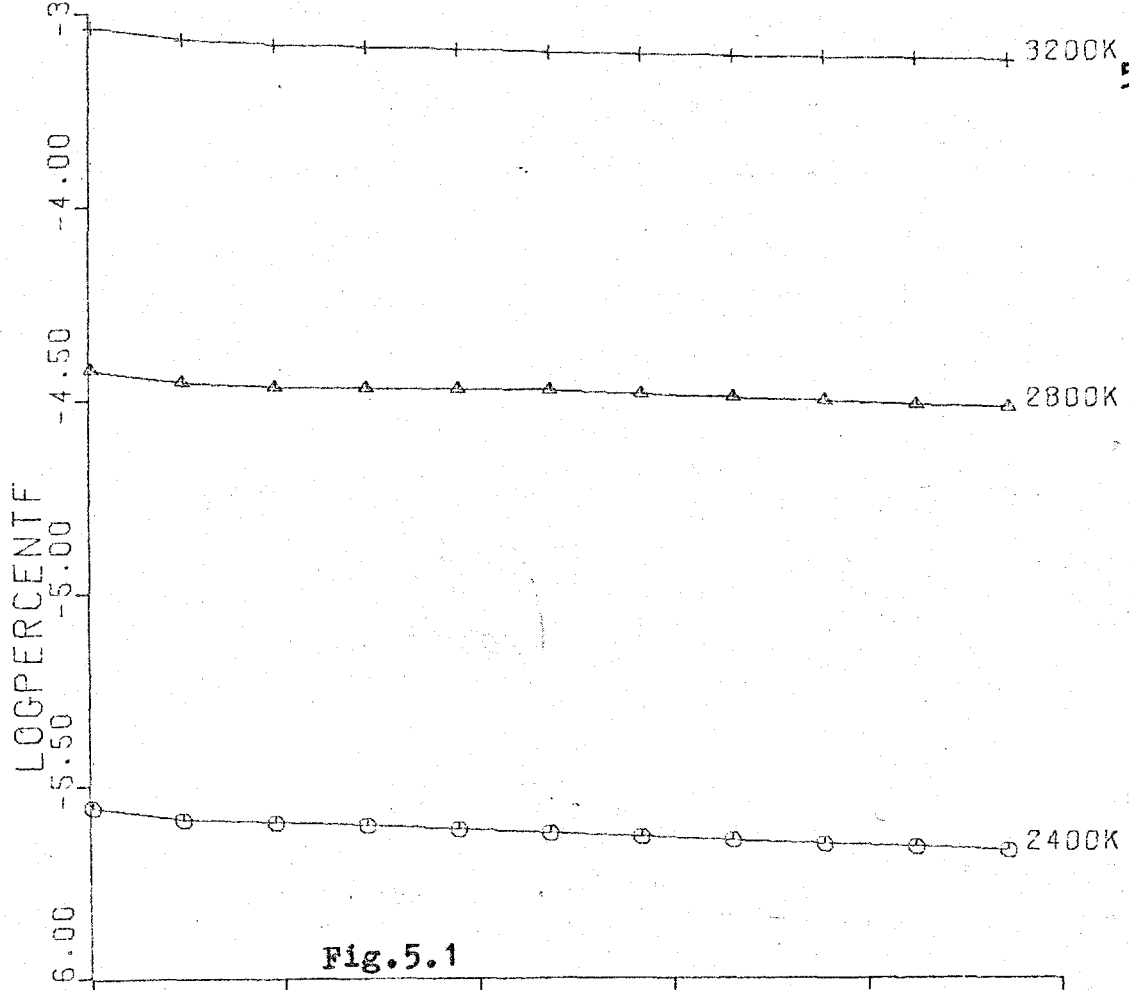


Fig. 5.1

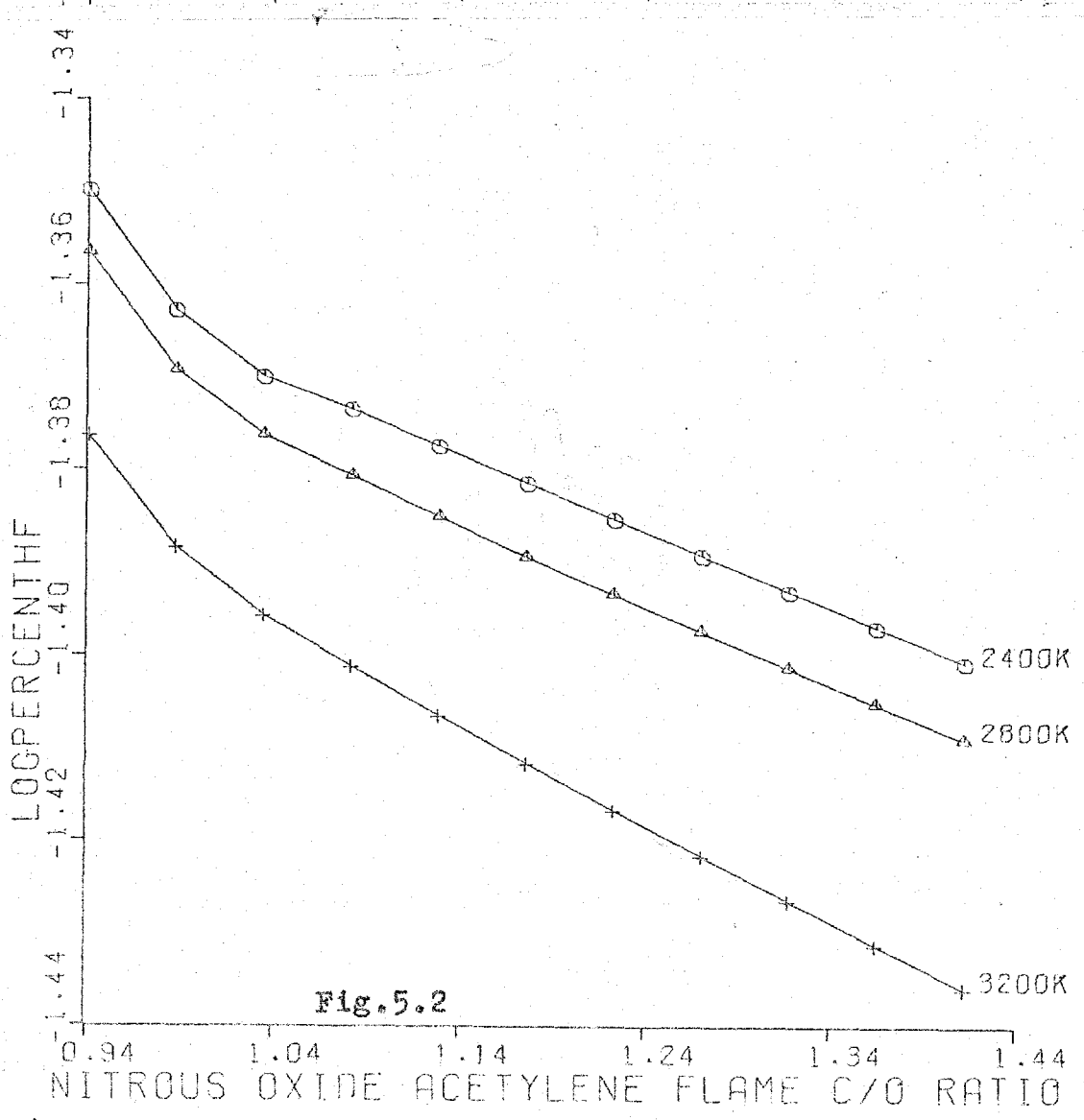


Fig. 5.2

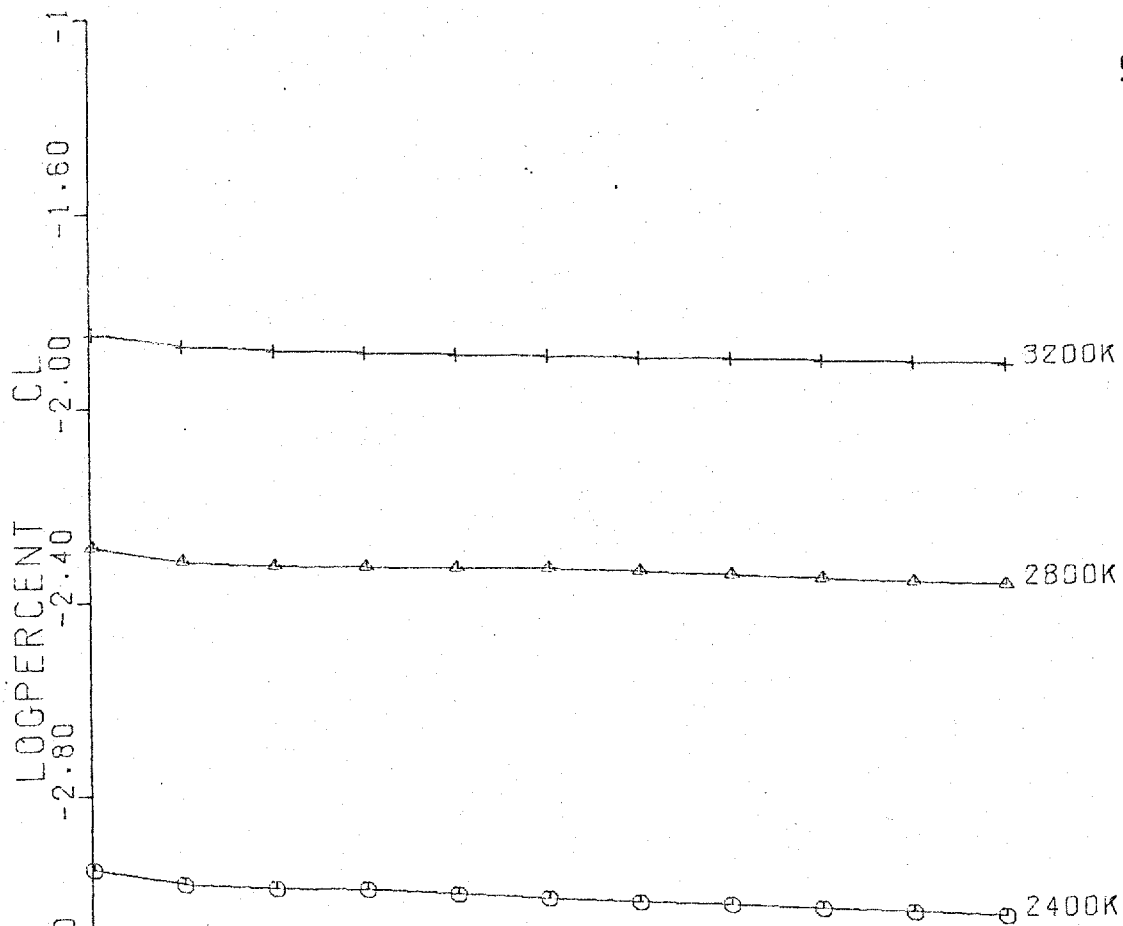


Fig.5.3

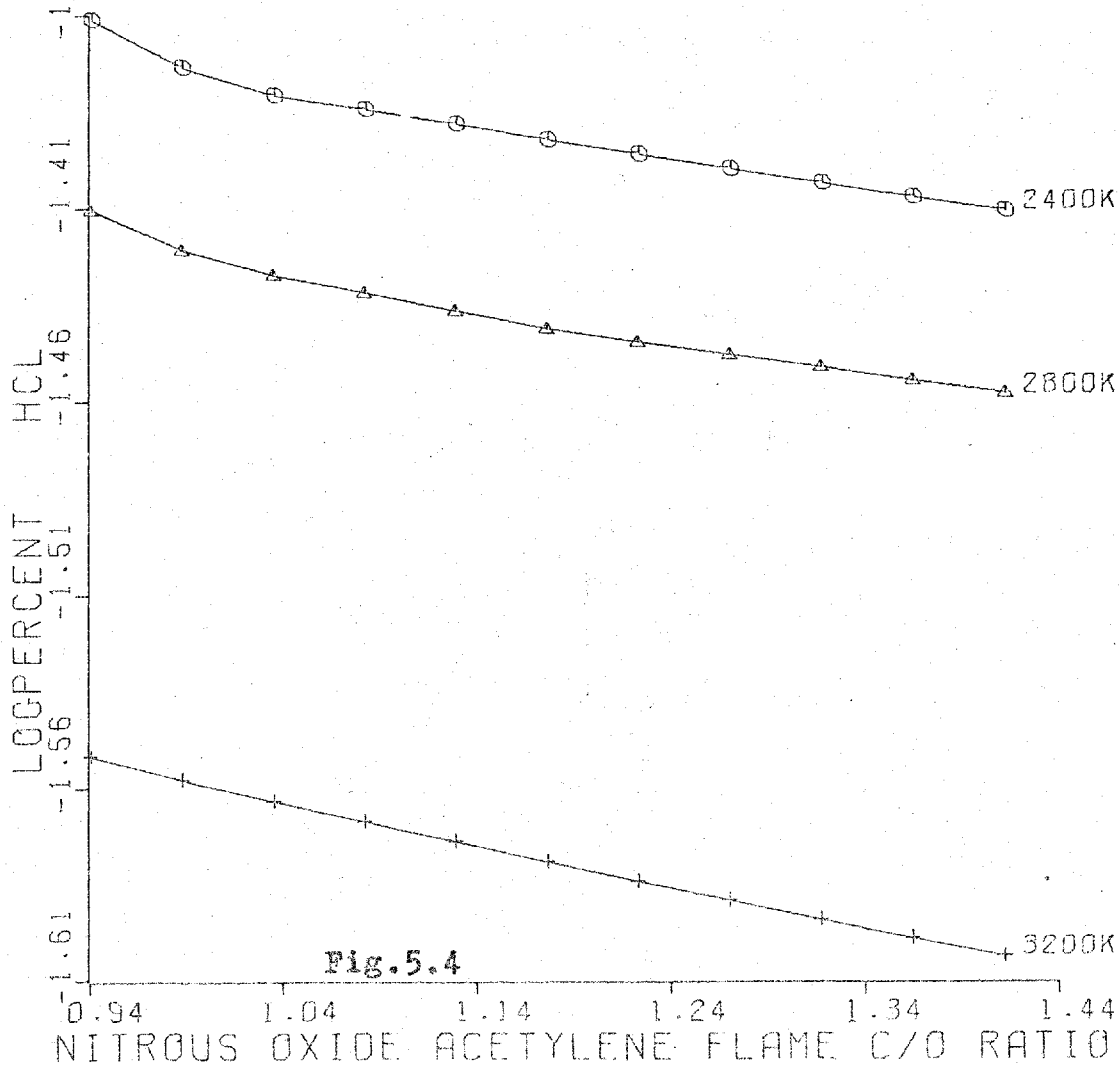
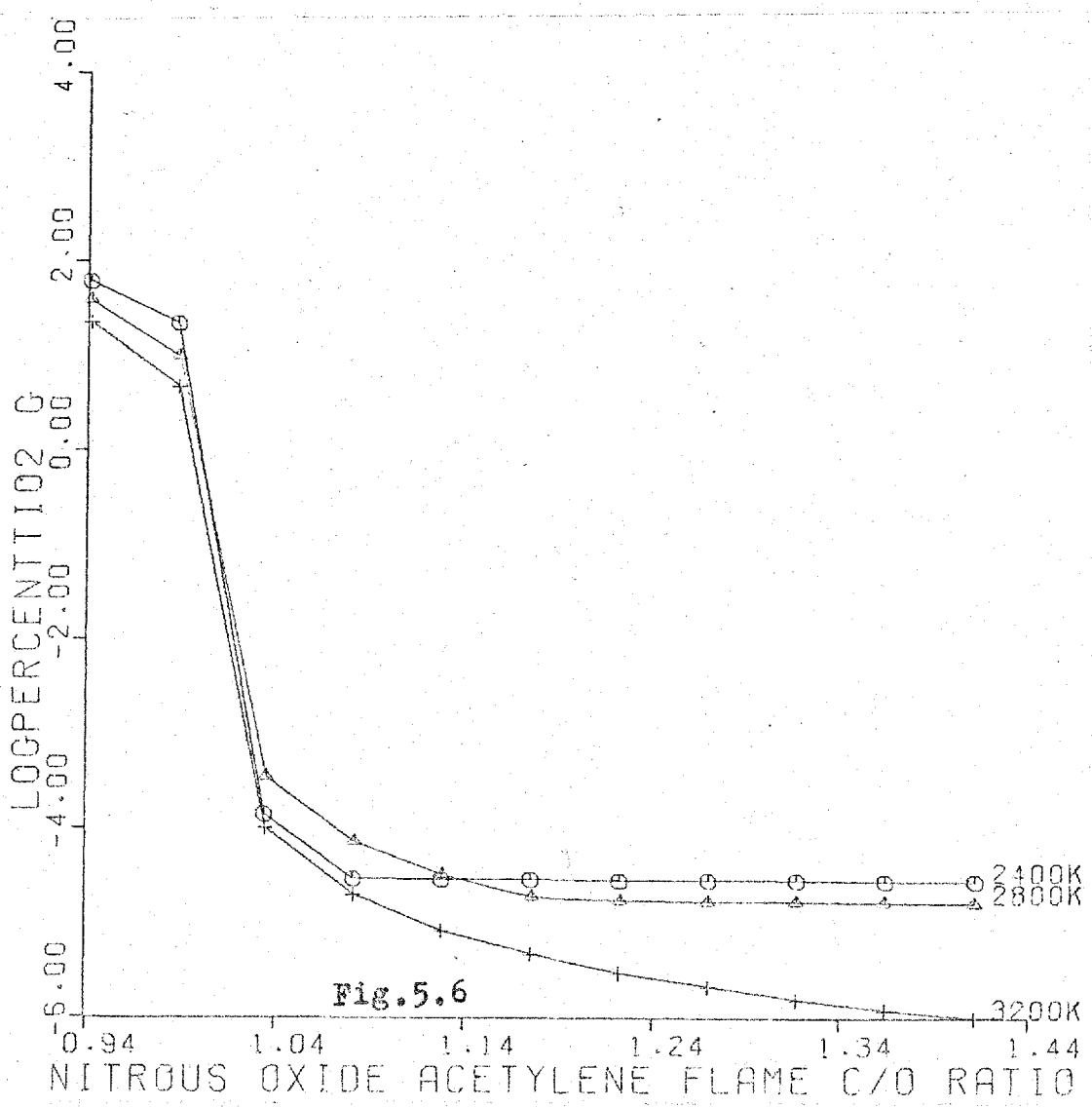
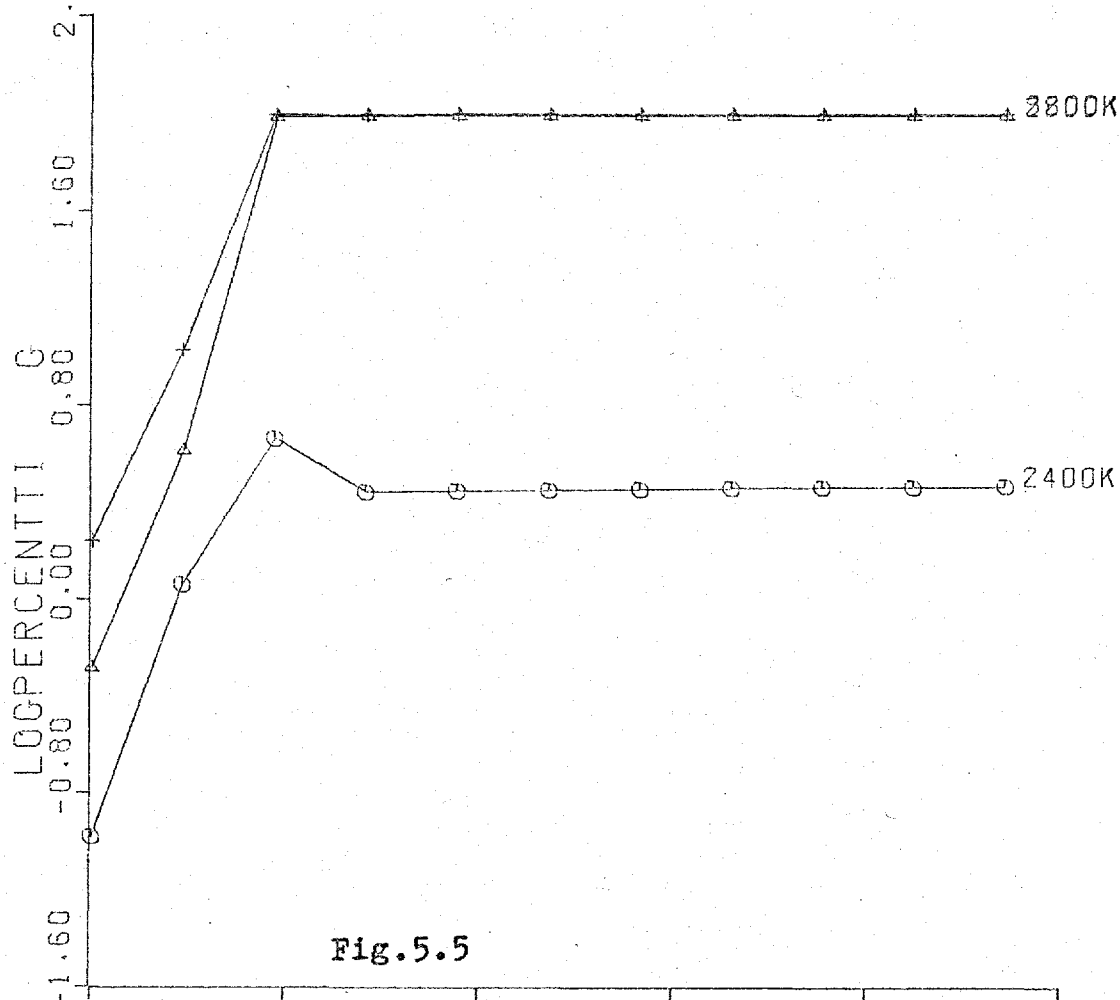
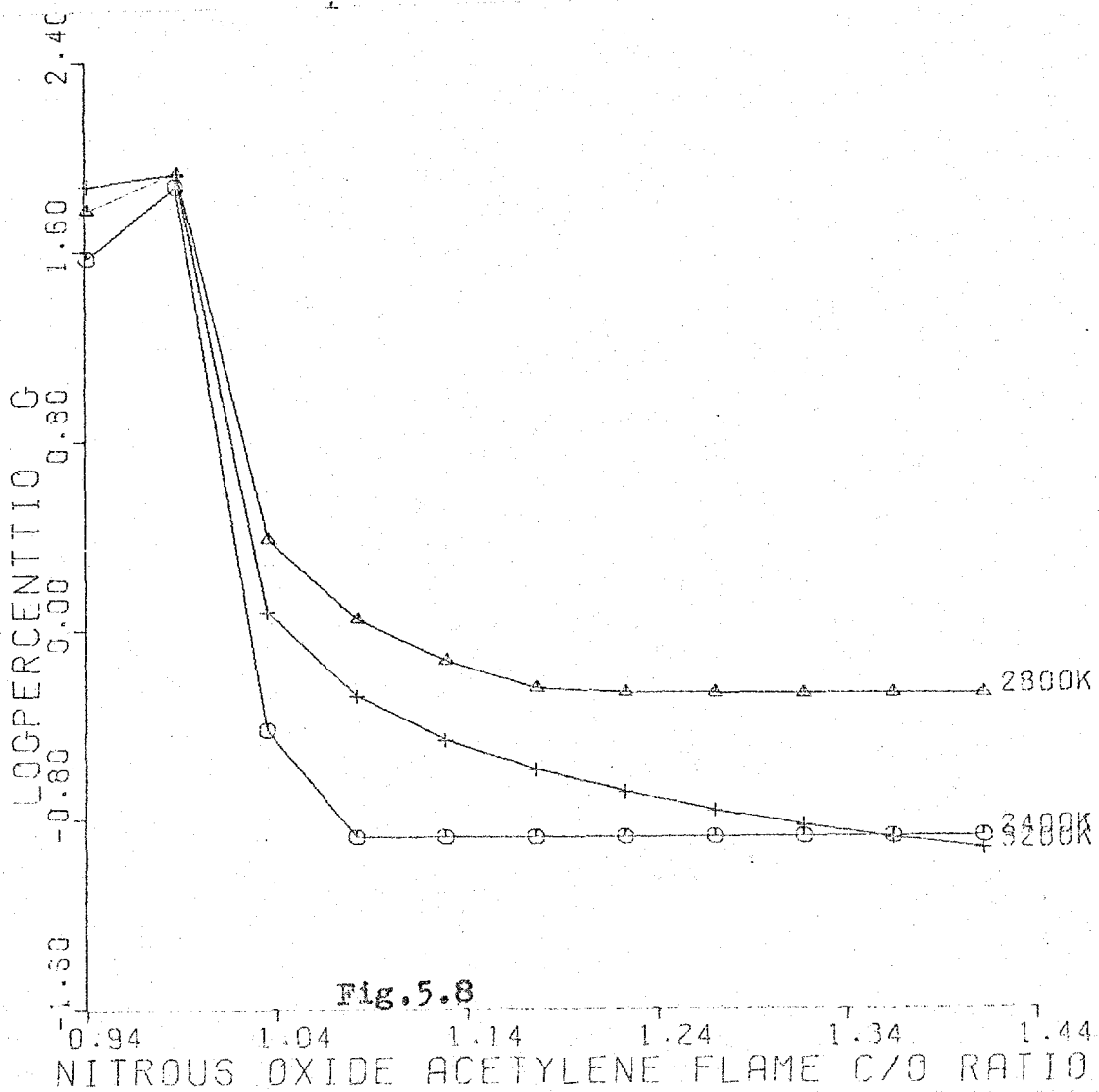
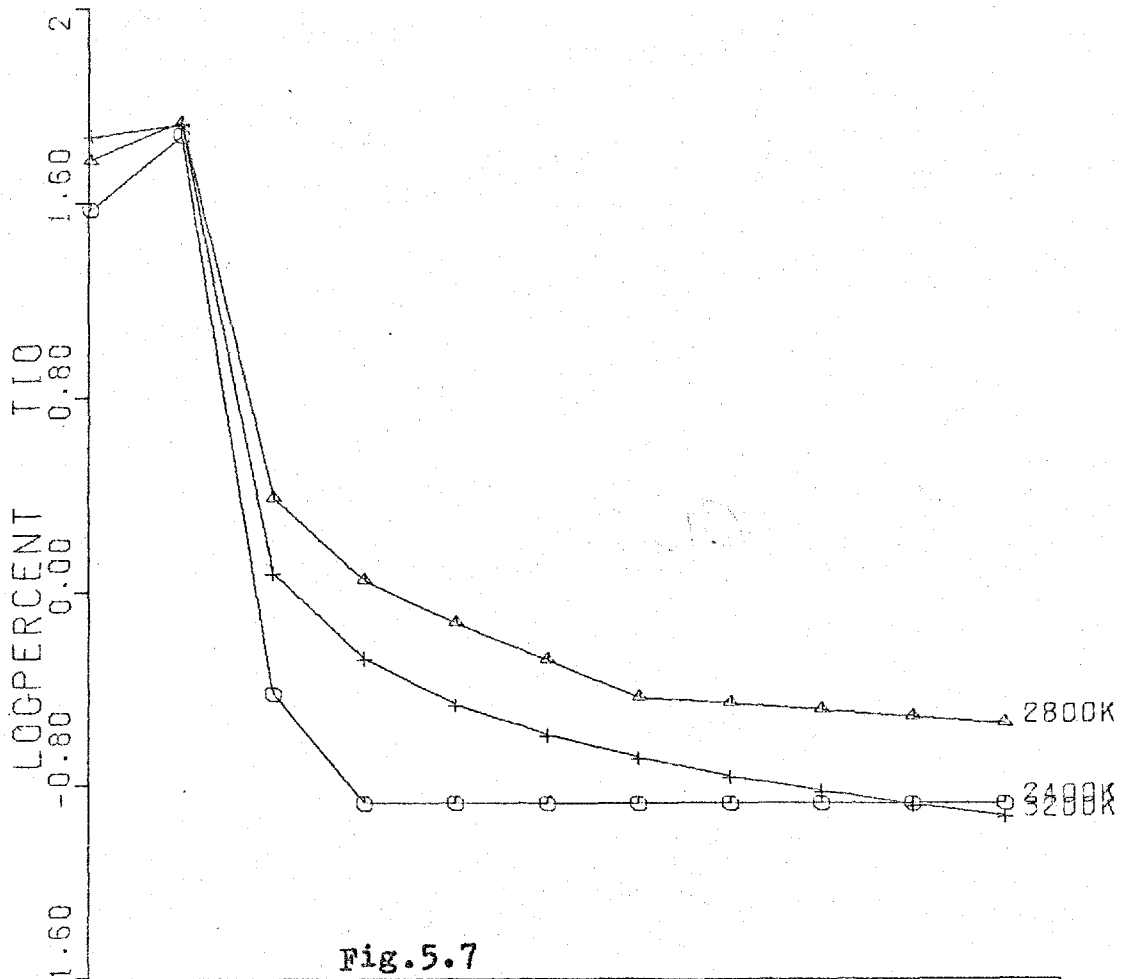
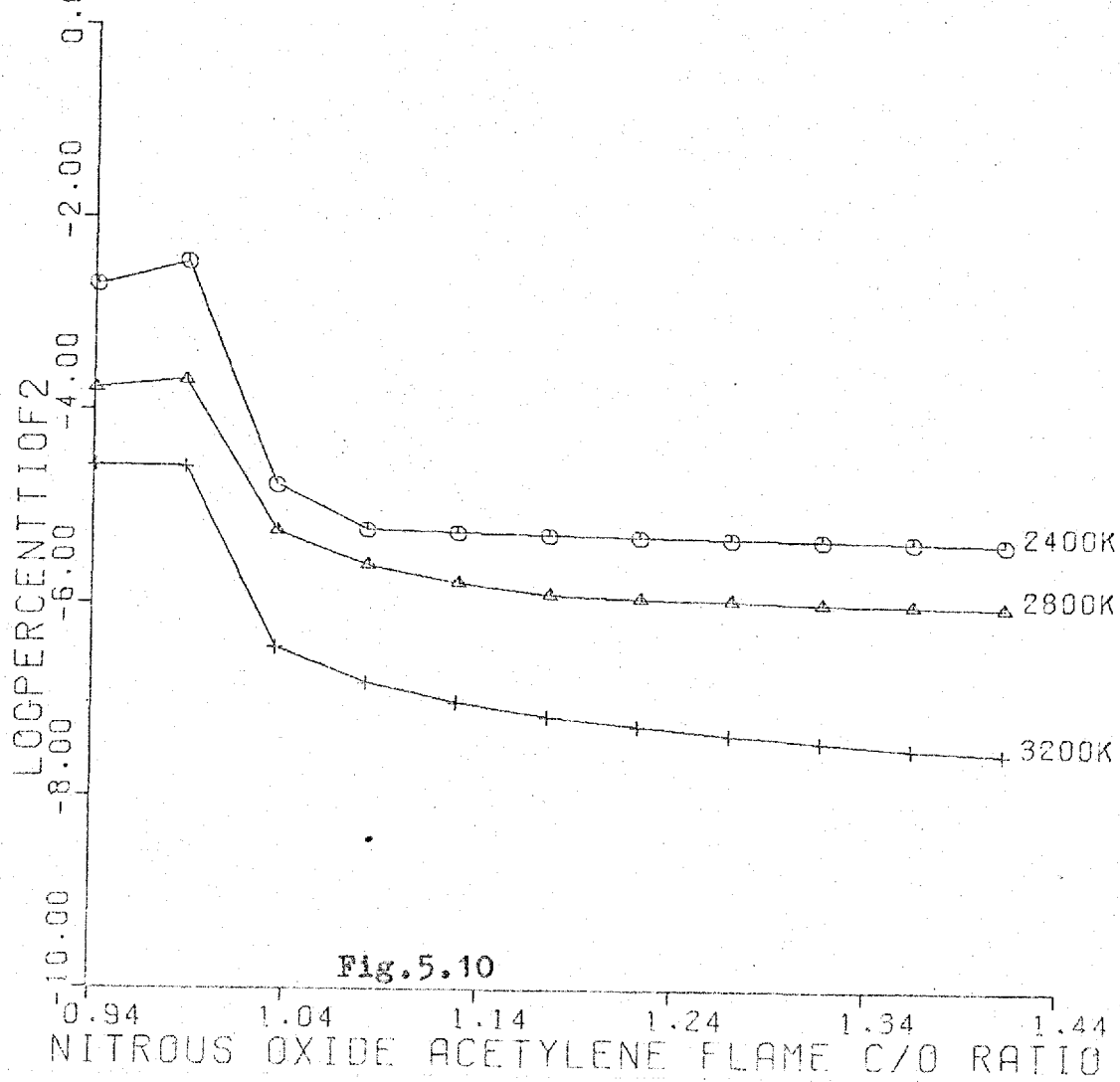
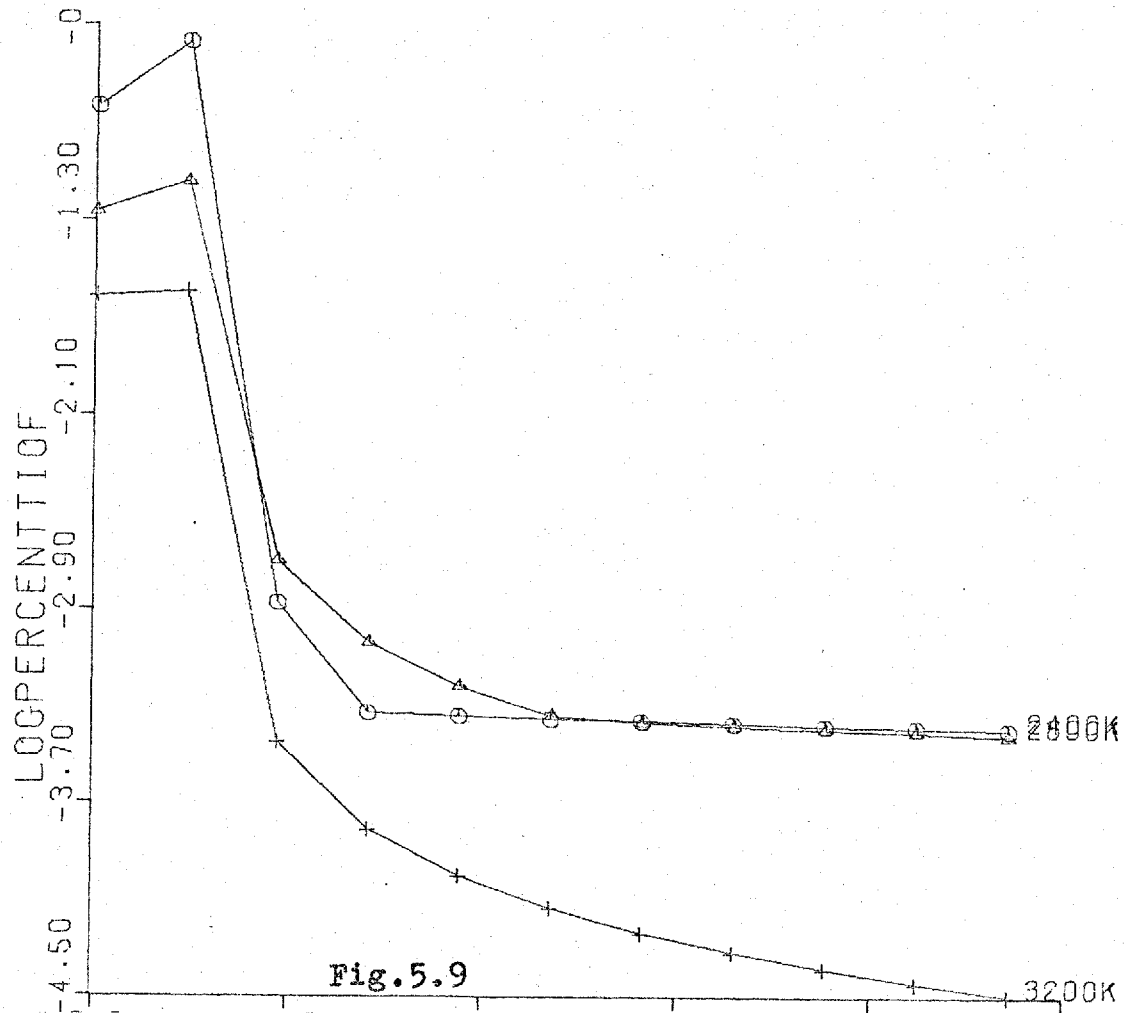


Fig.5.4







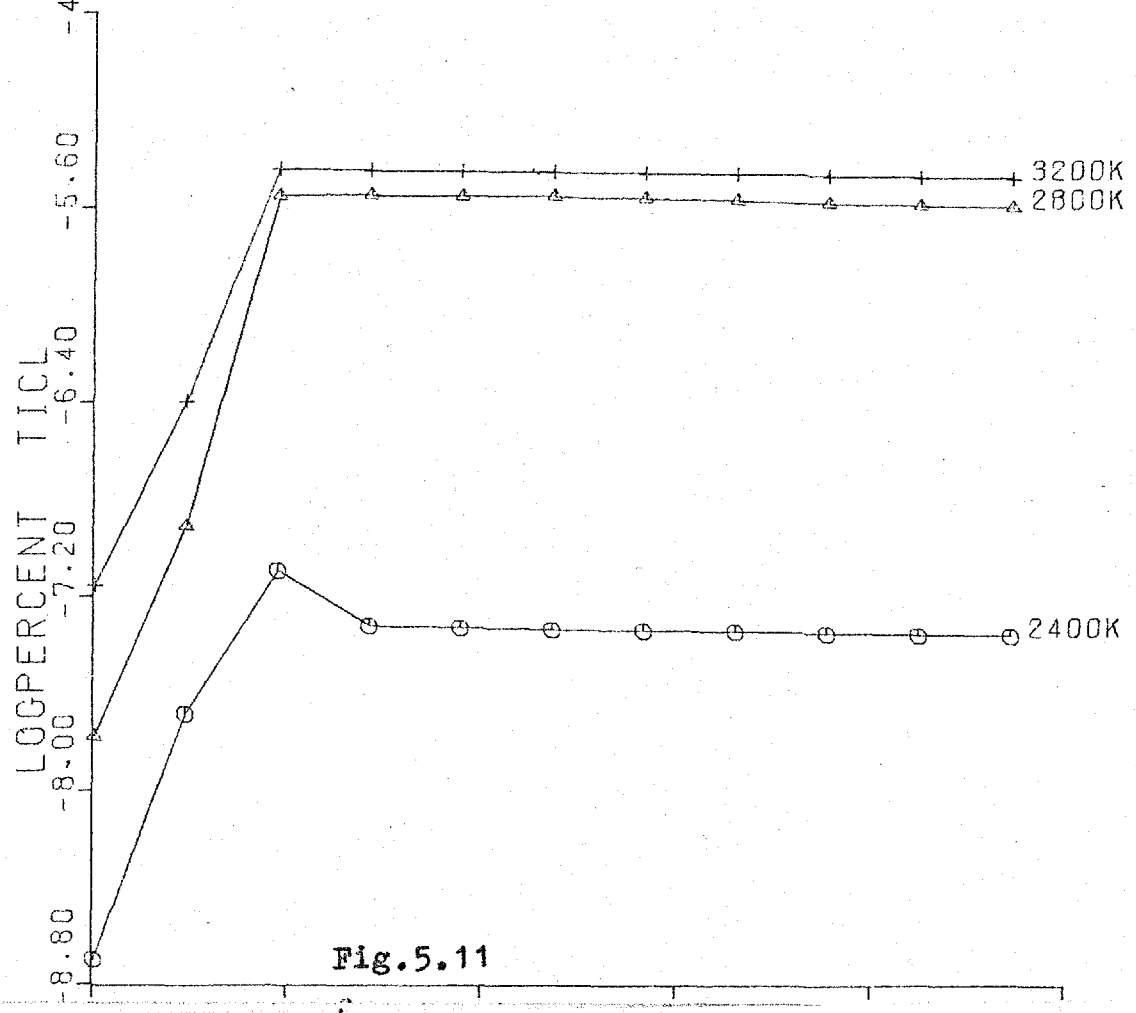


Fig.5.11

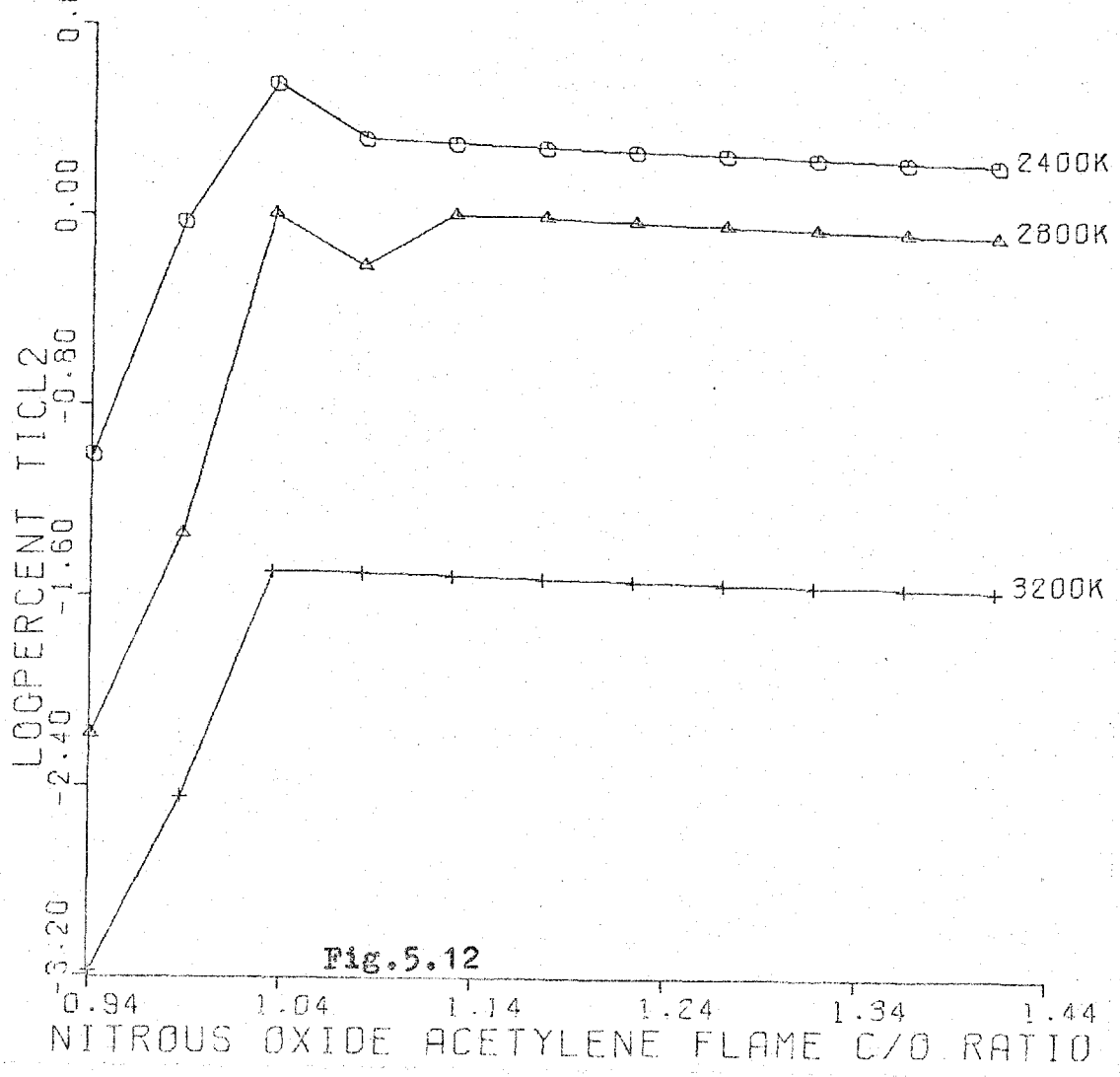


Fig.5.12

NITROUS OXIDE ACETYLENE FLAME C/O RATIO

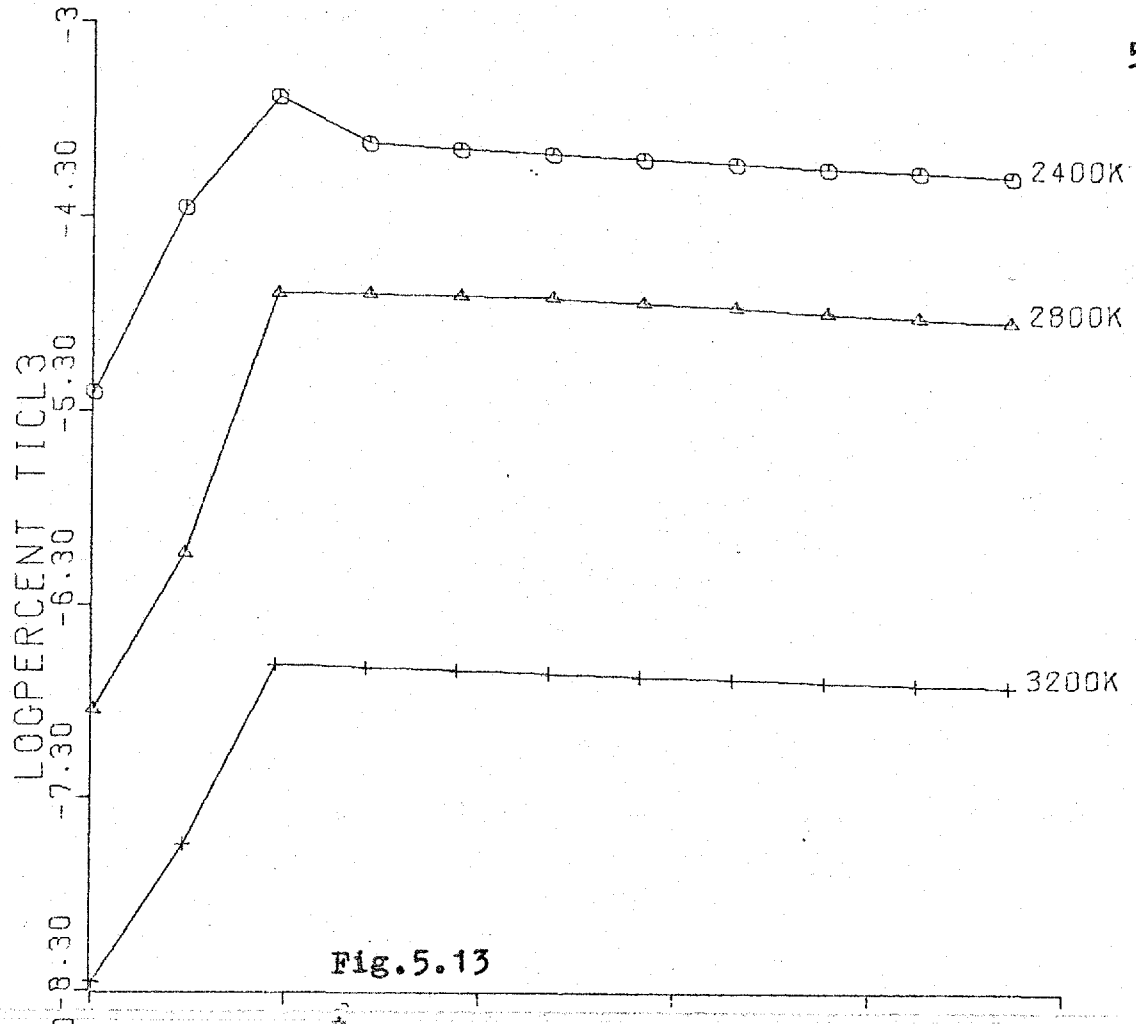


Fig. 5.13

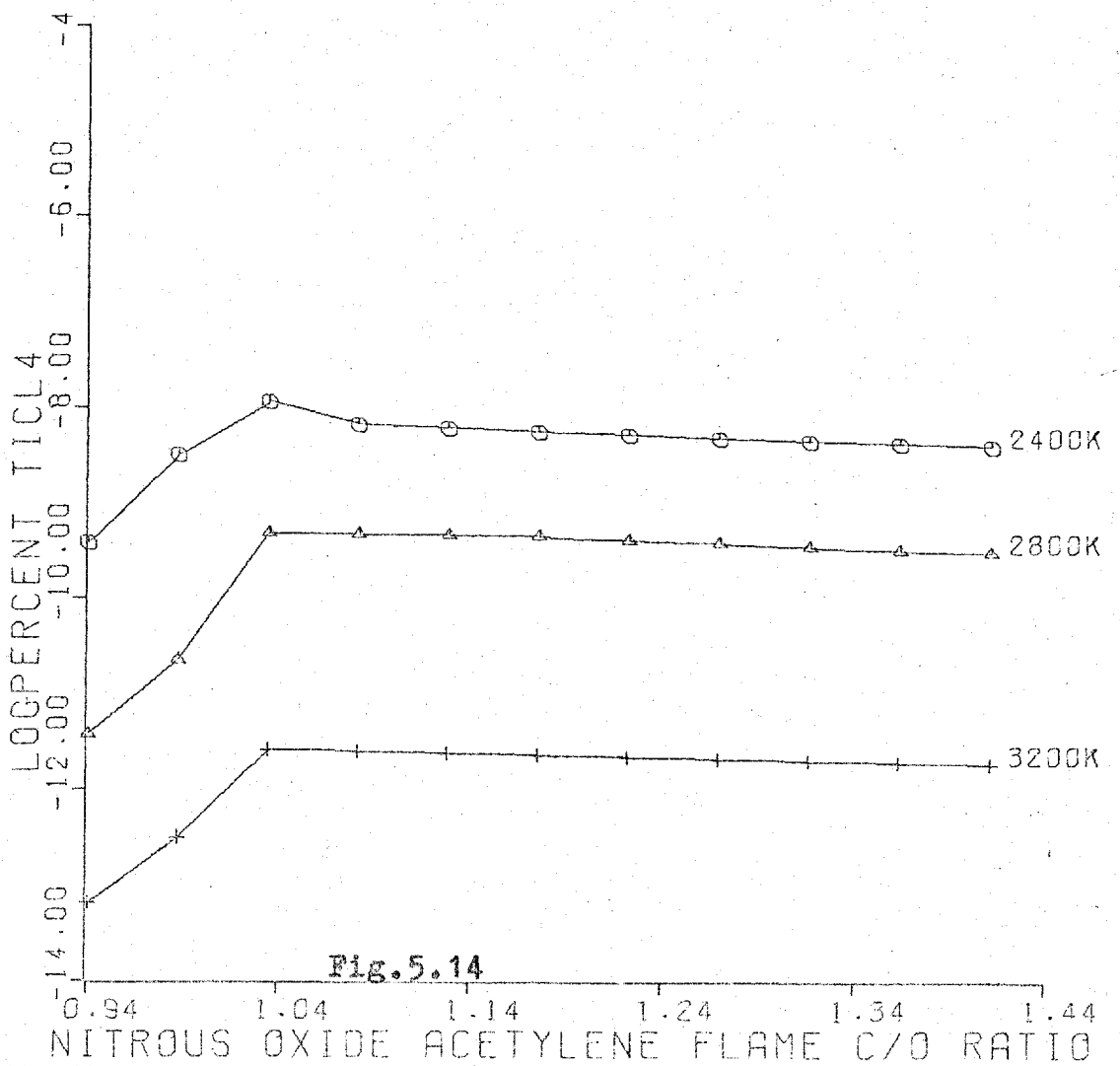


Fig. 5.14

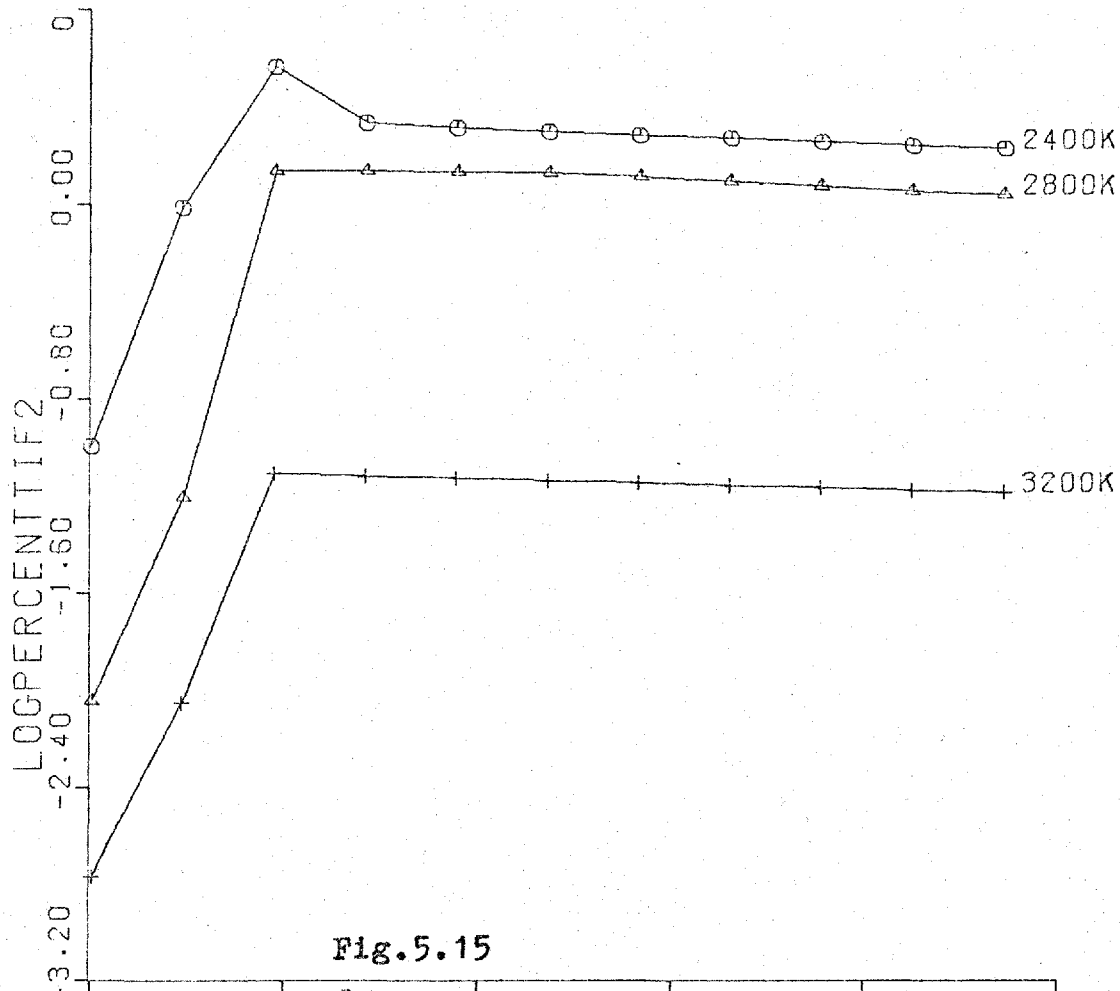


Fig.5.15

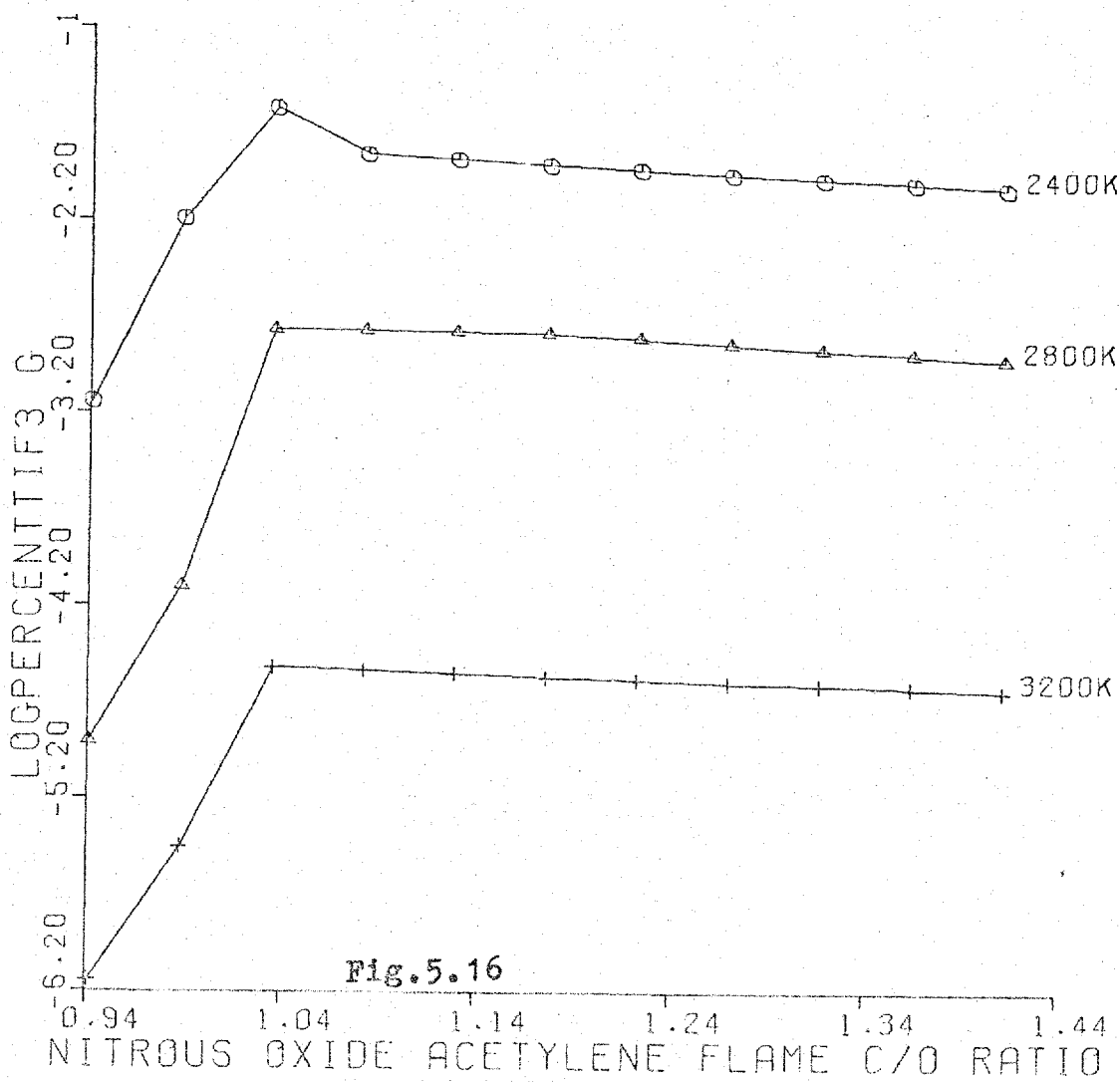
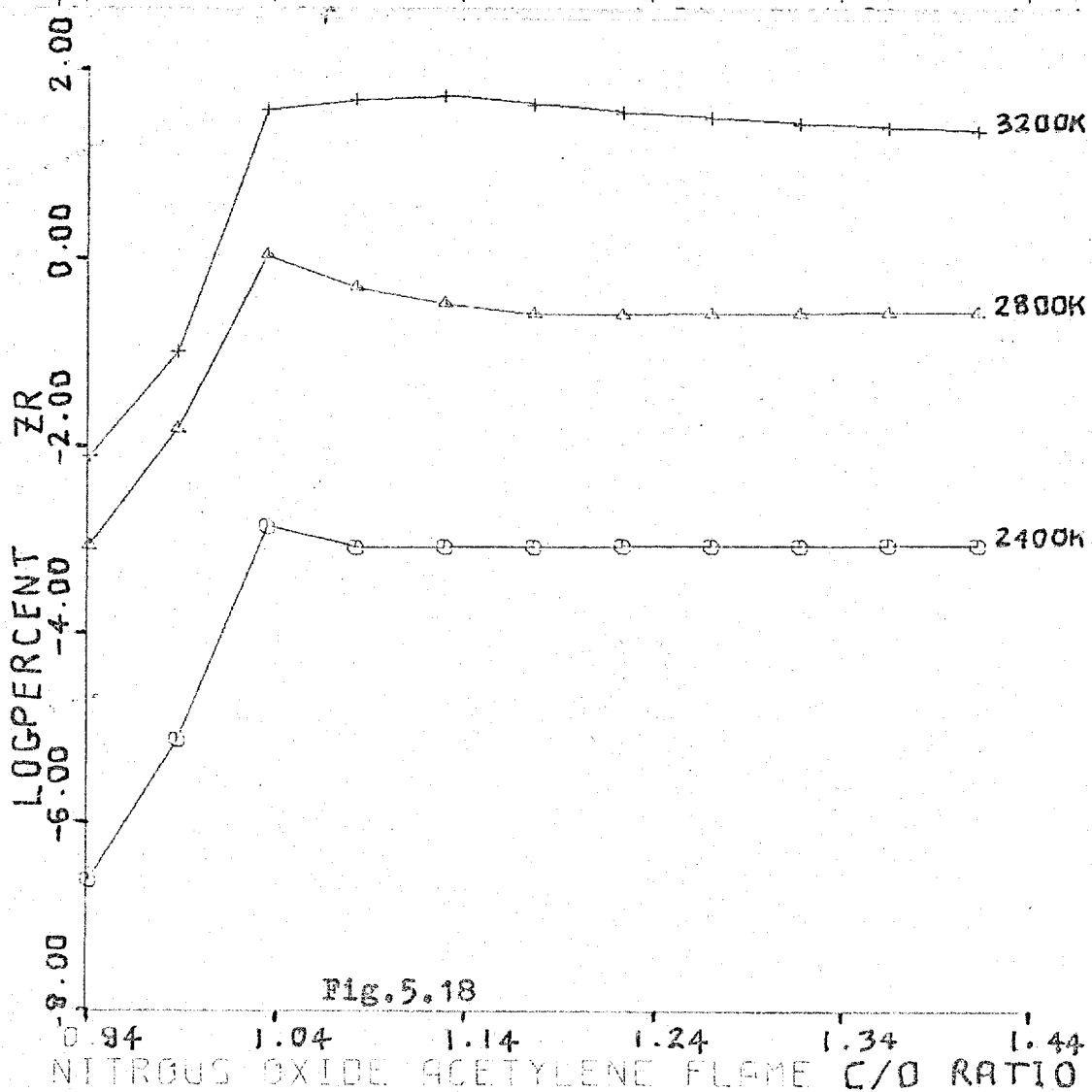
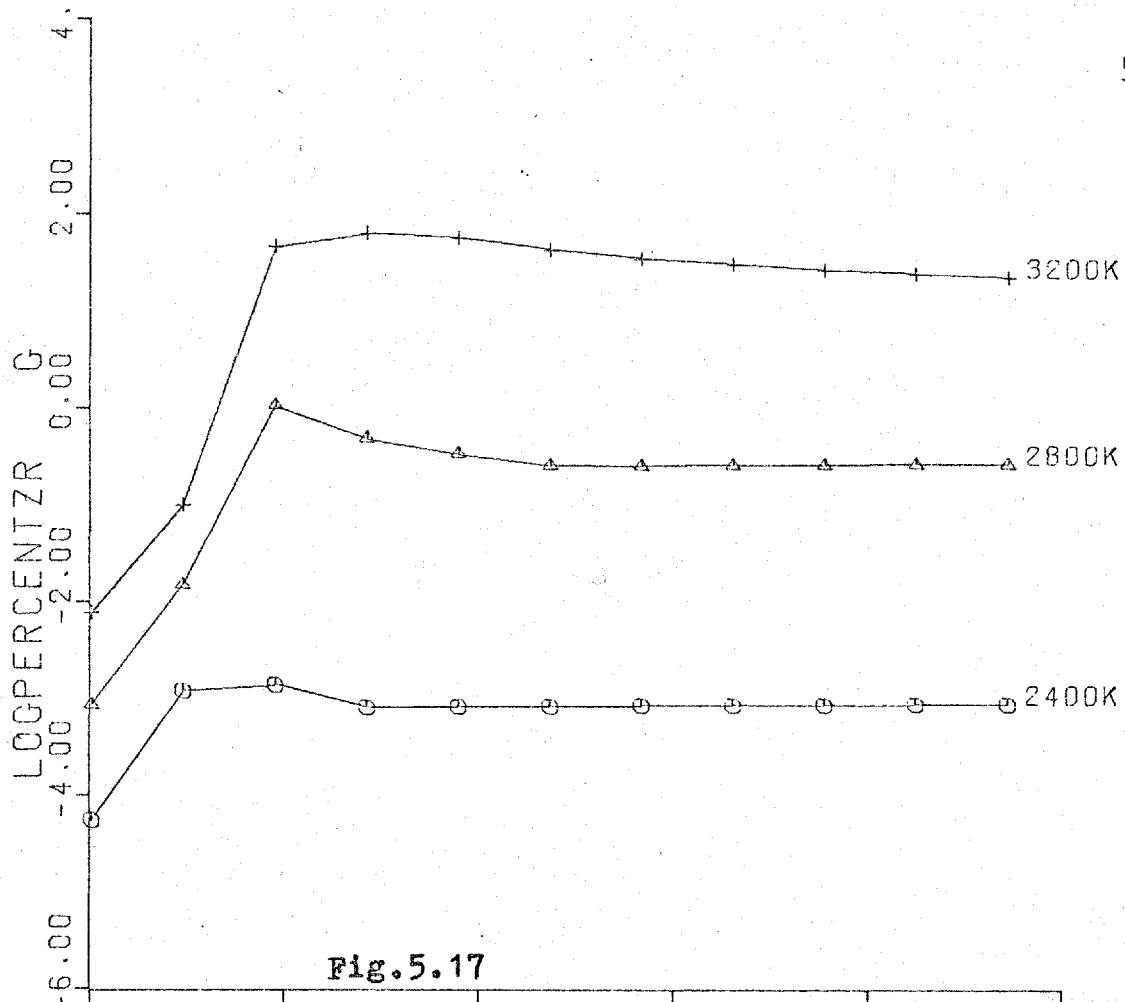
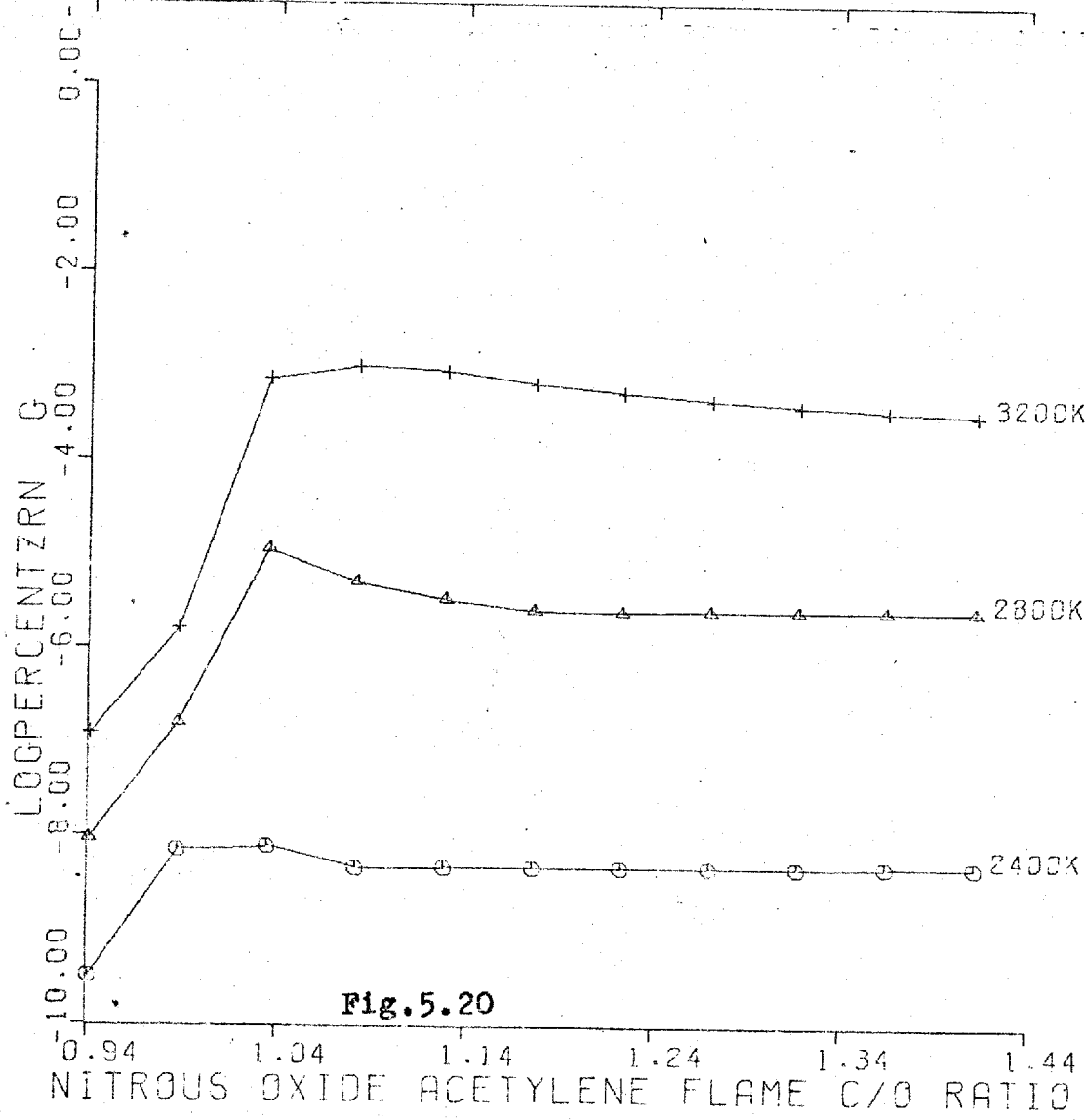
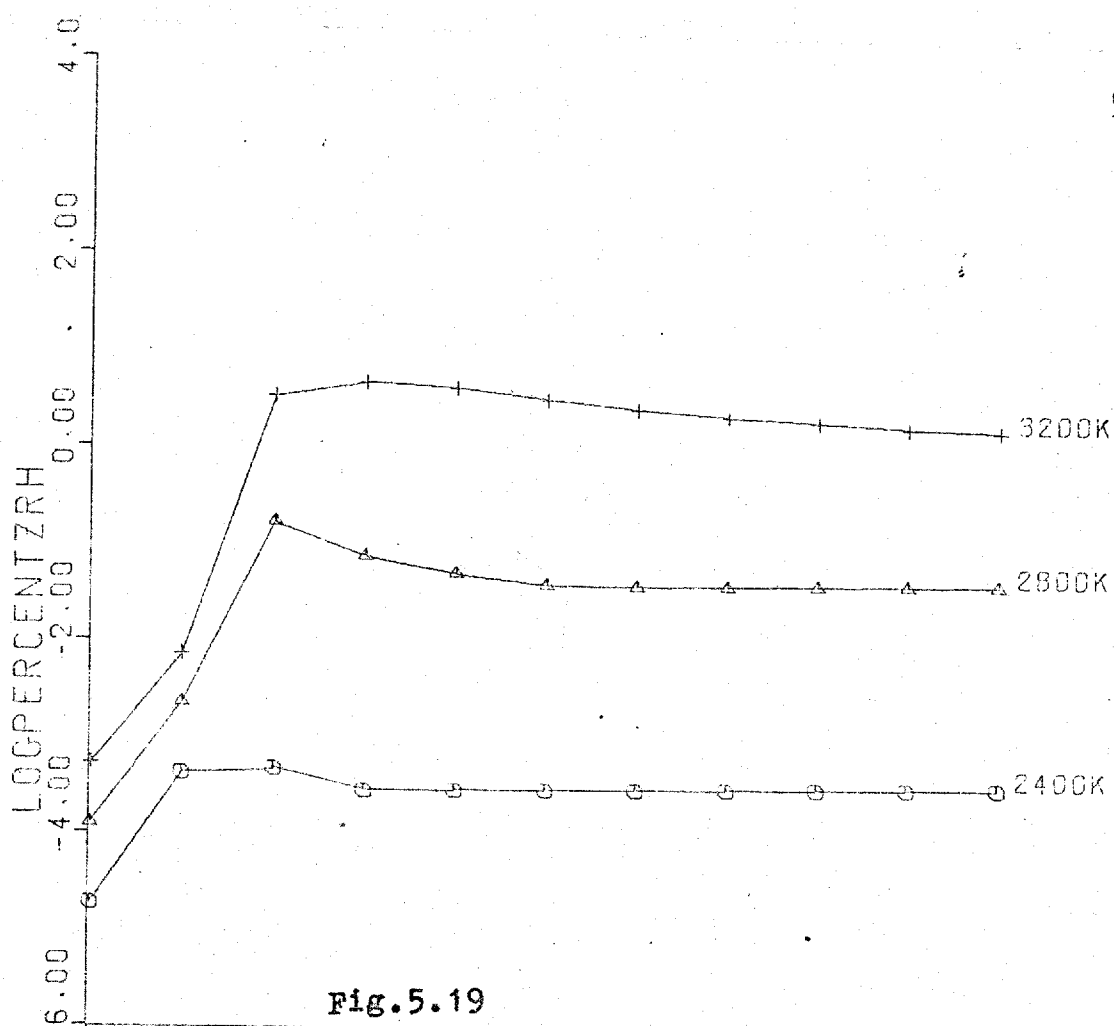
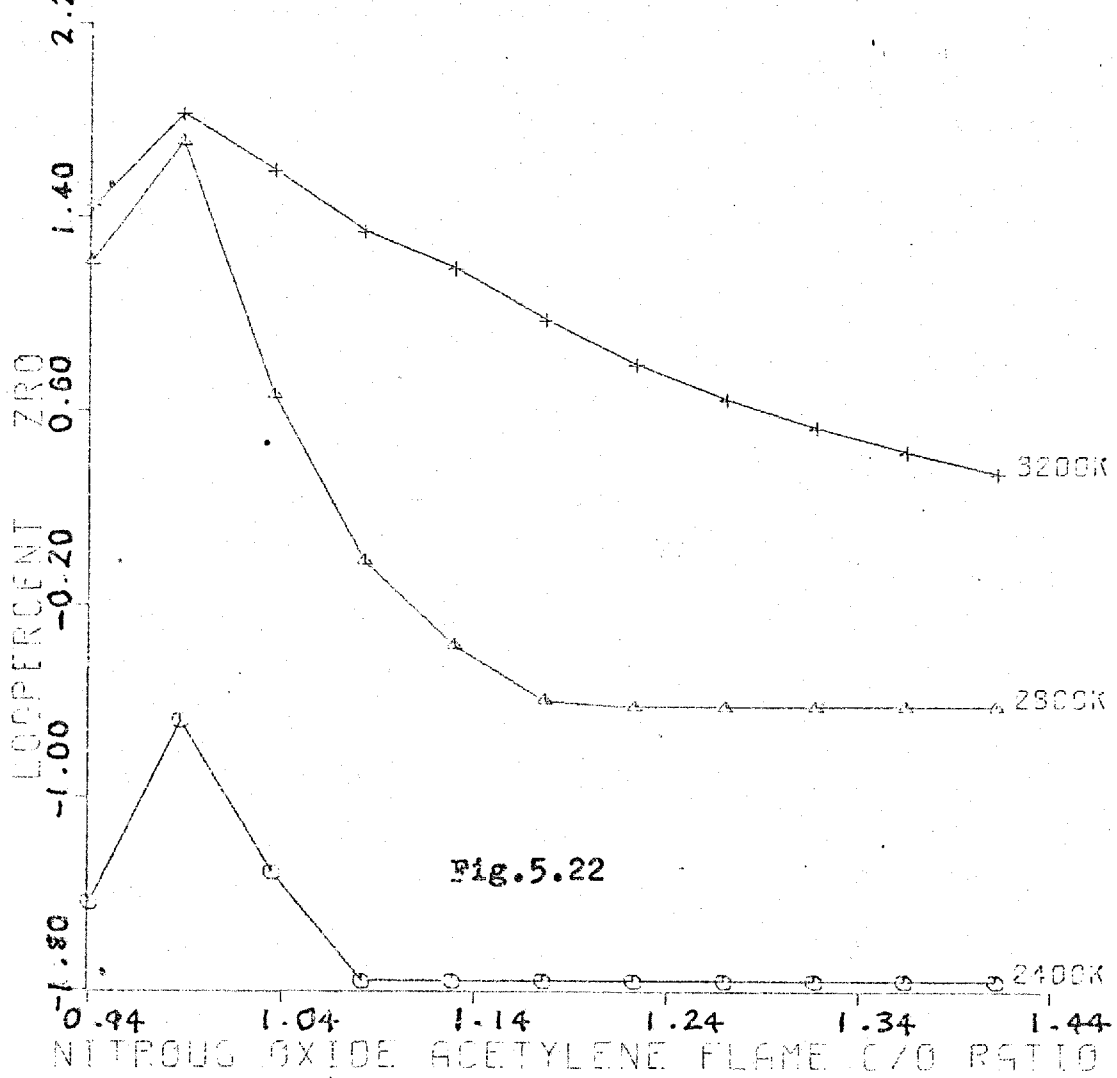
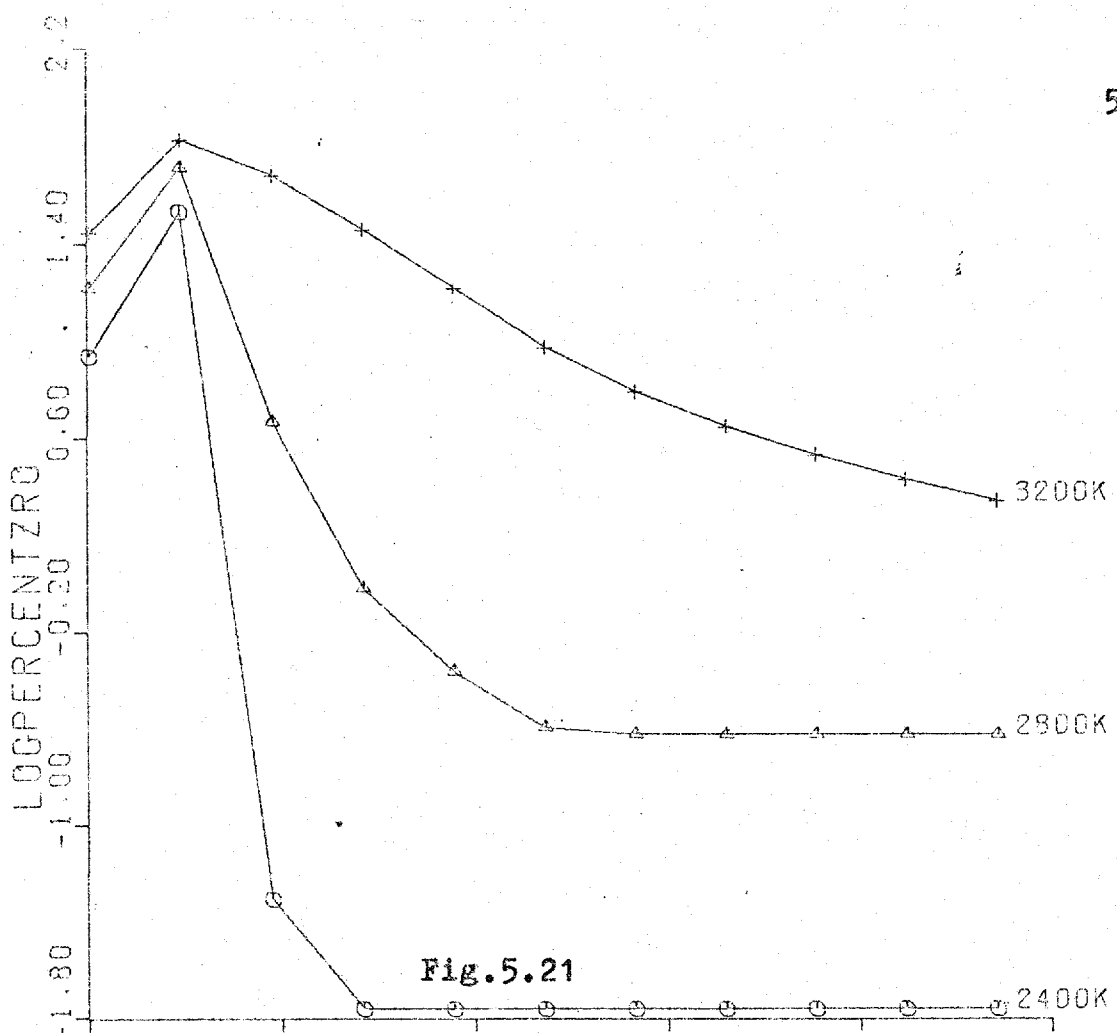


Fig.5.16

NITROUS OXIDE ACETYLENE FLAME C/O RATIO







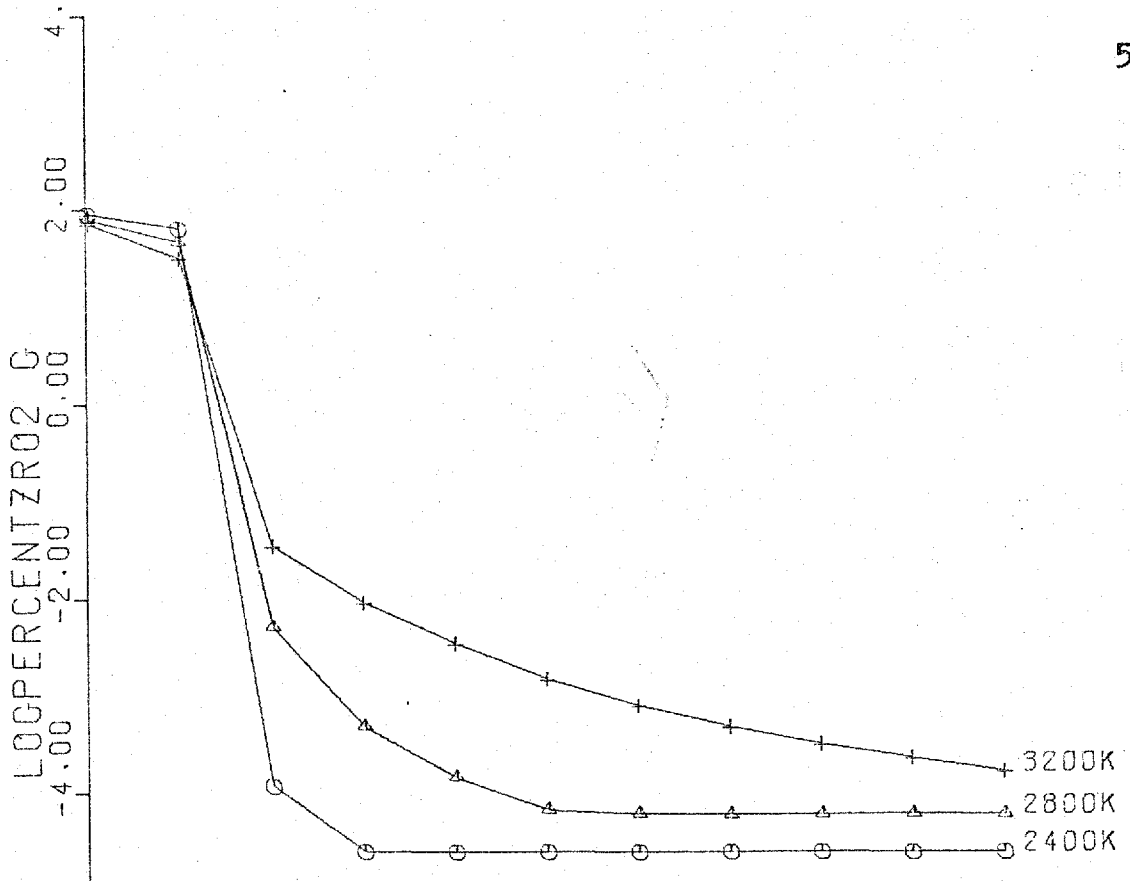


Fig.5.23

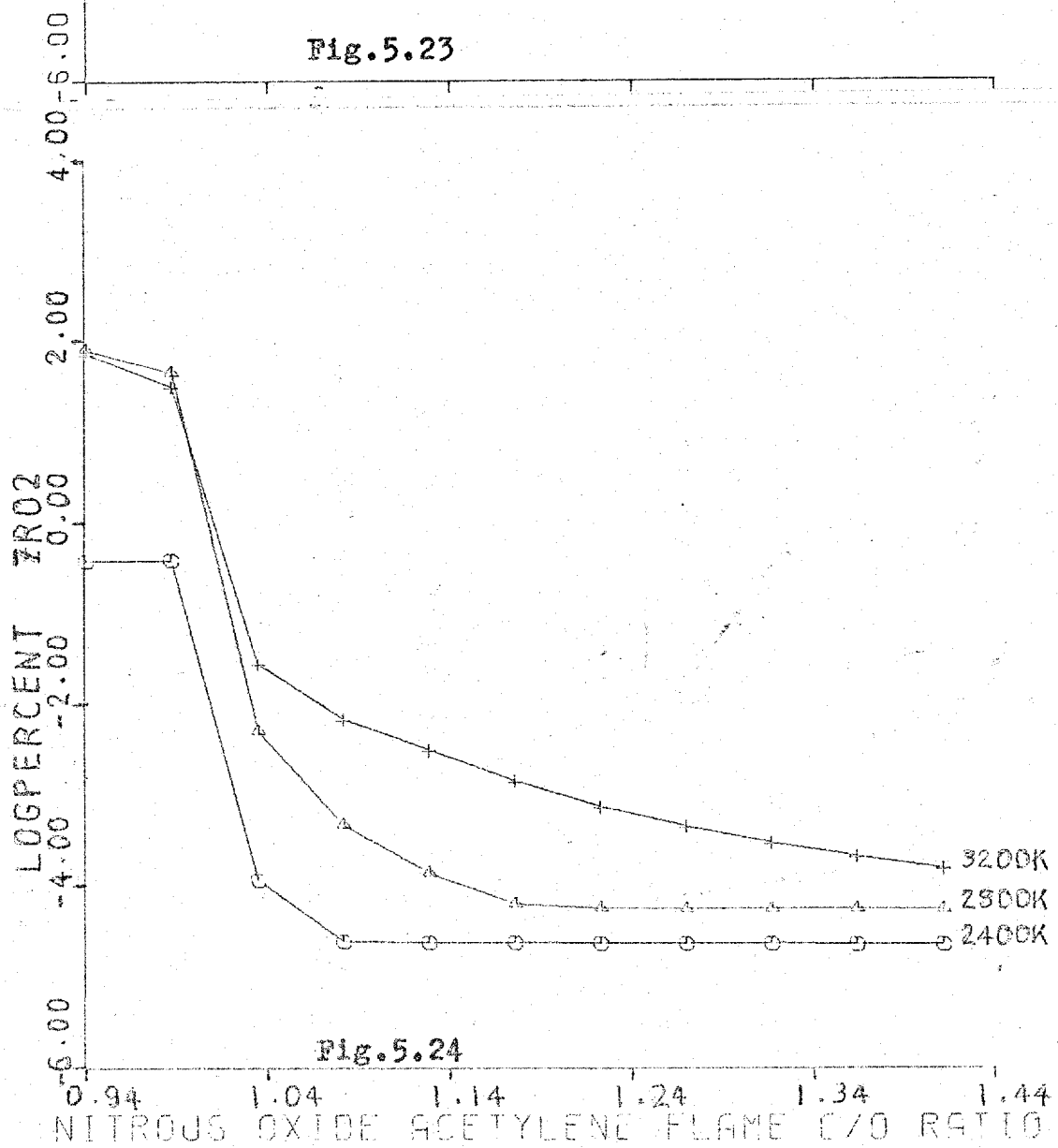
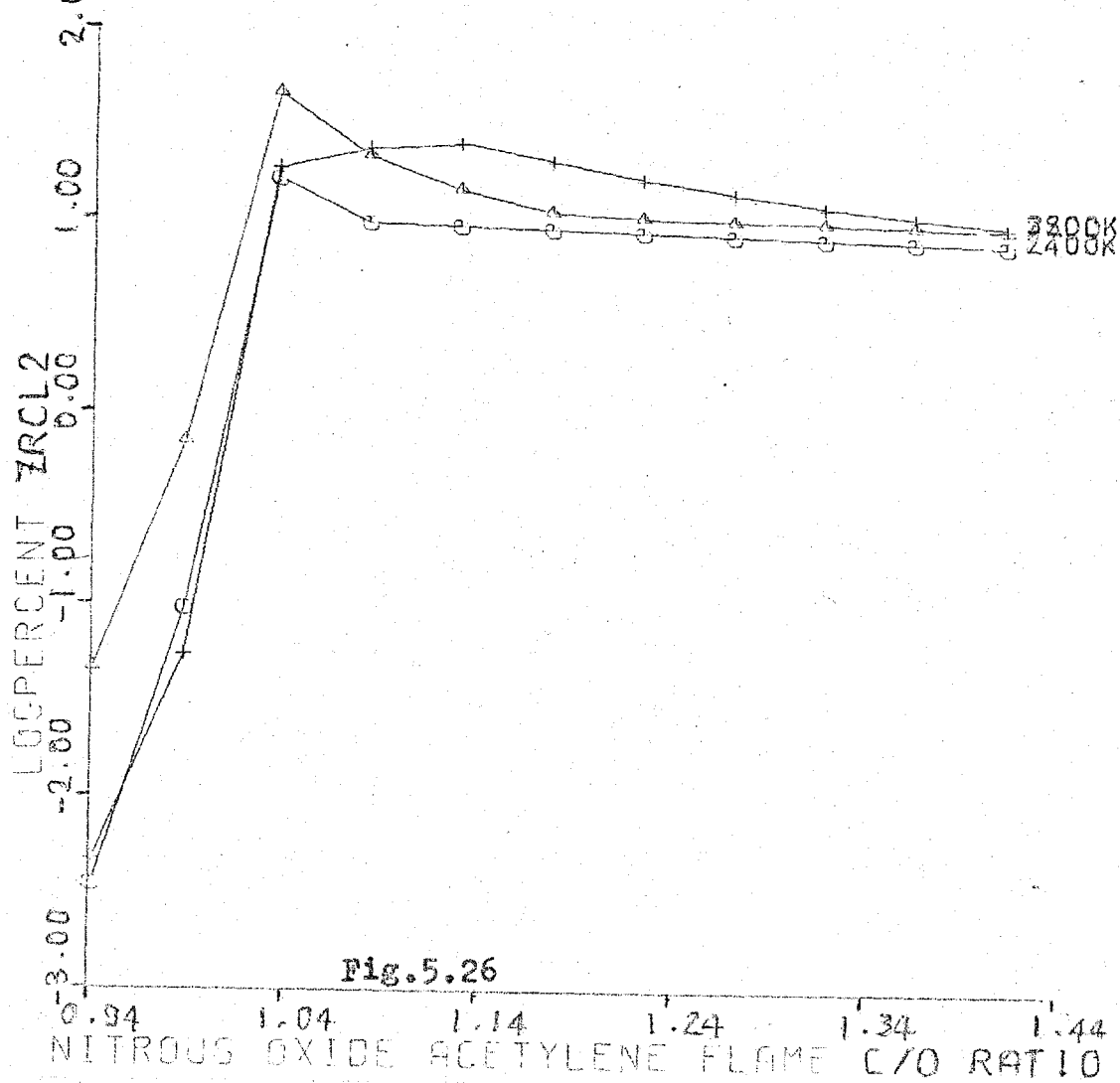
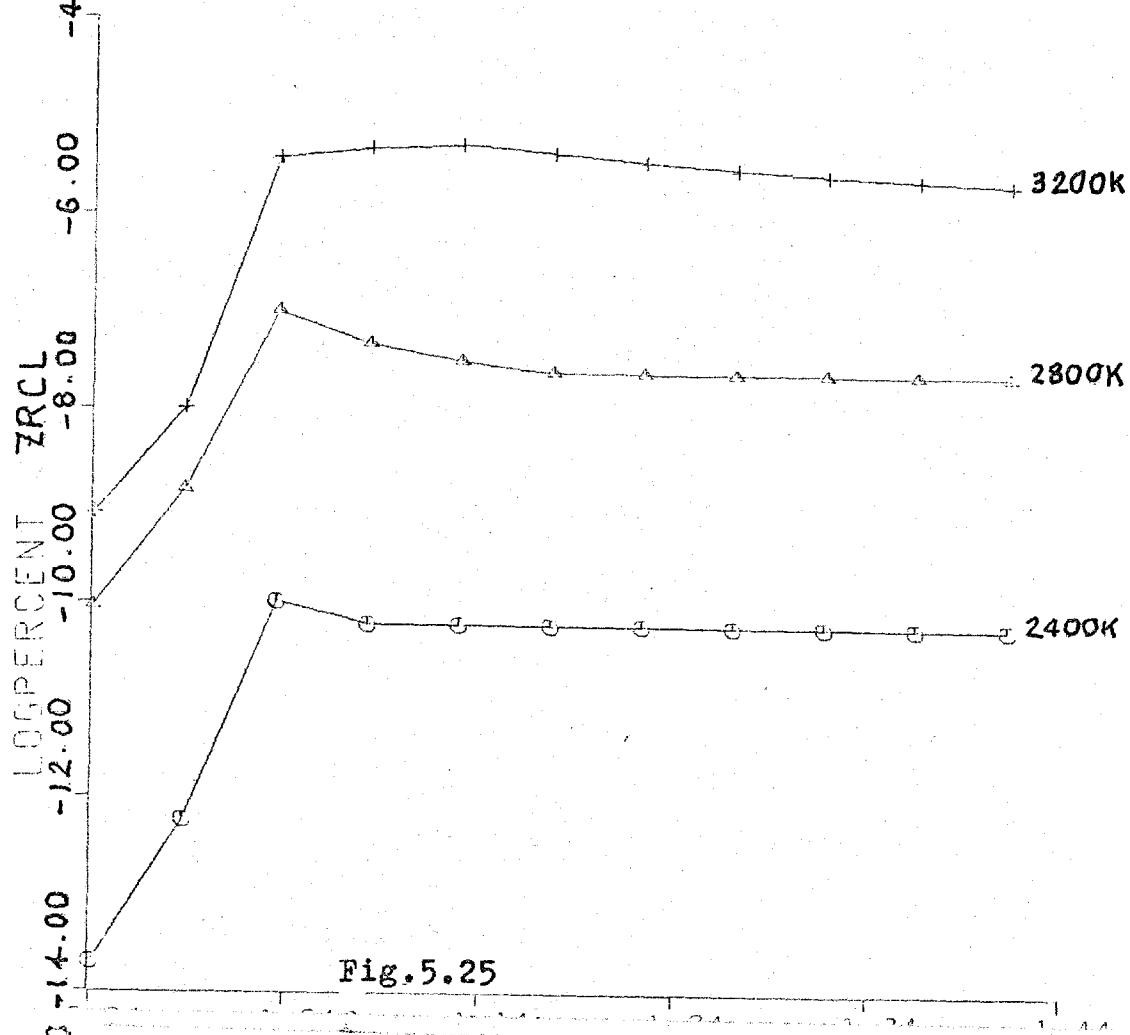
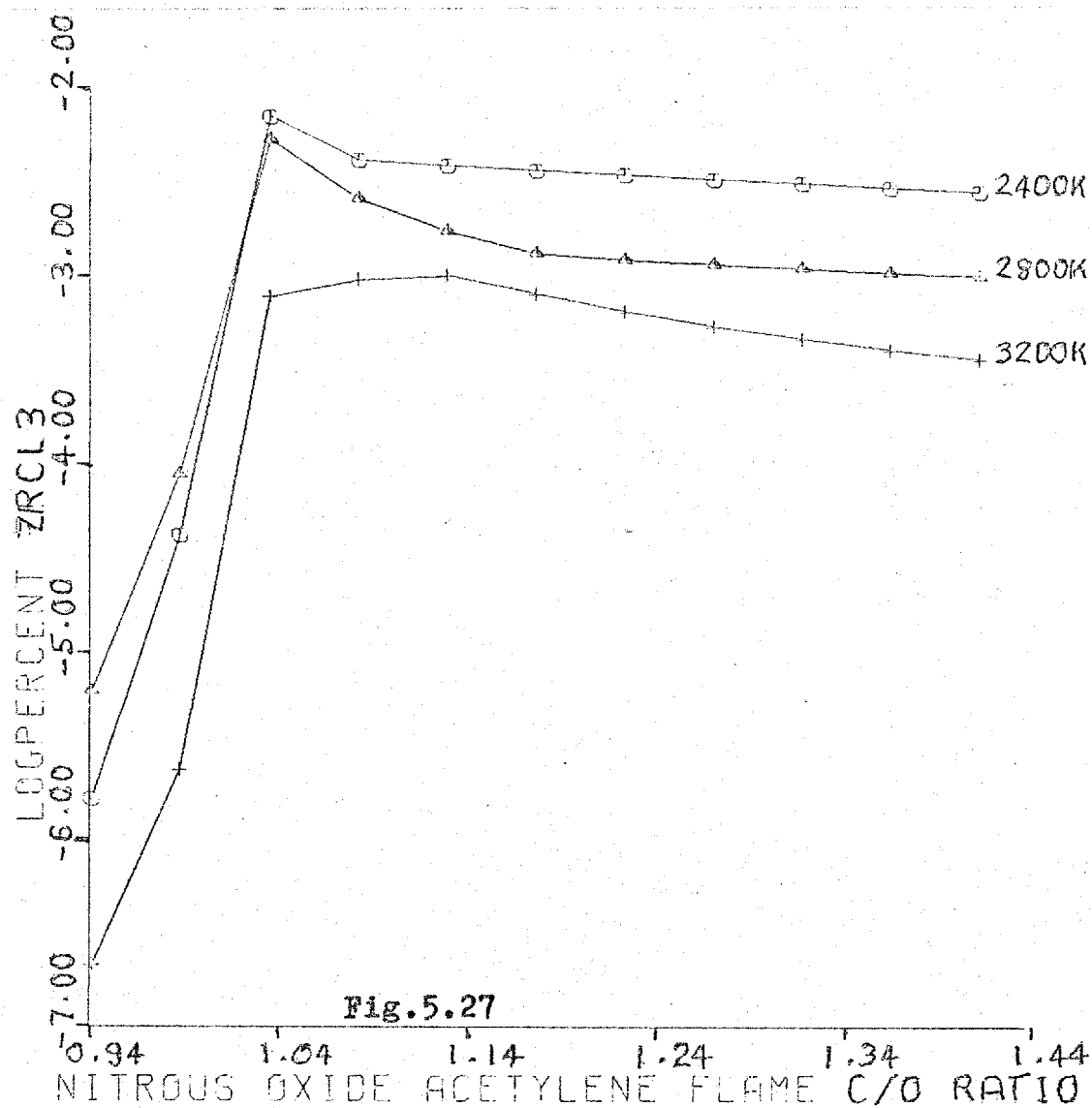
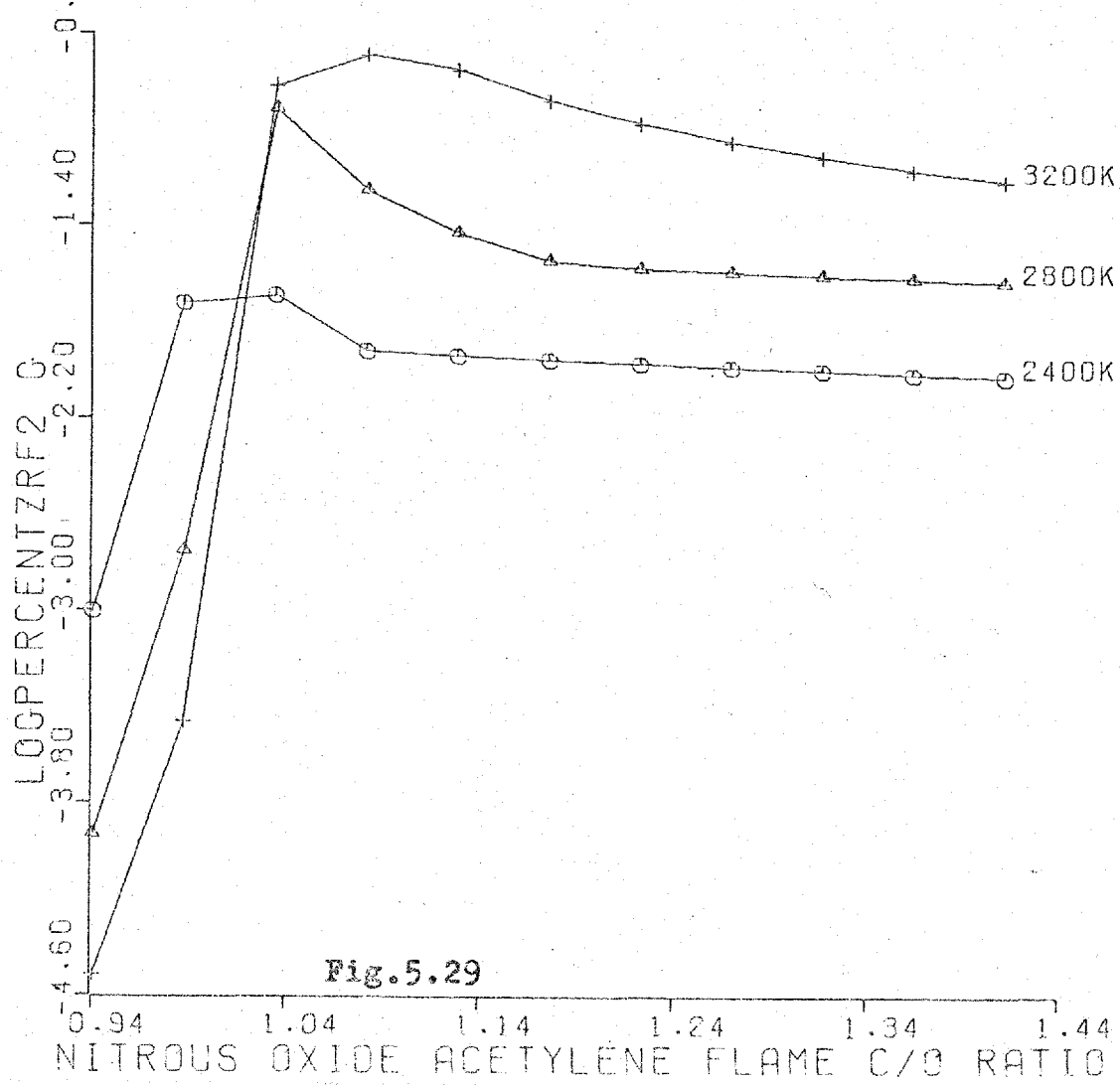
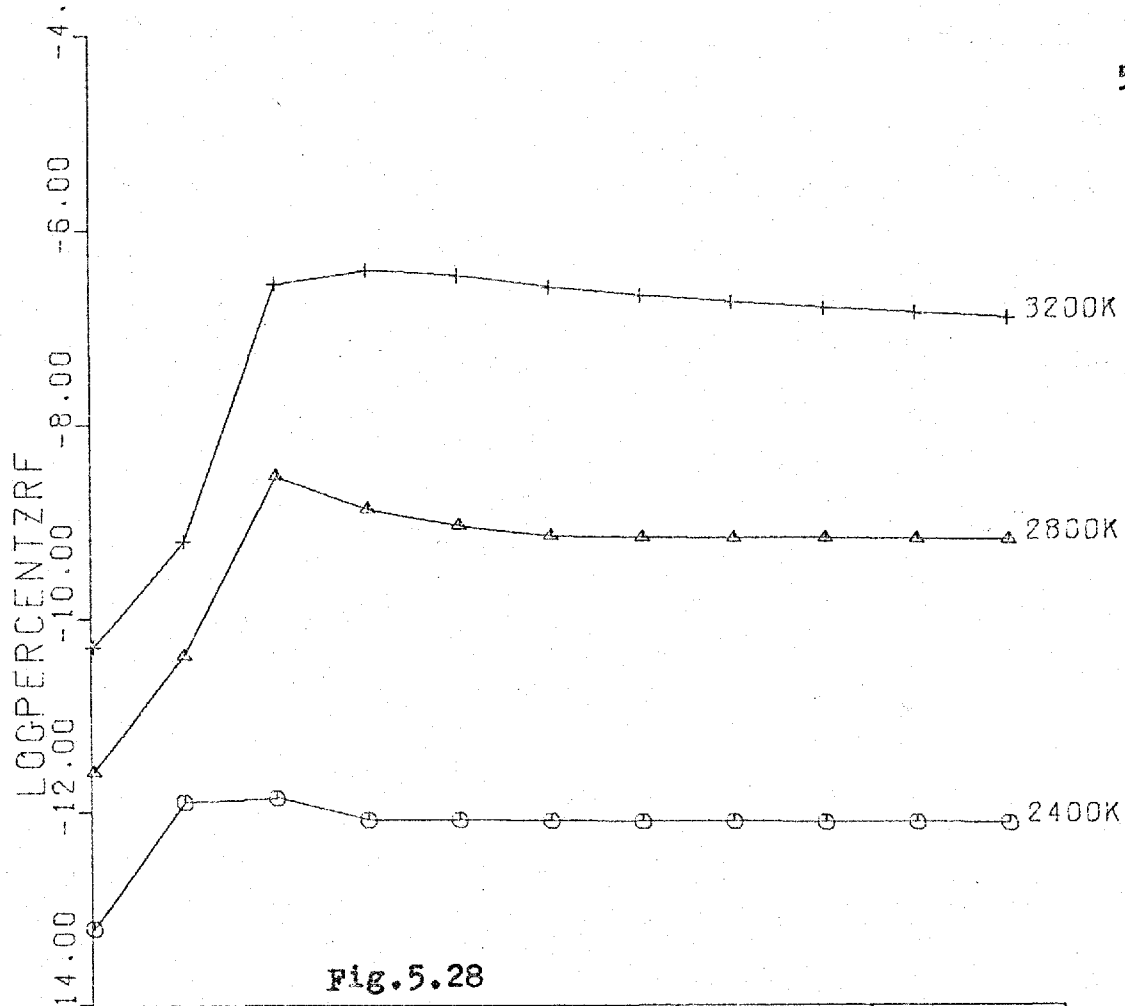
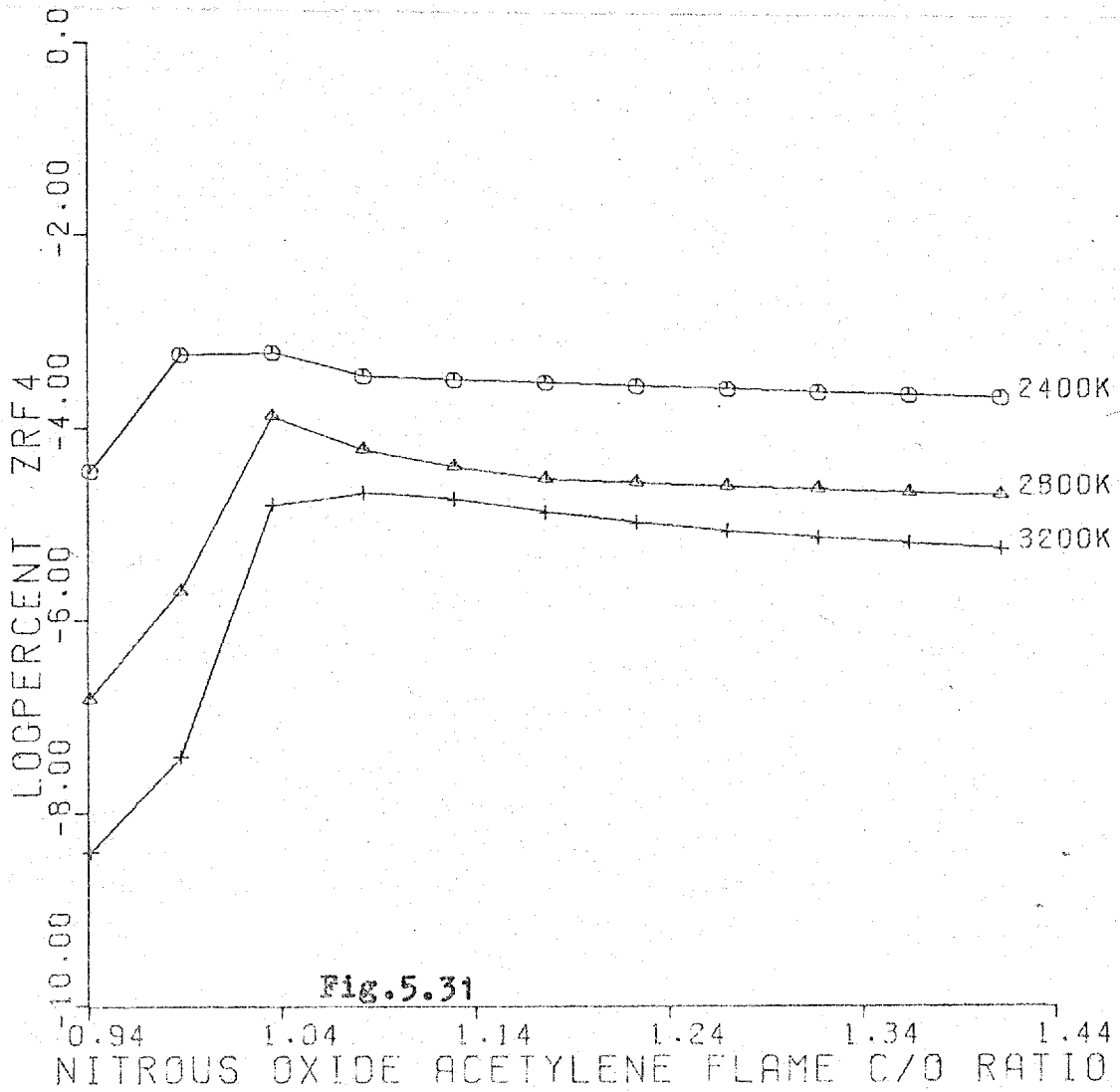
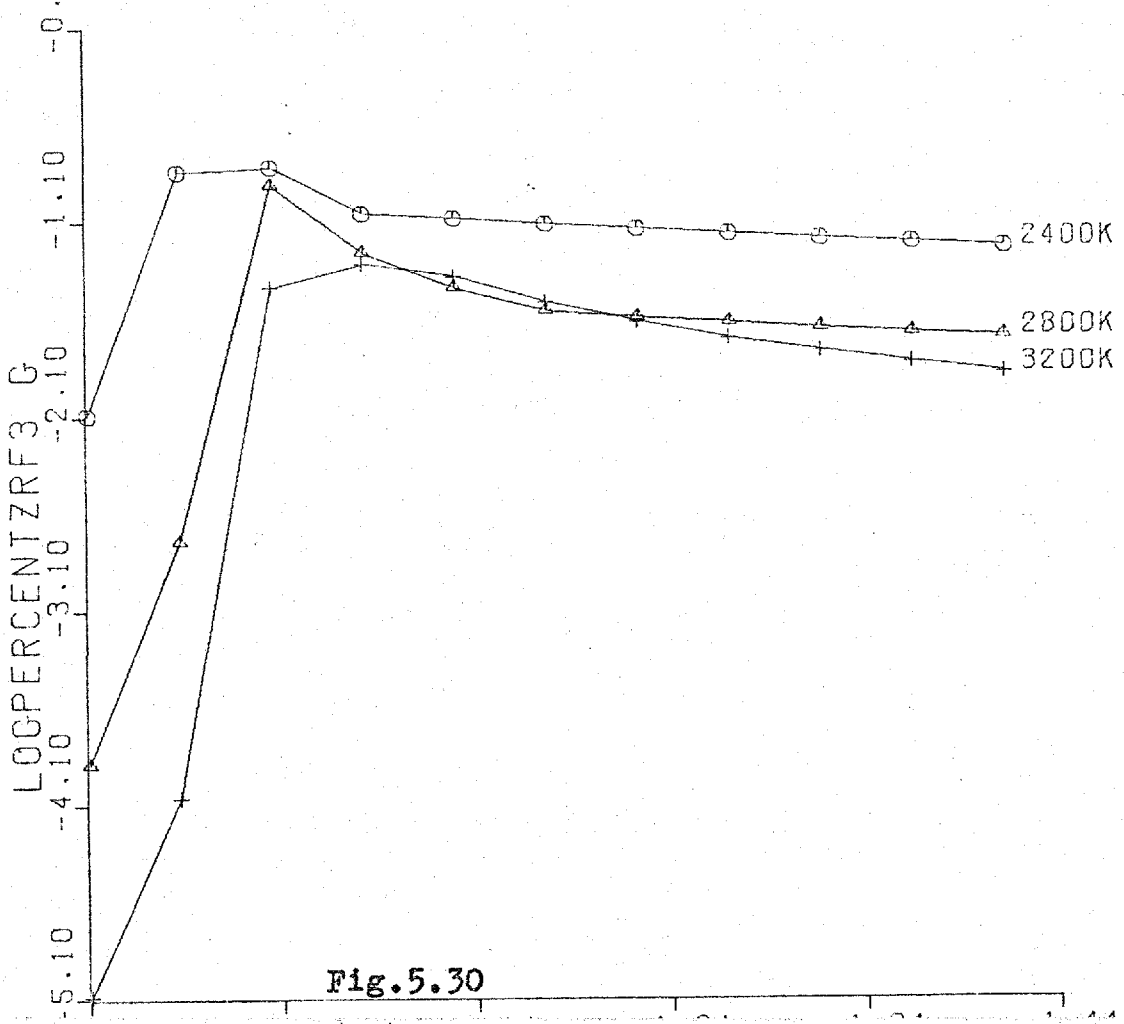


Fig.5.24









Bibliography

1. J.B. Willis
Nature 207 715 (1965)
2. D.W. Golightly
U.S.A.E.C. Published Report 15-T-26 (1965)
3. M.D. Amos, J.B. Willis
Spectrochimica Acta 22 1325 (1966)
4. G.F. Kirkbright, M.K. Peters, T.S. West
Talanta 14 789 (1967)
5. J.B. Headridge, D.P. Hubbard
Analytica Chimica Acta 37 151 (1967)
6. J.B. Willis, J.O. Rasmuson, R.N. Knisely, V.A. Fassel
Spectrochimica Acta 23B 725 (1968)
7. G.F. Kirkbright, M. Sargent, T.S. West
Talanta 16 1467 (1969)
8. D.N. Hingle, G.F. Kirkbright, T.S. West
Analyst 93 522 (1968)
9. A.M. Bond, T.A. O'Donnell
Analytical Chemistry 40 560 (1968)

APPENDIX

A DIGITAL COMPUTER PROGRAM TO DETERMINE SPECIES CONCENTRATIONS BY MINIMISATION OF FREE ENERGY.

The following program is basically that of C.F.ANDERSON¹, but modified for use with the Imperial College I.B.M. 7094 computer facility using a PUFFT (Purdue University Fast Fortran Translator) compiler, and also with the University of London C.D.C.6600 computer using a RUN compiler.

In addition to this a subroutine was written to make use of the CALCOMP (California Computers) graph-plotting facility available with the latter computer.

Mathematical Derivation of the Method.

The total free energy of a mixture of n gaseous and p condensed chemical species can be expressed as:

$$F(X) = \text{SIG}_i^n f_i^g + \text{SIG}_h^p f_h^c \quad (1)$$

Where SIG is the conventional series summation operator.

The free energy contributed by a gaseous species is given by the expression:

$$f_i^g = x_i^g (c_i^g + \ln(x_i^g/\bar{x})) \quad (2)$$

where

$$c_i^g = (F/RT)_i^g + \ln P \quad (3)$$

and

P is the total pressure in atmospheres,

$(F/RT)_i^g$ is the molal standard free energy function for the i^{th} gaseous species,

x_i^g is the mole number for the i^{th} gaseous species,

and

$$\bar{x} = \text{SIG}_i^n x_i^g$$

For a condensed species the effects of pressure and mixing are excluded so that the free energy expression becomes:

$$f_h^c = x_h^c \cdot c_h^c$$

where

$$c_h^c = (F/RT)_h^c \quad (5)$$

and

$(F/RT)_h^c$ is the molal standard free energy function for the h^{th} condensed species,

x_h^c is the mole number for the h^{th} condensed species

In the free energy expressions (3 and (5), $(F/RT)_i$ is defined in the following manner:

$$(F/RT)_i = 1/R \cdot ((F-H_{298})/T) + DH_{298}^f/RT \quad (6)$$

where

R is the universal gas constant,

T is the temperature in deg.K

DH_{298}^f is the standard enthalpy of formation at 298K

$((F-H_{298})/T)_i$ is the free energy function given in the JANAF Thermodynamic Tables for the i^{th} species.

Determination of the equilibrium composition requires finding a non-negative set of mole numbers $X = (x_1^g, x_2^g, \dots)$ which will minimise the total free energy of the system $F(x)$. However this set of mole numbers must also satisfy mass-balance considerations so that:

$$\text{SIG}_i^n a_{ij} \cdot x_i^g + \text{SIG}_h^p a_{hj}^c \cdot x_h^c = b_j, \quad j = 1, 2, \dots, m \quad (8)$$

where

m is the number of elements,

b_j is the total number of moles of the j^{th} element,

a_{ij} is the number of atoms of the j^{th} element in the i^{th} species

Let $Y^g = (y_1^g, y_2^g, \dots, y_n^g)$ be an initial guess for the mole numbers of the gaseous species $(x_1^g, x_2^g, \dots, x_n^g)$

Let $Y^c = (y_1^c, y_2^c, \dots, y_p^c)$ be an initial guess for the mole numbers of the solid species $(x_1^c, x_2^c, \dots, x_p^c)$

Let $Y = (Y^g, Y^c)$

Now choose Y such that it satisfies the mass-balance constraints and also such that it is a positive set. The free energy for this mixture is:

$$F(Y) = \text{SIG}_i^n y_i^g (c_i^g + \ln(y_i^g/\bar{y})) + \text{SIG}_h^p c_h^c \cdot y_h^c \quad (8)$$

where

$$\bar{y} = \text{SIG}_i^n y_i^g$$

An expression $Q(x)$ is obtained as an approximation for $F(x)$, the minimum free energy, by using a Taylor's expansion about the initial guess Y . Using this expansion technique, and substituting in values of the partial derivatives dF/dx_i^g and dF/dx_h^c the following expression can be obtained.

$$Q(x) = F(Y) + \text{SIG}_i^n (c_i^g + \ln(y_i^g/\bar{y})) D_i^g + \text{SIG}_h^p c_h^c \cdot D_h^c + 1/2(\text{SIG}_i^n y_i^g \cdot (D_i^g/y_i^g - D'/\bar{y})) \quad (9)$$

where

$$D_i^g = x_i^g - y_i^g,$$

$$D_h^c = x_h^c - y_h^c,$$

$$D' = \bar{x} - \bar{y}$$

In order to find a better approximation to the desired solution, $Q(x)$ is minimised subject to the mass-balance constraints of equation (7). First, however, it is necessary to define a function $G(x)$ as follows:

$$G(x) = Q(x) + \text{SIG}_j^m z_j (b_j - \text{SIG}_i^n a_{ij}^g \cdot x_i^g - \text{SIG}_h^p a_{hj}^c \cdot x_h^c) \quad (10)$$

where the z_{ij} 's are Lagrange multipliers. Setting

$$dG(X)/dx_i^g = dG(X)/dx_h^c = 0$$

the change in free energy with a change in moles of the gaseous species becomes

$$dG(X)/dx_i^g = (c_i^g + \ln(y_i^g/\bar{y})) + (x_i^g/y_i^g - \bar{x}/\bar{y}) - \text{SIG}_j^m z_j a_{ij}^g = 0 \quad (11)$$

and the change in free energy with change in moles of the condensed species is

$$dG(X)/dx_n^c = c_n^c - \text{SIG}_j^m z_j a_{ij}^c \quad (12)$$

Solving equation 11 for x_i^g and summing over i gives

$$x_i^g = -y_i^g (c_i^g + \ln(y_i^g/\bar{y})) + y_i^g (\bar{x}/\bar{y}) + \text{SIG}_j^m z_j a_{ij}^g y_i^g \quad (13)$$

and

$$\text{SIG}_j^m z_j \text{SIG}_i^n a_{ij}^g y_i^g = \text{SIG}_i^n y_i^g (c_i^g + \ln(y_i^g/\bar{y})) \quad (14)$$

Let

$$r_{jk} = r_{kj} = \text{SIG}_i^n (a_{ij}^g a_{ik}^g) y_i^g \quad j, k = 1, \dots, m \quad (15)$$

The substitution of equation (13) into equation (7) gives m equations which together with equations (12) and (14) give $m + p + 1$ linear equations in the unknowns z_1, \dots, z_m and x_1^c, \dots, x_p^c and \bar{x}/\bar{y} as follows

$$w_1 (\bar{x}/\bar{y}) + a_{11}^c x_1^c + a_{21}^c x_2^c + \dots + a_{p1}^c x_p^c + r_{11} z_1 + r_{12} z_2 + \dots + r_{1m} z_m = b_1 + \text{SIG}_i a_{i1}^g f_i^g$$

|
|
|
|

$$w_m (\bar{x}/\bar{y}) + a_{1m}^c x_1^c + \dots + r_{m1} z_1 + \dots = b_m + \text{SIG}_i a_{im}^g f_i^g$$

$$w_1 z_1 + w_2 z_2 + \dots + w_m z_m = \text{SIG}_i f_i^g$$

$$a_{11}^c z_1 + a_{12}^c z_2 + \dots + a_{1m}^c z_m = c_1^c$$

|
|
|

$$a_{m1}^c z_1 + a_{m2}^c z_2 + \dots + a_{pm}^c z_m = c_p^c$$

where

$$w_j = \text{SIG}_i^m a_{ij}^g y_i^g$$

The solution to this set of equations gives the new approximation to the condensed species, x_h^c , directly. To

find the new values of the gaseous species, x_i^g , it is necessary to substitute the w_j , \bar{x}/\bar{y} , and y_i^g values into equation (13). In this way a new set of x_i^g and x_h^c values are found which represent a new approximation to the desired result. In addition, values of trace gaseous species omitted from the system are computed by the formula

$$x_i^g = \bar{x} \cdot \exp(-c_i^g + \text{SIG}_j^m z_j a_{ij}^g)$$

where

$$1.0\text{E}-05 \leq x_i^g \leq 1.0\text{E}-35$$

and such species are added to the system again. The procedure is repeated using the x_i values thus calculated as new y_i values, until the differences between subsequent iterations are less than $1.0\text{E}-05$.

It is possible that the computed part of the new mole numbers x_i^g and x_h^c will include some negative numbers. If so, the computed values of mole numbers can not be used directly in the next approximation since zero or negative mole numbers are not permitted. Instead the new set is taken to be an indication of the desired direction of travel and x is allowed to proceed in this direction only so long as it remains a positive set.

This is done by choosing a value of k so that

$$y_i' = y_i + k(x_i - y_i)$$

is not zero or negative. The method of selecting k is to compute for each species where $(x_i - y_i)$ is negative a value of k' such that y_i' is zero.

$$k' = -y_i / (x_i - y_i)$$

The smallest value of k' is selected and k is set to $0.99k'$ so that all y_i are positive. The same value of k is used in adjusting all the mole numbers so that mass-balance is mai-

ntained throughout the set.

After each iteration and adjustment to a positive set, a test is applied to determine whether omitted condensed species should be added to the system. If for the h^{th} condensed species

$$\left| \frac{((F/RT)_h - \text{SIG}_j^m z_j a_{hj}^c)}{(F/RT)_h} \right| \geq 1.0\text{E}-03$$

then the species is added to the system with a value of $1.0\text{E}-08$.

In order to minimise matrix difficulties, any species which is present at a level of less than $1.0\text{E}-08$ is set to zero and omitted from calculation.

After convergence of the calculation the values calculated are used as initial guesses for calculations at the next highest temperature.

It will be noted from the above derivation that the thermodynamic function minimised by the program is not in fact the free energy, but a dimensionless quantity F/RT as suggested by WHITE, JOHNSON and DANTZIG .

Input

The input to the program is by punched cards both for the object program and data. A description of the data cards in turn is as follows:-

1st card; this is punched with the number of species under consideration in columns 1-2 and the number of temperatures considered in columns 5-6. The product of these two numbers is used by the program to determine the number of thermodynamic data cards to be read. This product may be denoted as 'n' .

2nd-(n+1)th card; these cards are punched with the following quantities: the name of the chemical species in

columns 2-7; the temperature at which the thermodynamic data applies in columns 10-13 (these quantities are not used in any manipulations by the program and the title section is later overwritten); the thermodynamic function from the JANAF tables - $-(F-H_{298})/T$ in columns 14-23; and the standard enthalpy of formation of the compound DH_{298}^f in columns 24-33. The order of these cards is very important; they must be arranged as follows. Each set of cards for one species should be together in order of ascending temperature, in steps of 100K. The number of cards for each species should correspond to the number of temperatures to be considered. All condensed species data should come at the end of the gaseous species data. The number of species must correspond to that given on the first card.

The previous $n+1$ cards constitute the bulk of all the data cards so to save confusion the remainder will be considered as a second set and numbered accordingly.

2nd set

1st card; this card is a flame title card and is punched in columns 1-30 with the name thus - e.g. OXYGEN-CYANOGEN FLAME . In columns 31-40 is punched the following C/O RATIO (or in case of air-hydrogen etc. H/O RATIO) The former label is used in labelling all output and the latter solely for labelling the CALCOMP plots.

2nd card; this card is punched with the variables NOMORE in columns 1-2, METALS in columns 5-6, and NOM in columns 9-10. The use of these parameters will be fully explained in the abridged namelist which follows.

3rd card; the number of elements in the system is punched in columns 1-4, the number of gaseous species in

columns 5-8, and the number of condensed species in columns 9-12. The starting temperature is punched in columns 13-18 and the pressure (in atmospheres) is in columns 19-24.

These latter are punched as floating-point numbers.

4th card; the chemical symbols of the elements present in the system are punched (right-justified) in 10 groups of 7 columns starting from column 1. The order must be; first the principal fuel element - carbon for hydrocarbon flames, -and with the metal under consideration coming last. The order of the other elements is relatively unimportant.

5th card; the atomic weights of the elements in the system are punched in groups of seven columns corresponding to those of the last card.

6th card; this is punched with the following parameters described more fully in the namelist, NOXY cols.1-2, RED(1) cols.3-9, DELTA cols.10-16, DIVO cols.17-23.

7th card; this is the first card of a group numbering the same as the number of elements . Each of these corresponds in order to the elements named on the 4th and 5th cards. The parameters punched on each card are, FRAC cols.1-7, and ADD cols.8-14. Their function will be described in the namelist.

8th card;(this may not be 8th in numerical order as it follows the group described above). The parameters LEAST cols.1-2, MOST cols.3-4, and INSTEP cols.5-6 are punched on this card.

9th card; this is the first of a group numbering the same as the number of species in the system. Each card is punched with the title of the species cols.1-6, an initial guess of the concentration of that species cols.7-12, and

the number of atoms of each element present in one molecule of that species, punched in groups of 6 columns. The order of the elements is the same as determined by cards 4 and 5 and the order of the cards of this group must be the same as that of the thermodynamic data cards.

10th card; (again this may well not be the 10th card)

This is punched with half of the legend of the ordinate axis of the CALCOMP plots in cols.1-10. Normally LOGPERCENT

11th card; this is punched with the temperature labels of the CALCOMP plots in cols.1-10, 11-20, & 21-30, in ascending order. These should be left-justified.

12th card; punched in cols.1-2 with the number of CALCOMP plots it is desired to obtain.

Abridged Namelist

The purpose of this namelist is to explain the purpose of the various parameters supplied by the card input.

NSPECY This is the total number of separate species considered in the program. For this purpose the same species is counted twice if present as gaseous and condensed phases. Although data are normally given for liquid and solid phases of the same species both above and below the melting and boiling points, obviously for a system in equilibrium, solid and liquid phases of the same species can not co-exist, nor can condensed phases exist above the boiling point. This point should be born in mind when deciding the number of species to be considered.

KELVIN The total number of temperatures to be considered. The product KELVIN.NSPECY determines the number of thermodynamic data cards required.

- TITLE** This is an alphabetic array used for storing the names of the species. The names actually stored and used are those read in from the second set of cards which also carry the initial concentration guesses.
- NTEMP** This array stores the temperature to calculate the free energy function.
- THERM1** The thermodynamic function $-(F-H_{298})/T$ is stored in this array.
- THERM2** The standard enthalpy of formation is stored in this array. These two variables are used to calculate the free energy function.
- FTITLE** An array to store the name of the flame and the rest of the label for the abscissal axis of the CALCOMP plots.
- NOMORE** The number of separate runs of the program at varying stoichiometry.
- METALS** The number of metal-containing species at the front of the block of thermodynamic data. This parameter, if greater than zero, affects the treatment of the CALCOMP variables of the first METALS species.
- NOM** This variable if greater than zero removes the mole fractions of the elements numbered from NOM to NE from calculation in the usual fashion; instead these are left constant at the value entered as ADD.
- NE** The number of elements.
- NGS** The number of gaseous species.
- NCS** The number of condensed species.
- STEMP** The starting temperature.

- P The pressure in atmospheres.
- ETITLE An array to store the chemical symbols of the elements present.
- WT This array stores the corresponding atomic weights to the above.
- NOXY This is the index of the major oxidising element and is used to calculate the fuel/oxidant ratio thus $B(1)/B(\text{NOXY})$.
- RED(1) This is the first value in an array for calculating the mole values of the various elements. It appears in the equation for setting the stoichiometry of the flame:- e.g. $2\text{N}_2\text{O} + \text{RED} \cdot \text{C}_2\text{H}_2 = \text{products}$.
- DELTA After each complete solution of the flame at one stoichiometry, the value of RED is increased by an amount DELTA and the process repeated.
- DIVO This is part of the normalising factor DIV used for calculating the mole fractions. In the equation:- $2\text{N}_2\text{O} + \text{RED} \cdot \text{C}_2\text{H}_2 + 0.125 \cdot \text{H}_2\text{O} = \text{products}$, DIVO would have the value 2.125 and DIV the value $2.125 + \text{RED}$.
- FRAC An array for the calculation of the mole fractions. Each element has a corresponding FRAC value used as detailed below.
- ADD This is a second array for the calculation of the mole fractions thus: $B(I) = (\text{FRAC}(I) \cdot \text{RED}(I) + \text{ADD}(I)) / \text{DIV}$
Obviously any element not present in the fuel gas will have a FRAC value of zero. For elements with an index greater than NOM the value of B is entered as ADD.
- LEAST This is the initial parameter of the 'DO'-loop used for entering values into the CALCOMP arrays.

MOST The maximum parameter of the above-mentioned 'DO'-loop

INSTEP The step size of the 'DO'-loop.

Y This is the array of mole numbers used in the free energy minimisation, the input values are arbitrary guesses and need not be close to the final ones.

A This is a two-dimensional array of the number of atoms of each element in one molecule of each species.

A1(1) This is the first half of the ordinate-axis legend.

DIG These three parameters are the labels used on the DDIG CALCOMP plots to denote temperature.

DDDIG " "

NGLYPH The number of CALCOMP plots desired to be plotted.

Output

The output of the program is in two basic forms: printed output, and CALCOMP plots.

Print-out

The printed output of the program is subdivided into two parts.

At the top of each page of results the program prints the chemical symbols of the elements present. below which are printed the mole numbers of the elements, the legend FUEL/OXIDANT RATIO followed by that value & the value of RED.

After this, on one half of the pages of results, the following legend is printed; 'EQUILIBRIUM CONCENTRATIONS OF(flame title) IN MOLES PER MOLE GAS FEED! On the other pages of results this legend is altered to; 'EQUILIBRIUM CONCENTRATIONS OF (flame title) IN VOLUME PERCENT OF PRODUCTS'. Below these titles are printed the temperatures in

columns followed by the corresponding concentrations.

Condensed species are not considered for inclusion in the 'volume percent' results since they are considered as having negligible volume.

Finally after the 'volume percent' results the mean molecular weight of the flame gases is printed.

CALCOMP

The CALCOMP graphic output is generated for plotting by a subroutine GLYPHO which is situated at the end of the main program. This subroutine will be described in some detail.

The subroutine obtains calculated values of concentration from the main program in the three-dimensional array ATOM. The values actually entered in this array are dependent upon the value of the variable METALS in the input. If this has a positive value n then the first n species entered in the ATOM array are calculated from the 'moles per mole feed' data in the following fashion;

$$\text{ATOM}(I,IT,\text{INDEX}) = \log_{10} Z(I,KT) \cdot A(I,NE) \cdot 100.0 / B(NE)$$

where

$Z(I,KT)$ is the mole number of the species No. I at temperature No. KT

$A(I,NE)$ is the number of atoms of the last element in the element list present in one molecule of the species.

$B(NE)$ is the total concentration of this last element.

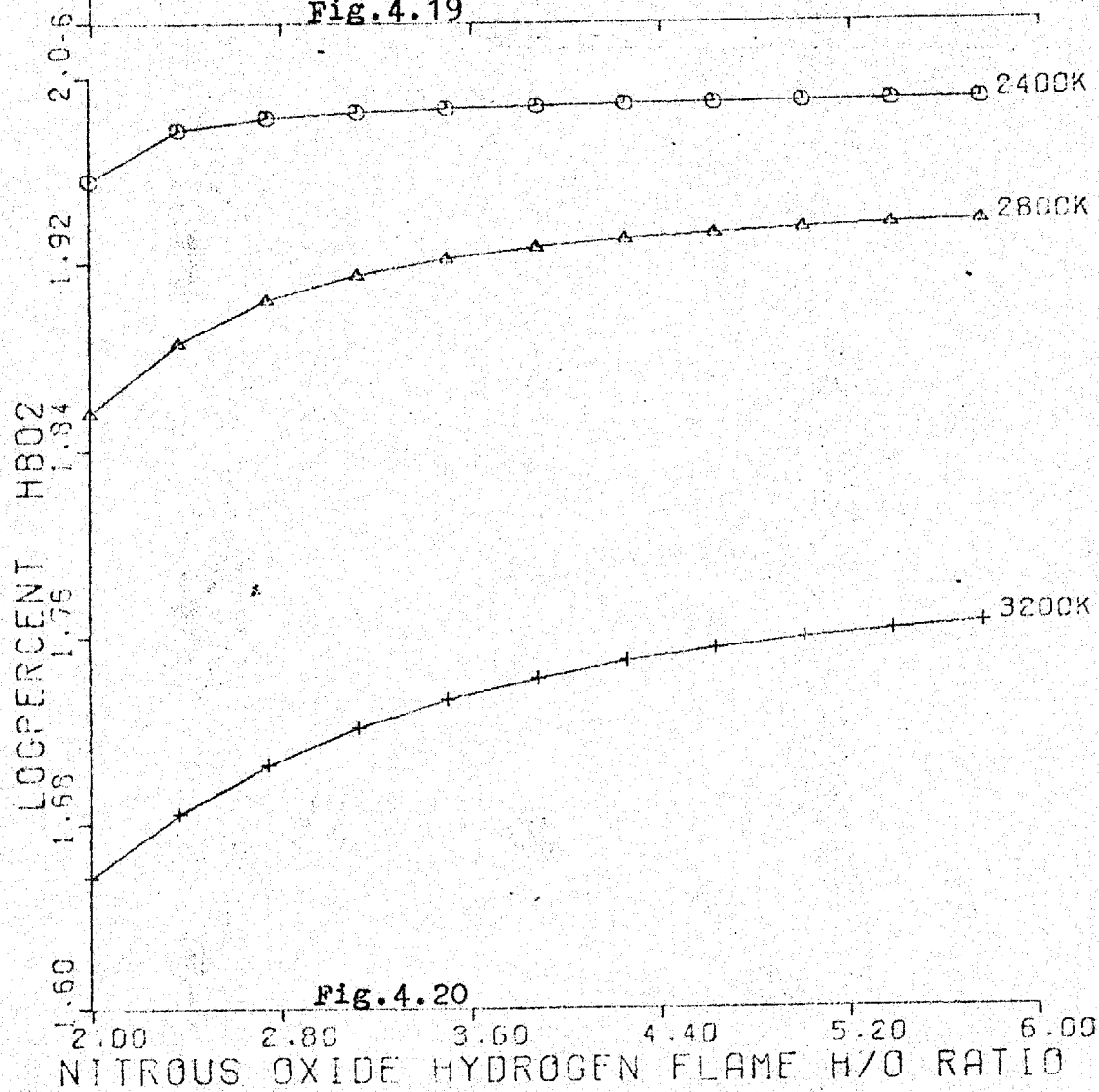
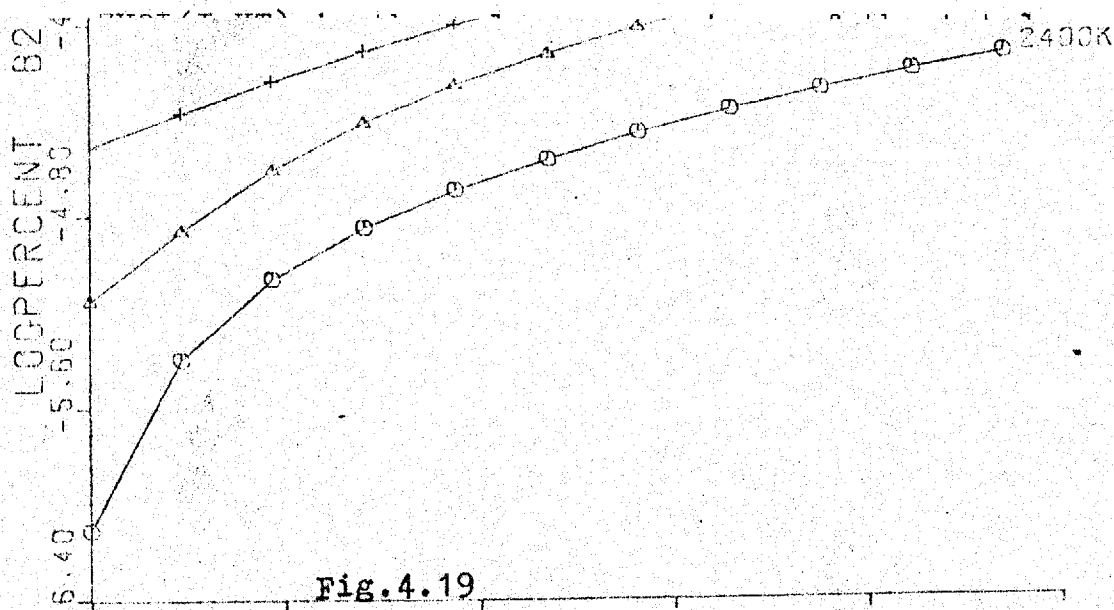
Thus it will be seen that the quantity entered into the ATOM array is the logarithm of the percentage of the final element in the element list, present as that parti-

cular species.

For species with an index number greater than n the quantity entered into the ATOM array is;

$$\text{ATOM}(I,IT,\text{INDEX})=\log_{10} \text{ZVOL}(I,KT)$$

where



els of each of the lines may be located. The axes are then drawn and labelled, the three lines plotted, and finally the temperature labels are drawn.

The process is then repeated for each of the species to be plotted.

The graphs produced by this subroutine are 5" square measured along the axes and the lines consist of a set of points (marked by a different symbol for each temperature) joined by straight lines. The graphs are presented four side by side on the standard CALCOMP graph plotter chart spaced at seven-inch intervals.

Program

A full program listing is given on pages A.16 to A.24


```
PROGRAM ANFLAM (INPUT,OUTPUT,TAPES=INPUT,TAPE6=OUTPUT,TAPE27,  
1TAPE25)
```

```
$IBFTC MAIN
```

```
C  
C  
C  
C  
C  
C
```

```
CALCULATION OF CONCENTRATIONS OF FLAME SPECIES BY MINIMISATION OF  
FREE ENERGY
```

```
READ IN DATA AND CALCULATE F/RT
```

```
DIMENSION FRT(60,10),NTEMP(10),TITLE(60),THERM1(60,10),
```

```
1 THERM2(60,10),TEMP(10)
```

```
2,Z(60,10)
```

```
COMMON FRT,KELVIN
```

```
READ(5,1914) NSPECY,KELVIN
```

```
1914 FORMAT(I2,2X,I2)
```

```
DO 10 NS = 1,NSPECY
```

```
DO 11 NT = 1,KELVIN
```

```
READ(5,1000)TITLE(NS),NTEMP(NT),THERM1(NS,NT),THERM2(NS,NT)
```

```
1000 FORMAT (1X,A6,I6,2F10.3)
```

```
TEMP(NT) = NTEMP(NT)
```

```
FRT(NS,NT) = -THERM1(NS,NT)/1.9872 + THERM2(NS,NT)/
```

```
1 (1.9872*TEMP(NT))*1000.0
```

```
11,CONTINUE
```

```
10 CONTINUE
```

```
CALL THERMO
```

```
STOP
```

```
END
```

\$IBFTC ATHERM

SUBROUTINE THERMO

```

DIMENSION TEMP(10),FRT(60,10),B(10),AW(10),TITLE(60),A(60,10),
1Y(60),F(60),ALPHA(10),R(10,10),Y1(60),X(41,42),NONCON(10),Z(60,10)
2,KTEMP(10),ZVOL(60,10),SUMZ(10),ETITLE(10),AVEMW(10),WT(10)
3,FTITLE(5),RED(20),ATOM(60,3,20),RATIO(20),NOUGHT(60)
4,FRAC(10),ADD(10)
COMMON FRT,KELVIN
DO 116 I = 1,60
116 NOUGHT(I) = -1
INDEX = 1
READ(5,119)(FTITLE(I),I=1,4)
119 FORMAT(4A10)
READ(5,120)NOMORE,METALS,NOM
120 FORMAT(12,2X,12,2X,12)
READ(5,121) NE,NGS,NCS,STEMP,P
121 FORMAT(3I4,F8.1,F6.2)
READ(5,140)(ETITLE(I),I=1,NE)
140 FORMAT(10(1X,A6))
READ(5,144)(WT(J),J=1,NE)
144 FORMAT(10F7.3)
READ(5,9111)NOXY,RED(1),DELTA,DIVO
9111,FORMAT(12,3F7.3)
READ(5,1999)(FRAC(I),ADD(I),I=1,NE)
1999 FORMAT(2F7.4)
READ(5,1998)LEAST,MOST,INSTEP
1998 FORMAT(3I2)
NS= NGS + NCS
DO 150 I =1,NS
READ(5,151)(TITLE(I),Y(I),(A(I,11),I1=1,NE))
151 FORMAT(A6,F6.4,10F6.1)
150 CONTINUE
C
C CALCULATE B VALUES FROM FLAME STOICHEOMETRY
C
414 CONTINUE
DIV = DIVO + RED(INDEX)
DO 415 I=1,NE
415 B(I) =(FRAC(I)*RED(INDEX) + ADD(I))/DIV
IF(NOM.LE.0) GO TO 417
DO 416 I=NOM,NE
416 B(I) = ADD(I)
417 RATIO(INDEX) = B(1)/B(NOXY)
WRITE(6,162)(ETITLE(I),I = 1,NE)
162 FORMAT(1H1,7X,10(3X,A6))
WRITE(6,163)(B(I),I = 1,NE)
163 FORMAT(1H0,5X,2HB=,10F9.6)
WRITE(6,8001)RATIO(INDEX),RED(INDEX)
8001 FORMAT(1H0,5X,22HFUEL/OXIDANT RATIO IS ,F8.4,5X,F8.4,10H MOLS FUEL
1 )
T1 = STEMP
ITEMP = I
C
C FIND SOLUTION FOR EACH TEMPERATURE
C
NGS1 = NGS + 1
NE1 = NE + 1
DO 1100 IT =1,KELVIN
LOOP = 0

```

```

NONCON(IT) = 0
260 DO 270 I = 1,NS
    IF ( Y(I) - 1.0E-8 ) 265,270,270
265 Y(I) = 0.0
270 Y1(I) = Y(I)
    LOOP = LOOP + 1
    IF ( LOOP - 100 ) 280,280,275
275 NONCON (IT) = 1
    GO TO 1085
280 N = NE1
    IF ( NS - NGS1 ) 350, 300, 300
300 DO 340 I = NGS1,NS
    IF ( Y(I) ) 320, 340, 320
320 N = N + 1
340 CONTINUE
350 N1 = N + 1
    DO 370 I =1,N
    DO 370 J =1,N1
370 X(I,J) = 0.0

```

```

C
C   FIND VALUES OF ALPHA, R AND F
C

```

```

400 YBAR = 0.0
    DO 420 I = 1,NGS
420 YBAR = YBAR + Y(I)
    DO 440 I = 1,NGS
    IF(Y(I).EQ.0.0) Y(I) = 1.0E-250
440 F(I) = Y(I)*(FRT(I,ITEMP) + ALOG(P) + ALOG( Y(I)/YBAR))
    DO 480 J = 1,NE
    ALPHA(J) = 0.0
    DO 460 K = 1,NE
    R(J,K) = 0.0
    DO 460 I = 1,NGS
460 R(J,K) = R(J,K) + A(I,J)*A(I,K)*Y(I)
    DO 480 I = 1,NGS
480 ALPHA(J) = ALPHA(J) + A(I,J)*Y(I)

```

```

C
C   SET UP THE SYSTEM OF EQUATIONS
C

```

```

C   EQUATIONS FOR GASEOUS SPECIES
C

```

```

DO 550 I = 1,NE
X(I,N1) = B(I)
X(I,1) = ALPHA(I)
II = N - NE + I
X(NE1,II) = ALPHA(I)
DO 530 J = 1,NE
JJ = N - NE + J
530 X(I,JJ) = R(I,J)
DO 550 J = 1,NGS
550 X(I,N1) = X(I,N1) + A(J,I)*F(J)
DO 570 I = 1,NGS
570 X(NE1,N1) = X(NE1,N1) + F(I)
    IF ( NS - NGS1 ) 680, 600, 600

```

```

C
C   EQUATIONS FOR CONDENSED SPECIES
C

```

```

600 NC = 0
    DO 650 I = NGS1,NS

```

```

        IF ( Y(I) ) 620, 650, 620
620 NC = NC + 1
        NN = NE1 + NC
        X(NN,N1) = FRT(I,ITEMP)
        DO 640 J = 1,NE
        NJ = N - NE + J
        X(J,NC+1) = A(I,J)
640 X(NN,NJ) = A(I,J)
650 CONTINUE

```

```

C
C   SOLVE THE SYSTEM OF EQUATIONS
C

```

```

680 CONTINUE
690 CALL GPIVOT(N,X)

```

```

C
C   COMPUTE NEW VALUES
C

```

```

        DO 780 I = 1,NGS
        SUM = 0.0
        DO 700 J = 1, NE
        NN = N - NE + J
700 SUM = SUM + X(NN,N1)*A(I,J)
        IF ( Y1(I) ) 720, 750, 720
720 Y(I) = Y1(I)*(-FRT(I,ITEMP) - ALOG(P) - ALOG(Y1(I)/YBAR)
        1 + X(I,N1) + SUM )
        GO TO 780
750 Y(I) = YBAR*EXP(-FRT(I,ITEMP) + SUM)
        IF ( Y(I) - 1.0E-5 ) 770, 770, 760
760 Y(I) = 1.0E-5
        GO TO 780
770 IF ( Y(I) - 1.0E-35 ) 775, 780, 780
775 Y(I) = 1.0E-35
780 CONTINUE
        IF ( NS - NGS1 ) 850, 800, 800
800 NC = 1
        DO 840 I = NGS1, NS
        IF ( Y1(I) ) 820, 840, 820
820 NC = NC + 1
        Y(I) = X(NC,N1)
840 CONTINUE

```

```

C
C   ADJUST NEW VALUES TO A POSITIVE SET
C

```

```

850 FLAM = 1.0
        DO 900 I = 1, NS
        IF ( Y(I) ) 855, 900, 900
855 IF ( Y(I) - Y1(I) ) 860, 900, 900
860 FL = - Y1(I) / ( Y(I) - Y1(I) )
        IF ( FLAM - FL ) 900, 900, 880
880 FLAM = 0.99*FL
900 CONTINUE
910 DO 920 I = 1, NS
920 Y(I) = Y1(I) + FLAM*( Y(I) - Y1(I) )
        IF ( NS - NGS1 ) 1050, 950, 950
950 DO 1000 I = NGS1, NS
        IF ( Y1(I) ) 955, 955, 1000
955 SUM = 0.0
        DO 960 J = 1, NE
        NN = N - NE + J

```

```

960 SUM=SUM + X(NN,N1)*A(I,J)
DIF = FRT(I,ITEMP) - SUM
IF ( DIF ) 980,1000,1000
980 IF ( ABS (DIF/FRT(I,ITEMP) ) - 1.0E-3 ) 1000,990,990
990 Y(I) = 1.0E-8
1000 CONTINUE
C
C CHECK FOR CONVERGENCE
C
1050 DO 1070 I = 1,NS
IF ( ABS( Y(I) - Y1(I) ) - 1.0E-6 ) 1070,260,260
1070 CONTINUE
IF ( FLAM - 1.0 ) 260,1080,260
1080 CONTINUE
C
C STORE VALUES OF Y(I) IN A TWO-DIMENSIONAL ARRAY SO THAT Y(I) CAN
C BE USED AS INITIAL GUESSES FOR THE NEXT TEMPERATURE
C
DO 2102 I=1,NS
Z(I,IT) = Y(I)
2102 CONTINUE
KTEMP(IT) = T1
T1 = T1 + 100.0
ITEMP = ITEMP + 1
1100 CONTINUE
GO TO 1086
C
C IF SYSTEM FAILS TO CONVERGE PRINT CURRENT VALUES OF CONCENTRATIONS
C AND TERMINATE PROGRAM
C
1085 WRITE(6,3110)T1
3110 FORMAT(1X,37HSYSTEM HAS FAILED TO CONVERGE AT TEMP,F6.1/
11X,40H VALUES OF Y(I) AFTER 50 ITERATIONS ARE )
WRITE(6,2555)(TITLE(I),Z(I,IT),I = 1,NS)
2555 FORMAT(1X,5(A6,1PE12.5))
STOP
1086 CONTINUE
C
C PRINT CONCENTRATIONS OF SPECIES IN MOLES PER MOLE GAS FEED
C
WRITE(6,2999) (FTITLE(I),I=1,3)
2999 FORMAT(1H0,6X,29HEQUILIBRIUM CONCENTRATIONS OF ,3A10,28H IN MOLES
1PER MOLE GAS FEED )
WRITE(6,2100)(KTEMP(IT) ,IT = 1,KELVIN)
2100 FORMAT(1H0,6H TEMP=/1X,10I12)
DO 6666 I = 1,NS
WRITE(6,2111)TITLE(I),(Z(I,IT),IT = 1,KELVIN)
2111 FORMAT(1X,A6,1X,1P10E12.5)
6666 CONTINUE
IF(METALS.EQ.0) GO TO 8012
DO 8000 I = 1,METALS
K = I
DO 8002 KT = LEAST,MOST,INSTEP
IF(KT.GT,KELVIN) GO TO 8000
EFFIC = Z(I,KT)*100.0/B(NE)
EFFIC = EFFIC*A(I,NE)
IF (EFFIC.LE.0.0) NOUGHT(I) = 1
IF (EFFIC.LE.0.0)GO TO 8000
ATOM(I,K,INDEX) = ALOG10(EFFIC)

```

```

8002 K=K+1
8000 CONTINUE
DO 8012 I = 1,METALS
IF(NOUGHT(I).EQ.-1) GO TO 8012
K = 1
DO 8011 KT = LEAST,MOST,INSTEP
ATOM(I,K,INDEX) = Z(I,KT)*A(I,NE)
8011 K = K+1
8012 CONTINUE

```

C
C
C

CALCULATE CONCENTRATIONS IN VOLUME PER CENT

```

DO 85 IT = 1,KELVIN
SUMZ(IT) = 0.0
DO 84 I = 1,NGS
SUMZ(IT) = SUMZ(IT) + Z(I,IT)
84 CONTINUE
85 CONTINUE
DO 88 IT = 1,KELVIN
DO 87 I = 1,NGS
ZVOL(I,IT) = 100.0*(Z(I,IT)/SUMZ(IT))
87 CONTINUE
88 CONTINUE
DO 95 IT = 1,KELVIN
SUMMW = 0.0
DO 94 I = 1,NGS
DO 93 J = 1,NE
SUMMW = SUMMW + ZVOL(I,IT)*A(I,J)*WT(J)
93 CONTINUE
94 CONTINUE
AVEMW(IT) = SUMMW/100.0
95 CONTINUE

```

C
C
C

PRINT CONCENTRATIONS OF SPECIES IN VOLUME PER CENT

```

WRITE(6,162)(ETITLE(I),I=1,NE)
WRITE(6,163)(B(I),I = 1,NE)
WRITE(6,8001)RATIO(INDEX),RED(INDEX)
WRITE(6,2998) (FTITLE(I),I=1,3)
2998 FORMAT(1H0,6X,29HEQUILIBRIUM CONCENTRATIONS OF ,3A10.31H IN VOLUME
1 PERCENT OF PRODUCTS )
WRITE(6,2100)(KTEMP(IT),IT=1,KELVIN)
DO 86 I = 1,NGS
86 WRITE(6,2997)TITLE(I),(ZVOL(I,IT),IT=1,KELVIN)
2997 FORMAT(1X,A6,1X,1P10E12.5)
NSTART = METALS + 1
DO 9020 NSPEC = NSTART,NGS
K = 1
DO 9021 KT = LEAST,MOST,INSTEP
IF(KT.GT.KELVIN) GO TO 9020
IF(ZVOL(NSPEC,KT).LE.0.0) NOUGHT(NSPEC) = 1
IF(ZVOL(NSPEC,KT).LE.0.0) GO TO 9020
ATOM(NSPEC,K,INDEX) = ALOG10(ZVOL(NSPEC,KT))
9021 K = K+1
9020 CONTINUE
DO 9022 NSPEC = NSTART,NGS
IF(NOUGHT(NSPEC).EQ.-1) GO TO 9022
K = 1
DO 9023 KT = LEAST,MOST,INSTEP

```

```
      ATOM(NSPEC,K,INDEX) = ZVOL(NSPEC,KT)
9023 K = K+1
9022 CONTINUE
      WRITE(6,3000)(AVEMW(IT),IT = 1,KELVIN)
3000 FORMAT(1X,44H AVERAGE MOLECULAR WEIGHTS OF FLAME PRODUCTS /1X,10(
1F12.5))
      IF(INDEX.EQ.NOMORE) CALL GLYPHO(ATOM,RED,TITLE,RATIO,FTITLE)
      IF(INDEX.GE.NOMORE) STOP
      RED(INDEX+1) = RED(INDEX) + DELTA
      INDEX = INDEX + 1
      GO TO 414
6667 CONTINUE
      RETURN
      END
```

```

$IBFTC APIVOT
SUBROUTINE GPIVOT (N,A)
DIMENSION A(41,42)
C
C GAUSSIAN ELIMINATION WITH PIVOTING
C
N1 = N + 1
4 DO 8 I = 1,N
  I1 = I + 1
  IF ( I - N ) 40,45,45
40 Q = ABS(A(I,I))
  MAX = 0
  DO 42 J = I1,N
    P = ABS(A(J,I))
    IF ( Q - P ) 41,42,42
41 Q = P
  MAX = J
42 CONTINUE
  IF (MAX) 45,45,43
43 DO 44 K = 1,N1
  B = A(I,K)
  A(I,K) = A(MAX,K)
44 A(MAX,K) = B
45 Z = A(I,I)
  DO 5 J = I1,N1
  5 A(I,J) = A(I,J)/Z
  IF ( I - N)6,8,6
  6 DO 7 K = I1,N
  DO 7 J = I1,N1
  7 A(K,J) = A(K,J) - A(K,I)*A(I,J)
  8 CONTINUE
  N2 = N - 1
  DO 9 K = 1,N2
  I = N - K
  I1 = I + 1
  DO 9 J = I1,N
  9 A(I,N1) = A(I,N1) - A(I,J)*A(J,N1)
RETURN
END

```


518FTC AGRAPH

```

SUBROUTINE GLYPHO(ATOM,RED,TITLE,RATIO,FTITLE)
  DIMENSION X(60),Y(60),RED(20),ATOM(60,3,20),NUM(10),SPEC(60)
  1,X1(20),Y1(20),Y2(20),Y3(20),TITLE(60),RATIO(20),A1(2),FTITLE(4)
  READ(5,117) A1(1)
  117 FORMAT(6A10)
  READ(5,1117) DIG,DDIG,DDDIG
  1117 FORMAT(6A10)
  READ(5,1118) NGLYPH
  1118 FORMAT(I2)
  CALL START
  CALL PLOT(1.0,1.0,-3)
  DO 9083 NSPEC = 1,NGLYPH
  A1(2) = TITLE(NSPEC)
  DO 9084 I = 1,10
  9084 NUM(I) = 11
  NTAG = NSPEC/4
  ITERO = NSPEC-(NTAG*4)
  DO 9082 KT = 1,3
  DO 9081 I = 1,11
  JEMMY = I + (11*(KT-1))
  Y(JEMMY) = ATOM(NSPEC,KT,I)
  9081 X(JEMMY) = RATIO(I)
  9082 CONTINUE
  CALL SCALE(X,5.0,33,1)
  CALL SCALE(Y,5.0,33,1)
  DO 9150 J = 1,11
  K = J+11
  L = J+22
  X1(J) = X(J)
  Y1(J) = Y(J)
  Y2(J) = Y(K)
  9150 Y3(J) = Y(L)
  X1(12) = X(34)
  X1(13) = X(35)
  Y1(12) = Y(34)
  Y1(13) = Y(35)
  Y2(12) = Y(34)
  Y2(13) = Y(35)
  Y3(12) = Y(34)
  Y3(13) = Y(35)
  XN1 = ((X1(11)-X1(12))/X1(13)) + 0.1
  YN1 = ((Y1(11)-Y1(12))/Y1(13))
  YN2 = ((Y2(11)-Y2(12))/Y2(13))
  YN3 = ((Y3(11)-Y3(12))/Y3(13))
  CALL AXIS(0.0,0.0,FTITLE,-40,5.0,0.0,X(34),X(35))
  CALL AXIS(0.0,0.0,A1,20,5.0,90.0,Y(34),Y(35))
  CALL LINE(X1,Y1,11,1,1,1)
  CALL LINE(X1,Y2,11,1,1,2)
  CALL LINE(X1,Y3,11,1,1,3)
  CALL SYMBOL(XN1,YN1,0.1,DIG,0.0,10)
  CALL SYMBOL(XN1,YN2,0.1,DDIG,0.0,10)
  CALL SYMBOL(XN1,YN3,0.1,DDDIG,0.0,10)
  IF(ITERO.EQ.0) CALL PLOT(8.0,-21.0,-3)
  IF(ITERO.NE.0) CALL PLOT(0.0,7.0,-3)
  9083 CONTINUE
  IF(ITERO.EQ.0) CALL PLOT(-8.0,0.0,-3)
  CALL ENPLOT(9.0)
  RETURN
  END

```

Bibliography

1. C.H. Anderson

Paper presented at the Pittsburgh Conference on Analytical Chemistry and Applied Spectroscopy. March 1968